UNIVERSITAT DE BARCELONA

The role of FGF21 in the metabolic response to amino acid restriction

Albert Pérez Martí

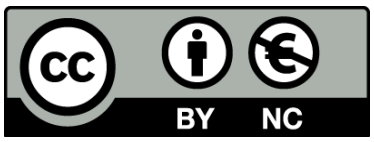

Programa de Doctorat en Biomedicina

Facultat de Farmàcia i Ciències de l'Alimentació

Departament de Nutrició, Ciències de l'Alimentació i Gastronomia

THE ROLE OF FGF21 IN THE METABOLIC RESPONSE TO AMINO ACID RESTRICTION

Memòria presentada per Albert Pérez Martí per optar al títol de doctor per la Universitat de Barcelona

Dr. Diego Haro	Dra. Joana Relat	Albert Pérez Martí
El Director	La Directora	El Doctorand

Aquesta tesi ha estat realitzada gràcies a la concessió d'una beca del programa "Ayudas para la formación de profesorado universitario" (FPU) del "Ministerio de Educación, Cultura y Deporte. (FPU12/01733)

[Success is going from failure to failure
without losing your enthusiasm.]

AGRAÏMENTS

Em sento molt afortunat de considerar la meva feina no sols una manera de guanyar-me la vida sinó també una part important d'ella, un estímul i un repte constant. Aprofitaré aquest espai doncs, per donar les gràcies a totes aquelles persones que fan que això sigui possible.

En primer lloc, donar les gràcies als caps de grup (els "jefes"), Diego, Pedro i Joana, per donar-me la oportunitat de formar part del vostre grup. He après moltíssim, a nivell professional i a nivell personal, dels moments bons però també dels dolents. He gaudit molt de la nostra feina, de les discussions científiques i de les persones que he anat coneixent. Gràcies per ensenyar-me a fer ciència rigorosa i honesta, per compartir amb mi la vostra manera de fer i de pensar, per no limitar-me i per deixar que m'equivoqués. He après molt més dels errors que dels encerts.

Gracias Diego por tener siempre claro donde vamos y por estar siempre, sin necesidad de estar. Gracias Pedro por tus aportaciones y por ser el contrapunto ácido y necesario. Gràcies Joana per ser el nexe indispensable, per tenir solucions per tot i sobretot pel teu positivisme incombustible.

Gràcies a les noies del laboratori per ajudar-me sempre que ho vaig necessitar sense posar mai mala cara. Mar, per fer-me començar amb bon peu i per fer que la ciència semblés fàcil. Mariona, per la teva predisposició a ajudar i a fer equip sempre. Anna Vilà, per imposar ritme al laboratori. *Elena, por generar buen ambiente y tener siempre una sonrisa en la cara*. *I Analu, gracias por nuestro trabajo "em parceria", aprendí mucho contigo y ha sido un placer continuar con tu proyecto.*

Gracias Xana por ser una gran compañera de laboratorio, por siempre echar una mano y por todas las horas que hemos pasado juntos.

Gràcies al "Torribera Team", Vivi i Maite, pel vostre bon rotllo, per donar un cop de mà sempre que ha fet falta i per la fantàstica acollida al nou laboratori.

Gràcies a tots els estudiants que he tingut: Adrian, Pablo, Edu, Gerard, Paula, Ilona, Cristina, Raquel, Miriam, Liza, Úrsula i Felix. Perquè ensenyant s'aprèn moltíssim.

A tota la gent del departament, que en algun moment o altre m'heu ajudat, ja sigui amb aquell reactiu, aparell o protocol o simplement fent-la petar pels passadissos. També a la gent de l'estabulari, per fer que la feina amb els ratolins sigui molt més fàcil.

Gràcies a les noies del laboratori CCVN per acollir-me quan més ho necessitava, m'ho he passat molt bé amb vosaltres. *Xenia, gracias por tu puntito de locura, el mundo seria un lugar muy aburrido sin gente como tu*. Anna, gràcies per ser molt més que una companya de feina i per estar incondicionalment al meu costat.

I per últim, gràcies als amics i la família, que sense acabar d'entendre molt bé el que faig, sempre us heu interessat i preocupat per mi.

INDEX

PRESENTATION AND OBJECTIVES

Obesity and associated metabolic diseases have reached epidemic proportions, affecting not only high-income countries but also low- and middle-income ones. In this context, the search for therapeutic approaches to treat obesity is becoming a priority worldwide.

In this regard, the metabolic hormone fibroblast growth factor 21 (FGF21) has been identified as a potential candidate for the treatment of obesity and metabolic syndrome. Previous work by our group described that FGF21 is highly induced in liver in response to leucine deprivation and that the transcription factor ATF4 mediates this induction. The present work is the follow-up of this initial observation. To better expose our observations, some results from the thesis of Dr De Sousa-Coelho titled "*Metabolic signalling during nutrient deprivation*" (2012) are included. When this is the case, they are accurately labelled.

This manuscript has been divided in three sections: the role of Rev-Erbα in the induction of *Fgf21* upon leucine deprivation, the role of FGF21 in the metabolic response to leucine deprivation, and the role of FGF21 in the metabolic response to protein restriction. Accordingly, the current study has three general objectives:

- To extend our understanding of the molecular mechanisms that regulate *Fgf21* expression during amino acid deprivation.

- To determine whether FGF21 mediates the metabolic response observed under amino acid deprivation.

- To study the effects of a low protein diet on *Fgf21* expression and its mediated effects on target tissues.

INTRODUCTION

1 FGF21 AS A THERAPEUTIC AGENT FOR METABOLIC DISEASES.

Obesity is a worldwide health problem mainly due to its associated comorbidities, such as non-alcoholic fatty liver disease (NAFLD), certain cancers, insulin resistance, and type 2 diabetes (DMT2), which all reduce life expectancy and life quality.

FGF21 is an atypical member of fibroblast growth factors (FGFs) family that function as a hormone involved in metabolic homeostasis in healthy individuals and considered a promising therapeutic candidate for the treatment of obesity. Since it was described in 2005 as an unexpected regulator of metabolism, extensive investigation has situated FGF21 as a key component of the complex metabolic networks.

Fibroblast Growth Factor 21 (FGF21) increases energy expenditure (EE). It thus has beneficial effects on glucose/lipid homeostasis and on body weight control. In rodent and primate models of metabolic diseases, FGF21 has the capacity to restore glycaemia and lipid profile, and to improve insulin resistance (Kharitonenkov & Shanafelt 2009; Kharitonenkov et al. 2005)

Given the patently beneficial pharmacology of FGF21 in multiple animal models, the prospect of FGF21 emerging as a drug has steadily progressed through the past decade.

It is widely accepted that FGF21 participates in metabolic homeostasis in health but its action takes on greater relevance in metabolic diseases.

To date, the pharmacological use of FGF21 is limited due to its half-life of around 1-2 h. In order to improve the pharmacokinetics, selectivity, and potency of FGF21, several laboratories have focused on designing FGF21 analogs. Two such analogs (LY2405319 and PF05231023) are currently being tested in clinical trials and have yielded similar results: benign toxicology, decreased plasma TGs and LDL cholesterol, increased HDL cholesterol, modest weight loss, elevated adiponectin, reduced insulin levels, and elevated plasma ketones. Surprisingly, no glucose-lowering effect was registered in any trial. This is a major setback since both compounds were assessed mainly as anti-

diabetic drugs. However, the results of these two trials highlight the capacity of FGF21 to ameliorate lipid and cholesterol metabolism (Gaich et al. 2013; Weng et al. 2015; Talukdar, Zhou, et al. 2016).

Given the complex pharmacokinetics properties of FGF21, other approaches such as increasing FGF21 endogenous levels and sensitizing target tissues are being considered.

2 FGF21 SIGNALLING MACHINERY

FGF21 acts as a hormone-like peptide and its signalling pathway requires FGF21 binding to a fibroblast growth factor receptor (FGFR). FGFRs are tyrosine kinase receptors, and seven isoforms have been described (1b, 1c, 2b, 2c, 3b, 3c and 4).

FGFR1c has been defined as the main mediator of FGF21 response *in vivo* (Yang et al. 2012) through an obligate dimerization with the co-receptor β-Klotho (KLB) (Ding et al. 2012). The C-terminus of FGF21 binds with high affinity to KLB (Yie et al. 2012), which enables its interaction with the FGFR. The co-expression of these two receptors determines the sensitivity of a tissue or organ to FGF21 signalling.

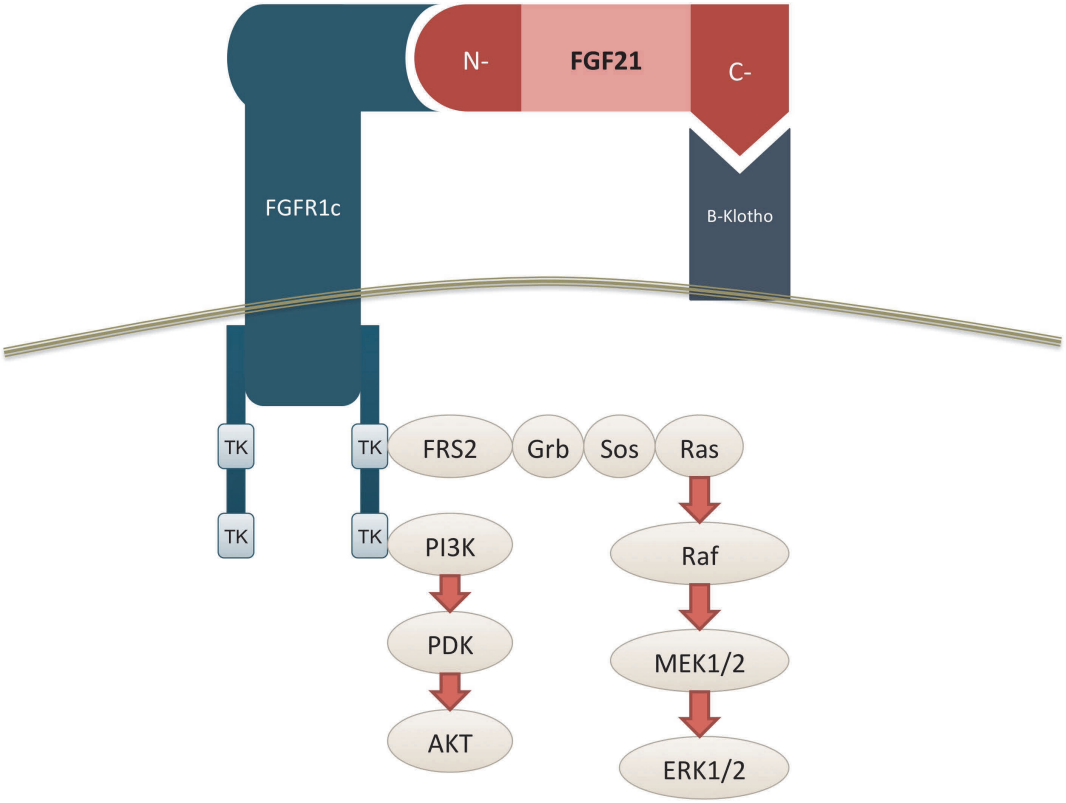

Figure I 1 FGFR1c-FGF21-KLB complex signalling transduction

Regarding the signal transduction pathway, the binding of FGF21 to the FGFR-KLB dimer stimulates the dimerization of FGFR and the autophosphorylation of tyrosines. This action facilitates binding and activation of FGFR substrate 2α

(FRS2α), which transduces the signal to MAPK signalling cascades via the recruitment of several adaptor molecules. The activation of extracellular signal-regulated kinase 1/2 (ERK1/2) and PI3K is critical to induce transcription of early response genes, including c-fos and early growth response 1 (EGR1) resulting in numerous changes in gene expression (Fisher & Maratos-Flier 2016).

However, inhibiting ERK signalling does not always attenuate FGF21 effects, and thus, novel signalling pathways are being studied (Ge et al. 2011).

3 FGF21 REGULATION

3.1 PEROXISOME PROLIFERATOR-ACTIVATED RECEPTOR (PPAR) α, CAMP-RESPONSIVE ELEMENT-BINDING PROTEIN H (CREBH) AND MANY OTHERS

FGF21 was initially described as a protein induced in the liver to regulate metabolic adaptation to long periods of starvation. This mRNA induction is orchestrated through PPARα (Badman et al. 2007; Inagaki et al. 2007; Lundåsen et al. 2007) and CREBH (Kim et al. 2014; Lee et al. 2011). Later, several studies showed that FGF21 expression is regulated not only by fasting but also by other nutritional states. Reviewed in (Pérez-Martí et al. 2016) (Annex 3).

In addition to PPARα and CREBH, FGF21 expression responds positively or negatively to a broad set of factors: the retinoic acid (RA) receptor β (RARβ) (Li et al. 2013), the RA receptor-related orphan receptor α (RORα) (Wang et al. 2010), the glucocorticoid receptor (GR)(Patel et al. 2015), the thyroid hormone receptor β (TRβ) (Adams et al. 2010), the activating transcription factor-4 (ATF4) (De Sousa-Coelho et al. 2012), Rev-erbα (Estall et al. 2009), the farnesoid X receptor (FXR) (Cyphert et al. 2012), the liver X receptor (LXR) (Archer et al. 2012) and the carbohydrate responsive element binding protein (ChREBP) (Iizuka et al. 2009).

Given the complexity and variety of mechanisms that control FGF21 expression, the following sections will focus on its regulation by the two factors of interest in this work, namely ATF4 and Rev-erbα.

3.2 ATF4

3.2.1 Amino Acid Response

Amino acid homeostasis is achieved through the sensing of amino acid and trough the activation of proper signalling pathways. While the mTOR signalling pathway monitors amino acid sufficiency and promotes protein translation and cell growth, among many other processes (Laplante & Sabatini 2013), depletion

of amino acids is sensed by the GCN2/ATF4 pathway, which activates the Amino Acid Response (AAR).

GCN2 kinase is a direct sensor of amino acid supply via the binding of deacylated tRNAs (Qiu et al. 2001). When levels of an indispensable amino acid fall below a threshold, its tRNA becomes deacylated (i.e uncharged). When activated by uncharged tRNAs, GCN2 increases eiF2α phosphorylation (Anthony et al. 2004; Hao et al. 2005) which results in the slowing or stalling of the initiation step of mRNA translation. Hence, phospho-eiF2α reduces general protein synthesis rates.

Paradoxically, the delay in the reinitiation rate promotes an increase in the translation of discrete mRNAs that contain alternative upstream open reading frames in the 5`-UTR region; including that coding for ATF4. Once induced, ATF4 directly or indirectly triggers the transcription of a subset of specific target genes in order to adapt to dietary stress (Harding et al. 2003; Shan et al. 2009).

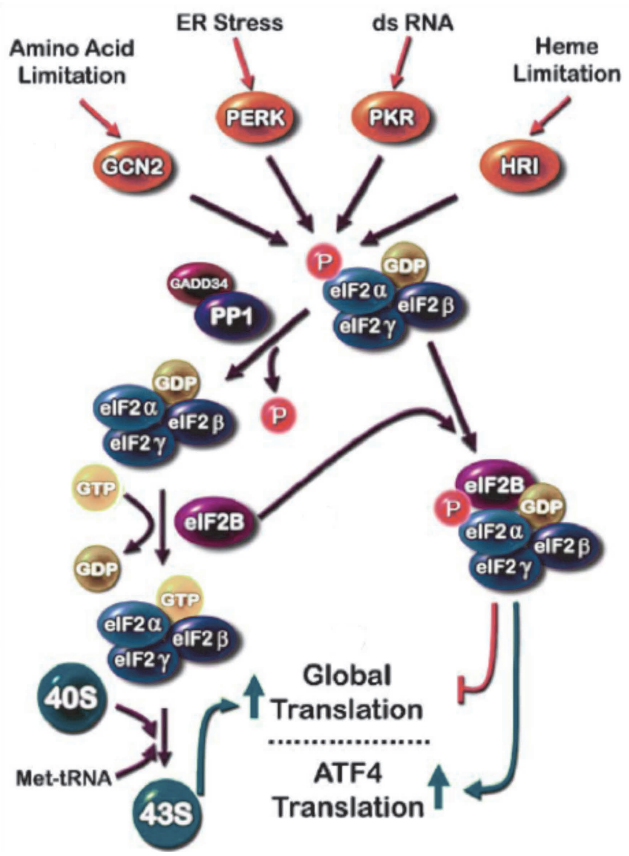

Figure I 2 The AAR pathway. Adapted from (Kilberg et al. 2009)

ATF4 is expressed by enhanced translation from pre-existing mRNA in response to a variety of stress conditions (Vattem et al. 2004). GCN2 is one of four known eIF2α kinases that collectively respond to a wide array of cellular stress. Other members include the protein kinase-like endoplasmic reticulum (ER)-resident kinase (PERK), the heme-regulated kinase (heme-controlled inhibitor, HRI) and the interferon-inducible, double-stranded RNA-activated protein kinase (PKR). Indeed, ER stress (Harding et al. 2000), the presence of dsDNA (Zhang et al. 2001), and heme deficiency (Zhan et al. 2002) each lead to eIF2α phosphorylation that, in turn, promotes increased ATF4 translation.

ATF4 triggers increased transcription by binding to CCAAT-enhancer binding protein-activating transcription factor (C/EBP-ATF) response elements (CAREs). CAREs are composed of a half-site for the C/EBP family and a half-site for the ATF family of transcription factors, also called amino acid response elements (AARE) (Fawcett et al. 1999). Among the known ATF4-activated genes are the transcription factors C/EBPβ (Thiaville et al. 2008), ATF3 (Pan et al. 2007) and C/EBP homology protein (CHOP) (Cherasse et al. 2007), which

then act as ATF4 counter regulatory signals. The numerous dimerization and interacting partners of ATF4 determine its diverse functions (Ameri and Harris, 2008).

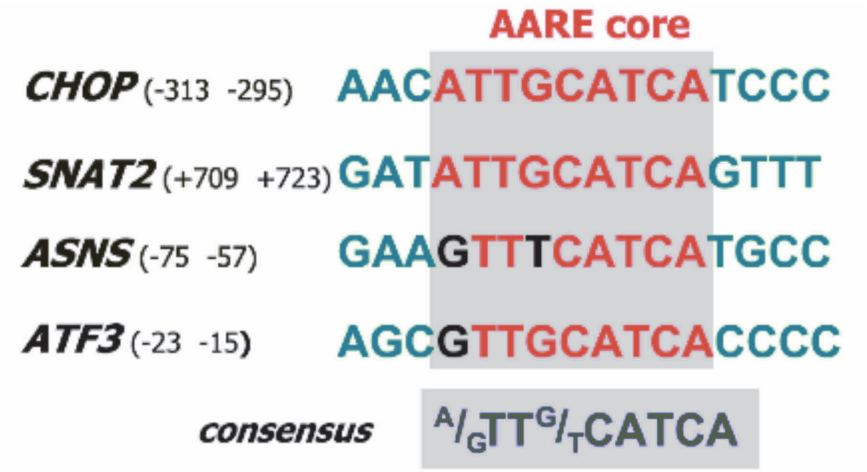

Figure I 3 Genomic C/EBP-ATF composite sites that serve as ATF4-responsive elements for the induction of well-established ATF4 target genes in response to amino acid starvation. Adapted from (Chaveroux et al. 2010)

3.2.2 ATF4 regulation of FGF21

In 2012, our laboratory identified human *FGF21* gene as a target gene for ATF4 and localized two evolutionarily conserved ATF4-binding sequences in the 5' regulatory region of the gene. These sequences are responsible for the ATF4-dependent transcriptional activation of FGF21 (De Sousa-Coelho et al. 2012).

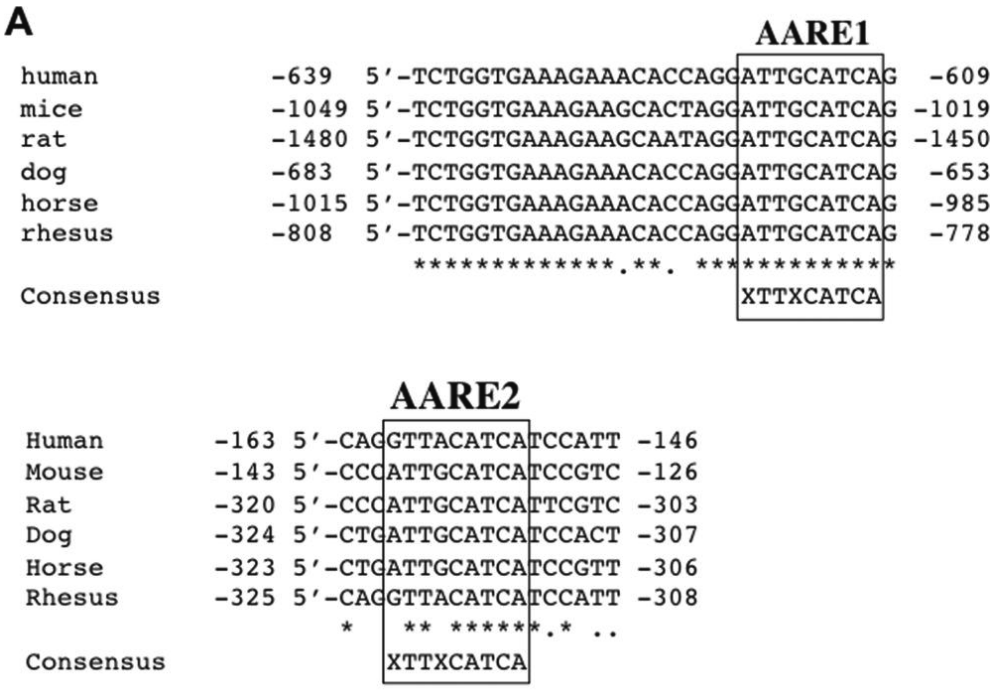

Figure I 4 Alignment of FGF21 promoter sequences of different mammals. Two conserved AAREs are boxed and asterisks indicate the sequence identity. Consensus sequence is shown at the bottom. (De Sousa-Coelho et al. 2012).

Consequently, FGF21 is induced by amino acid deprivation both in mice and in cultured HepG2 cells. This induction occurs in liver but not in other FGF21-expressing tissues such as white adipose tissue (WAT) and brown adipose tissue (BAT).

Later studies confirmed that ER stress inducers, such as tunicamycin (Schaap et al. 2013) and thapsigargin (Wan et al. 2014), as well as methionine restriction (Lees et al. 2014), trigger FGF21 expression through ATF4 activation. In addition, mitochondrial dysfunction leads to ATF4-dependent induction of FGF21 in liver (Kim, Jeong, Kim, et al. 2013) and also in muscle (Kim, Jeong, Oh, et al. 2013; Keipert et al. 2014).

Many lines of data support the notion that FGF21 regulation by ATF4 is a common feature of the response to intracellular stresses. Consequently, other intracellular stress signalling pathways that converge at eIF2α/ATF4, may regulate FGF21 expression.

3.3 REV-ERBα [NUCLEAR RECEPTOR SUBFAMILY 1 GROUP D MEMBER 1 (NR1D1)]

3.3.1 Linking circadian rhythms to metabolism

Circadian rhythmicity is present in almost all physiological processes, including the sleep-wake cycle, the rest-activity cycle, blood pressure, hormone secretion and metabolism. The rhythmicity is driven by the cellular clock machinery, which is comprised of transcription factors that act on one another to generate near-24 hours oscillations. CLOCK and BMAL1 initiate the transcription of their target genes, including *Per* and *Cry* (Schibler & Sassone-Corsi 2002). PER and CRY form heterodimers that translocate to the nucleus to repress their own expression by repressing CLOCK/BMAL1 complex (Kume et al. 1999). This feedback loop takes approximately 24 hours to complete a cycle and constitutes a circadian oscillation of the molecular clock.

Circadian clocks and metabolism are tightly connected, and the nuclear receptor *Rev-erbα,* which functions both as a core repressive component of the cell autonomous clock and as a regulator of metabolic genes, is central to complex interactions between circadian rhythms and metabolism.

Rev-erbα is a core clock component but it also has tissue-specific functions. Interestingly, different mechanisms have been proposed for circadian regulation and tissue-specific actions.

Rev-erbα represses transcription by recruiting the histone deacetylase 3 (HDAC3) and nuclear receptor corepressor (NcoR) (Yin & Lazar 2005). The cofactor heme is a natural Rev-erbα ligand that potentiates the recruitment of NcoR, thereby enhancing the transcriptional repression of its target genes (Yin et al. 2007; Raghuram et al. 2007). Furthermore, overexpression of Delta-aminolevulinate synthase 1 (Alas-1), the rate-limiting enzyme of hepatic heme biosynthesis, also enhances the recruitment of NcoR and HDAC3 (Estall et al. 2009).

The regulation of the clock requires Rev-erbα to bind directly to its classical canonical binding sequences, namely ROREs and RevDR2 (Harding & Lazar

1995; Giguere et al. 1994), where it competes with activating ROR transcription factors.

In contrast, it has recently been described that Rev-erbα regulates metabolic genes primarily by recruiting the HDAC3 corepressor to sites to which it is tethered by cell type-specific transcription factors. (Zhang et al. 2015)

Therefore, competition between Rev-erbα and RORs provides a universal mechanism for molecular clock regulation across all tissues, whereas Rev-erbα uses tissue-specific lineage-determining factors to direct metabolism in circadian cycles in function of the specific needs of that tissue.

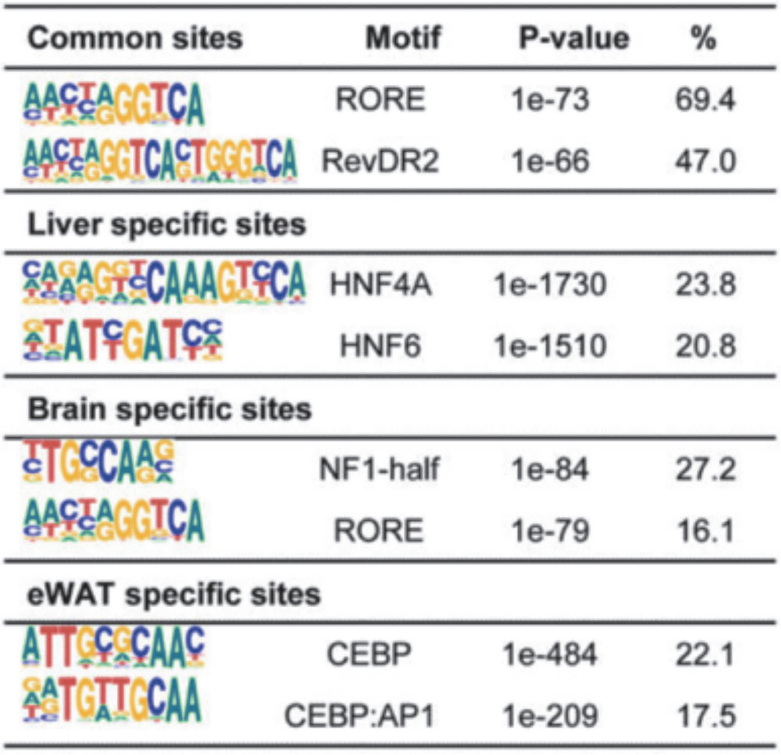

Figure I 5 Most significantly enriched motifs by ChIP seq in different tissues. (Zhang et al. 2015)

In the liver, hepatocyte nuclear factor 6 (HNF6) and hepatocyte nuclear factor 4 (HNF4) are the main Rev-erb α tethering factors. However, many other transcription factors, such as CEBP, NFY, PPAR and ATF4, can also tether Rev-erb α to chromatine (Zhang et al. 2016).

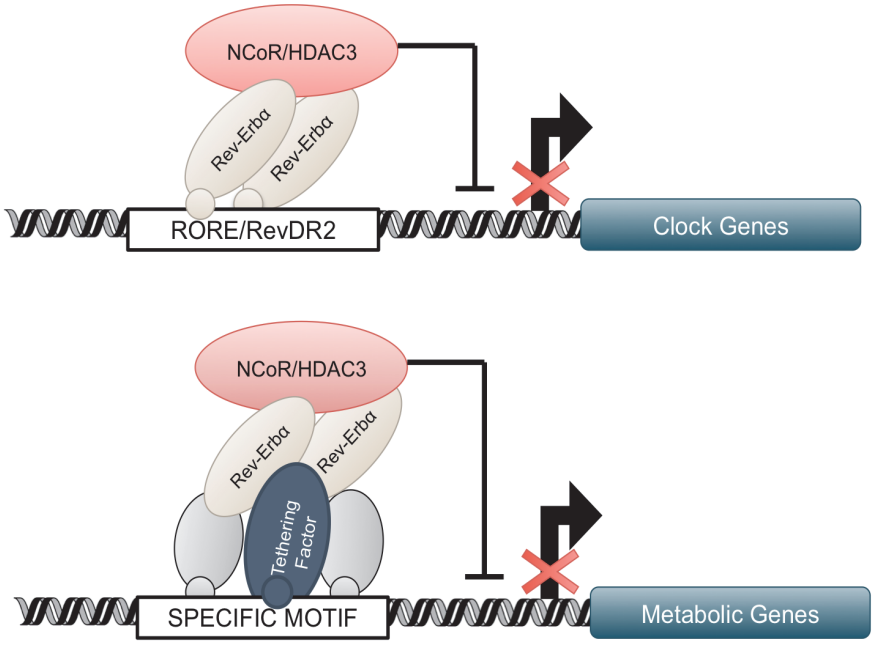

Figure I 6 Model of different mechanisms of Rev-erbα function

3.3.2 Rev-erbα regulation of FGF21

Since Rev-erb aplha connects the circadian clock to liver metabolism (Zhang et al. 2016) and *Fgf21* presents a marked circadian expression pattern, it is feasible that these two molecules are linked. In this regard, *FGF21* levels inversely correlate to the expression pattern of *Rev-erb*α and *ALAS-1* in liver (Kaasik & Lee 2004; Oishi et al. 2008).

In fact, peroxisome proliferator-activated receptor gamma coactivator 1-α (PGC-1α) negatively regulates *Fgf21* hepatic expression modulating the heme/Rev-erbα axis (Estall et al. 2009). PGC-1α not only directly modulates the expression of Rev-erb α but also increases heme levels in response to hormonal cues. Furthermore, heme feeds back to inhibit PGC-1α expression through the activation of Rev-erbα (Wu et al. 2009).

The mechanism proposed for Rev-erbα repression of *Fgf21* consists of a repressor complex that includes LXRβ, RORα, Rev-erb α and HDAC3 onto the proximal *Fgf21* promoter region, although the direct binding sites have yet to be determined (Archer et al. 2012).

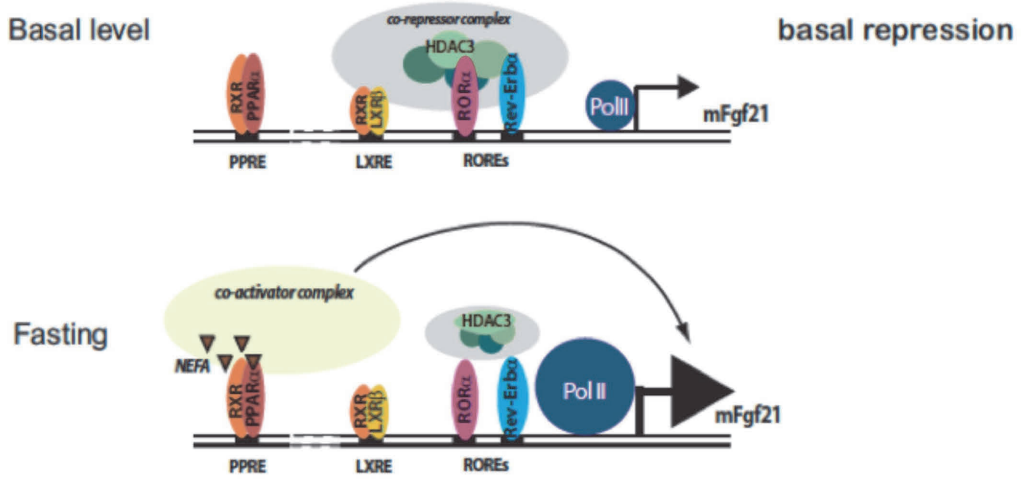

Figure I 7 Model of the repressor complex onto the FGF21 promoter. Adapted from(Archer et al. 2012)

Interestingly, and in disagreement with this model, ChIP-seq results from Mitchell Lazar's lab (GSE67973) point to Rev-erbα binding to DNA regions that contain the described AARE1 and AARE 2 of the *Fgf21* promoter (De Sousa-Coelho et al. 2012).

4 FGF21 IN LIVER

4.1 LIVER IS THE PRINCIPAL FGF21 PRODUCER

FGF21 is expressed and produced by multiple tissues. However, under normal physiological conditions, all circulating protein appears to derive from the liver (Markan et al. 2014). In liver, FGF21 expression is induced in response to stress. FGF21 was initially described as a fasting-adaptation hormone, since its hepatic production coupled to plasma levels is dramatically increased during prolonged fasting (Inagaki et al. 2007; Potthoff et al. 2009).

It is now known that hepatic FGF21 expression is also induced in other liver-stress circumstances such as in obesity, specific nutritional conditions, liver injury, viral infection, chemical insult, hepatosteatosis, steatohepatitis, NAFLD, cirrhosis, and liver cancer (Dushay et al. 2010; Dasarathy et al. 2011; Domingo et al. 2010; Zhang et al. 2008; Yang et al. 2013).

4.2 AUTOCRINE EFFECTS

Hepatic overexpression of FGF21 triggers ketogenesis, gluconeogenesis, and FA oxidation (FAO) and suppresses lipogenesis in the liver (Dasarathy et al. 2011; Fisher et al. 2011). However, the autocrine effects of FGF21 on this organ are still under debate. FGFR4 is the predominant isoform in the liver, but the FGFR4-KLB complex cannot activate the FGF21 transduction pathway (Yang et al. 2012). In contrast, hepatic FGFR1 levels are low, and it is unclear whether they are enough to ensure FGF21 signalling.

Later studies reported contradictory results regarding the role of FGF21 in ketogenesis, thereby suggesting that the physiological effects of this molecule may differ from the pharmacological ones (Hotta et al. 2009).

4.3 FGF21 AS A HEPATOKINE

FGF21, as well as FGF19 and FGF23, lacks heparin binding domain. This detail allows FGF21 to be secreted and act as a hormone.

As a hepatokine, FGF21 affects WAT and BAT, tissues in which it regulates lipid metabolism—mainly by inducing lipolysis and browning and by increasing thermogenic capacity (De Sousa-Coelho et al. 2013; Hotta et al. 2009). FGF21 also exerts action in the brain, where it is able to reduce physical activity, induce torpor, and regulate circadian behaviour (Bookout et al. 2013; Ishida 2009). In conclusion, all data indicate that FGF21 is produced and secreted by the liver when the function of this organ is compromised by stress and that it is responsible for restoring and maintaining metabolic homeostasis.

5 FGF21 IN ADIPOSE TISSUE

5.1 SHADES OF FAT: WHITE, BEIGE, BROWN

WAT comprises unilocular adipocytes and its principal function is to store lipids, which prevents their lipotoxic accumulation in other organs. Additionally, WAT can act as an endocrine organ by signalling to other tissues through the so-called adipokines. The lipid storage capacity of WAT is adaptable, but when its maximum capacity is exceeded, it cannot properly store these fats or act as an endocrine organ. This impairment of WAT function can result in the accumulation of lipids in peripheral tissues and can contribute to insulin resistance and dyslipidemia (Virtue & Vidal-Puig 2010).

The primary function of BAT is to produce heat in order to maintain core body temperature in response to cold stress. Multilocular brown adipocytes contain large numbers of mitochondria enriched in uncoupling protein 1 (UCP1), which uncouples substrate oxidation from ATP, thereby producing heat. Hence, BAT has potent machinery for oxidising metabolic substrates, and accordingly, efficient mechanisms for lipid and glucose uptake and catabolism.

Persistent thermogenic activation (e.g. cold stress) causes the upregulation of the genes encoding UCP1, mitochondrial oxidative machinery, and lipid catabolism and uptake. Moreover, long-term thermogenic induction leads to the enlargement of BAT mass through hyperplasia and hypertrophy.

As part of the same response, the so-called beige or “brite” (brown in white) cells are recruited in WAT in a process known as browning of WAT (Young et al. 1984). Beige adipose tissue (BeAT) is composed of UCP1-expressing adipocytes with great capacity for thermogenic stimulation, UCP1 expression induction and uncoupled respiration. Thus, stimulated beige adipocytes resemble brown adipocytes in terms of uncoupled respiration and UCP1 expression (Wu et al. 2012).

Thermogenic activation leads BAT/BeAT to increase EE and act as a lipid and glucose sink, with a significant impact on whole body glucose homeostasis and body weight.

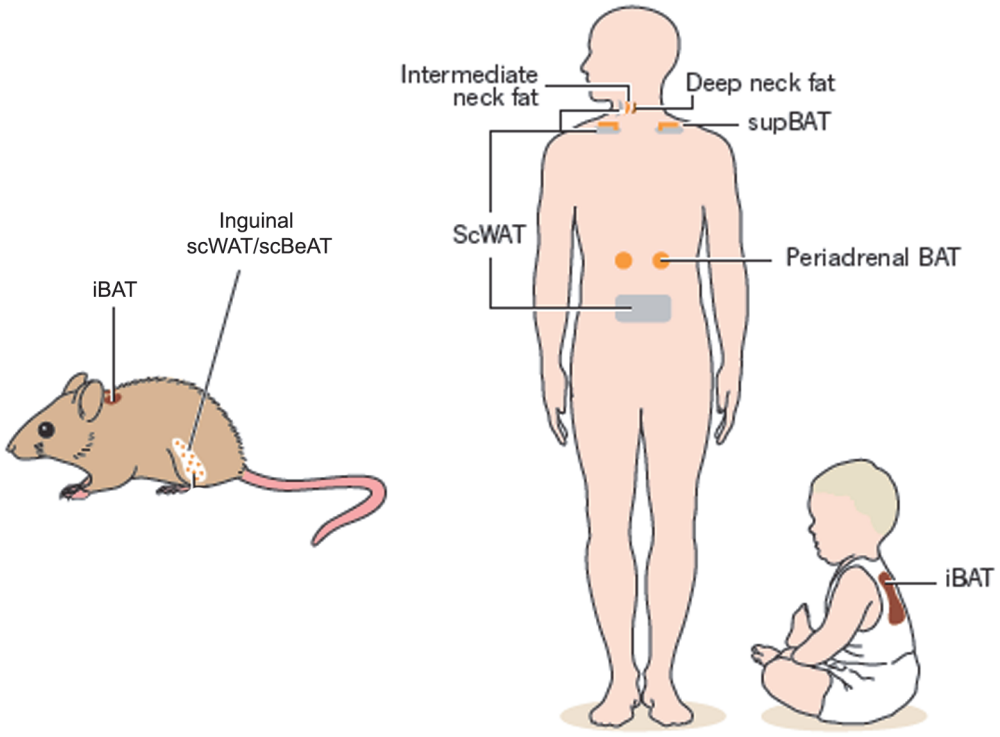

Figure I 8 BAT and BeAT localization. iBAT, interscapular BAT. scWAT, subcutaneous WAT. scBeAT, subcutaneous BeAT. supBAT, supraclavicular BAT. Adapted from (Peirce et al. 2014)

5.2 TARGETING BAT FOR THE TREATMENT OF METABOLIC DISEASES

The recent discovery that adult humans have BAT (Hany et al. 2002; Nedergaard et al. 2007; Virtanen et al. 2009; van Marken Lichtenbelt et al. 2009; Cypess et al. 2009) has paved the way for new therapeutic strategies and placed BAT in the spotlight of the research into metabolic diseases.

Thermogenesis is an extremely high energy-consuming process. Consequently, significant attention has been directed toward the activation of BAT as a potential strategy for promoting EE and protecting against obesity (Cereijo et al. 2015; Hankir et al. 2016; Peirce et al. 2014).

Given the roles of BAT in the regulation of circulating lipids and glucose, it has been argued that this tissue is also a target for the treatment of diabetes

mellitus II, independently of weight loss. (Peirce & Vidal-Puig 2013; Kajimura et al. 2015)

5.2.1 BAT/BeAT activators

Thermogenic activation is mediated mainly by the activation of the sympathetic nervous system (SNS). The release of norepineprhine by sympathetic nerve endings activates β-adrenergic receptors, therby inducing the thermogenic response.

Pharmacological activators of the SNS have succeeded in inducing weight loss but their strong cardiovascular side effects outweigh their benefits. Thus, the lack of sensitivity shown by sympathomimetics drugs, make them unsuitable as a treatment option. The identification of new BAT/BeAT activators that act independently or in association with the SNS may provide more specific ways to activate BAT and bypass the cardiovascular effects.

In addition to the SNS, the thyroid system is the other major player in BAT activation. Triiodothyronine (T3) is converted to thyroxine (T4) in BAT by type II thyroxine 5'-deionidase (Dio2), which activates the thermogenic programme and upregulates UCP1. The SNS and thyroid system are complexly linked in a complex manner since *Dio2* is controlled by norepinephrine and, T3 stimulates sympathetic outflow in the hypothalamus (Lopez et al. 2010).

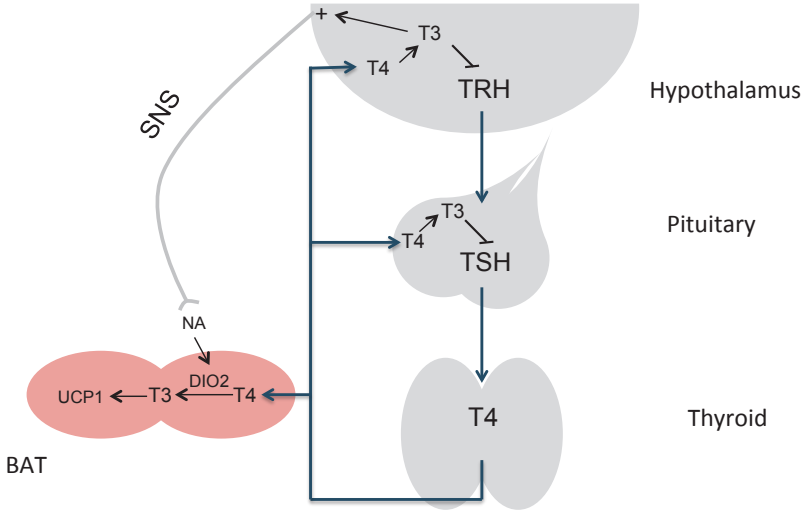

Figure I 9 Sympathetic nervous system (SNS) and thyroid system crosstalk. TRH: thyrotropin-releasing hormone, TSH: thyroid-stimulating hormone, NA: noradrenaline, BAT: brown adipose tissue, UCP1: uncoupling protein 1, DIO2: type II thyroxine 5'-deionidase

The hypothalamic–pituitary–adrenal axis (HPA), which regulates processes in response to stress, is also involved in thermogenesis activation. The paraventricular nucleus of the hypothalamus synthesises and secretes the neuropeptide corticotropin releasing factor (CRF) which acts on pituitary cells to stimulate the secretion of adrenocorticotropic hormone (ACTH). The i.c.v administration of CRF elicits sustained increases in BAT sympathetic nerve activity, BAT temperature, expired CO_2, and heart rate (Cerri & Morrison 2006).

In addition to the SNS, the HPA axis and the thyroid system, several new players act as BAT activators. Vitamin A, and more specifically, its metabolites retinal and retinoic acid, are modulators of BAT thermogenesis (Kiefer et al. 2012).

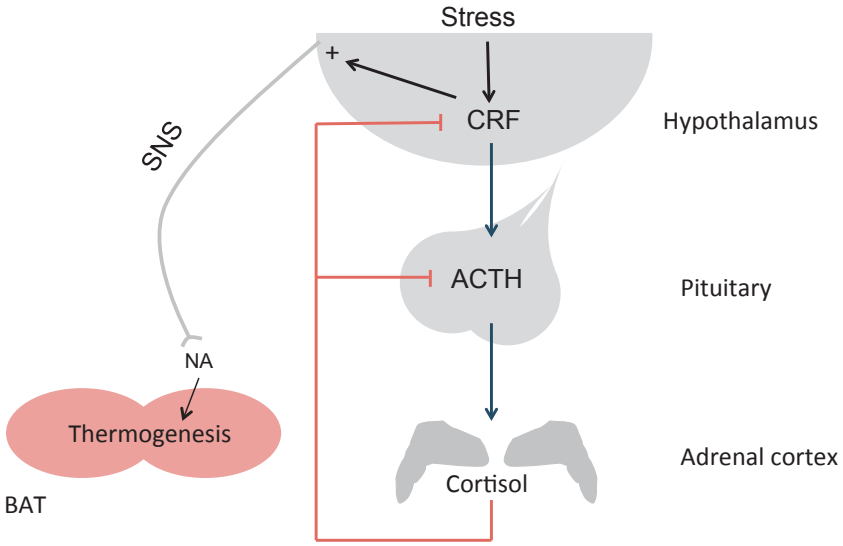

Figure I 10 Hypothalamic–Pituitary–Adrenal axis (HPA) and Sympathetic Nervous System (SNS) crosstalk. CRF: corticotropin releasing factor, ACTH: adrenocorticotropic hormone, NA: noradrenaline, BAT: brown adipose tissue, UCP1: uncoupling protein 1, DIO2: type II thyroxine 5'-deionidase

Liver and BAT activity are tightly connected. Bile acids released after meals induce *Dio2* in BAT leading to a local increase in T3, which in turn induces *Ucp1* expression (Watanabe et al. 2006). FGF21 is another key hepatic factor that regulates BAT activity. The mechanisms by which FGF21 exerts this function are discussed in section 5.4 of the introduction.

Exercise increases BAT activity and the release of myokines such as irisin, thus indicating a connection between muscle and BAT. In addition, irisin is a potent stimulator of browning of WAT (Bostrom et al. 2012).

The heart is also a source of BAT activators, namely atrial natriuretic peptide (ANP), ventricular natriuretic peptide (VNP) and cardiotrophin-1, which all enhance BAT thermogenesis, as well as browning of WAT (Bordicchia et al. 2012; Moreno-Aliaga et al. 2011).

Unexpectedly, recent findings report that immune cells are BAT activators. Activated macrophages regulate BAT thermogenesis via the local release of cathecolamines (Nguyen et al. 2011), and the adipose-resident invariant natural killer T cells release FGF21, thus causing browning of WAT (Lynch et al. 2016).

Several thermogenesis regulators act both in the hypothalamus and directly in BAT. As an example, bone morphogenic protein-8b sensitises BAT to SNS stimulation but also modulates sympathetic outflow (Whittle et al. 2012).

Finally, ion channels such as transient receptor potential melastin 8 (TRPM8) and transient receptor potential vainilloid-4 (TRVP-4), participate in the regulation of BAT activation. TRPM8 agonist (e.g., menthol) induces BAT activity and pharmacological inhibition of TRVP leads to browning of WAT(Ma et al. 2012; Ye et al. 2012) .

5.3 FGF21 IN WAT

Adipose tissue is the main target tissue of FGF21 and the major mediator of its beneficial effects. While the physiological effects of FGF21 during fasting remain elusive, most data on its signalling in WAT derive from studies in which it was pharmacologically administered or overexpressed in obese mice. Nevertheless, FGF21 shows paradoxical actions on WAT depending on its source. *Fgf21*-overexpressing mice show induced lipolysis (Inagaki et al. 2007; Li et al. 2009). In contrast, *Fgf21*-knockout mice present enhanced lipolysis in late fasting (Hotta et al. 2009). In addition, while FGF21 suppresses lipolysis in

mouse and human adipocytes (Arner et al. 2008), it is induced by peroxisome proliferator activating receptor g (PPARg) in WAT upon feeding, thus stimulating adipogenesis (Dutchak et al. 2012; Muise et al. 2008).

Regarding glucose metabolism, FGF21 induces glucose uptake in 3T3L1 adipocytes by increasing glucose transporter 1 (GLUT1) independently of insulin action (Kharitonenkov et al. 2005; Ge et al. 2011). Moreover, later studies showed increased glucose uptake in both WAT and BAT of lean mice infused with FGF21 and fed a chow diet (Camporez et al. 2013).

In summary, in WAT, FGF21 induces genes involved in glucose uptake, lipogenesis and lipolysis, depending on the metabolic state of the adipocytes. This apparently contradictory effects may be due to compensatory effects of genetic modifications in mice, different nutritional status and different FGF21 concentrations reached between pharmacological administration and physiological secretion.

WAT is not only a FGF21 target tissue but also a mediator of the effects of this growth factor. In this regard, the glucose- and insulin-sensitizing effects of FGF21 require the production and secretion of adiponectin from WAT. Accordingly, FGF21 stimulates this mechanism in rodents, and adiponectin-knockout mice fail to reproduce the sensitizing effects of FGF21 (Lin et al. 2013). Similarly, FGF21 also reduces the levels of the sphingolipid ceramide. Sphingolipid ceramides have been associated with insulin resistance caused by lipotoxicity. By inducing adiponectin secretion, FGF21 diminishes the accumulation of ceramides in obese animals (Holland et al. 2013). Overall, despite some contradictory effects of FGF21 in adipose fat depots, adipose tissue is considered indispensable for the physiological and pharmacological effects of FGF21.

Finally, FGF21 induces the expression of Ucp1, thus producing browning of WAT in an autocrine, paracrine or endocrine fashion (De Sousa-Coelho et al. 2013; Fisher et al. 2012).

5.4 FGF21 IN BAT

BAT is a FGF21 target tissue since it expresses FGFR1 and KLB; however, it is also a source of FGF21. In BAT, FGF21 stimulates glucose uptake and thermogenesis through the induction of UCP1 in the interscapular depot in an autocrine and paracrine fashion (Hondares et al. 2011). Upon cold exposure, FGF21 expression is increased in BAT and other cold-sensitive fat depots in the β-adrenergic/ATF2-dependent pathway (Fisher et al. 2012; Hondares et al. 2011; Chartoumpekis et al. 2011). In this regard, Fgf21-deficient mice respond poorly to cold exposure and show greater shivering (Fisher et al. 2012). The mechanisms underlying the action of FGF21 on BAT/WAT are still not well understood. Part of the FGF21-induced activation of the thermogenic program is driven by PGC-1α, as FGF21 increases the protein levels of this molecule. Similarly, Pgc-1α-knockout mice show an impaired response to FGF21 (Fisher et al. 2012).

Furthermore, hepatic FGF21-mediated thermogenesis has also been described in response to maternal milk consumption in neonatal pups (Hondares et al. 2010), and also in situations of metabolic stress, for example, as described in this thesis, upon amino acid restriction (De Sousa-Coelho et al. 2013). These observations suggest that the hepatic FGF21-mediated increase in thermogenic capacity is an adaptive response to metabolic stress.

It has been proposed that the effect of FGF21 on EE and weight loss may be due to an increased thermogenic capacity of BAT and WAT (browning). However, recent experiments in Ucp1–null mice and interscapular BAT-excised mice show that when FGF21 is administered pharmacologically, UCP1 is not required for the improvement of the glucose, cholesterol, and free FA profile. Nonetheless, the increment in metabolic rate associated with the administration of FGF21 is diminished in these mice (Samms et al. 2015; Véniant et al. 2015; Bernardo et al. 2015). These data suggest that the metabolic benefits of FGF21 are partly UCP1-independent.

6 FGF21 IN OTHER TISSUES

6.1 FGF21 IN SKELETAL MUSCLE

FGF21 expression in muscle was first described in Akt1 transgenic mice in which the mRNA and serum levels of FGF21 were induced (Izumiya et al. 2008). In normal conditions, basal expression of FGF21 in skeletal muscle is low but its expression is increased by insulin (Izumiya et al. 2008; Hojman et al. 2009), exercise (Kim, Kim, et al. 2013), mitochondrial myopathies (Tyynismaa et al. 2010), impaired mitochondrial FAO (Vandanmagsar et al. 2016), muscle-specific autophagy deficiency (Kim, Jeong, Oh, et al. 2013) and transgenic overexpression of Akt1, perilipin-5 (Harris et al. 2015) or Ucp1 (Keipert et al. 2014) in skeletal muscle. The induction of FGF21 in muscle due to a metabolic dysfunction is driven by the transcription factor ATF4, which is activated by endoplasmic reticulum (ER) stress. The AMPK and PI3K/Akt1 signalling pathways are also able to increase FGF21 expression (Vandanmagsar et al. 2016).

The impact of FGF21 on skeletal muscle is not clear, as the expression levels of KLB do not seem to be sufficient to respond to FGF21. Several studies suggest that FGF21 administration can improve glucose uptake *in vitro* (Lee et al. 2012; Mashili et al. 2011), and a model of impaired mitochondrial FAO has recently shown the same *in vivo* (Vandanmagsar et al. 2016).

In contrast, the role of FGF21 as a myokine is more evident. In the abovementioned conditions where FGF21 is overexpressed in muscle, the plasma levels of this growth factor also increase. The metabolic effects of this increase include the reduction of fat content in liver, increased FAO, resistance to a HFD and browning of WAT. These results show that FGF21 can act as a myokine when secreted in response to muscle stress and that it exerts its effects on metabolism in an endocrine fashion.

6.2 FGF21 IN HEART

Initially, the heart was discarded as a target tissue or source of FGF21 due to the low levels of FGF21 and KLB mRNA detected in this organ. However, later studies showed that FGF21 is expressed and secreted by cardiac cells in response to various stress conditions, including obesity, type 1 diabetes, fasting, ER stress, inflammation, infarct or hypertrophy, and some cardiovascular diseases (Brahma et al. 2014; Planavila et al. 2015). In the heart, FGFR1 and KLB have been detected in cardiac cells, where FGF21 exerts protective effects in an autocrine and endocrine fashion. The mRNA expression of FGF21 in these cells is driven by the transcriptional activation of Sirtuin1 (Sirt1) – PPARα (Planavila et al. 2015) in response to cardiac insults; however, it can also be regulated by ATF4, especially when FGF21 induction is caused by ER or oxidative stress (Brahma et al. 2014; Dogan et al. 2014).

It is now well established that FGF21 plays a key role in cardiac remodelling and pathophysiology. FGF21 protects cardiomyocytes from hypertrophy through a mechanism that involves the activation of the cAMP Responsive Element Binding protein (CREB), the induction of PGC-1α expression, and the reduction of the NF-kB pro-inflammatory pathway (Planavila et al. 2015). Cardiac FGF21 also induces the expression of anti-oxidant genes such as Ucp3 and superoxide dismutase (Sod2), thus preventing the production of reactive oxygen species (ROS) in cardiac cells and oxidative stress in the heart (Planavila et al. 2014). In an autocrine fashion, FGF21 modulates cardiac lipid homeostasis (Brahma et al. 2014) and protects against diabetes-induced cardiomyopathy by activating the ERK-p38MAPK-AMPK pathway (Planavila et al. 2015). Finally, as an endocrine peptide, FGF21 can also inhibit cardiomyocyte apoptosis, thus reducing damage to the heart (Liu et al. 2013; Joki et al. 2015).

6.3 FGF21 IN THE CENTRAL NERVOUS SYSTEM

FGF21 has the potential to act in the central nervous system (CNS) since FGFRs are widely expressed in this tissue and KLB is specifically expressed in the suprachiasmatic nucleus, the dorsal vagal complex of the hindbrain, the

area postrema, the nucleus tractus solitari, the nodose ganglia, and the paraventricular nucleus (Fon Tacer et al. 2010; Bookout et al. 2013; Liang et al. 2014). Immunoblotting experiments have revealed that FGF21 is expressed in several regions of the brain, such as the substantia nigra, striatum, hippocampus, and cortex (Makela et al. 2014); however, this growth factor also crosses the blood brain barrier and is present in the cerebrospinal fluid in a linear relationship with serum levels (Tan et al. 2011). FGF21 modulates circadian rhythm and fertility (Bookout et al. 2013; Owen et al. 2013), but current data point to the CNS as a mediator of the effects of FGF21 on EE and browning (Douris et al. 2015a). However, in all cases, the presence of KLB appears to be required for FGF21 to exert its effects. This observation thus indicates that this growth factor is an endocrine signal. Regarding the effects of FGF21 on EE and browning, experiments with diet-induced obese (DIO) mice show that the lack of KLB in the CNS abrogates all the effects of FGF21 on body weight, insulin sensitivity, metabolic regulation in liver, WAT, and BAT. These data suggest that direct signalling in the CNS causes an increase in the sympathetic outflow.

In the hypothalamus, FGF21 affects the expression of CRF. Intracerebroventricular injection of FGF21 in Fgf21-KO mice restores the metabolic effects of FGF21 essentially through the CRF and the activation of CREB, which finally enhances hepatic gluconeogenesis and sympathetic nerve activity in BAT (Liang et al. 2014; Owen et al. 2014; Arase et al. 1988). According to that, lack of KLB in the brain blunts these effects (Liang et al. 2014; Owen et al. 2014; Douris et al. 2015a). Finally, treatment with the b-blocker propranolol diminishes the effects of FGF21 when it is centrally administered but not when delivered peripherally (Douris et al. 2015b).

Given the wide range of biological processes regulated by the CNS and the capacity of FGF21 to act in the brain, it is likely that future studies will reveal new actions of FGF21 signalling through the CNS.

6.4 FGF21 IN PANCREAS

FGF21 is highly expressed in the pancreas and has protective effects against cerulein-induced pancreatitis (Johnson et al. 2009). Supporting data show that FGF21-deficient mice are more susceptible to damage, and FGF21-overexpressing mice are partly protected. In addition, FGF21 may be involved in enhancing islet engraftment (Uonaga et al. 2010) and in the preservation of b-cell function and survival (Wente et al. 2006). Another point is that KLB expression is critical for these beneficial effects, but the expression of KLB is reduced when islets are treated with high glucose concentrations (So et al. 2013). In the pancreas, FGF21 increases insulin content and glucose-dependent secretion and inhibits glucagon release in isolated islets (Wente et al. 2006).

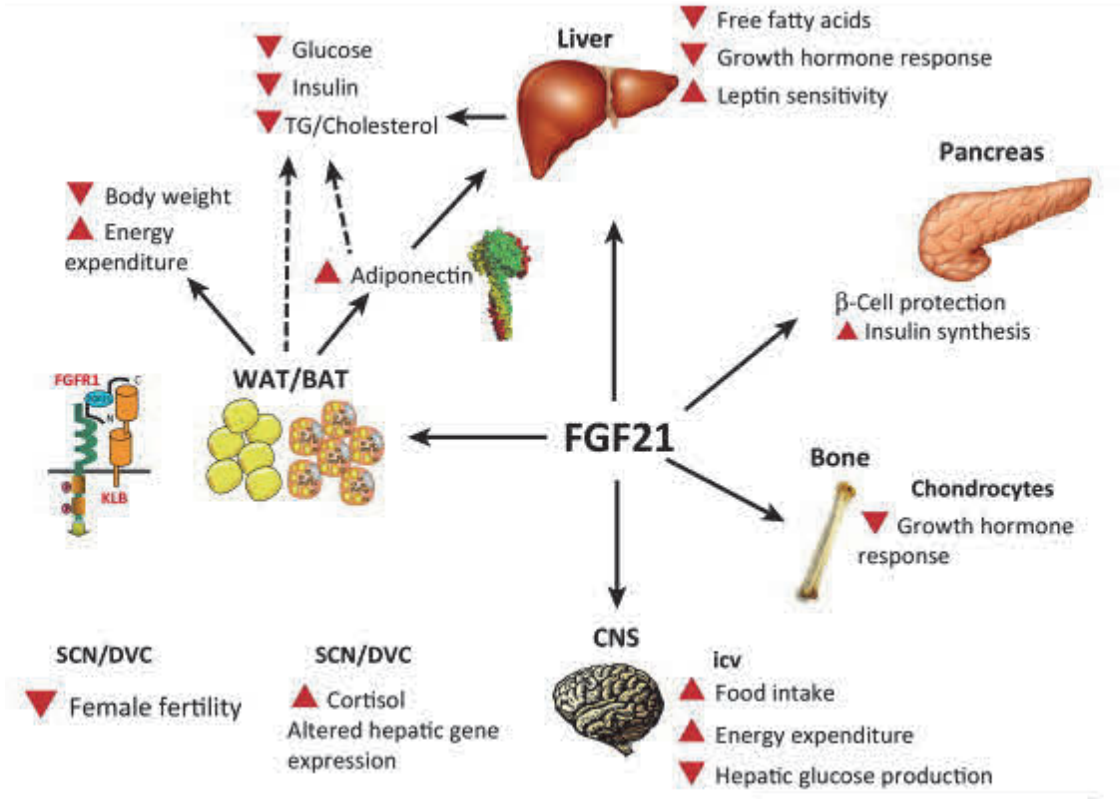

Figure I 11 Metabolic effects of exogenous FGF21. (Gimeno & Moller 2014)

7 OTHER EFFECTS OF FGF21

In addition, and consistent with its metabolic benefits, FGF21 transgenic overexpression extends lifespan in mice. The authors of that study proposed that inhibition of the GH/IGF-1 signalling pathway would explain life extension in Fgf21 transgenic mice. Furthermore, microarray analysis showed that FGF21 modulates gene expression in the liver in a similar manner to caloric restriction (which is known to extend lifespan in mammals). These data suggest that FGF21 extends lifespan by acting as a selective caloric restriction mimetic in the liver (Zhang et al. 2012).

Interestingly, FGF21 appears to be not only a metabolic regulator but also a nutrient intake and taste regulator. Both pharmacologic administration and hepatic secretion of FGF21 produce a satiety signal that suppresses the intake of "sweets" (von Holstein-Rathlou et al. 2016; Talukdar, Owen, et al. 2016). In addition, two genome-wide meta-analyses associated genetic variations in a locus including Fgf21 with significant differences in macronutrient intake (Tanaka et al. 2013; Chu et al. 2013).

While FGF21 boasts numerous beneficial effects, a major adverse effect is a decrease in bone mass. Both, genetic overexpression of *Fgf21,* and pharmacological administration of this molecule lead to the inhibition of osteoblastogenesis and the stimulation of adipogenesis. In contrast, the absence of *Fgf21* leads to a high bone mass phenotype. The mechanism underlying bone mass loss is the potentiation of PPARγ activity (Wei et al. 2012). Although this non-desirable effect has been described only in rodents, it has to be taken into account when considering FGF21 as a potential drug candidate.

8 NUTRITIONAL REGULATION OF FGF21

Nutritional signals play an important role in controlling gene expression in mammals. Macronutrients (carbohydrates, fatty acids (FAs), proteins), micronutrients (minerals and vitamins), and some bioactive dietary compounds have the capacity to regulate gene expression and thus metabolic homeostasis. In this context, it has been described that endogenous FGF21 levels are regulated by various nutritional challenges.

Carbohydrates ingestion modulates FGF21 expression. A dextrose enriched diet induce hepatic FGF21 expression in mice (Hao et al. 2016), and human FGF21 promoter responds to xylitol and fructose through ChREBP. In addition, humans and rodents ingestion of fructose but not glucose leads to increased FGF21 serum levels after an acute load (Dushay et al. 2015) .

High-fat diets (HFDs) induce FGF21 resistance (Fisher et al. 2010) although there is still some controversy due to the variety of fatty acids included in the diet. In vitro, oleate, linolate and trans-10, cis-12 conjugated linoleic induce FGF21 expression and secretion (Yu et al. 2011; Mai et al. 2009). Moreover, in neonatal mice, initiation of suckling induces hepatic FGF21 expression mainly due to high FA content of maternal milk (Hondares et al. 2010). PPARα and CREBH are the mediators of FGF21 induction in response to fatty acids.

Amino acid-deficient and low protein diets (LPD) diminish aminoacidemia and trigger AAR, thereby resulting in elevated FGF21. This will be the focus of the results and discussion of the present work.

Finally, bioactive dietary compounds such as polyphenols induce FGF21 expression in liver and improve its signalling. Nevertheless, mechanisms driving these effects need further studies (Monika & Geetha 2015; Yu et al. 2013)

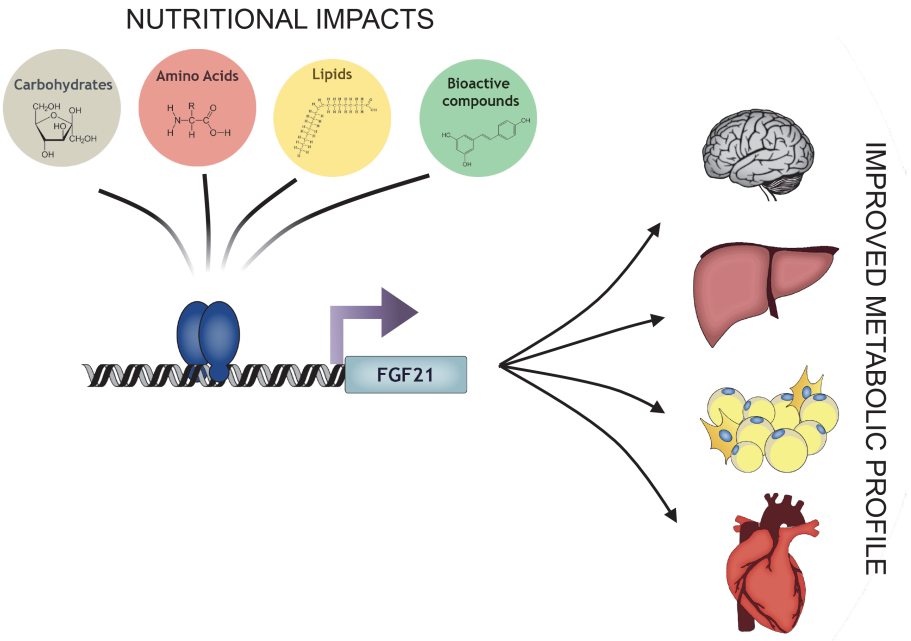

Figure I 12 FGF21 is regulated by different nutritional impacts to adapt the metabolic profile.(Pérez-Martí et al. 2016)

9 AMINO ACID DEFICIENCY

In eukaryotic cells, amino acids are the building blocks for the synthesis of proteins and other biomolecules. Furthermore, amino acids are required as energy supply and also as signalling molecules.

Multicellular organisms are unable to synthesise all amino acids. In this regard, nine essential amino acids (valine, isoleucine, leucine, lysine, methionine, phenylalanine, threonine, histidine and tryptophan) cannot be synthesised de novo or at least not in sufficient amounts to meet cellular needs. Furthermore, under certain conditions, non-essential amino acids may become indispensable (the so-called conditionally essential amino acids). All essential amino acids must be supplied by diet. Moreover, there is no dispensable amino acid store in mammals. Thus, when necessary, the organism has to hydrolyse muscle protein to produce free amino acids.

In mammals, the blood concentration of amino acids can be affected by nutritional or pathological situations. Protein undernutrition caused by a low protein diet or imbalanced diets (which are common in mammals confronted with deficient sources of selected amino acids like legumes, grains or corn) strongly affects aminoacidemia (Placko & Graham 1974; Grimble & Whitehead 1970). In addition, pathological situations involving various forms of stress such as trauma, thermal burn, sepsis and fever, can lead to a negative nitrogen balance.

At the cellular level, the size of the pool of each amino acid is the result of a balance between inputs and outputs. The metabolic outputs for amino acids are protein synthesis and amino acid degradation, whereas the inputs are de novo synthesis (for non-essential amino acids), protein breakdown and dietary supply.

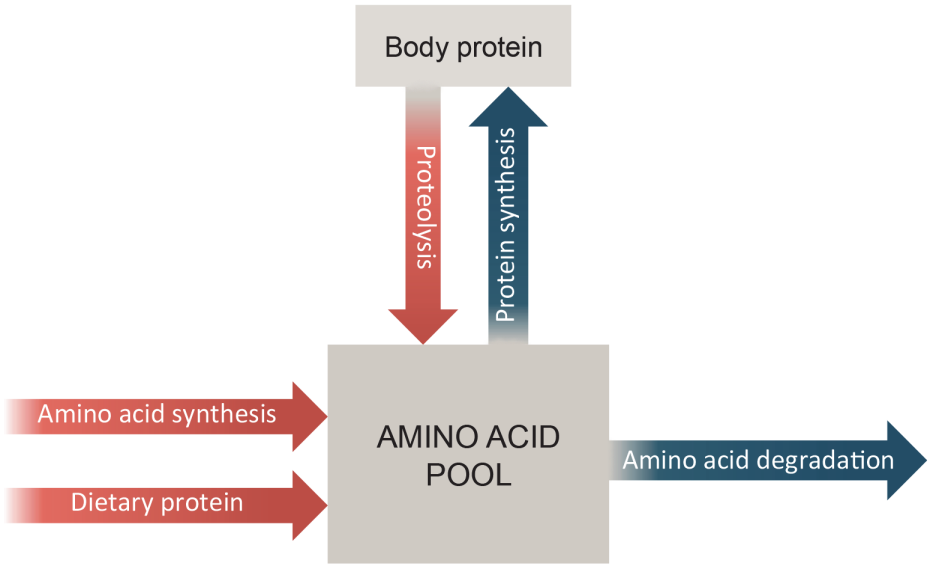

Figure I 13 Biochemical systems involved in the homeostasis of proteins and amino acids.

Dietary amino acid availability alters metabolic pathways beyond protein homeostasis since there is a link between dietary amino acids and lipid metabolism.

Leucine deprivation causes dramatic changes in lipid metabolism. In liver, leucine deprivation inhibits fatty acid synthase activity, decreases the expression of lipogenic genes, and increases the mobilisation of lipid stores. In WAT, it decreases fatty acid synthase activity and the expression of lipogenic genes, while it increases the expression of β-oxidation genes. Finally, in BAT, increased expression of UCP1 is observed (Cheng et al. 2010; Cheng et al. 2009)

The aforementioned effects of leucine deprivation on lipid metabolism match the effects of FGF21 on liver, WAT and BAT. This observation, in addition to our previous results indicating that leucine deprivation increases FGF21 hepatic expression and serum levels (De Sousa-Coelho et al. 2012), led us to hypothesise that FGF21 mediates the leucine deprivation effects on lipid metabolism.

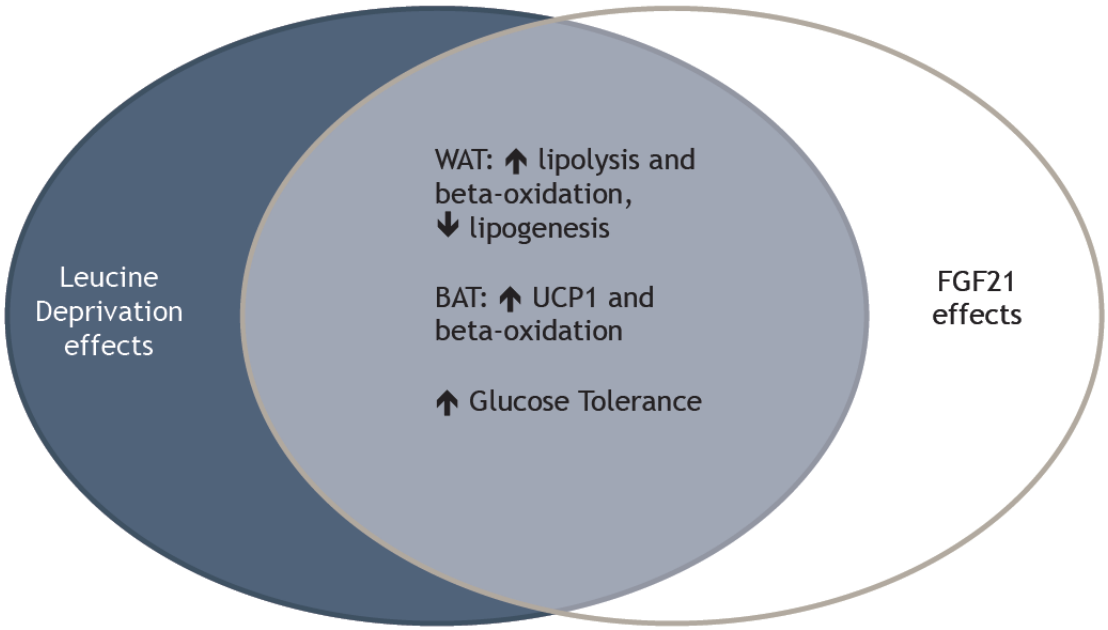

Figure I 14 Overlapping metabolic effects of FGF21 and leucine deprivation

MATHERIALS AND METHODS

1 CELL CULTRE – MAMMALIAN CELL LINES

1.1 HepG2 - human liver carcinoma cell line (ATCC No. HB-8065).

HepG2 are adherent, epithelial-like cells growing as monolayers and in small aggregates. HepG2 cell line was derived from the liver tissue of fifteen-year-old male with differentiated hepatocellular carcinoma. Cells were cultured in Eagle's Minimum Essential Medium (MEM) supplemented to contain 1x nonessential amino acids, 4 mM glutamine, 100 µg/ml streptomycin sulfate, 100 units/ml penicillin G, and 10% (v/v) fetal bovine serum (FBS). Cells were incubated at 37ºC in humidified atmosphere with 5% CO2. Culture medium was discarded and changed every 2-3 days. To passage cells, cells were briefly rinsed with 1x PBS twice and 0.05% Trypsin-EDTA solution was added. Once cell layer was dispersed (3-4 min at 37ºC), trypsin was deactivated by adding complete growth medium. Cells were splited 1:2 dilution twice a week or counted and plated according the final experiment.

1.2 AML12- transgenic mouse liver cell line (ATCC No. CRL-2254)

AML12 (alpha mouse liver 12) are adherent, epithelial-like cells growing as monolayers. AML12 cell line was established from hepatocytes from a mouse (CD1 strain, line MT42) transgenic for human TGF alpha. These cells exhibit typical hepatocyte features such as peroxisomes and bile canalicular like structure. Expression of liver specific proteins decreases with time in culture, but is reactivated by growing the cells in serum free medium. Cells were cultured in A 1:1 mixture of Dulbecco's modified Eagle's medium and Ham's F12 medium with 0.005 mg/ml insulin, 0.005 mg/ml transferrin, 5 ng/ml selenium, and 40 ng/ml dexamethasone, 4 mM glutamine, 100 µg/ml streptomycin sulfate, 100 units/ml penicillin G, and 10% (v/v) fetal bovine serum (FBS). Cells were incubated at 37ºC in humidified atmosphere with 5% CO2. Culture medium was discarded and changed every 2-3 days. To passage cells, cells were briefly rinsed with 1x PBS twice and 0.05% Trypsin-EDTA solution was added. Once cell layer was dispersed (1-2 min at 37ºC), trypsin was deactivated by adding complete growth medium. Cells were splited 1:10 dilution twice a week or counted and plated according the final experiment.

1.3 3T3-L1 Mus musculus embryo cell line (ATCC No. CL-173)

3T3-L1 is a cell line derived from mouse 3T3 (Swiss albino) cells developed through clonal isolation. 3T3-L1 cells have a fibroblast-like morphology, but, under appropriate conditions, the cells differentiate into an adipocyte-like phenotype (Diaz-Delfin et al. 2012). The cells undergo a pre-adipose to adipose like conversion as they progress from a rapidly dividing to a confluent and contact inhibited state. High serum content in the medium enhances fat accumulation.

Cells were cultured in Dubelcco's Modified Eagle's Medium (DMEM) supplemented to contain 4 mM glutamine, 100 µg/ml streptomycin sulfate, 100 units/ml penicillin G, and 10% (v/v) calf serum (CS). Cells were incubated at 37ºC in humidified atmosphere with 5% CO2. Culture medium was discarded and changed every 2-3 days. To passage cells, cells were briefly rinsed with 1xPBS twice and 0.05% Trypsin-EDTA solution was added. Once cell layer was dispersed (1-2 min at 37ºC), trypsin was deactivated by adding complete growth medium. Cells were splited 1:5 dilution twice a week or counted and plated according the final experiment.

1.4 Reagents used in cell culture maintainance

Reagent	Company	Ref
Minimum Essential Media (MEM)	GIBCO	61100-087
Dubelcco's Modified Eagle's Medium (DMEM)	GIBCO	12100-061
DMEM (Dulbecco's Modified Eagle Medium) /F-12	GIBCO	11320074
Fetal Bovine Serum (FBS)	GIBCO	10270-106
Calf Serum	GIBCO	12100-061
L-Glutamine 200mM	GIBCO	25030-024
Pen Strep (Penicillin-Streptomycin)	GIBCO	15140-122
Sodium bicarbonate solution 7.5%	Sigma-Aldrich	S8761

MEM Non Essential Amino Acids (NEAA) 100x	GIBCO	11140-035
Tripsin-EDTA 10X	GIBCO	15400-054
Insulin-Transferrin-Sodium Selenite Supplement	GIBCO	11074547001
Dexamethasone	Sigma-Aldrich	D2915

1.5 Reagents used in cell culture transfection

Reagent	Company	Ref
OPTI-MEM	GIBCO	31985-047
Lipofectamine LTX Reagent	Invitrogen	15338-100
Plus Reagent	Invitrogen	11514015

1.6 Reagents used in cell culture specific treatments

Reagent	Company	Ref	Description	Treatment conditions
L-histidinol (HisOH)	Sigma-Aldrich	H6647	Reversible inhibitor of protein synthesis. Dissolved in water to 50mg/mL.	2mM / 8h
SR8278	Sigma-Aldrich	S9576	Nuclear Heme Receptor REV-ERB antagonist. Dissolved in DMSO to 1mM	10μM / 24h
Hemin	Sigma-Aldrich	H9039	Heme is a small molecule present either free or bound to hemoglobin in the bloodstream of mammals. It is the natural ligand of REV-ERB. Dissolved in 1.4M NaOH to 30mM	30μM / 24h
PD98059	ThermoFisher Scientific	PHZ1164	PD98059 is a potent and selective cell permeable inhibitor of MAP kinase kinase	30μM /16h

	(MEK). It selectively blocks the activation of MEK, thereby inhibiting the phosphorylation and the activation of MAP kinase. Dissolved in DMSO.

Following reconstitution stock solutions aliquots were stored at -20°C.

2 PLASMID CONTRUCTS

All plasmid constructs were generated by PCR from human or mouse genomic DNA (HepG2 cells or C57BL/6 mouse strain), using Taq polymerase (Biotools) and primers introducing restriction sites when needed (see primer sequences below). The PCR products were cloned in the vector pGEM-T (Promega) and sequenced. The plasmids were digested with the corresponding restriction enzymes and subcloned into pGL3b vector (Promega), forming pGL3b-hFGF21 *wt*, pGL3b-mFgf21 *wt* and pGL3b-mRev-erbα *wt*. (For more information of the cloning strategies see Annex 2)

The sequences and orientations of the constructions were verified by sequencing (Macrogen sequencing service).

2.1 Reporter constructions

Construction	Insert	Clonning targets	Primers
pGL3b-hFGF21 *wt*	-768/+115	Kpn I / Sac I	DH1309 / DH1310
pGL3b-mFgf211 *wt*	-1497/+5	Sma I / Xho I	DH1195 / DH1196B
pGL3b-mRev-erbα	-393/+629	Mlu I / Xho I	DH1415/DH1416

List of primers (restriction sites italicized and bolded)

DH1195	5'- AGTC***CCCGGG***ATTAATTAATCGCATGGAGT-3'
DH1196b	5'- GCAAT***CTCGAG***GCTGTCTGGTGAACGCAGA-3'
DH1309	5'- ***GGTACC***AGCCAACCTGTCTTCCCTCT-3'
DH1310	5'-CTCTGGCCCACACTCACTTT- 3'
DH1415	5'-AA***ACGCGT***AATCTCTCCTCCCAGCTTGT-3'
DH1416	5'-AA***CTCGAG***GTCTTCACCAGCTGAAAGCG-3'

2.2 Expression constructions

Construction	Clonning targets	Inserts species	Origin
pRK-ATF4	Sal I / Not I	Human	Addgene (ref. 26114)
pSG-Egr-1	EcoR I	Rat	CSIC
pSG5-hReverbα	N.A	Human	Dr J.C. Rodríguez

*N.A. Not Available

3 DNA OLIGONUCLEOTIDE (PRIMERS AND PROBES)

All DNA oligos were synthesized by Sigma-Aldrich with technology ultra-high base coupling efficiency, combined with optimized cartridge purification and 100% quality control by mass spectrometry.

4 TRANSIENT TRANSFECTION AND LUCIFERASE ASSAY

HepG2 cells (1 x 10^5 cells/well) or AML12 cells (0.6 x 10^5) were seeded on 24-well plates 18–24h before transfection with Lipofectamine® LTX reagent (Invitrogen) at a ratio of 2 µl of Lipofectamine® and 0.5 µl of Plus™ reagent to 1µg of DNA. For each transfection, 0.2µg of the reporter plasmid was used along with 0.01µg of Renilla (pRL-CMV), as an internal control, and the indicated amounts of the transcription factor expression plasmids (in general 0.25µg). The total amount of transfected DNA was kept constant among experimental groups by the addition of empty pcDNA3 plasmid. 24h following transfection, cells were transferred to fresh complete MEM medium and treated with Hemin or SR8278 when indicated. In this work every transfection with pSG5-hReverbα was treated with hemin. At approximately 48h following transfection, cellular extracts were prepared for analysis of luciferase activity. Cells were washed twice with PBS, and harvested in 100µl of 1x Passive lysis buffer (Promega). The lysates were collected and a 10µl aliquot was used for Firefly luciferase assays using the Dual-Luciferase Reporter Assay System (Promega). Relative luciferase activity was given as the ratio of relative luciferase unit / relative renilla unit.

5 PROTEIN EXTRACTION

Whole-cell lysates from HepG2 cells were isolated using NP40 lysis buffer. Cells plated in MW6 were washed twice with ice-cold PBS, harvested with a rubber policeman, and centrifuged for 10min at 1000 x g at 4°C. The resulting pellet of cells was lysed with 50-100µL of NP40 lysis buffer with agitation for 15-20min at 4°C, and centrifuged for 5-10min at 12000 x g at 4°C. The supernatant corresponding to the proteins extract was collected, frozen, and stored at -80°C.

Nuclear extracts were prepared from HepG2 cells plated in 100-mm-diameter dishes (p100). Cells were washed twice with ice-cold PBS, harvested with a rubber policeman in 1mL PBS, and centrifuged for 5min at 800 x g at 4°C. Cell pellets were resuspended in 1mL of HB buffer, centrifuged at 800 x g for 5min. To obtain liver nuclear extracts, frozen liver was first triturated within a mortar in liquid nitrogen and immediately homogenized with a Dounce homogenizer in

1mL of HB buffer, and centrifuged at 800 x g for 5min. From here the protocol was the same for both cultured cells and tissues. The resulting pellet was resuspended in 100µL of HB buffer supplemented with 0.05% Triton X-100 (Sigma), and centrifuged for 1 min at 1000 x g. Nuclear pellets were washed with 1mL of HB buffer supplemented with 0.05% Triton X-100 and 1mL of HB buffer. Nuclei were incubated on ice for 30min in 50µL of HB buffer containing 36mM KCl and centrifuged for 5min at 10000 x g. The supernatant corresponding to the nuclear extract was collected, frozen, and stored at -80°C.

To obtain total extracts from epididimal White Adipose Tissue (eWAT), Brown Adipose Tissue (BAT) or Liver, tissue was homogenized in RIPA (Radio-Immunoprecipitation Assay) buffer and centrifuged at 12000 x g for 15min at 4°C. The supernatant was collected and frozen at -80°C until analysis.

NP40 lysis buffer	RIPA buffer	HB buffer
Tris-HCl 50mM pH 8	Tris HCl 10mM pH 7	Tris-HCl 15mM pH 8
NaCl 150mM	Triton X-100 1%	NaCl 15mM
NP40 1%	NaCl 150mM	KCl 60mM
	EDTA 5mM	EDTA 0.5mM

All of the buffers were supplemented with a mixture of protease inhibitors (Sigma Aldrich), 0.1mM phenylmethylsulfonyl fluoride (PMSF), and a phosphatase inhibitor cocktail (IPC3, Sigma Aldrich). Protein concentration was estimated by using the Bio-Rad protein assay with bovine serum albumin (BSA) as standard.

6 WESTERN BLOTTING ANALYSIS

Protein extracts were resolved by 8-10% SDS-polyacrylamide gel electrophoresis and transferred onto a PVDF membrane (Millipore) at 200mA for 2-3h or with iBlot 2 Dry Blotting System (ThermoFisher Scientific) programme 0 (20V 1 minute, 23V 4 minutes, 25V 5 minutes). Generally, membranes were blocked for 1 h at room temperature and the blots were then incubated with primary antibody in blocking solution overnight at 4ºC. In

general, antibodies were diluted according to the manufacturer's instructions. Specific blocking solutions and antibody dilutions are described above.

Antibody	Blocking solution	Dilution	2ari antibody
ACC1	TBS, 0.5%Tween, 5%Milk	1:500	Rabbit
ACTIN	PBS, 1%Tween, 5% Milk	1:1000	Rabbit
ATF4	TN, 0.1%Tween, 5%Milk	1:200	Rabbit
ERK1/2	TBS, 0.1%Tween, 5%BSA	1:1000	Rabbit
FASN	TBS, 0.5%Tween, 5%Milk	1:20000	Rabbit
HSL	TBS, 0.1%Tween, 5%Milk	1:1000	Rabbit
p38α/βMAPK	TBS, 0.1%Tween, 5%Milk	1:1000	Mouse
phospho-HSL	TBS, 1%Tween, 5%Milk	1:1000	Rabbit
phospho-ACC1	TBS, 0.5%Tween, 5%Milk	1:500	Rabbit
phospho-ERK1/2	TBS, 0.1%Tween, 5%BSA	1:1000	Rabbit
phospho-p38MAPK	TBS, 0.1%Tween, 5%BSA	1:1000	Rabbit
SREBP1c	TBS, 0.5%Tween, 5%Milk	1:500	Rabbit
TUBULIN	PBS, 0.1% Tween, 5%Milk	1:5000	Mouse

TBS	**PBS**	**TN**
25 mM Tris	NaCl 137mM	50mM Tris-HCl pH 8.0
150 mM NaCl	KCl 2.7mM	150mM NaCl
2mM KCl	Na2HPO4 10mM	
pH 7.4	KH2PO4 1.76mM	
	pH 7.5	

The blots were washed three times for 10min and incubated with horseradish peroxidase-conjugated secondary antibody in blocking buffer for 2 h at room temperature. After three washes, the blots were developed using the EZ-ECL Chemiluminescence Detection Kit for HRP (Biological Industries). Briefly, after the final washings, membranes were incubated with substrate for peroxidase and chemiluminescence's enhancer for 1 minute and immediately exposed to ImageQuant LAS 4000 (GE Healthcare Lifesciences). Quantification was performed by densitometry using Image J software.

7 ANTIBODIES

7.1 Primary antibodies

Antibody	Company	Ref
HSL	Cell Signaling Technology	#4107
phospho HSL	Cell Signaling Technology	#4126
ERK1/2	Cell Signaling Technology	#4695
phospho-ERK1/2	Cell Signaling Technology	#4370
phospho-p38	Cell Signaling Technology	#9211
ATF4	Santa Cruz Biotechnology	sc-200
p38α/β	Santa Cruz Biotechnology	A-12, sc-7972
SREBP1c	Santa Cruz Biotechnology	C-20. sc-36
FASN	Abcam	ab128870
ACC1	Millipore	04-322
phospho-ACC1	Millipore	07-303
ACTIN	Sigma-Aldrich	A2066
TUBULIN	Calbiochem	#CP06

7.2 Secondary antibodies

Antibody	Company	Ref
Donkey anti-rabbit IgG, whole Ab ECL antibody, horseradish peroxidase (HRP) conjugated	Amersham Biosciences	NA934V
Sheep anti-mouse IgG, HRP-Linked whole Ab (from sheep)	Amersham Biosciences	NA931V

8 ISOLATION OF TOTAL RNA

Total RNA was extracted from HepG2 cells or from frozen tissues using TRI Reagent Solution (Ambion) following the manufacter's instructions. RNA was pretreated with DNase I (Ambion) to eliminate genomic DNA contamination. Frozen tissues were chopped in liquid nitrogen and then crushed in TRI Reagent solution with the help of a politron. RNA was dissolved in DNase, RNase, protease free water (Sigma-Aldrich) and the concentration and purity of each sample was obtained from A_{260}/A_{280} measurements in a micro-volume spectrophotometer NanoDrop-1000 (NanoDrop Technologies, Inc. Thermo Scientific)

9 ANALYSIS OF MRNA EXPRESSION

To measure the relative mRNA levels, quantitative (q)RT-PCR was performed using SYBR Green or TaqMan reagents. cDNA was synthesized from 1 µg of total RNA by MLV reverse transcriptase (Invitrogen, Thermo Fisher Scientific) with random hexamers (Roche Diagnostics), following the manufacturer's instructions. The TaqMan Gene Expression Master Mix (and SYBR® Green PCR Master Mix, supplied by Applied Biosystems (ThermoFisher Scientific), were used for the PCR step. Amplification and detection were performed using the Step-One Plus Real-Time PCR System (Applied Biosystems, ThermoFisher Scientific). Each mRNA from a single sample was measured in duplicate, using 18S, Beta-Actin, and 36b4 as housekeeping genes. The primer sequences are

shown above. Results were obtained by the Relative Standard Curve Method and expressed as fold increase versus the experimental control.

	Gene	**Sequence/Ref**
SYBR Green	*18S*	F- 5'-CGGCTACCACATCCAAGGAA-3' R- 5'-GCTGGAATTACCGCGGCT-3'
SYBR Green	*36b4*	F- 5'-AGATGCAGCAGATCCGCAT-3' R- 5'-GTTCTTGCCCATCAGCACC-3'
SYBR Green	*Alas-1*	F- 5'-GCCAGGCTGTGAAATTTACT-3' R- 5'-CTGTTGCGAATCCCTTGGAT-3'
SYBR Green	*beta-Actin*	F- 5'-GCTCTGGCTCCTAGCACCAT-3' R- 5'-GCCACCGATCCACACAGAGT-3'
SYBR Green	*Cebp-beta*	F- 5'-GGGTTGTTGATGTTTTTGGTTT-3' R- 5´-GAAACGGAAAAGGTTCTCAAAA-3'
SYBR Green	*Dio2*	F- 5'-TGCGCTGTGTCTGGAACAG-3' R- 5'-CTGGAATTGGGAGCATCTTCA-3'
SYBR Green	*Glut1*	F-5'-GCCCCCAGAAGGTTATTGA-3' R-5'-CGTGGTGAGTGTGGTGGAT-3'
SYBR Green	*Pgc1-alpha*	F- 5'-AACCACACCCACAGGATCAGA-3' R- 5'-CTCTTCGCTTTATTGCTCCATGA-3'
SYBR Green	*Ppar-gamma*	F- 5'-GCATCAGGCTTCCACTATGGA-3' R- 5'-AATCGGATGGTTCTTCGGAAA-3'
SYBR Green	*Prdm16*	F- 5'-CAGCACGGTGAAGCCATT-3' R- 5'-GCGTGCATCCGCTTGTG-3'
SYBR Green	*Rev-erb alpha*	F- 5'-TTACCAAGCTGAATGGCATGGTGC-3' R- 5'- ATATTCTGTTGGATGCTCCGGCGA-3'
Taqman	*Acadm*	Mm01323360_g1
Taqman	*Acadl*	Mm00599660_m1
Taqman	*Acaca (Acc1)*	Mm01304257_m1
Taqman	*Acox*	Mm01246834_m1
Taqman	*Adrb3*	Mm02601819_g1
Taqman	*Atf4*	Mm00515325_g1
Taqman	*Atgl (Pnpla2)*	Mm00503040_m1

Taqman	*ASNS* *Asns*	Hs04186194_m1 Mm00803785_m1
Taqman	*Cd36*	Mm00432403_m1
Taqman	*Cpt1a*	Mm01231183_m1
Taqman	*Cidea*	Mm00432554_m1
Taqman	*Dio2*	Mm00515664_m1
Taqman	*Fabp4*	Mm00445878_m1
Taqman	*Fasn*	Mm00662319_m1
Taqman	*Fgf21* *FGF21*	Mm00840165_g1 Hs00173927_m1
Taqman	*Fgfr1*	Mm00438930_m1
Taqman	*Hsl (Lipe)*	Mm00495359_m1
Taqman	*Klb*	Mm00473122_m1
Taqman	*Lpl*	Mm00434764_m1
Taqman	*Ppargamma*	Mm00440940_m1
Taqman	*Pgc-1alpha*	Mm01208835_m1
Taqman	*Plin1*	Mm00558672_m1
Taqman	*Srebp1c (Srebf1)*	Mm00550338_m1
Taqman	*Ucp1*	Mm01244861_m1

ANIMAL EXPERIMENTATION

1 MICE HOUSING

Mice were housed at the Animal Facility of the School of Pharmacy of the University of Barcelona. Mice were kept in a temperature-controlled room (22±1°C) on a 12/12 h light/dark cycle and were provided free access to commercial rodent chow and tap water prior to the experiments.

All procedures were performed with male mice aged two to three months.

2 MOUSE STRAINS

The following mouse strains were used.

Mouse	Nomenclature	Origin
Wild type	C57Bl/6J	Harlan-Animals
FGF21-KO	B6N;129S5-Fgf21tm1Lex/Mmcd	Dr Villaroya Laboratory
$Fgf21^{loxP}$	B6.129S6(SJL)-*Fgf21*$^{tm1.2Djm}$/J	The Jackson Laboratory
Ob/Ob	B6.V-*Lep*^{ob}/JRj	Janvier Labs
Albumin-cre	FVB(Cg)-Tg(Alb1-cre)1Dlr/J	Dr. Zorzano Laboratory
L*Fgf21*KO	$FGF21^{fl/fl;Albumin-Cre}$	Dr Haro and Dr Marrero Laboratory

3 ANIMAL EXPERIMENTATION ETHICS COMMITTEE APPROVAL

All of the experimental protocols with mice were performed with the approval of the animal experimentation ethics committee of the University of Barcelona. All experiments were performed following the below approved procedures.

Title	CEEA Register	Acceptance date
Estudi de l'expressió d'FGF21 en ratolins alimentats amb una dieta deficient en leucina i els efectes de la deprivació d'aminoàcids en el metabolisme	389/11 593/13	04/10/2011
Estudi de l'efecte de l'FGF21 hepàtic sobre el metabolisme lipídic i la homeòstasi energètica en ratolins alimentats amb una dieta amb baix contingut proteic	48/15	16/12/2014
Estudi de l'efecte de l'FGF21 a través del sistema nerviós simpàtic sobre el metabolisme lipídic i la homeòstasi energètica en ratolins alimentats amb una dieta amb baix contingut proteic	328/16	16/12/2016
Colònia de ratolí	C-0086	13/11/2014

4 FGF21 LIVER SPECIFIC KNOCKOUT MOUSE COLONY MANAGEMENT

To generate the *Fgf21* liver specific knockout mice (L*Fgf21*KO), *Fgf21*^{loxP} mice (*Fgf21*$^{tm1.2Djm}$/J) that have *Fgf21* flanked by two *loxP* sites (Jackson Laboratory) were crossed with Albumin-cre (Tg(Alb1-cre)1Dlr/J) mice (kindly provided by Dr. A. Zorzano). The latter express the CRE recombinase enzyme under control of albumin promoter/enhancer elements, thus allowing liver-specific gene deletions. *Fgf21*^{LoxP} mice were used as controls.

4.1 Genomic DNA extraction from tails

To extract genomic DNA (gDNA) from mice tail, the last 2mm of the tail were snipped and placed into 1.5mL microcentrifuge tube (eppendorf). At his point tails can be directly frozen at -20ºC and stored until use. 500 µl of Tail buffer (supplemented with proteinase K to a final concentration of 100 µg/mL) were added to each tube. Snipped tails were incubated at 55ºC with constant mixing for at least 4h in a water bath with agitation at 55ºC. Samples were occasionally vortexed until tissue was degraded. Once tails were dissolved, they were centrifuged at 1400rpm for 10 min at RT. The supernatant was transferred to a new tube and 500 µL of isopropanol and 2µl of GlycoBlue (Ambion) were added. Tubes were mixed without vortexing and centrifuged at 14000rpm for 5 min at 4ºC. Supernatant was discarded, the pellet washed with 500 µl of cold 70% ethanol and centrifuge at 14000 rpm for 5 min at 4ºC. Next, pellet was air-dried and resuspended with 50µl of TE pH8. Samples were incubated for 5-10 min in a 65ºC bath. Finally, to check out integrity of the DNA in the sample, an aliquot can be loaded in a 0.8-1% agarose gel and a single band in the top of the gel should be visualized.

Tail buffer	TE pH 8
Tris-HCl 20 mM pH 8 EDTA 5mM pH 8 SDS 0.5% NaCl 200mM	Tris-HCl 10mM pH 8 EDTA 1mM

4.2 PCR Detection of Cre

Detection of Cre recombinase was performed by PCR using genomic DNA from mice tails. H_2O instead of gDNA was used as a negative control, and when possible, a positive control was used.

PCR reaction		PCR programme
dNTPs (10mM each)	1µL	Step 1: 95ºC 5min
Buffer (10x)	2.5µL	Step 2: 94ºC 1sec
Primer Cre-Fw (10µM)	1uL	Step 3: 50ºC 1min
Primer Cre-Rv (10µM)	1uL	Step 4: 72ºC 1 min
Taq polymerase	0.5µL	Step 5: Go to step 2 for 30 times
H2O	14µL	Step 6: 72ºC 7 min
gDNA (~ 25 ng/µL)	5µL	Step 7: STOP

PCR product will be around 100bp, so it should be loaded in a 2% agarose gel.

4.3 PCR Detection of LoxP

Detection of LoxP sites was performed by PCR using genomic DNA from mice tails. H_2O instead of gDNA was used as a negative control, and when possible, a positive control was used.

PCR reaction		PCR programme
dNTPs (10mM each)	1µL	Step 1: 95ºC 5min
Buffer (10x)	2.5µL	Step 2: 94ºC 30sec
Primer LoxP-Fw (10µM)	1uL	Step 3: 60ºC 1min
Primer LoxP-Rv (10µM)	1uL	Step 4: 72ºC 1 min
Taq polymerase	0.5µL	Step 5: Go to step 2 for 32 times
H2O	14µL	Step 6: 72ºC 10 min
gDNA (~ 25 ng/µL)	5µL	Step 7: STOP

PCR product will present a single 450bp band for homozygous mutants, single 319bp band for wild type and both bands for heterozygous mutants. Thus, it should be loaded in a 2% agarose gel.

5 DIETARY MANIPULATIONS

5.1 Leucine-deficient diet

Control (Ctl) (nutritionally complete amino acid) and leucine-deficient ((-)leu) diets were obtained from Research Diets, Inc. All diets were isocaloric and compositionally the same in terms of carbohydrate and lipid components (detailed composition shown in Annex 1). At the beginning of the feeding experiment, twelve- to fifteen-week old male mice were first acclimated to the control diet for 7 days, and then randomly assigned to either the control diet group, with continued free access to the nutritionally complete diet, or the (-)leu diet group, with free access to the diet devoid of the essential amino acid leucine for 7 days. Food intake and body weight were recorded at least every two days

5.2 Low protein diet

The Control Diet (CD) and Low Protein Diet (LPD) were obtained from Research Diets, Inc. Both diets were isocaloric. They had the following composition (in percentage of mass): 20% protein, 66% carbohydrates and 5% fat for the CD, and 5% protein, 81% carbohydrates and 5% fat for the LPD (detailed composition shown in Annex 1). For the feeding experiment, 8-week-old male mice were first fed the CD for 7 days and then randomly assigned to either the CD or LPD group with free access to food and water for 7 days. Food intake and body weight were recorded daily.

5.3 Pair-feeding

To compensate the reduction in food intake caused by leucine-deficient diet, in some experiments, a control pair-fed group was included. Food intake of mice on leucine-deficient diet was measured every day. Control pair-fed group was caged individually and administered the exact amount of food that leucine-deprived mice ingested the previous day.

5.4 Fasting

Animals were fasted for 15 hours. At 20:00h (Zeitgeber Time 12) mice were moved to new cages and food was removed while water was maintained *at libitum*. At 11:00 (Zeitgeber Time 3) mice were euthanized, tissues were isolated and immediately snap-frozen and stored at −80°C for future analysis.

5.5 Food intake measurement

Animals were distributed in 2-3 mice per cage. Food was daily weighted with a tabletop scale measured to the closest 0.1 g and restocked during 7 days. Food intake was assumed to be the same for every mouse in the cage.

6 Glucose Tolerance Test (GTT) Protocol

GTT was carried out on Fgf21 liver specific knockout or *Fgf21*^{loxP} mice, aged 8 weeks and maintained for 7 days on either CD or LPD.

To perform the GTT the following protocol was performed:

Material

- filter-sterilized glucose solution 10%(w/v)
- glucometer and strips Ascencia Elite XL (Bayer)
- razor blades
- timer
- glucose solution 10% (w/v)

Preparation

Mice were fasted for 6h [from 08:00h (Zeitgeber Time 0) to 14:00h (Zeitgeber Time 6)]. Mice were transferred to clean cages with new clean bottles of water but not food. Before starting the fast, each mouse was weighted (weight determines the amount of glucose to inject) and their tails marked in the order of injection. Glucose solution was freshly prepared before the beginning of the procedure.

Glucose solution 10%(w/v): 9mL H2O + 1g D-glucose (then add H2O to have 10mL).

Mice were located at the experimentation room at least 30 minutes before the beginning of the protocol.

Method

To obtain baseline blood glucose, the tail was nicked with a fresh razor blade by a horizontal cut of the very end, and measured using a glucometer. Each mouse was injected intraperitoneally (ip) with a filter-sterilized solution of D-glucose, with the size of the bolus determined by animal weight (1.5 mg glucose/g body weight). At 30. 60. 90 and 120 min blood glucose was sampled from the tail of each mouse by gently massaging a small drop of blood onto the glucometer strip. Glucose injections and blood glucose sampling were timed to take approximately the same amount of time per animal, so that the samples time were accurate for each animal. The data were plotted as blood glucose concentration (mg/dL) over time (min) and as the area under the curve (AUC) of the % of basal glucose calculated by the trapezoidal rule.

7 INSULIN TOLERANCE TEST (ITT) PROTOCOL

ITT was carried out on Fgf21 liver specific knockout or *Fgf21*^{loxP} mice, aged 8 weeks and maintained for 10 days on either CD or LPD.

To perform the ITT the following protocol was performed:

Material

- Filter-sterilized insulin solution 0.05 I.U/ml
- Glucometer and strips Ascencia Elite XL (Bayer)
- Razor blades
- Timer

Preparation

Mice were fasted for 6h [from 08:00h (Zeitgeber Time 0) to 14:00h (Zeitgeber Time 6)]. Mice were transferred to clean cages with new clean bottles of water but not food. Before starting the fast, each mouse was weighted (weight determines the amount of insulin to inject) and their tails marked in the order of injection. Insulin solution was freshly prepared before the beginning of the procedure.

Mice were located at the experimentation room at least 30 minutes before the beginning of the protocol.

Method

To obtain baseline blood glucose, the tail was nicked with a fresh razor blade by a horizontal cut of the very end, and measured using a glucometer. Each mouse was injected intraperitoneally (ip) with a filter-sterilized insulin solution, with the size of the bolus determined by animal weight (0.75 I.U insulin/kg body weight). At 30. 60 and 90 minutes blood glucose was sampled from the tail of each mouse by gently massaging a small drop of blood onto the glucometer strip. Insulin injections and blood glucose sampling were timed to take approximately the same amount of time per animal, so that the samples time were accurate for each animal. The data were plotted as blood glucose

concentration (mg/dL) over time (min) and as the inverted area under the curve below baseline glucose calculated by the trapezoidal rule.

8 β-ADRENOCEPTOR ANTAGONISM (PROPRANOLOL TREATMENT)

For the β-adrenergic blockade experiment, 8-week-old male mice were first daily i.p. injected with saline solution and fed the CD for 7 days. Then, mice were randomly assigned to either the CD or LPD group and given daily ip injections with ((s)-(-) propranolol hydrochloride; Sigma) at 5 mg/kg·d or saline vehicle alone for 7 more days. Food intake and body weight were recorded daily.

9 TISSUES HARVESTING

Animals were anesthetized by isoflurane inhalation (4% for induction and 2% for maintenance), the thoracic cavity was opened and blood was collected from heart by intracardiac puncture. Then, blood was prepared for serum or plasma extraction. After sacrifice, tissues were isolated and immediately snap frozen and stored at -80ºC for future analysis.

9.1 Serum extraction

Mouse serum was obtained by clotting whole blood (30 min, RT) and posterior centrifugation (1500G, 15 min, 4ºC). Serums were stored at -80°C for posterior analysis.

9.2 Plasma extraction

Mouse plasma samples were obtained by centrifuging (1500G, 15 min, 4ºC) whole blood collected in EDTA-treated tube. The plasma was stored at −80°C for posterior analysis.

10 PLASMA/SERUM MEASUREMENTS

10.1 Plasma free fatty acids (FFA) measurement

Free fatty acids (non-esterified fatty acids, NEFA) were determined in mice serum by an enzymatic colorimetric assay. The Free fatty acids, Half-micro test

was obtained from Roche. The measure was performed according to the manufactures' instructions. Briefly, Free fatty acids are converted to Acyl-Coenzyme A, AMP and pyrophosphate in the presence of acyl-CoA synthetase. Acyl-CoA reacts with oxigen in the presence of acyl-CoA oxidase to form 2,3-enoyl-coenzyme A. The resulting hydrogen peroxide converts TBHB and 4-AA to a red dye in the presence of peroxidase. The dye is measured in the visible wavelenght range at 546nm.

10.2 FGF21 analysis

Mouse FGF21 enzyme-linked immunosorbent assay (ELISA) kit was obtained from Millipore for the quantification of FGF21 in mice serum. The assay was conducted according to the manufacturer's protocol.

Briefly, FGF-21 molecules from samples were captured to the wells of a microtiter plate coated with a polyclonal goat anti-FGF-21 antibody, a second biotinylated polyclonal goat anti-FGF-21 antibody bound to the captured molecules. After washing, streptavidin-horseradish peroxidase conjugate bound to the immobilized biotinylated antibodies. After washing the excess of free enzyme conjugates, quantification of immobilized antibody-enzyme conjugates was performed by monitoring horseradish peroxidase activities in the presence of the substrate 3,3',5,5'-tetramethylbenzidine. A calibration curve was constructed by plotting the difference of absorbance values at 450 and 590nm versus the FGF21 concentrations of the calibrators, and concentrations of unknown samples (performed in duplicate) were determined by using this calibration curve.

10.3 Adiponectine measurement

Mouse adiponectine enzyme-linked immunosorbent assay (ELISA) kit was obtained from Millipore for the quantification of adiponectine in mice serum. The assay was conducted according to the manufacturer's protocol. The principle of procedure is the same as the abovementioned FGF21 ELISA kit.

Briefly, a calibration curve was constructed by plotting the difference of absorbance values at 450 and 590nm versus the adiponectine concentrations

of the calibrators, and concentrations of unknown samples (performed in duplicate) were determined by using this calibration curve.

10.4 Free T3 measurement

Free T3 ELISA kit was obtained from Abnova for the quantification of free T3 in mice plasma. The assay was conducted according to the manufacturer's protocol.

Tested specimen is placed into the microwells coated by specific rabbit polyclonal to T3-antibodies simultaneously with conjugated fT3-peroxidase. fT3 from the specimen competes with the conjugated fT3 for coating antibodies. After washing procedure, the remaining enzymatic activity bound to the microwell surface is detected and quantified by addition of chromogen-substrate mixture, stop solution and photometry at 450 nm. Optical density in the microwell is inversely related to the quantity of the measured analyte in the specimen. A calibration curve was constructed by plotting the absorbance values at 450nm versus the free T3 concentrations of the calibrators. Concentrations of unknown samples (performed in duplicate) were determined by using this calibration curve.

10.5 ACTH measurement

The ACTH (Mouse/Rat) ELISA Kit was obtained from Abnova for the quantification of ACTH in mice plasma. It is a two-site lumELISA for the measurement of the biologically active 39 amino acid chain of ACTH. A goat polyclonal antibody to ACTH, and a mouse monoclonal antibody to ACTH are specific for well-defined regions on the ACTH molecule. One antibody is prepared to bind only the C-terminal ACTH 34-39 and this antibody is biotinylated. The other antibody is prepared to bind only the mid-region and N-terminal ACTH 1-24 and this antibody is labeled with horseradish peroxidase for detection. Calibrators, controls, or samples are simultaneously incubated with the enzyme labeled antibody and a biotin coupled antibody in a streptavidin-coated microplate well. At the end of the assay incubation, the microwell is washed to remove unbound components. Upon the addition of the luminol substrate, the enzyme activity in the enzyme-bound fraction is directly

proportional to the concentration of the ACTH in the sample. A calibration curve was constructed by plotting the relative light units (RLU) after 10 seconds of integration versus the ACTH concentrations of the calibrators. Concentrations of unknown samples (performed in duplicate) were determined by using this calibration curve.

10.6 Noradrenaline measurement

Epinephrine/Norepinephrine ELISA kit was obtained from Abnova for the quantification of norepinephrine in mice plasma. Noradrenaline (norepinephrine) is extracted by using a cis-diol-specific affinity gel, then acylated and then converted enzymatically.

The competitive ELISA kit uses the microtiter plate format. The antigen (coverted noradrenaline) is bound to the solid phase of the microtiter plate. The solid phase bound analytes compete for a fixed number of antibody binding sites. After the system is in equilibrium, free antigen and free antigen-antibody complexes are removed by washing. The antibody bound to the solid phase is detected by an anti-rabbit IgG-peroxidase conjugate using TMB as a substrate.

A calibration curve is constructed by plotting the absorbance values at 450nm versus the noradrenaline concentrations of the calibrators. Concentrations of unknown samples and controls (performed in duplicate) were determined by using this calibration curve.

11 HISTOLOGICAL EXAMINATIONS

For the histological analysis, a little piece of each fresh tissue (liver and epididymal WAT) was cut and fixed in 10% formalin (Sigma-Aldrich) at 4°C o/n and processed for embedding in paraffin. Subsequent processing was performed by the Pathology Department of the Hospital Clinic of Barcelona. Four-micrometer-thick sections were obtained and stained with hematoxylin and eosin (H&E) and examined at 20X magnification. Images of adipose tissue were analyzed to establish cell size, and of liver to determine fat accumulation. At least 10 random and independent fields were acquired from each individual mouse tissue staining, using a Leica CTR 4000 microscope with the Leica

Application Suite Version 2.7.OR1 software. Quantitative data were obtained using the IMAT program developed in the Science and Technology Center of the University of Barcelona (CCIT-UB). The selection of the test objects has been performed according to color and choosing the same limits for binarization for all images.

OTHER

1 HUMAN SAMPLES

We used plasma samples from 78 participants randomly selected from the nodes of the Hospital Clinic (Barcelona) and Reus (Tarragona) and included in the PREDIMED trial. This was a 5-year randomized clinical trial to compare the effects of either a Mediterranean diet supplemented with extra virgin olive oil or nuts versus a low-fat control diet. A total of 7447 asymptomatic men but at high cardiovascular risk (aged 55–80 years) and women (aged 60–80 years) were recruited. All participants had type 2 diabetes or three or more cardiovascular risk factors. Details of the recruitment method and study design have been described elsewhere (Estruch et al. 2013) and are also available at www.predimed.es. In addition to the plasma samples, we also gathered information from these 78 individuals, including a 137-item semi-quantitative food frequency questionnaire (FFQ), and a general questionnaire that provided data on lifestyle habits, concurrent diseases, anthropometry, and medication use. Total energy intake and nutrient intake were calculated on the basis of Spanish food composition tables (Mataix Verdú 2003). The study protocol was approved by the institutional review boards of the participating centers (ISRCTN35739639).

2 STATISTICAL ANALYSIS

For human samples, baseline characteristics are presented as means ± standard error of the mean (SEM) for continuous variables, frequencies and percentages for categorical variables across quartiles of protein intake at baseline. Differences between quartiles were tested by a 1-factor ANOVA test

for continuous variables and by the chi-square test for the categorical ones. We performed multiple linear regressions to evaluate the relationship between protein intake (exposure variable) and FGF21 hormone levels (dependent variable). Protein intake was previously adjusted for calories using the residual method. Regression analyses were unadjusted (model 1) or adjusted by body mass index (BMI) and total energy intake (model 2)

All statistical analyses were conducted using SAS software, version 9.3 (SAS Institute, Inc.). All t tests were 2-sided and P values below 0.05 were considered statistically significant.

3 INFORMATION TECHNOLOGIC TOOLS

Entrez-Pubmed, National Center for Biotechnology Information (NCBI, USA) - http://www.ncbi.nlm.nih.gov/pubmed/

Basic Local Alignment Search Tool (BLAST), National Center for Biotechnology Information (NCBI, USA) - http://blast.ncbi.nlm.nih.gov/Blast.cgi

Webcutter 2.0 - http://bio.lundberg.gu.se/cutter2/

Primer3 (v. 0.4.0) - http://frodo.wi.mit.edu/primer3/

PROMO (ver 8.3) - http://alggen.lsi.upc.es/cgibin/promo_v3/promo/promoinit.cgi?dirDB=TF_8.3

UCSC Genome Browser - https://genome.ucsc.edu

4 ADDITIONAL INFORMATION

Any missing information regarding the experimental procedures, which also cannot be found in the ANNEX, means that the procedure was performed according to the detailed information given by “Molecular Cloning, a Laboratory Manual” (Sambrook, Fritsch and Maniatis) and/or “Current Protocols in Molecular Biology” (Ausubel, Bent, Kingston, Moore, Seidman, Smith and Struhl), or following the protocols provided in the instructions of the commercial kits used.

RESULTS

THE ROLE OF REV-ERBα IN THE INDUCTION OF FGF21 UPON LEUCINE DEPRIVATION

Rev-erbα is a core component of the molecular clock and a transcriptional repressor (Harding & Lazar 1995). It is highly expressed in the liver, skeletal muscle, adipose tissue, and brain, repressing many genes in order to regulate metabolism in a circadian rhythm.

Given that Rev-erbα links the circadian clock to liver metabolism (Zhang et al. 2016), that *FGF21* levels inversely correlate with the expression pattern of *REV-ERBα* and *ALAS-1* in liver (Kaasik & Lee 2004; Oishi et al. 2008) and that PGC-1α negatively regulates hepatic *Fgf21* expression by modulating the heme/Rev-erbα axis (Estall et al. 2009), we hypothesised that Rev-erbα participates in the regulation of *Fgf21* during amino acid deprivation.

Moreover, the analysis of the ChIP-seq results from Mitchell Lazar's group (Figure R0) points to an indirect binding of Rev-erbα to DNA regions containing AARE1 and AARE 2 of the *Fgf21* promoter, thus presenting the interesting idea of competition between the activator ATF4 and the repressor Rev-erbα for the occupancy of this promoter. The putative tethering factor CEBPβ (Zhang et al. 2015) also binds to the DNA region enriched by Rev-erbα immunoprecipitation.

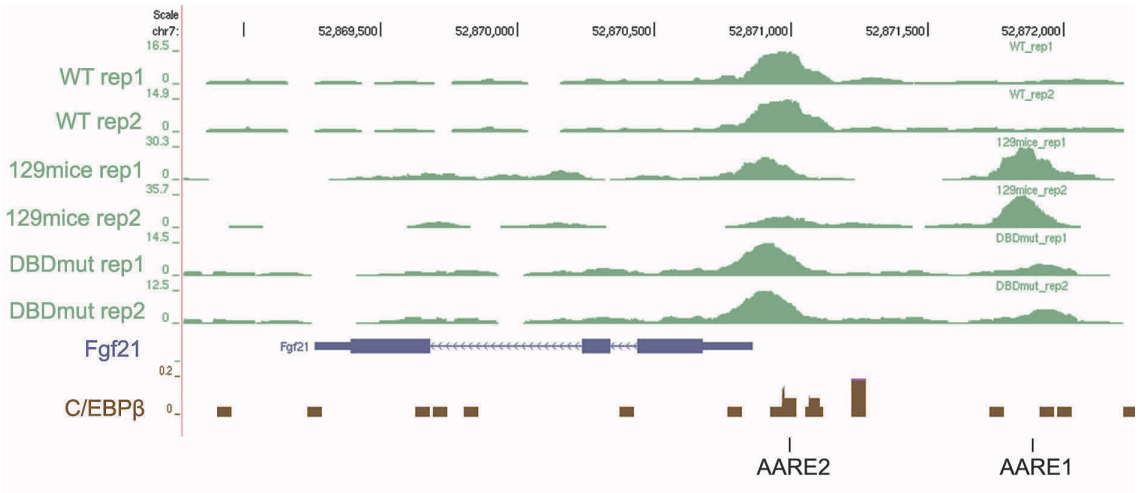

Figure R 0 Analysis of ChIP-seq results from Mitchell Lazar's group (GSM1659686). Sequences enrichment after immunoprecipitation of Rev-erbα is shown in green. WT: liver of C57BL/6J mouse. 129mice: liver of 129S1/SvlmJ mouse. DBDmut: liver of C57BL/6J Rev-erbα DNA binding domain (DBD)

mutant mouse. Fgf21 gene representation is shown in blue. Sequences enrichment after immunoprecipitation of CEBPβ in C2C12 cells is shown in brown (from Caltech TFBS database).

All together, these considerations led us to address the role of Rev-erbα in the regulation of *Fgf21* during amino acid deprivation.

1 *Rev-erbα* and *Fgf21* expression is negatively correlated across various nutritional states and different tissues

To address the contribution of Rev-erbα to the regulation of *Fgf21,* wild-type mice were challenged with nutritional conditions known to increase the expression of this gene, namely leucine deprivation (De Sousa-Coelho et al. 2012), fasting (Lundåsen et al. 2007) or both. mRNA levels of *Fgf21* and *Rev-erbα,* as well as of other factors involved in the Heme/Rev-erbα axis, were analysed.

1.1 *Fgf21* is repressed by fasting in mice fed a leucine-deficient diet

First, we analysed FGF21 serum concentration of mice administered *ad libitum* a control diet (Ctl) or a leucine-deficient diet ((-)leu) for 7 days. Two other groups on the Ctl or (-)leu diet were fasted 15 h before sacrifice.

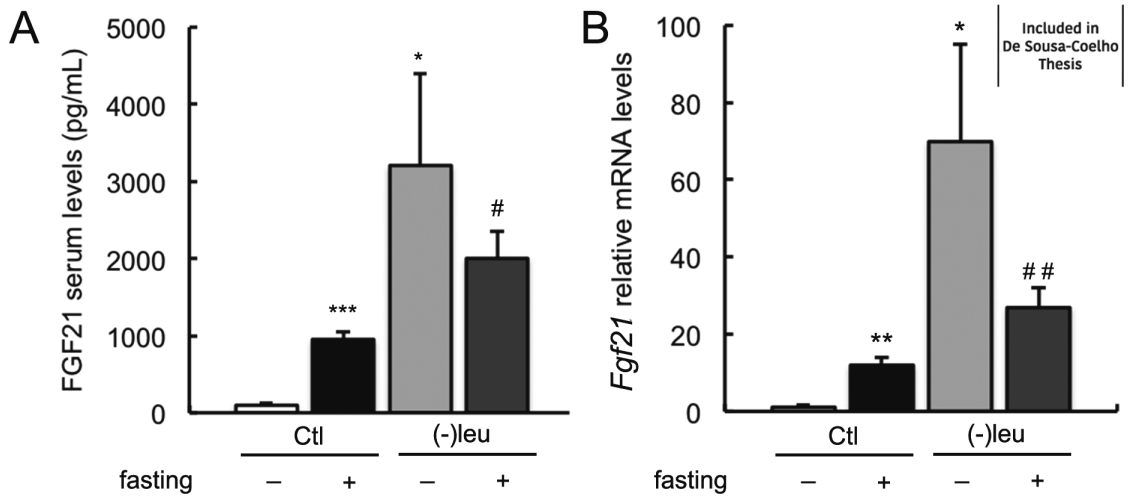

Figure R 1 FGF21 Expression under a leucine-deficient diet is differentially induced in the fed and in the fasted state. Serum FGF21 protein concentrations were measured by ELISA (A). *Fgf21* mRNA in liver was measured by qRT-PCR (B). Error bars represent the mean ± standard error of the mean (SEM) *p<0.05 **p<0.01 versus Ctl ad libitum; #p<0.05, # # p<0.01 versus (-)leu *ad libitum* (n=6/group).

As previously described, fasting caused an increase in FGF21 serum concentration (Inagaki et al. 2007) and leucine deprivation strikingly did it too

(De Sousa-Coelho et al. 2012). However, surprisingly, when leucine-deprived animals were fasted, FGF21 serum concentrations were significantly lower than in leucine-deprived animals fed *ad libitum*. The addition of two conditions known to increase *Fgf21* expression, namely, leucine deprivation and fasting, did not increase FGF21 levels but rather decreased them (Figure R1A). *Fgf21* mRNA levels in liver accurately paralleled FGF21 serum levels (Figure R1B). The weaker induction of *Fgf21* in fasted leucine-deprived mice led us to study the role of the transcriptional repressor Rev-erbα in these conditions.

1.2 mRNA levels of factors involved in the heme/Rev-erbα axis in liver of leucine-deprived and fasted mice

To analyse the role of *Rev-erbα* during fasting and leucine deprivation, we measured the expression of *Rev-erbα* and the factors involved in its activity.

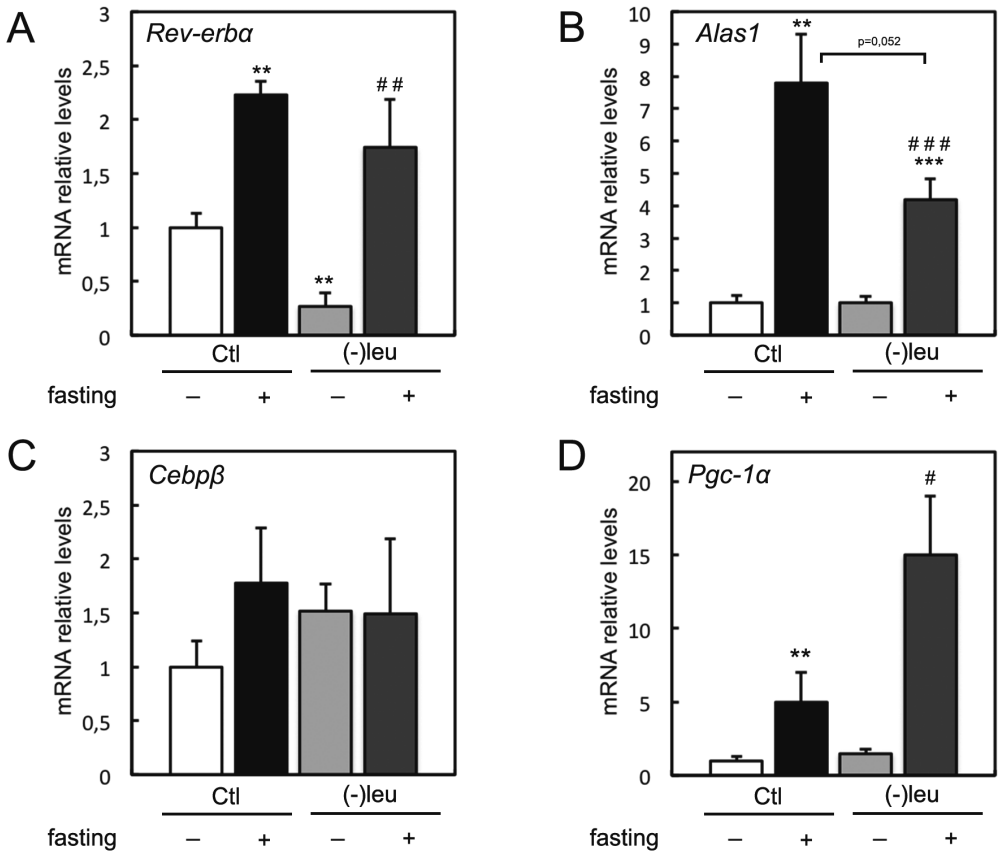

Figure R 2 *Rev-erbα* is downregulated by leucine deprivation and upregulated by fasting. *Rev-erbα, Alas1, Cebpβ* and *Pgc-1α* mRNA in liver was measured by qRT-PCR (B). Error bars represent the mean ± standard error of the mean (SEM) * p<0.05, ** p<0.01, ***p<0.001 versus Ctl ad libitum; #,p<0.05; # # p<0.01 versus , # # # p<0.001 versus (-)leu *ad libitum* (n=6/group).

Analysis of hepatic mRNA levels showed that *Rev-erbα* expression was repressed by leucine deprivation and increased by fasting (Figure R2A). The expression of *Alas1*, (the rate-limiting enzyme of the biosynthesis of the Rev-erbα ligand, heme) increased in response to fasting in both dietary groups (Figure R2B), while the expression of the putative tethering factor *Cebpβ* remained unchanged between conditions (Figure R2C). Finally, *Pgc-1α*, which positively regulates *Rev-erbα* and *Alas1*, was increased by fasting in mice on both diets, but the induction was much higher in leucine-deprived animals (Figure R2D).

These results reveal a negative correlation between *Fgf21* expression and the heme/Rev-erbα axis. In mouse liver, leucine deprivation causes the upregulation of *Fgf21* and the downregulation of *Rev-erbα.* When leucine-deprived mice were fasted, *Rev-erbα* and *Alas1* increased, resulting in the blunted upregulation of *Fgf21*.

1.3 *Fgf21* is downregulated and *Rev-erbα* is upregulated in eWAT of leucine-deprived mice

We also checked whether the negative correlation between *Fgf21* and *Rev-erbα* mRNA level observed under leucine deprivation was translatable to other *Fgf21*-expressing tissues such as eWAT.

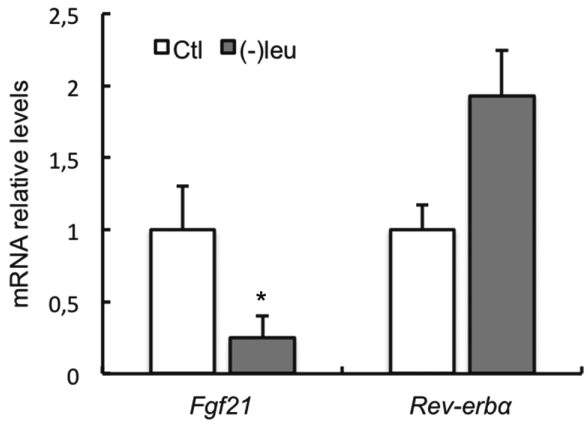

Figure R 3 *Fgf21* and *Rev-erbα* expression in eWAT of leucine-deprived mice. *Rev-erbα* and *Fgf21* mRNA in liver was measured by qRT-PCR (B). Error bars represent the mean ± standard error of the mean (SEM) * p<0.05 Ctl diet; (n=6/group).

Contrary to liver, leucine deprivation caused a decrease in *Fgf21* expression in eWAT. Consistent with its role as a repressor, *Rev-erbα* mRNA levels tended to increase (p= 0,17) in response to leucine deficiency. (Figure R3)

These results, together with the abovementioned data (Figure R1, R2), show a consistent negative correlation between *Fgf21* and *Rev-erbα* expression across tissues and nutritional states.

2 Rev-erbα represses Fgf21 promoter activity

Given the negative correlation between expression patterns of *Fgf21* and *Rev-erbα* and the published data suggesting that Rev-erbα regulates *Fgf21* (Estall et al. 2009; Archer et al. 2012), we studied the effect of Rev-erbα on the *FGF21* promoter.

2.1 Inhibition of Rev-erbα increases *FGF21* promoter activity

To imitate the leucine deprivation state in the liver, AML12 cells were transiently co-transfected with the reporter construction pGL3b-hFGF21 (-768/+115 of the human *FGF21*) and an ATF4 expression plasmid. Rev-erbα activity was inhibited by treating the cells with its synthetic antagonist SR8278.

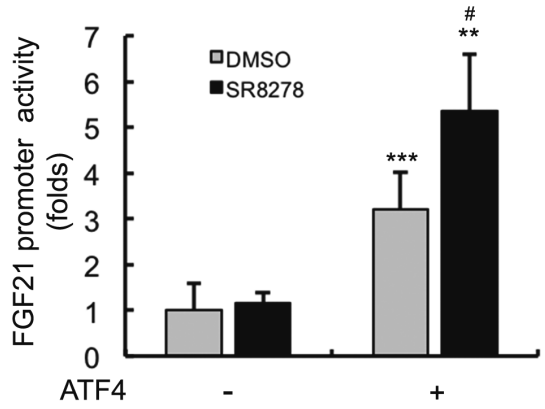

Figure R 4 Rev-erbα antagonism enhances ATF4 activation of FGF21 promoter. Luciferase activity of the human *FGF21* promoter reporter construct co–transfected with an expression plasmid for human ATF4 in the presence or absence of the Rev-erbα antagonist SR8278 (10μM). Data are means ± SEM from three independent experiments with two plates each. **p<0.01, ***p<0.001 versus reporter construction treated with vehicle. # p<0.05 versus reporter construction cotransfected with ATF4 treated with vehicle.

As previously reported by our group (De Sousa-Coelho et al. 2012), the transcriptional activity of the *FGF21* promoter increased in the presence of

ATF4. Remarkably, the inhibition of the endogenous Rev-erbα protein by SR8278 enhanced the activation induced by ATF4. This result is consistent with the analysis of the mRNA levels, suggesting that a decrease in Rev-erbα activity enhances the ATF4-mediated upregulation of Fgf21.

2.2 CEBPβ represses Fgf21 promoter activity

We next co-transfected the *Fgf21* promoter with expression plasmids for the activator ATF4, the repressor Rev-erbα and the tethering factor CEBPβ.

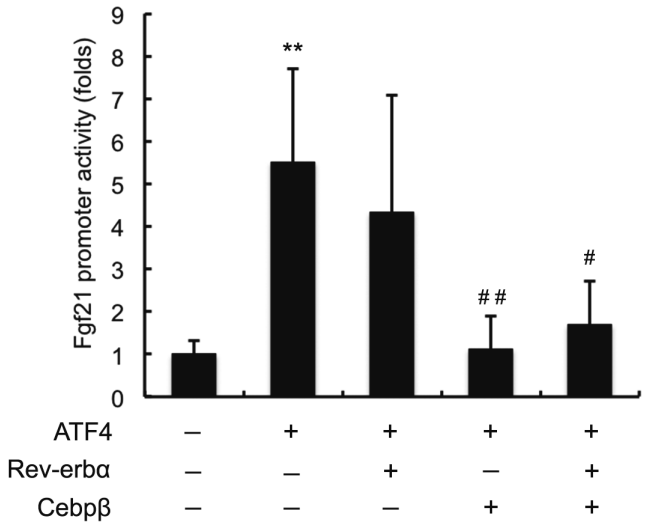

Figure R 5 CEBPβ blocks ATF4 activation of *Fgf21* promoter. Luciferase activity of the mouse *Fgf21* promoter reporter constructs co–transfected with an expression plasmid for human ATF4, Rev-erbα or Cebpβ as indicated. Data are means ± SEM from three independent experiments with two plates each. **p<0.01, versus reporter construction alone. # p<0.05, # # p<0.05 versus reporter construction cotransfected with ATF4.

The single addition of Rev-erbα did not alter the activation induced by ATF4. However, when Rev-erbα was cotransfected with Cebpβ, the activation of the promoter decreased dramatically. This effect occurred independently of the presence of Rev-erbα. A feasible explanation for this observation is that CEBPβ repress the promoter by thethering the endogenous Rev-erbα protein of the cells.

3 EGR-1 represses Rev-erbα promoter activity

Rev-erbα is downregulated in mouse liver during leucine deprivation, and this effect correlates with the upregulated expression of *Fgf21* (Figures R1, R2).

During leucine deprivation, early growth response protein 1 (*Egr-1*) is highly induced in cultured cells in a partially Gcn2 dependent manner (Deval et al. 2009), and this observation is consistent with our results showing an induction of *Egr-1* in liver of leucine-deprived mice (Figure R6A). In addition, *Egr-1* can act as a transcriptional repressor by competing with specific protein 1 (*Sp1*) for its binding elements. Consequently, we hypothesised that *Egr-1* is responsible for the downregulation of *Rev-erbα* during amino acid deprivation.

To study the possible effect of EGR-1 on *Rev-erbα* expression, we co-transfected AML12 cells with a reporter plasmid containing 1022pb (-393/+629) of the mouse promoter and increasing amounts of an Egr-1 expression plasmid.

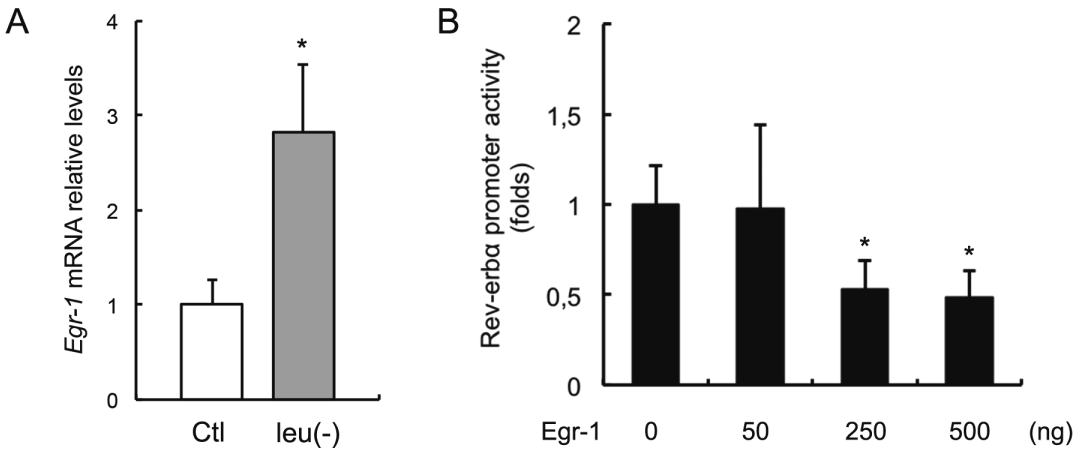

Figure R 6 *Egr*-1 is induced by leucine deprivation in liver and EGR-1 diminishes *Rev-erbα* promoter activity. *Egr-1* mRNA in liver was measured by qRT-PCR (A). Error bars represent the mean ± standard error of the mean (SEM) * p<0.05 versus Ctl diet; (n=6/group). Luciferase activity of the mouse *Rev-erbα* promoter reporter construct co–transfected with various amounts of an expression plasmid for rat Egr-1 (B). Data are means ± SEM from three independent experiments with two plates each. *p<0.05, versus reporter construction alone.

When the reporter construction was cotransfected with 250 or 500 ng of the Egr-1 expression plasmid, the activity of the promoter was significantly lower (Figure R6B). This finding proposes EGR-1 as a possible effector of the *Rev-erbα* repression under leucine deprivation.

THE ROLE OF FGF21 IN THE METABOLIC RESPONSE TO LEUCINE DEPRIVATION

The coincidence between the metabolic response to essential amino acid deprivation and to FGF21, the induction of *Fgf21* under amino acid deprivation (De Sousa-Coelho et al. 2012), together with the repression of the transcription and maturation of sterol regulatory element binding protein (SREBP) 1c induced by FGF21 in HepG2 cells (Zhang et al. 2011), led us to consider that FGF21 could be an important mediator between amino acid deprivation and lipid metabolism in liver, WAT and BAT.

To investigate this hypothesis, we examined the response of FGF21-deficient mice to deprivation of the essential amino acid leucine.

1 FGF21 gene expression is induced by leucine deprivation specifically in liver but not BAT or WAT

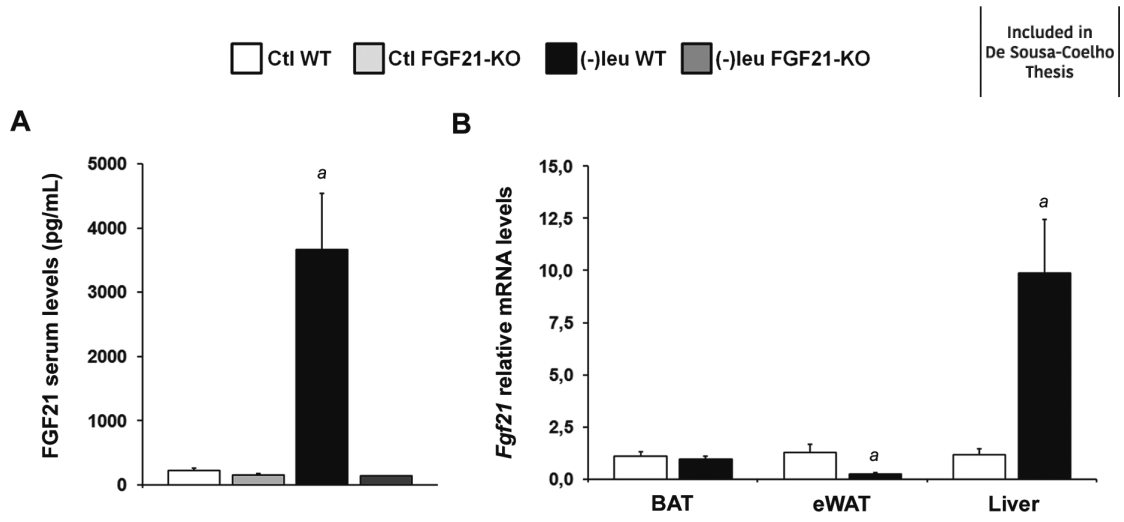

Figure L 1. FGF21 is differently regulated by leucine deprivation in liver and adipose tissues. Serum FGF21 protein concentrations were measured by ELISA (A). *Fgf21* mRNA in BAT, eWAT and liver was measured by qRT-PCR (B). Error bars represent the mean ± standard error of the mean (SEM) a, $p<0.05$ versus Ctl WT; b, $p<0.05$ versus Ctl FGF21-KO; c, $p<0.05$ versus (-)leu WT (n=6/group).

According to our previously reported results (De Sousa-Coelho et al. 2012), mice maintained on a leucine-deficient diet showed a dramatic increase in FGF21 circulating levels (Figure L1A). To check the origin of this circulating

FGF21 we analysed *Fgf21* gene expression in several tissues. Consistent with the liver as the main site of FGF21 production and release into the blood, *Fgf21* mRNA levels in liver paralleled those in serum, whereas mRNA levels were unchanged in BAT and, unexpectedly, significantly decreased in epididymal (e) WAT in wild-type mice maintained on a (-)leu diet (Figure L1B). As expected, *Fgf21* mRNA levels were undetectable in any analysed tissue in the *FGF21-KO* mice. According with previous reports (Badman et al. 2009), the circulating levels of FGF21 in knockout mice were below the threshold for correct quantification.

2 FGF21 deficiency significantly attenuates weight loss under leucine deprivation

When fed a leucine-deprived diet, mice undergo rapid weight loss (Cheng et al. 2009). The goal of the present study is to investigate whether this phenomenon is FGF21-dependent. For this purpose, wild-type and FGF21-KO mice were fed a control or leucine-deficient diet for 7 days.

2.1 Total body weight after 7 days on a leucine-deficient diet

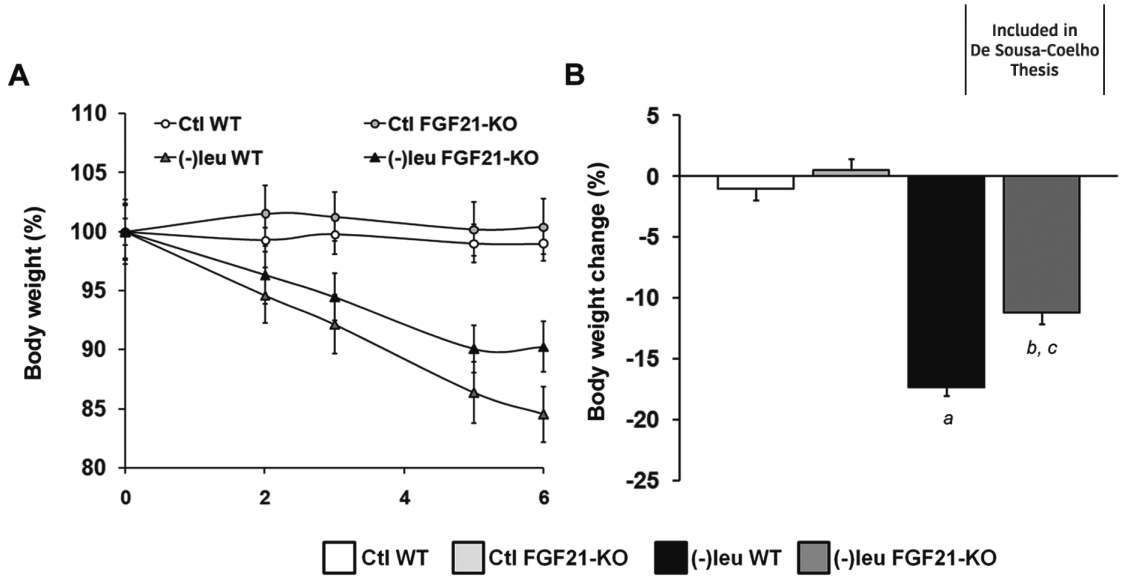

Figure L 2. FGF21 is required for leucine-deficient diet effects on body weight. Body weight of mice fed with Ctl or (-)leu diet (A). The weight on the first day was considered 100%. Body weight change (%) after 7 days of feeding the Ctl or (-)leu diet (B). Error bars represent the mean ± standard error of the mean (SEM). a, $p<0.05$ versus Ctl WT; b, $p<0.05$ versus Ctl FGF21-KO; c, $p<0.05$ versus (-)leu WT (n=6/group).

Accordingly to previous reports, mice on a leucine-deficient diet experienced a drastic weight loss. *Fgf21* deficiency modestly reduced weight loss from 17% of total body weight to 11% indicating that FGF21 is partially responsible for the weight loss under leucine deprivation.

2.2 Tissue weight after 7 days on a leucine-deficient diet

To better understand the contribution of each tissue to the total body weight loss, BAT, eWAT, scWAT and liver weight were analysed.

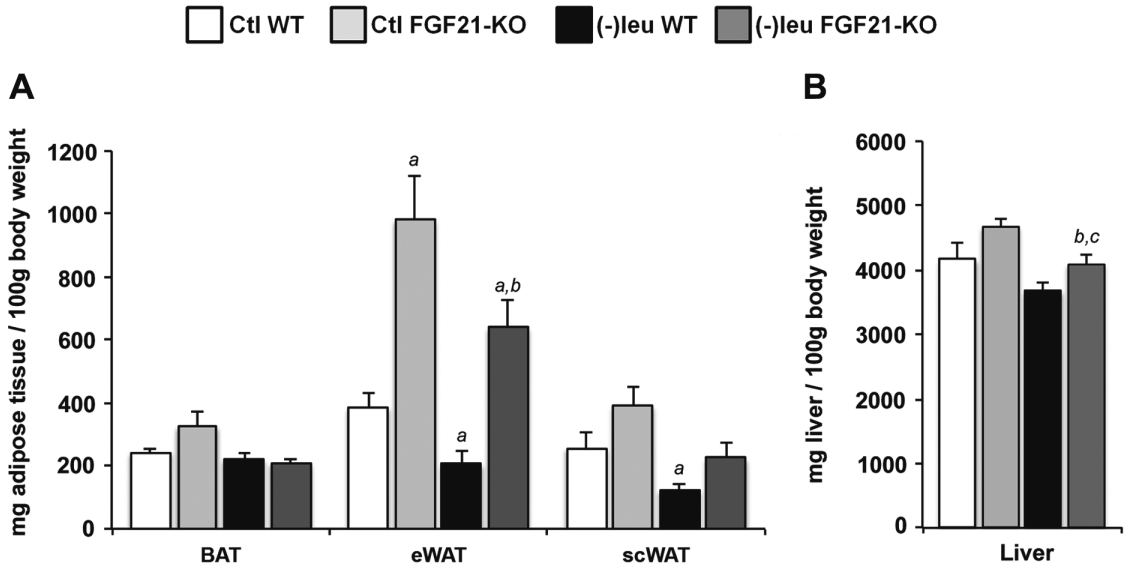

Figure L 3. FGF21 is required for leucine-deficient diet effects on eWAT, scWAT and liver weight. BAT, eWAT and scWAT weight of mice fed with Ctl or (-)leu diet related to 100 mg of body weight (A). Liver weight of mice fed with Ctl or (-)leu diet related to 100 mg of body weight (B). Error bars represent the mean ± standard error of the mean (SEM). a, $p<0.05$ versus Ctl WT; b, $p<0.05$ versus Ctl FGF21-KO; c, $p<0.05$ versus (-)leu WT (n=6/group).

Together with total body weight loss, mice fed a leucine-deprived diet underwent a fat mass loss, both epididymal and subcutaneous. Liver showed the same tendency although didn't reach statistical significance (Figure L3). We found that these effects were partially blunted in FGF21-KO mice

2.3 Food intake of mice fed a leucine-deficient diet

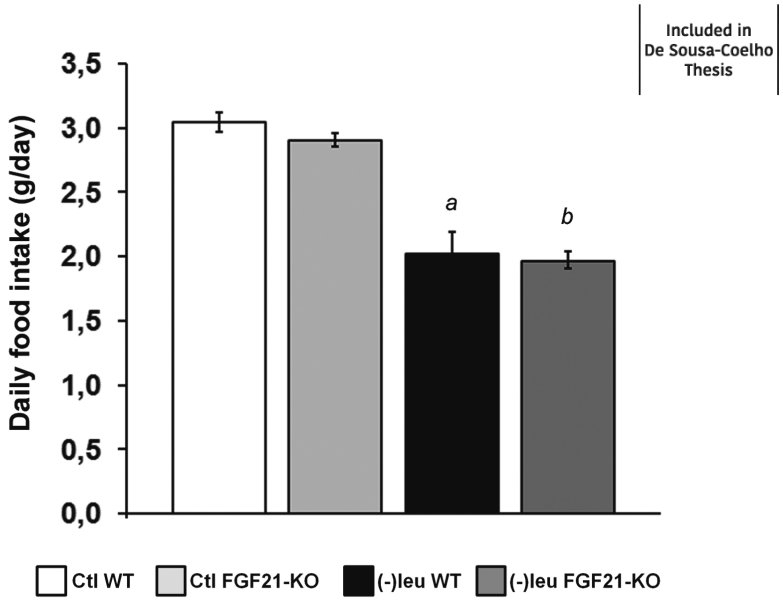

Figure L 4. FGF21 is not responsible for reduced food intake in leucine-deprived mice. Food intake was recorded daily for seven days. Error bars represent the mean ± standard error of the mean (SEM). a, $p<0.05$ versus Ctl WT; b, $p<0.05$ versus Ctl FGF21-KO; (n=6/group).

The reduction in food intake caused by leucine deprivation (~30%), which is partially responsible for the body weight loss, was unchanged between genotypes (Figure L4). This result suggests that *Fgf21* is not involved in the food aversion caused by a leucine-deficient diet.

3 FGF21 deficiency prevents changes in WAT of leucine-deprived mice

The reported observation that white adipocytes from FGF21 transgenic mice are substantially smaller than those from wild-type mice (Inagaki et al. 2007; Kharitonenkov et al. 2005), and that leucine deprivation decreases adipocyte volume (Cheng et al. 2009), together with the abovementioned partially FGF21-dependent weight loss of WAT in mice fed a leucine-deficient diet (FigureL3), led us to examine whether this effect was mediated by FGF21.

3.1 FGF21 mediates the reduction of adipocytes size upon leucine deficiency

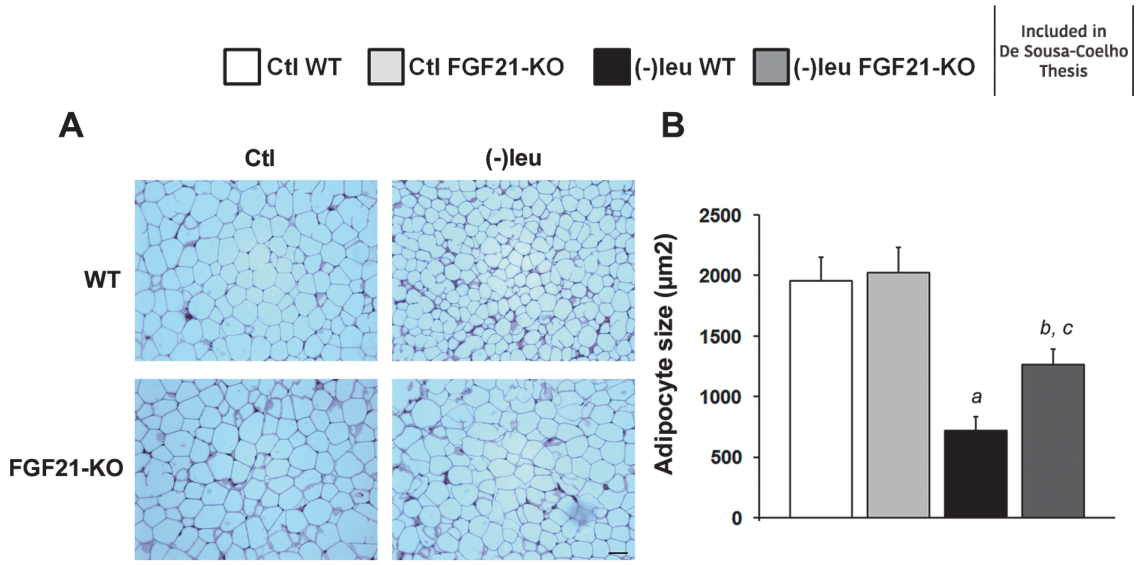

Figure L 5. Leucine-deficient diet effects on adipocyte size are FGF21-dependent. Representative hematoxylin and eosin (H&E)-stained eWAT sections from WT and FGF21-KO mice (×20 magnification). Scale bar, 50 mM (A). Adipocyte size was measured by IMAT programme , using at least three different randomly chosen fields of eWAT sections from each mouse. Error bars represent the mean ± standard error of the mean (SEM). a, $p<0.05$ versus Ctl WT; b, $p<0.05$ versus Ctl FGF21-KO; c, $p<0.05$ versus (-)leu WT (n=6/group).

The histological analysis of eWAT showed that leucine deprivation resulted in a reduction in adipocyte volume compared with mice fed a control diet. By contrast, the adipocyte volume was only slightly reduced in (-)leu-fed *FGF21-KO* animals and remained unchanged in FGF21-KO mice on the control diet (Figure L5A). We note that other groups reported increased (Hotta et al. 2009) or decreased (Dutchak et al. 2012) adipocyte size in FGF21-KO mice on regular diets.

3.2 FGF21 mediates increased lipolysis upon leucine deficiency

It has been previously described that leucine deprivation increases lipolysis in WAT (Cheng et al. 2010). It has also been suggested that FGF21 stimulates lipolysis in WAT during normal feeding, but inhibits it during fasting (Hotta et al. 2009). Therefore, to examine the role of FGF21 in lipolysis, we evaluated the mRNA levels of adipose triglyceride lipase (*Atgl*), hormone-sensitive lipase (*Hsl)*, and perilipin 1(*Plin1)*, and the levels of phosphorylated HSL.

3.2.1 Leucine deficiency doesn't change mRNA levels of lipolysis related genes in eWAT.

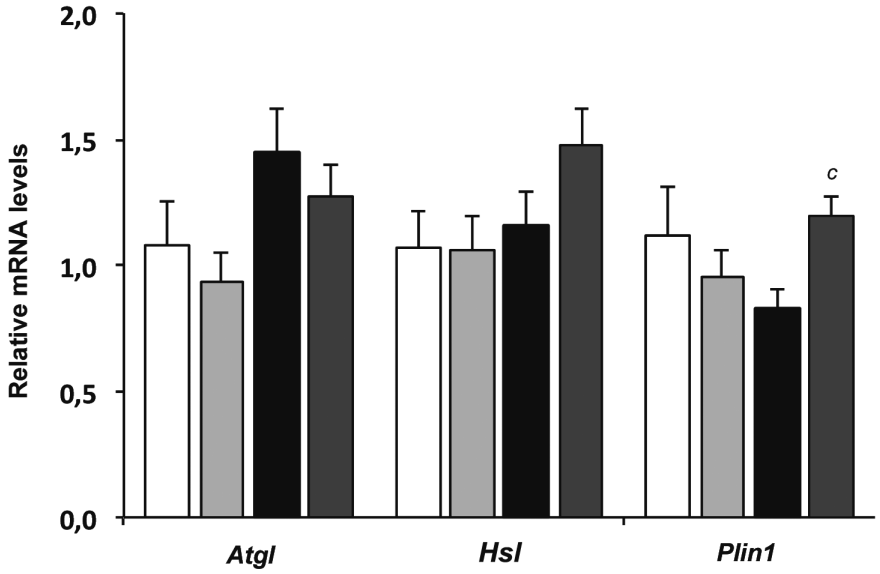

Figure L 6 . mRNA levels of lipolysis-related genes in eWAT. *Atgl, Hsl* and *Plin1* gene expression was measured by qRT-PCR in mice eWAT. Error bars represent the mean ± standard error of the mean (SEM). a, $p<0.05$ versus Ctl WT; b, $p<0.05$ versus Ctl FGF21-KO; (n=6/group).

The analysis of eWAT mRNA levels of *Atgl*, *Hsl* and *Plin1* did not find any statistically significant changes upon leucine deprivation (Figure L6). However, HSL activity is mainly modulated by its phosphorylation by protein kinase A (PKA). Thus, we next analysed HSL phosphorylation by Western blot.

3.2.2 *Increased phosphorylation of HSL under leucine deprivation is FGF21 dependent*

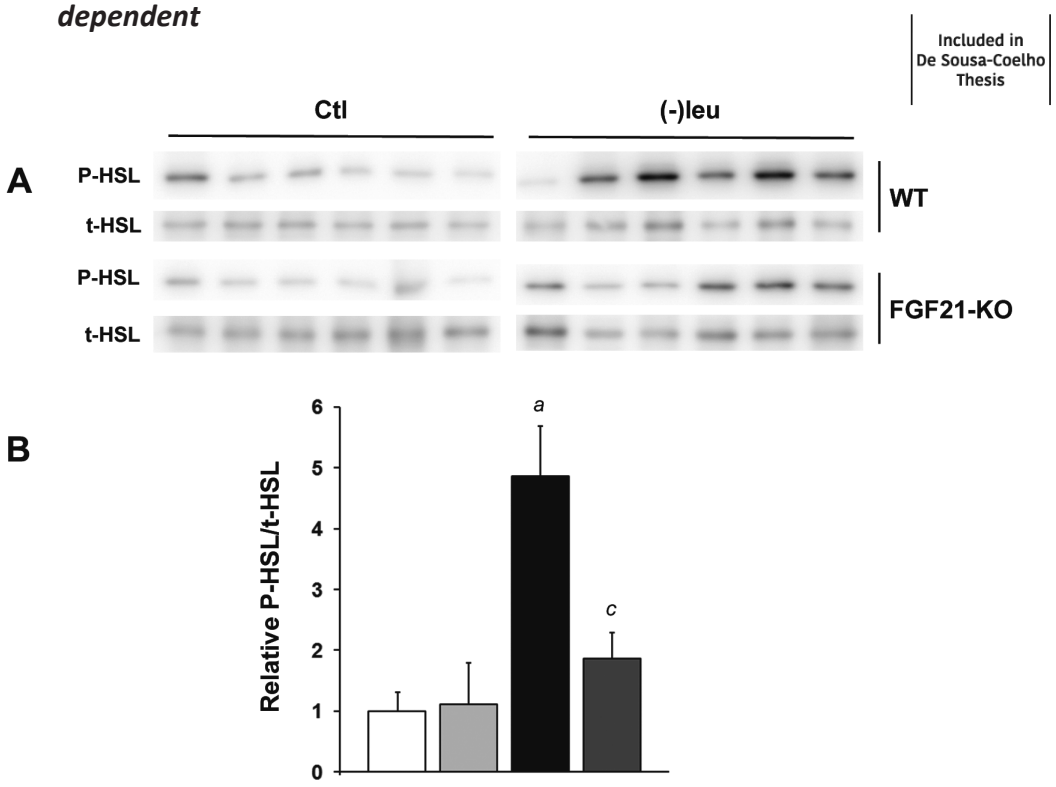

Figure L 7. FGF21-dependent phosphorylation of HSL in mice fed a leucine-deficient diet. Phosphorylated and total HSL protein levels were measured in WT and FGF21-KO eWAT homogenates by Western blot analysis (A). The bottom panel shows quantification by densitometry of phosphorylated HSL normalized to total HSL, using Image J software (B). Error bars represent the mean ± standard error of the mean (SEM). a, $p<0.05$ versus Ctl WT; c, $p<0.05$ versus (-)leu WT (n=6/group).

Consistent with changes in body weight and adipocytes size, lack of FGF21 significantly decreased levels of phosphorylated HSL in WAT under leucine deprivation (Figure L7), which suggests that lipolysis was impaired in these mice. Despite the evidence of increased lipolysis under leucine deprivation, levels of free fatty acids in serum were not significantly altered in the conditions analysed (Table1, Section 6). This observation suggests increased fatty acid utilization by other tissues.

3.3 FGF21 mediates the downregulation of lipogenesis-related genes upon leucine deficiency in eWAT

As lipogenic genes are downregulated in eWAT of leucine-deprived mice (Cheng et al. 2010), we speculated that FGF21 might regulate their expression. To investigate this possibility, we examined the expression of genes involved in

lipogenesis in eWAT of wild-type and FGF21-KO mice maintained either on Ctl or (-)leu diet.

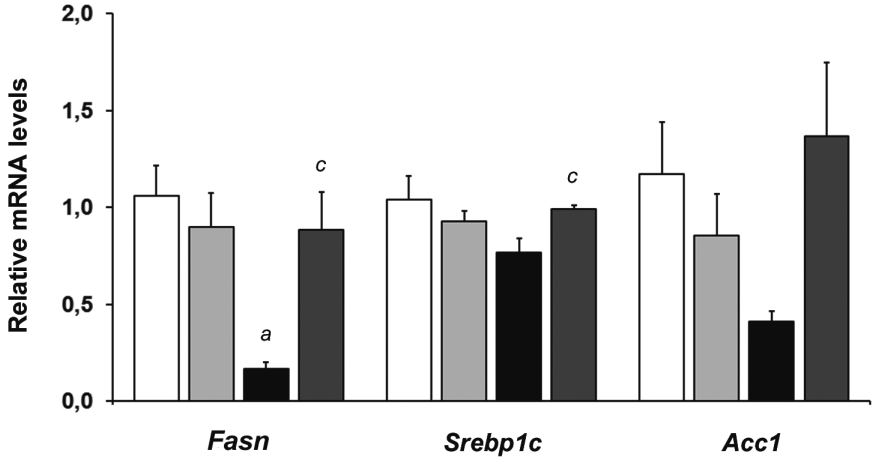

Figure L 8. mRNA levels of lipogenic genes in eWAT. *Fasn, Srebp1c* and *Acc1* gene expression was measured by qRT-PCR in mice eWAT. Error bars represent the mean ± standard error of the mean (SEM). a, p<0.05 versus Ctl WT; c, p<0.05 versus (-)leu WT (n=6/group).

As expected, gene expression analysis in eWAT revealed that the mRNA levels of the lipogenic genes fatty acid synthase (*Fasn)*, sterol regulatory element-binding protein 1c (*Srebp1c)* and acetyl CoA carboxylase 1 (*Acc1)* were lower in this tissue in mice maintained on the (-)leu diet. These changes were blunted in the FGF21-KO animals, particularly for *Fasn* (Figure L8). The analysis of FASN, protein abundance showed a good correlation with the gene expression data (Figure L9). All together, this data show that FGF21 mediates the impairment of lipogenesis in eWAT of leucine-deprived mice.

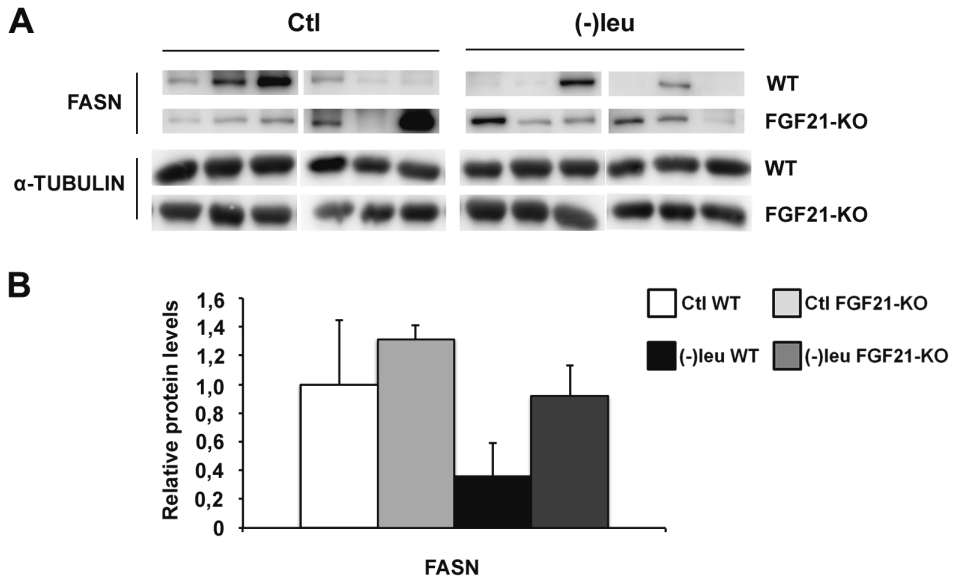

Figure L 9. FASN protein levels are downregulated by FGF21 in mice on a leucine-deficient diet. FASN protein levels were detected by western blot analysis in mice eWAT (A). The bottom panel shows quantification by densitometry of the immunoblotted proteins, using Image J software (B). Error bars represent the mean ± standard error of the mean (SEM), (n=6/group).

3.4 Leucine deficiency induces both *Klb and Fgf21r1c* in eWAT

Given the shocking effects of FGF21 on eWAT of leucine-deprived mice, we questioned whether additional mechanisms enhancing FGF21 were acting. Consequently, we analysed the expression of the FGF21-receptor *Klb* and *Fgfr1*.

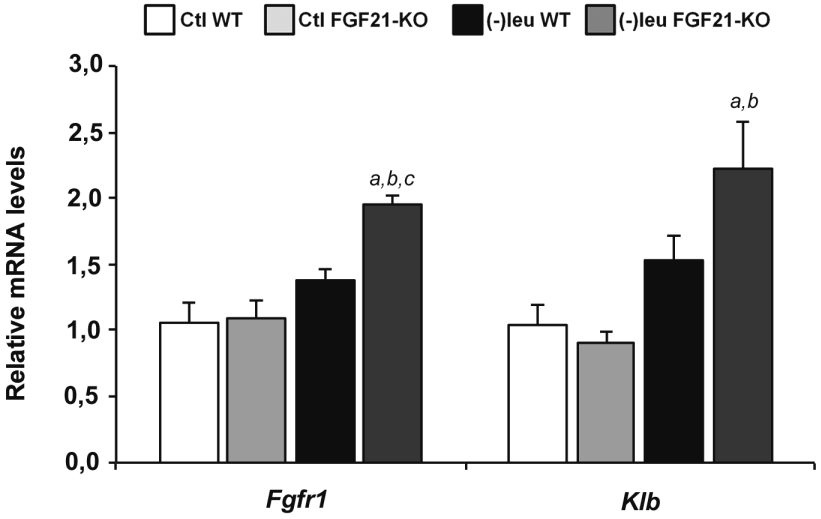

Figure L 10 *FgfR1* and *Klb* are upregulated in eWAT of leucineB deprived mice. *FgfR1* and βt *Klotho* gene expression was measured by qRTt PCR in mice eWAT. Error bars represent the mean ± standard error of the mean (SEM). a, p<0.05 versus Ctl WT; b, p<0.05 versus Ctl FGF21---KO; c, p<0.05 versus (---)leu WT (n=6/group).

Leucine deprivation increased *Klb* and *Fgfr1* mRNA levels in both genotypes but only reached statistic significance in the FGF21-KO mice (Figures L10). A compensative mechanism can explain this observation. The components of the receptor complex are overexpressed to compensate lack of FGF21 signalling in the FGF21-KO animals.

3.5 Expression of lipogenic and lipolytic genes in 3T3L1 treated with FGF21

To further confirm the results obtained in mice, we analysed the expression of lipid metabolism genes in 3T3L1 cells treated with FGF21.

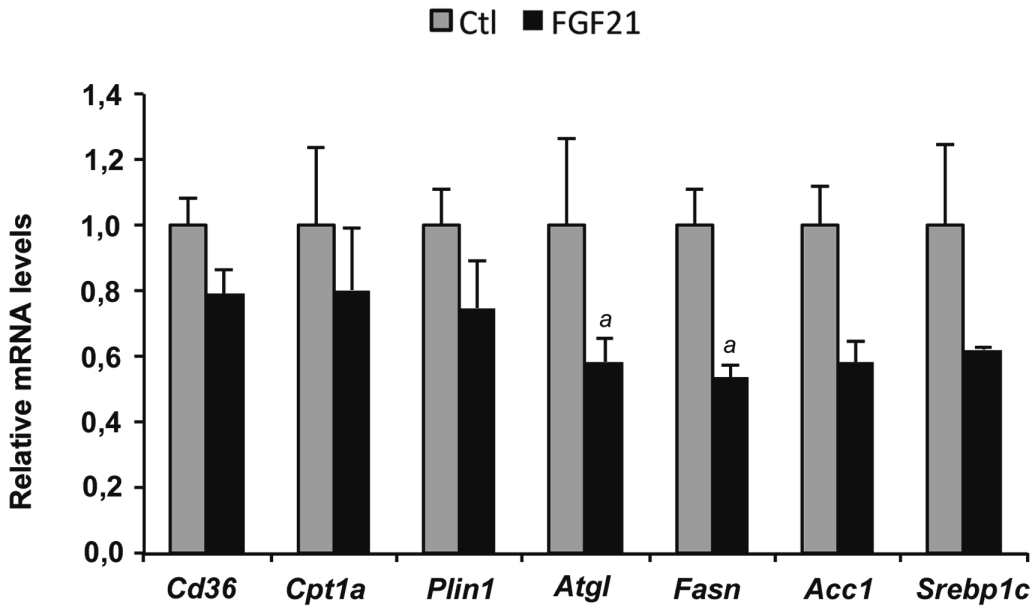

Figure L 11. Regulation of lipid metabolism genes by FGF21 in 3T3L1 adipocytes. The expression of genes related with lipid metabolism pathways was measured by qRT-PCR in 3T3L1 adipocytes treated with recombinant FGF21 (100nM) for 24h. Error bars represent the mean ± standard error of the mean (SEM). a, $p<0.05$ versus Ctl (n=3).

Consistent with mice results, the expression of the lipogenic genes *Fasn, Srebp1c*, and *Acc1* was repressed by FGF21 treatment. In addition, *Atgl* expression was also decreased. (Figure L11).

3.6 Increased FGF21 expression under leucine deprivation do not affect adiponectin circulating levels

Adipose tissue is not only the main target tissue of FGF21 but also a necessary mediator of its actions. Adiponectin secretion by adipocytes mediates the effects produced by the pharmacological administration of FGF21, including changes in EE, lower blood glucose levels and insulin sensitizing effects (Holland et al. 2013; Lin et al. 2013). Given the high levels of FGF21 reached in leucine-deprived mice we examined whether adiponectin serum levels were changed in this condition.

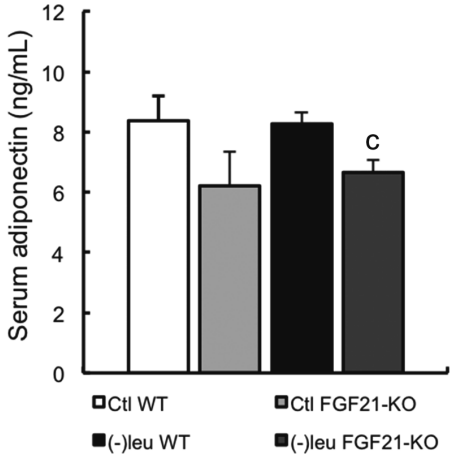

Figure L 12. Circulating Adiponectin is diminished in FGF21 null mice. Serum adiponectin protein concentrations were measured by ELISA. Error bars represent the mean ± standard error of the mean (SEM). c, $p<0.05$ versus (-)leu WT (n=6/group).

Leucine deprivation, and associated increased FGF21 blood levels, did not produce changes in adiponectin circulating levels. However, and consistent with the role of FGF21 in the regulation of adiponectin secretion, FGF21 deficiency decreased serum adiponectin concentration (Figure L12).

4 FGF21 deficiency prevents changes in liver of leucine-deprived mice

4.1 FGF21 mediates the downregulation of lipogenesis-related genes upon leucine deficiency in liver

A link between FGF21 and SREBP1c during lipogenesis in cultured hepatocytes has recently been proposed (Zhang et al. 2011). As lipogenic

genes are downregulated in liver of mice deprived of leucine (Guo & Cavener 2007), we speculated that FGF21 might regulate their expression.

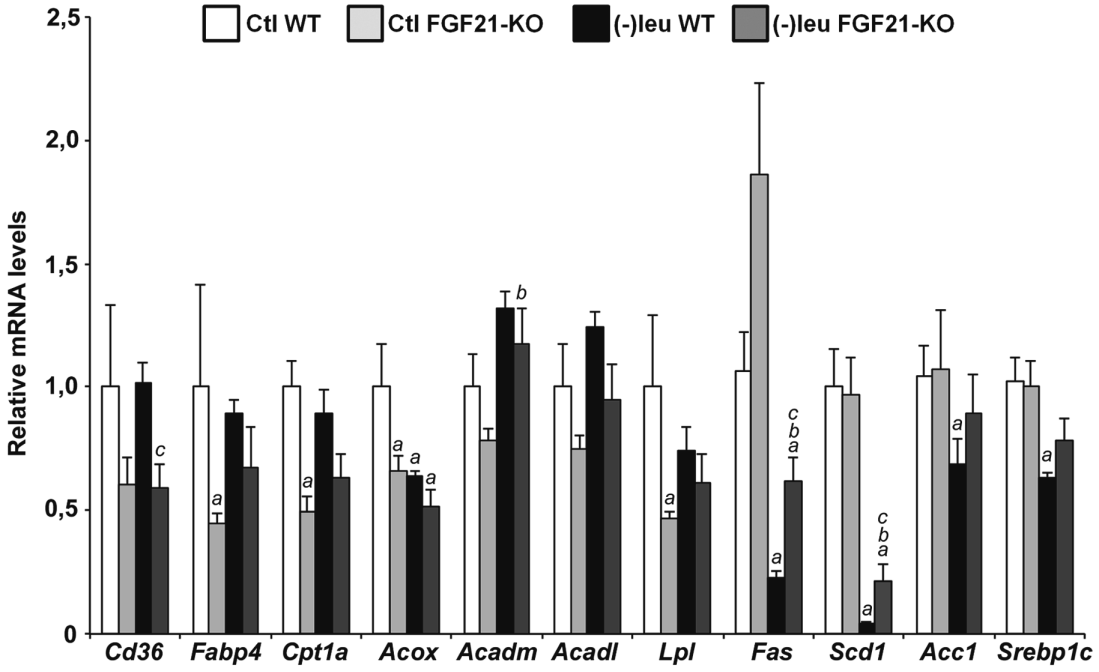

Figure L 13. FGF21 regulation of of lipid metabolism genes in liver of leucine-deprived mice. Expression of genes related with lipid handling was measured by qRT-PCR in mouse liver. a, p<0.05 versus Ctl WT; b, p<0.05 versus Ctl FGF21-KO; c, p<0.05 versus (-)leu WT (n=6/group).

As expected, levels of *Fasn*, *Srebp1c* and *Acc*1 mRNA were significantly decreased on the (-)leu diet. However, in mice lacking FGF21, the reduction of *Fasn* expression was statistically significantly blocked, and, although not statistically significant, *Srebp1c* and *Acc1* showed both the same tendency (Figure L13). The expression of other genes involved in fatty acid uptake [cluster of diferentiation 36 (*Cd36),* fatty acid binding protein 4 *(Fabp4*)] or oxidation [carnitine palmytoiltransferase 1a (*Cpt1a*)] was decreased in the absence of *Fgf21*.

The analysis of FASN, SREBP1c, and ACC1 protein abundance showed a good correlation with the gene mRNA levels (Figure L14). In addition, ACC1 phosphorylation (which inhibits its activity) was decreased under leucine deprivation in both wild-type and *FGF21-KO* mice.

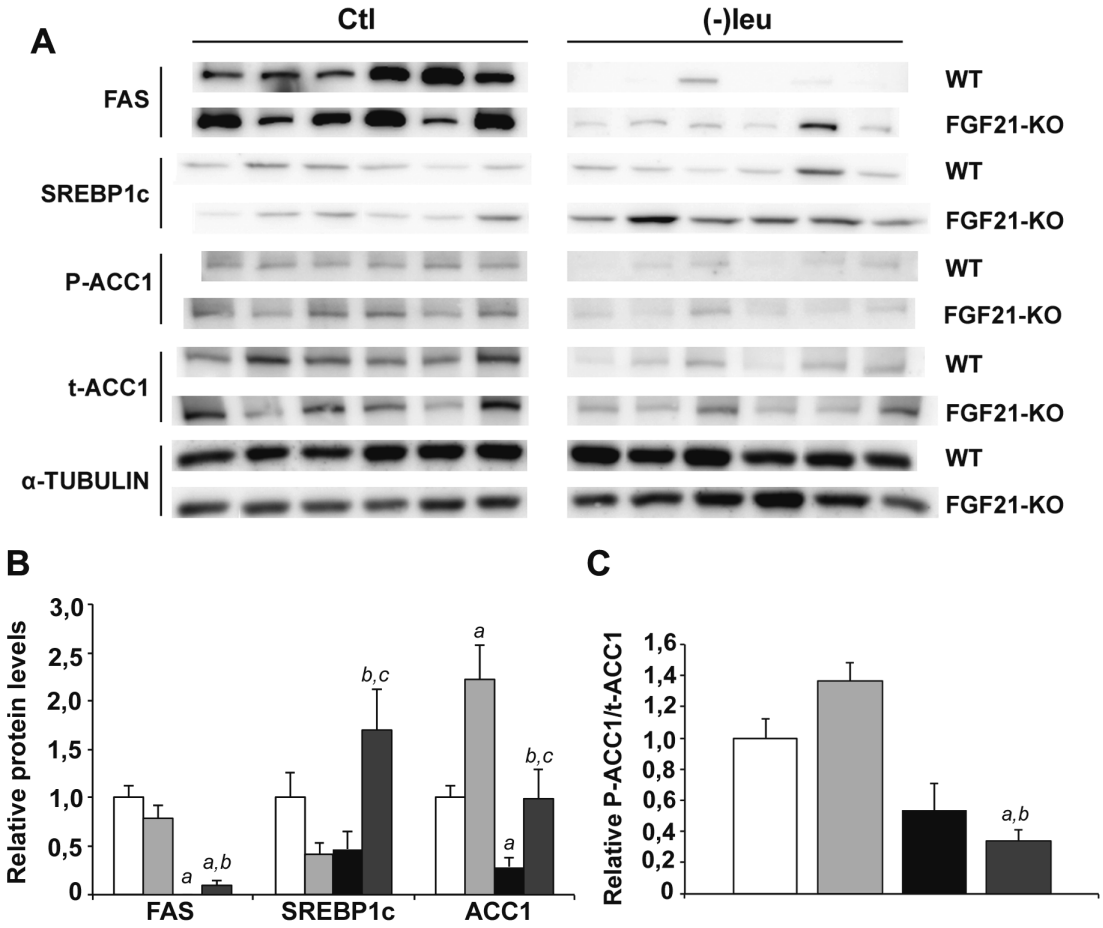

Figure L 14. FGF21 reduces abundance of lipogenesis related proteins in liver of mice fed a leucine-deficient diet. FASN, SREBP1c and p-ACC1 and total ACC1 protein levels were detected by western blot analysis in mouse liver (A). The bottom panels (B,C) show quantification by densitometry of the immunoblotted proteins, using Image J software. Error bars represent the mean ± standard error of the mean (SEM). a, $p<0.05$ versus Ctl WT; b, $p<0.05$ versus Ctl FGF21-KO; c, $p<0.05$ versus (-)leu WT (n=6/group).

4.2 FGF21 deficiency abolish the reduction in lipid content in liver upon leucine deficiency

Although liver triglyceride levels, measured by extraction and posterior quantification, did not reflect the expression pattern of the lipid synthesis genes, haematoxylin and eosin staining revealed it.

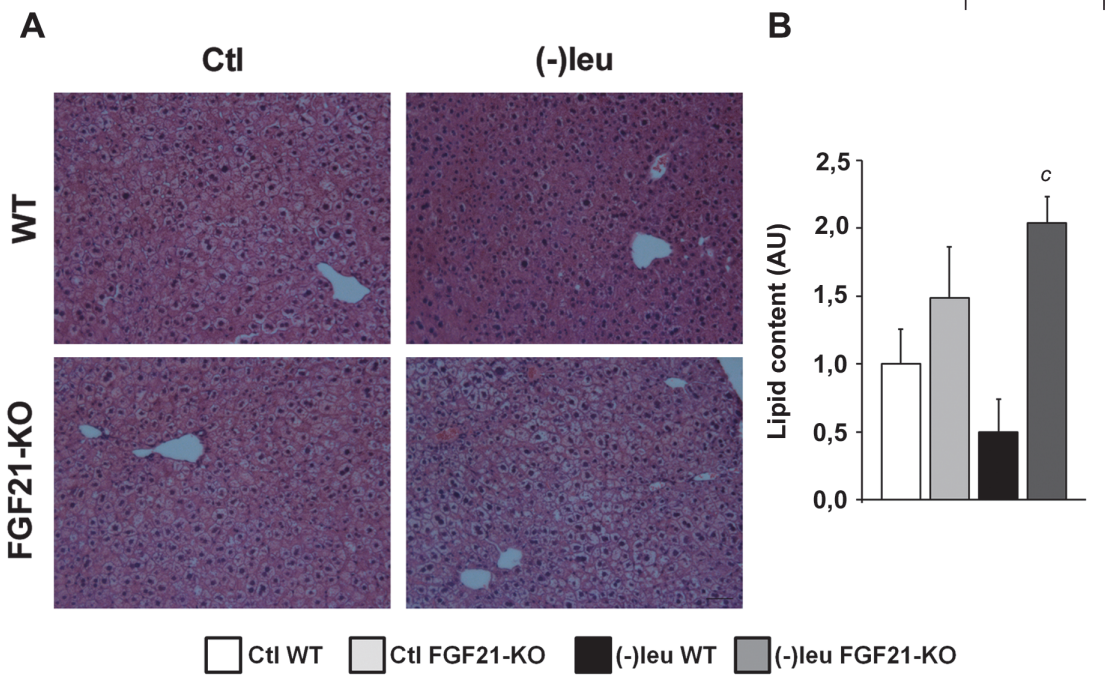

Figure L 15. FGF21-KO liver has impaired lipid accumulation in response to leucine deprivation. Histological appearance and hepatic lipid accumulation of H&E liver staining of WT and FGF21-KO mice maintained either on a Ctl or a (-)leu diet. Representative H&E-stained hepatocytes are shown (×20 magnification) (A). Scale bar, 50 mM. Lipid accumulation (B) was measured by IMAT programme, using at least three different randomly chosen fields of liver sections from each mouse. c, $p<0.05$ versus (-)leu WT (n=6/group).

The staining and consequent quantification of lipid content suggested a decreased lipid accumulation under leucine deprivation in wild-type animals that does not seem to occur in the FGF21-KO mice (Figure L15).

5 FGF21 deficiency prevents BAT activation of leucine-deprived mice

5.1 FGF21 mediates the upregulation of *Ucp1* and *Dio2* upon leucine deficiency in BAT

Thermogenesis in BAT is mediated by the upregulation of UCP1 (Matthias et al. 2000). It has been proposed that the induction of FGF21 production by the liver mediates direct activation of brown fat thermogenesis during the fetal-to-neonatal transition (Hondares et al. 2010). FGF21 also regulates PPAR gamma coactivator 1 (PGC1) α and browning of white adipose tissues in adaptive thermogenesis (Fisher et al. 2012). Therefore, in order to analyse the effect of high FGF21 circulating levels during leucine deprivation on thermogenesis, we

analysed the expression of several genes involved in thermogenesis in BAT of wild-type or FGF21 null mice fed a Ctl or (-)leu diet.

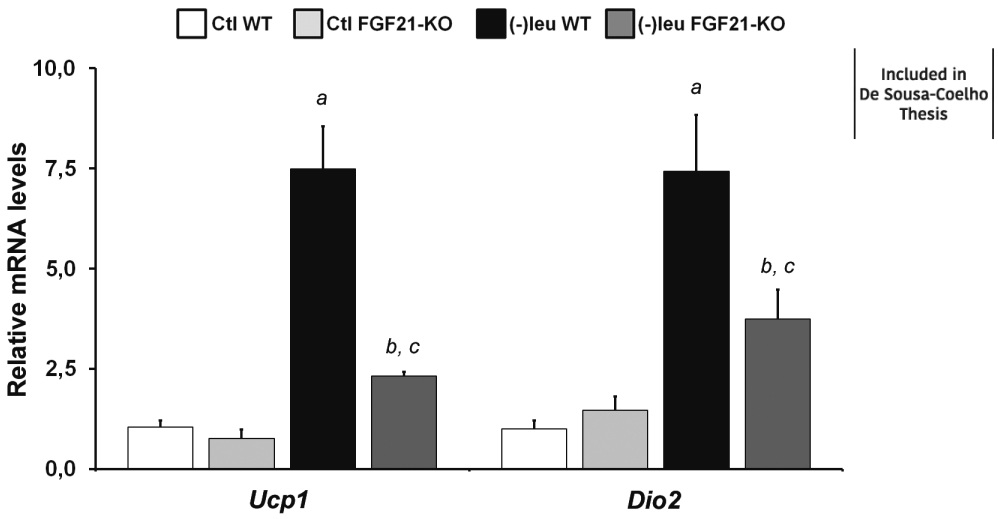

Figure L 16. FGF21 is required for inducing BAT activation during amino acid deprivation. *Ucp1* and *Dio2* gene expression was measured by qRT-PCR in mice BAT. Error bars represent the mean ± standard error of the mean (SEM). a, $p<0.05$ versus Ctl WT; b, $p<0.05$ versus Ctl FGF21-KO; c, $p<0.05$ versus (-)leu WT (n=6/group).

Consistent with previous results (Cheng et al. 2009), leucine deprivation caused an increase of *Ucp1* and *Dio2* mRNAs in wild-type mice. These changes were blocked in FGF21-KO mice (Figure L16). Because *Ucp1* expression is related to EE, the absence of induction of *Ucp1* in FGF21-KO under leucine deprivation may contribute to the decrease in weight loss observed under these circumstances.

5.2 Leucine deprivation triggers expression of *Pgc-1α, PparϒΥ* and *Adrb3* in BAT

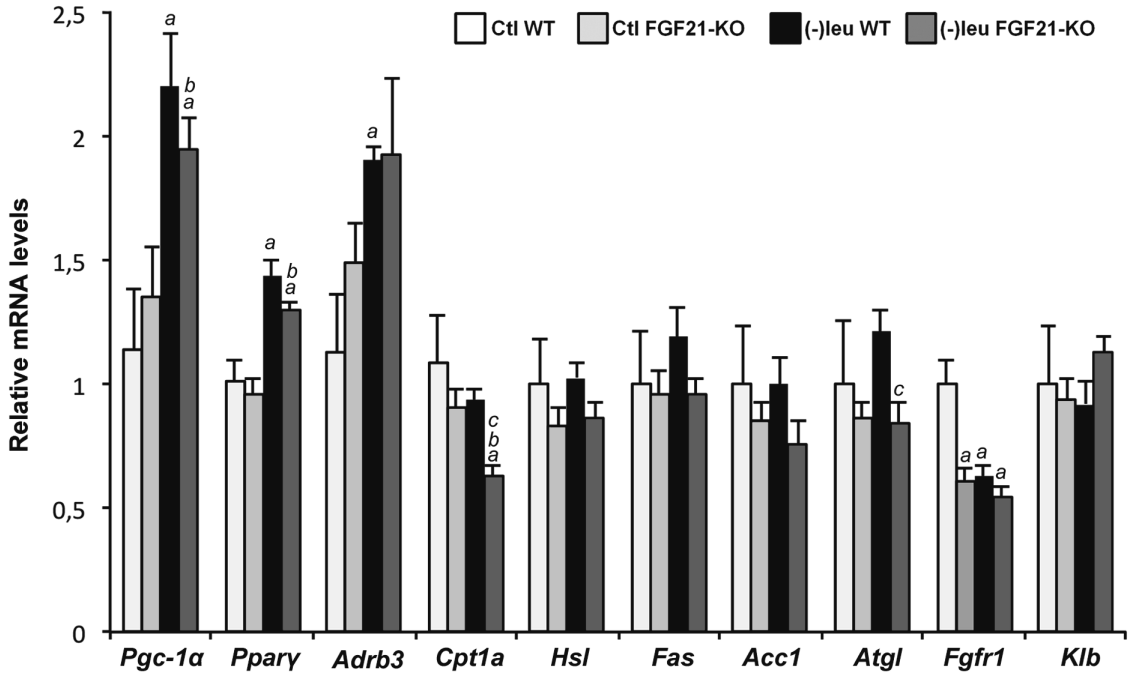

Figure L 17. The role of FGF21 in the expression of genes related with lipid metabolism in BAT of leucine-deprived mice. The expression of genes related with lipid metabolism was measured by qRT-PCR in mice BAT. Error bars represent the mean ± standard error of the mean (SEM). a, p<0.05 versus Ctl WT; b, p<0.05 versus Ctl FGF21-KO; c, p<0.05 versus (-)leu WT (n=6/group).

The analysis of other genes involved in thermogenesis and lipid metabolism revealed interesting data. mRNA levels of *Pgc1α*, which regulates the expression of UCP1 (Handschin & Spiegelman 2006), were increased by leucine deprivation. However, they did not differ between wild-type and FGF21-KO mice under either control or (-)leu diet conditions. The same pattern as for peroxisome proliferator-activated receptor gamma (*Pparγ)* and *Pgc1α*, was observed for adrenoreceptor beta 3 (*Adrb3)* mRNA levels (Figure L17). These data propose that part of the thermogenic programme is induced by leucine deficiency independently of FGF21.

5.3 Upregulation of *Ucp1* is independent of the p38 MAPK signalling

Given the upregulation of *Adrb3* mRNA levels by leucine deficiency (FigureL17) and the well described role of p38MAPK in the regulation of *Ucp1* (Cao et al. 2001), we tested the possibility that the activation of p38 by the ADRB3 participated in the induction of *Ucp1* gene in BAT under this situation.

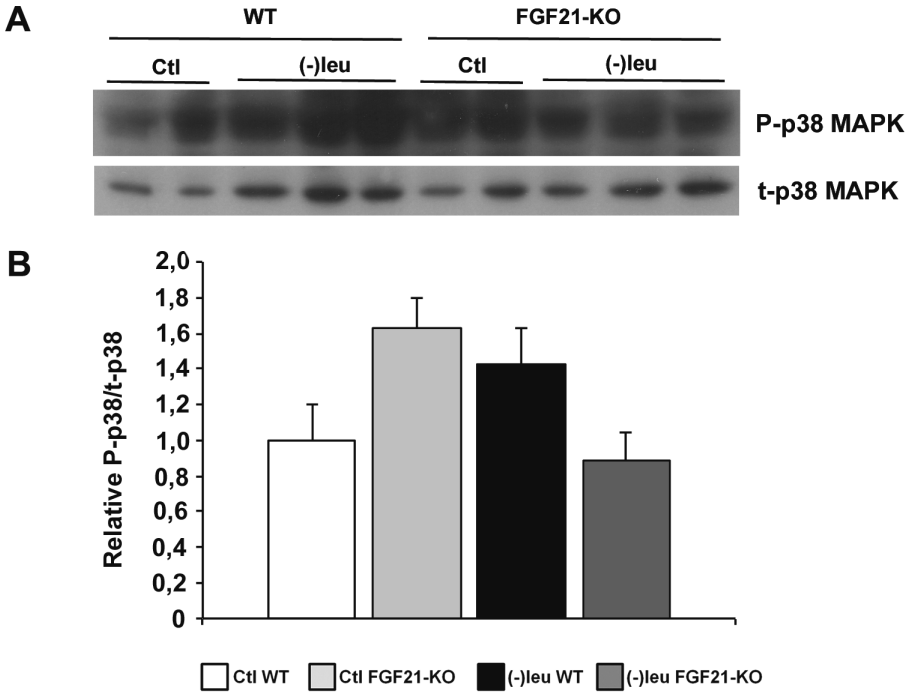

Figure L 18. Phosphorylation of p38MAPK does not change upon leucine deprivation or FGF21 deficiency. Phosphorylated and total p38 MAPK levels were measured in WT and FGF21-KO mouse liver extracts by Western blot analysis. The below panel (B) shows quantification by densitometry of phosphorylated p38 MAPK normalized to total p38 MAPK, using Image J software.

However, phosphorylated p38 levels remained unchanged between diets and genotypes (Figure L18). This result discards p38MAPK pathway as the mediator of FGF21 effects on BAT during leucine deprivation.

5.4 FGF21 treatment represses *Fasn* and increases glycerol release in primary brown adipocytes

To better understand the effect of FGF21 on BAT, and to characterize it as a direct effect, we analysed the expression of lipogenic and lipolytic genes and glycerol release in primary brown adipocytes treated with FGF21.

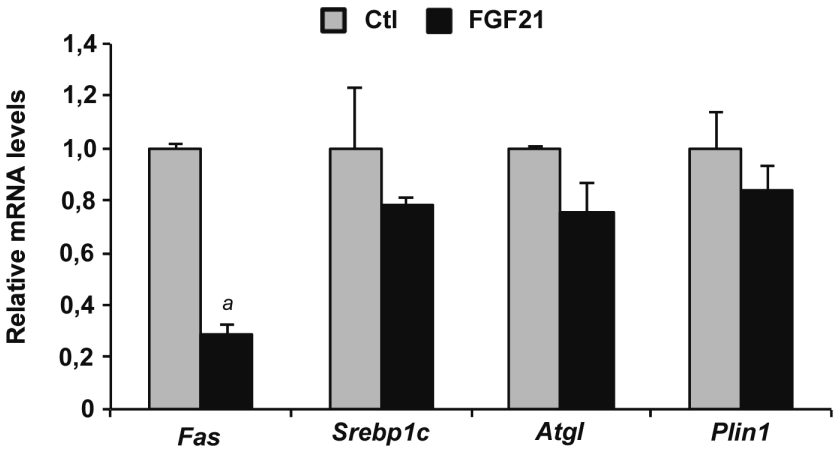

Figure L 19 Expression of genes related with lipid metabolism in FGF21-treated primary brown adipocytes. *Fasn*, *Srebp1c*, *Atgl* and *Plin1* gene expression was measured by qRT-PCR in differentiated primary BAT treated with FGF21 (50nM) for 24h.). a, p<0.05 versus Ctl (n=3)

This treatment decreased the expression of *Fasn* and increased glycerol release without significant changes in the expression of *Atgl* and *Plin* (Figure L19 and L20). Accordingly, mRNA levels of *Hsl* and *Atgl* as well as HSL phosphorylation did not change in BAT of *Fgf21*-deficient mice (Figures L17 and L21).

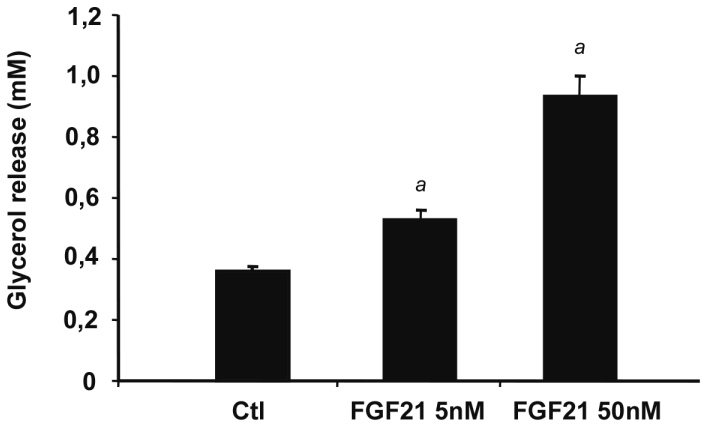

Figure L. 20 FGF21 increases glycerol release in primary brown adipocytes. Glycerol release in differentiated primary BAT treated with FGF21 (5nM and 50nM) for 24h. a, p<0.05 versus Ctl (n=3)

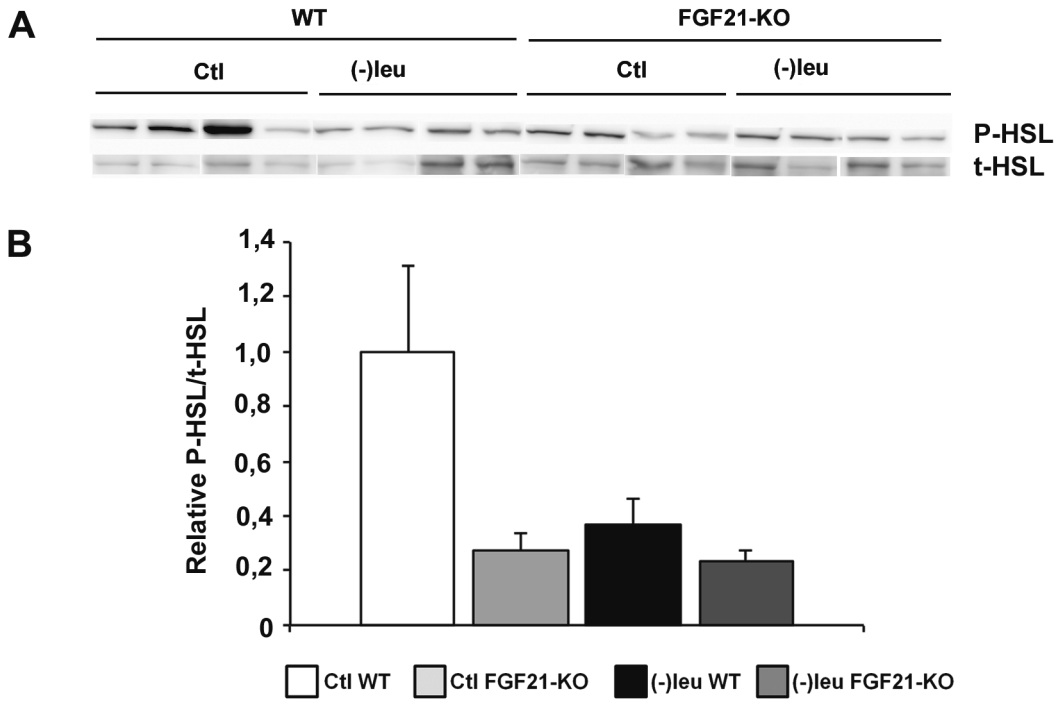

Figure L 21 Phosphoryation of HSL do not change upon leucine deprivation or FGF21 deficiency. Phosphorylated and total HSL protein levels were measured in WT and FGF21-KO BAT homogenates by Western blot analysis. The bottom panel shows quantification by densitometry of phosphorylated HSL normalized to total HSL, using Image J software. Error bars represent the mean ± standard error of the mean (SEM. Error bars represent the mean ± standard error of the mean (SEM). (n=6/group).

6 Serum biochemical parameters of leucine-deprived mice

Since leucine deprivation, via FGF21, caused striking metabolic changes in liver, WAT and BAT, we examined how this changes were affecting basic serum biochemical parameters. Thus, we measured non-esterified fatty acids (NEFAs), triglycerides, cholesterol, glucose, glycerol and insulin in wild-type and FGF21 null mice fed a complete diet or a leucine-deficient diet.

Table 1. Serum measurements in mice maintained on different diets

	Ctl WT	Ctl FGF21-KO	(-)leu WT	(-)leu FGF21-KO
NEFA (nmol/l)	0,79±0,11	1,05±0,11	0,73±0.09	0,82±0.06
Triglycerides (mg/dl)	95,79±7,18	153,73±11,62[a]	99,39±15,36	186,08±27,38[a,c]
Cholesterol (mg/dl)	101,13±13,13	147,65±4,21[a]	96,40±7,69	122,55±3,08[b,c]
Glucose (mg/dl)	209,43±10,45	212,90±7,88	185,53±14,87	187,02±9,55

Glycerol (μmol/l)	393,50±38,32	520,95±23,10[a]	313,93±26,56	372,16±19,99[b]
Insulin (μg/l)	1,26±0,23	2,01±0,52	0,41±0.04[a]	1,21±2,20[c]

All data are expressed as means ± SEM. Significant differences were assessed by a two-tailed Student's *t*-test. P<0.05 was considered statistically significant. N=6/group of mice. [a] P<0.05 versus Ctl WT mice. [b] P<0.05 versus Ctl FGF21-KO mice. [c] P<0.05 versus (-)leu WT mice

When pharmacologically administered, FGF21 reduces circulating glucose and NEFAs (Fisher et al. 2010) as well as triglycerides (Kharitonenkov et al. 2005) and cholesterol (Emanuelli et al. 2015). In addition, leucine deprivation decreases glycerol and NEFAs (Cheng et al. 2009).

Among all parameters analysed, only insulin was modified by leucine deprivation. Insulin levels were significantly lower in leucine-deprived mice and lack of FGF21 reverted this effect. Although not significant, glycerol and NEFAs presented the same tendency of previously reported data. Finally, lack of FGF21 significantly increased triglycerides, cholesterol and glycerol levels, which agrees with the beneficial effects of pharmacological administration of FGF21 on these parameters.

7 Leucine deprivation activates the mitogen activated protein kinase ERK1/2 signalling pathway in liver independently of FGF21.

As described, MAPK ERK1/2 signalling is required for the amino acid starvation response (Thiaville et al. 2008; Pan et al. 2007) and a downstream signal of FGF21 (Adams et al. 2012; Fisher et al. 2011). Thus, we next studied the role of ERK1/2 signalling in the FGF21-mediated response to amino acid starvation.

7.1 Inhibition of ERK1/2 phosphorylation blocks the amino acid deficiency response mediated by ATF4

To study the relation between amino acid limitation and ERK1/2 signalling pathway, HepG2 cells were treated with the MEK inhibitor PD98 and histidinol, which blocks charging of histidine onto the corresponding tRNA, and thus mimics histidine deprivation,

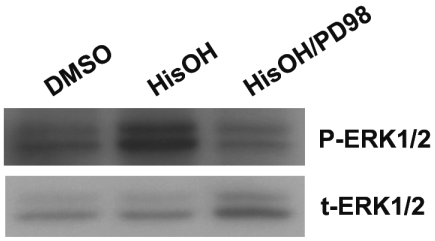

Figure L 22 Histidinol induces ERK1/2 phosphorylation. HepG2 cells were incubated for 8h with HisOH (2mM) and the MEK inihibitor PD98 (30µM), when indicated. Phosphorylation of ERK1/2 was analyzed by Western blot in HepG2 extracts.

Histidinol treatment of HepG2 cells induced the phosphorylation of ERK1/2, which was reversed by PD98. (Figure L22).

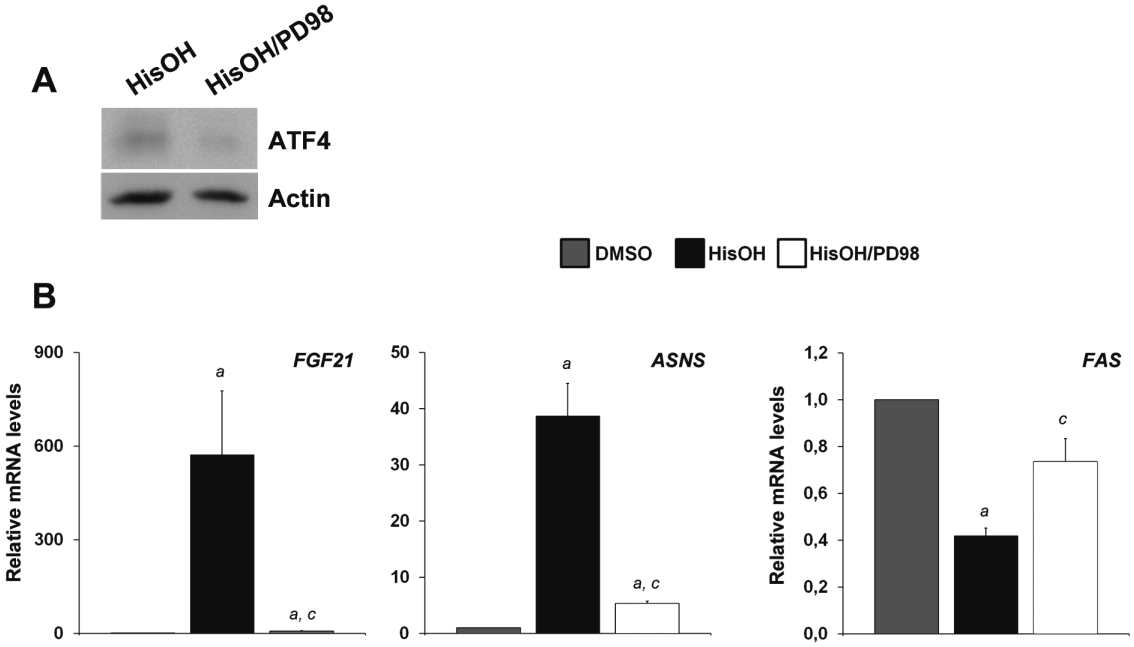

Figure L 23. Increased expression of *Fgf21* is a downstream signal of ERK1/2 phosphorylation. ATF4 protein levels (A) were analyzed by Western blot in nuclear HepG2 extracts. mRNA levels for *FGF21, ASNS* and *FASN* (B) were analyzed by qRT-PCR. a, $p<0.05$ versus DMSO; c, $p<0.05$ versus HisOH (n=3).

In addition, histidinol treatment increased ATF4 protein levels (Figure L23A), as well as its target genes *FGF21* and asparagine synthetase (*ASNS*) mRNA levels (Figure L23B). The MEK inhibitor considerably reduced these increases. In these cells, *FASN* expression is opposed to that of *FGF21* (Figure L23B), mimicking what we observed in leucine-deprived wild-type (high FGF21) or *Fgf21* null mice (Figure L13).

7.2 ERK1/2 phosphorylation is induced in liver of leucine-deprived mice independently of FGF21

As it has been described that exogenous FGF21 is able to induce ERK1/2 phosphorylation in the liver and WAT of acutely treated mice (Fisher et al. 2011), we checked ERK1/2 phosphorylation in leucine-deprived wild-type and FGF21 null mice.

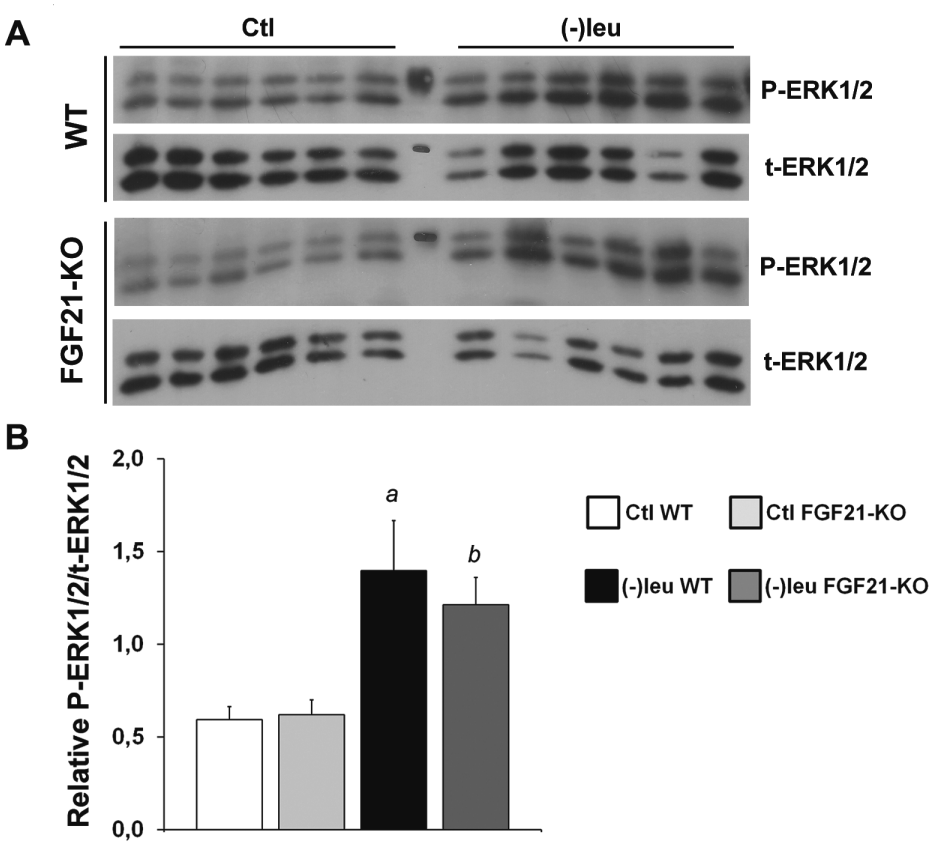

Figure L 24. Activation of the MEK/ERK pathway in the liver by leucine deprivation is independent of FGF21. Phosphorylated and total ERK1/2 levels were measured in WT mouse liver homogenates by Western blot analysis. Error bars represent the mean ± standard error of the mean (SEM). a, $p<0.05$ versus Ctl WT; b, $p<0.05$ versus Ctl FGF21-KO (n=6/group).

ERK1/2 phosphorylation was induced in liver of leucine-deprived animals, although there were no differences between genotypes (Figure L24). Accordingly, the amino acid starvation response programme was correctly initiated in FGF21-KO mice, as shown by the increased levels of ATF4 protein and mRNA levels of *Asns* (Figure L25).

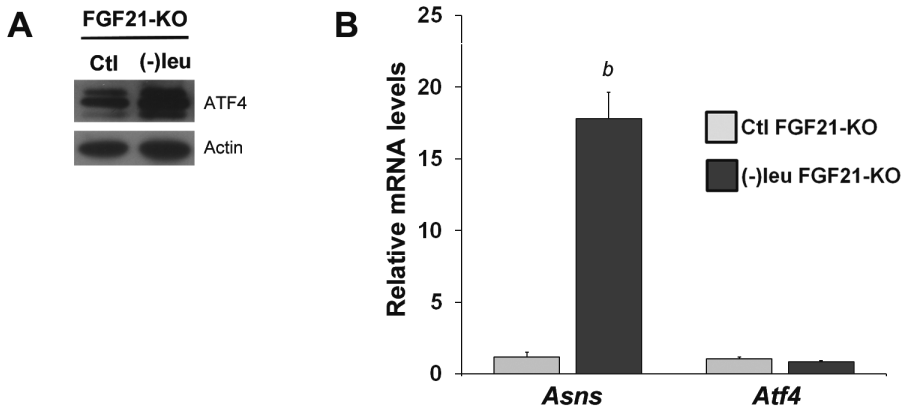

Figure L 25 Leucine deprivation increases ATF4 protein levels and Asns mRNA synthesis in liver of *FGF21-KO* mice. Nuclear ATF4 protein levels (A) and *Asns* and *Atf4* mRNA levels (B) were measured in FGF21-KO mouse liver by qRT-PCR and Western blot, respectively. Actin was used as a loading control. A representative blot is shown. Error bars represent the mean ± standard error of the mean (SEM). b, $p<0.05$ versus Ctl FGF21-KO (n=6/group).

Moreover, despite the fact that FGF21 serum levels are highly increased in leucine-deprived mice (Figure L1A), ERK1/2 phosphorylation is not modified in WAT (Figure L26).

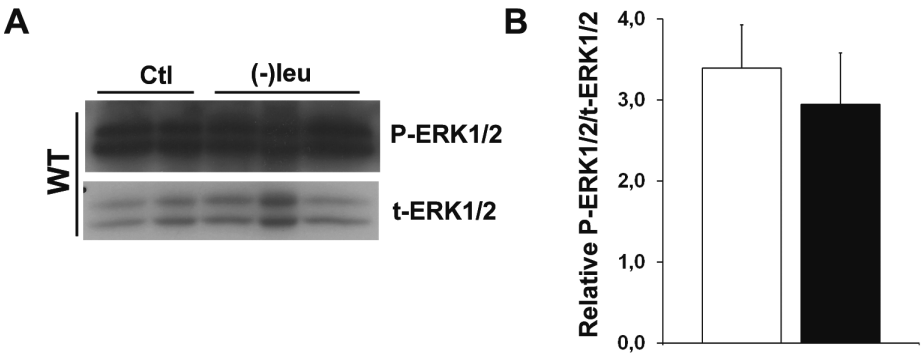

Figure L 26. ERK1/2 phosphorylation is not modified by leucine deprivation in mice eWAT. Phosphorylated and total ERK1/2 levels (A) were measured in WT mice eWAT homogenates by Western blot analysis. The right panel (B) shows quantification by densitometry of phosphorylated ERK1/2 normalized to total ERK1/2, using Image J software. Error bars represent the mean ± standard error of the mean (SEM). (n=6/group).

8 Obesity lessen leucine deprivation effects on energy expenditure

FGF21 mediates most of the beneficial metabolic effects of leucine deprivation (De Sousa-Coelho et al. 2013). In lean mice, leucine deprivation increases

Ucp1 expression increasing EE and drastically reduces body weight in an FGF21-dependent manner. To analyse the putative beneficial effects of leucine deprivation on pathological situations such obesity we maintained Ob/Ob mice under leucine deprivation for 7 days.

8.1 Leucine deprivation reduces food intake in Ob/Ob mice

In lean mice, leucine deficiency decreased daily food intake approximately 1g (Figure L4). Despite disrupted leptin signalling, in Ob/Ob mice, the decrease in food intake is maintained and even higher (1,5g) than in lean animals (Figure L27).

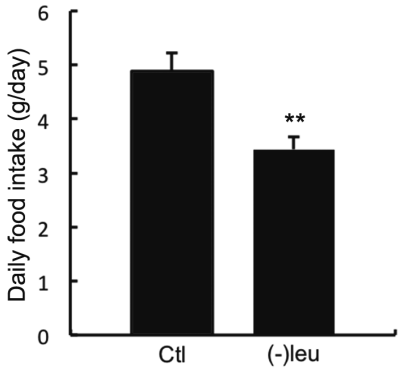

Figure L 27. Leptin is not involved in food aversion caused by leucine-deficient diets. Ob/Ob mice were maintained for 7 days on Ctl diet and 7 days on leucin deficient diet. Food intake was measured daily. **, p<0.01 (n=6/group)

8.2 Ob/Ob mice under leucine deprivation under go the same weight loss than a pair pair-fed Ob/Ob pair-fed mice

To exclude the changes on caloric intake from the effect of the (-)leu diet on body weight, we pair-fed Ob/Ob mice with (-)leu and Ctl diets.

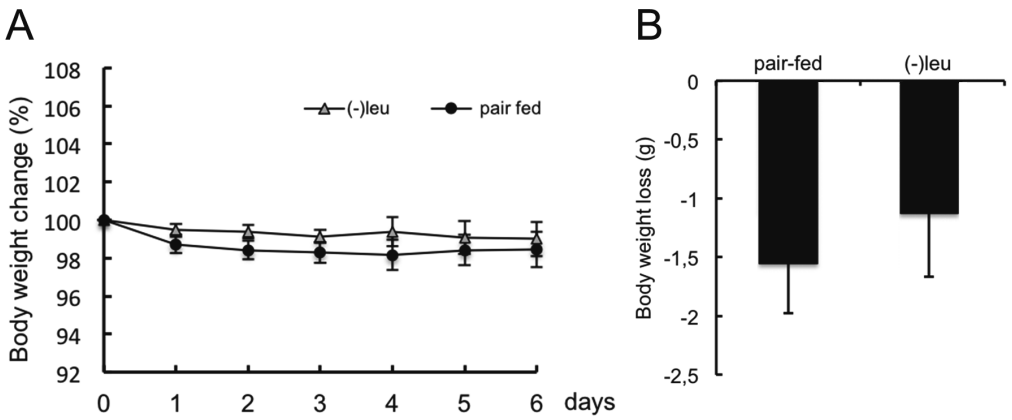

Figure L 28. Leucine-deficient diet causes same weight loss than control pair-fed diet. Body weight of Ob/Ob mice fed with (-)leu diet or a control pair-fed diet (A). The weight on the first day was considered 100%. Body weight change (g) after 7 days of feeding the Ctl or (-)leu diet (B). Error bars represent the mean ± standard error of the mean (SEM). (n=6/group).

Both groups, leucine-deprived and control pair-fed, lost weight in a similar way and no statistical differences were observed (Figure L28A-B). Hence, the reduced food intake is the major responsible for the weight loss in both groups.

8.3 Leucine deprivation induces Ucp1 expression in BAT of Ob/Ob mice

In leucine-deprived lean mice, triggered levels of *Ucp1* in BAT increases thermogenesis and EE (Figure L16) (Cheng et al. 2010). To evaluate this observation in a context of obesity, we analysed *Ucp1* mRNA levels in BAT of Ob/Ob mice fed a (-)leu diet or pair-fed with a Ctl diet.

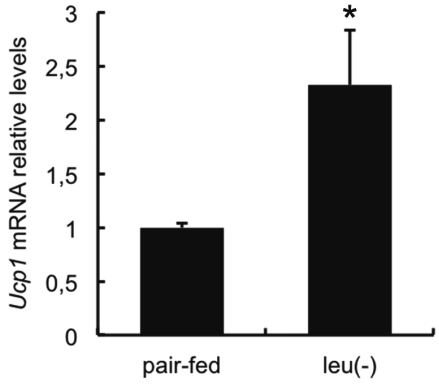

Figure L 29. Ucp1 expression is induced in BAT of Ob/Ob leucine-deprived mice. *Ucp1* gene expression was measured by qRT-PCR in Ob/Ob mice BAT. Error bars represent the mean ± standard error of the mean (SEM). *, $p<0.05$ vs control pair-fed (n=6/group).

Leucine-deprived Ob/Ob mice presented a modest but statistically significant *Ucp1* induction. In these obese mice a 2 fold induction was observed (Figure

L29), while in lean animals the induction was much more higher and reached 7,5 folds (Figure L16).

8.4 *Fgf21* is slightly induced in liver of leucine-deprived Ob/Ob mice

Given that FGF21 partially mediates the weight loss and *Ucp1* induction upon leucine deprivation, we analysed FGF21 serum levels and *Fgf21* hepatic expression in leucine-deprived and pair-fed Ob/Ob mice.

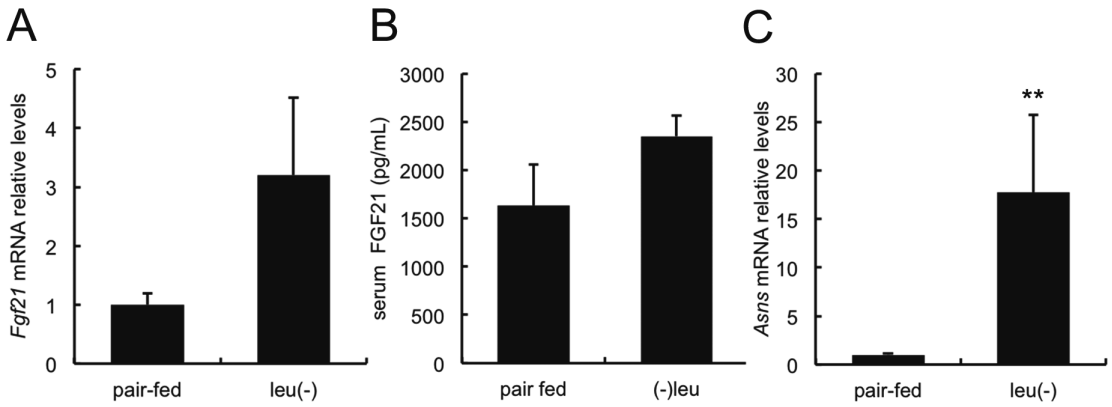

Figure L 30*. Fgf21* mRNA levels and serum concentration of Ob/Ob mice on a leucine-deficient diet. *Fgf21* in liver was measured by qRT-PCR (A). Serum FGF21 protein concentrations were measured by ELISA (B). *Asns* in liver was measured by qRT-PCR (C). Error bars represent the mean ± standard error of the mean (SEM) **, p<0.01 versus Ctl pair-fed (n=6/group).

Fgf21 hepatic expression was slightly induced in leucine-deprived Ob/Ob mice and serum levels paralleled the expression pattern (Figure L30A-B). The induction of *Fgf21* in Ob/Ob mice was much smaller than the induction observed in lean animals (Figure L1). Actually, it didn't reach statistical significance (p=0,12). Remarkably, the pair-fed group presented elevated FGF21 serum levels. This observation is consistent with the notion that obesity is an FGF21-resistant state (Fisher et al. 2010).

To evaluate the AAR in the liver of Ob/Ob mice, we analysed the mRNA levels of the ATF4 target gene *Asns.* Leucine deprivation normally induced *Asns* in the liver of Ob/Ob mice (Figure L30C). This result discards trunked AAR as the mechanism underlying the abnormally slight induction of *Fgf21* in response to leucine deprivation.

THE ROLE OF FGF21 IN THE METABOLIC RESPONSE TO PROTEIN RESTRICTION

Given the unfeasibility to translate single amino acid deprivation to humans, we focussed on low-protein diets (LPDs) instead of amino acid-deficient diets as a more realistic approach.

During the development of the present work, some other groups published data in the same direction that our results. Protein restriction brings about weight loss and an increase in both food intake and EE (Ozaki et al. 2015). Moreover, LPD induces thermogenic markers in BAT of obese rats (Pezeshki et al. 2016). Furthermore, serum concentrations of FGF21 in both rodents and humans increase upon exposure to a LPD, regardless of overall calorie intake. This observation thus reveals that FGF21 is involved in the metabolic response to protein-restricted diets (Laeger et al. 2014).

Here we addressed whether a LPD exerts similar effects on lipid metabolism to those of a (-)leu diet and whether these effects are dependent on hepatic FGF21 production. To this end, we examined the metabolic response of wild-type and *Fgf21* liver-specific knockout mice (L*Fgf21*KO) to a LPD (up to 5% of energy as protein).

1 Generation and characterization of the *Fgf21* liver-specific knockout mice (L*Fgf21*KO)

Although liver is well established as the main source of FGF21, autocrine and endocrine actions of FGF21 in different tissues still on debate. To elucidate the specific role of liver-derived FGF21 during protein restriction we generated the *Fgf21* liver-specific knockout mice (L*Fgf21*KO).

To generate the L*Fgf21*KO mice, $Fgf21^{loxP}$ mice that have *Fgf21 loxP* sites flanking exons 1-3 were crossed with Albumin-cre mice. The latter express the CRE recombinase enzyme under control of albumin promoter/enhancer

elements, thus allowing liver-specific gene deletions. After several generations, the homozygous mutant was obtained. *Fgf21*^{LoxP} mice were used as controls.

Mice were genotyped by PCR (Figure 0A) and the expression of *Fgf21* was analysed in liver, BAT, eWAT and scWAT.

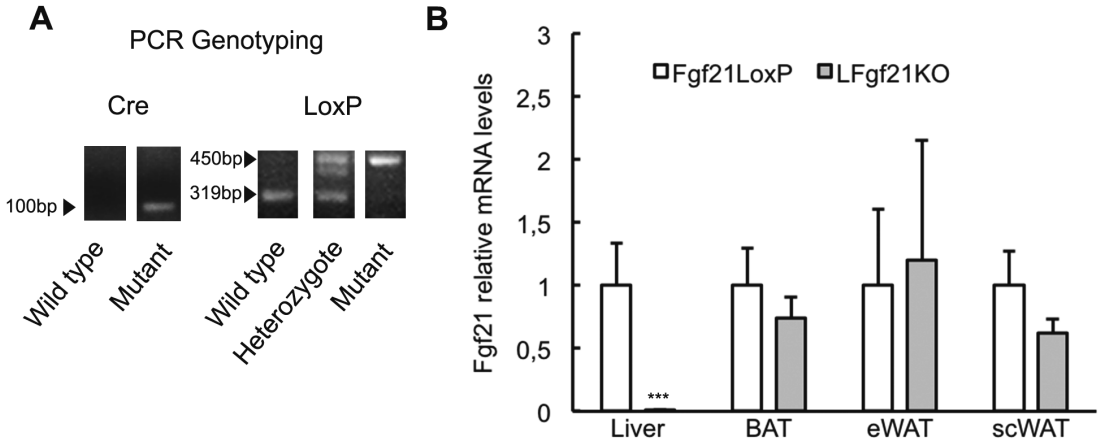

Figure P 0 Genotyping and characterization of the L*Fgf21*KO mice. PCR genotyping was performed using 50ng of genomic DNA (A). *Fgf21* mRNA levels in liver, BAT, eWAT and scWAT were measured by qRT-PCR (B). Error bars represent the mean ± SEM. ***p<0.001 versus Fgf21LoxP mice (n=7–9/group).

As expected, *Fgf21* mRNA levels were undetectable in liver while no compensatory effects were detected in adipose depots.

2 A LPD induces FGF21 gene expression in the liver, but not in BAT or WAT.

2.1 LPD increase plasma levels of FGF21 in parallel with its hepatic expression

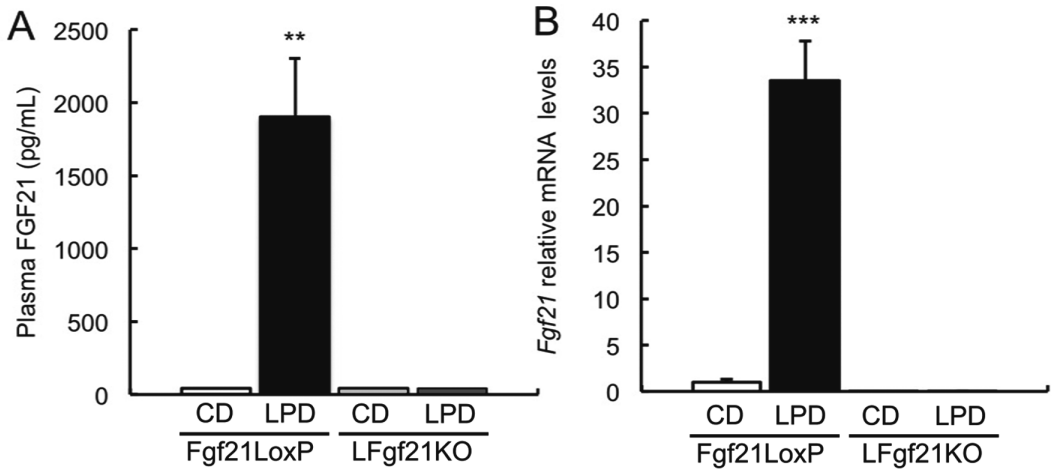

Figure P 1 FGF21 is induced by a LPD in liver and this induction correlates positively with plasma concentration in mice. Plasma protein concentration of FGF21 was measured by ELISA (A). Fgf21 mRNA levels in liver (B) were measured by qRT-PCR. Error bars represent the mean ± SEM. ** p<0.01 ***p<0.001 versus Fgf21LoxP mice fed a CD (n=7–9/group).

The liver is the main site of FGF21 production and release into the blood. Accordingly, we observed a great induction of *Fgf21* mRNA synthesis in the liver of mice on the LPD (Figure P1B). This increase correlated positively with plasma levels (Figure P1A).

To determine the specific role of hepatic FGF21 in the metabolic response to a LPD, we fed L*Fgf21*KO mice a LPD diet. As expected, *Fgf21* mRNA levels were undetectable in the livers of these animals (Figure P1B),

2.2 LPD do not increase FGF21 expression in BAT, eWAT or scWAT

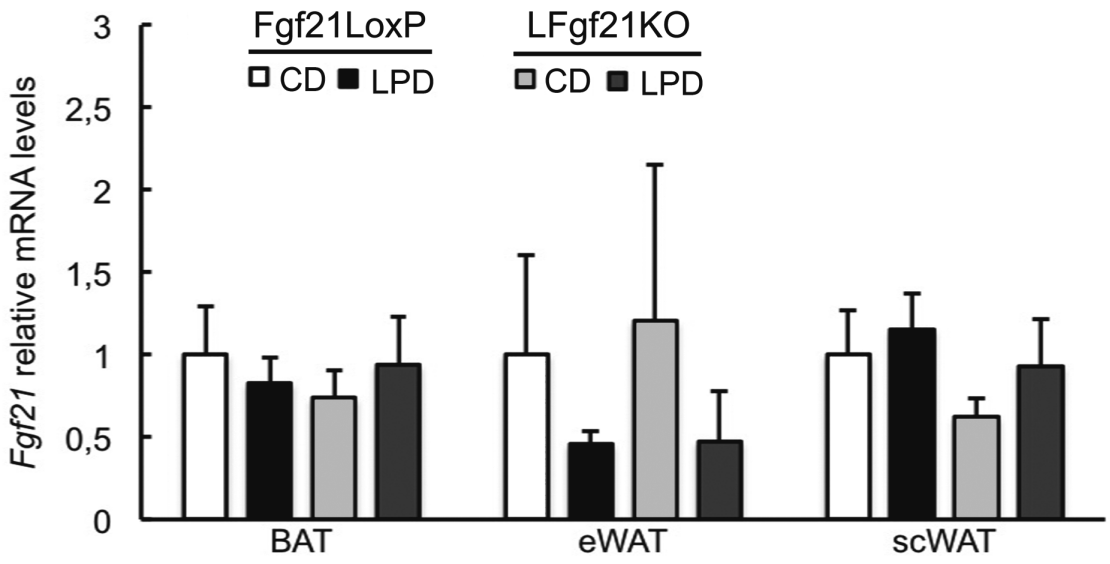

Figure P 2. FGF21 is not induced by a LPD in in BAT or WAT. *Fgf21* mRNA levels were measured by qRT-PCR. Error bars represent the mean ± SEM. (n=7–9/group).

In contrast to liver upregulation, *Fgf21* expression did not increase in BAT, eWAT and scWAT of control mice on the LPD (Figure P2) while no statistically significant changes were detected in L*Fgf21*KO mice when compared to the same tissues in control mice (Figure 2P). Interestingly, in the same direction as leucine deprivation, *Fgf21* mRNA levels showed a decreasing tendency in eWAT of animals on a LPD.

3 A LPD increases ATF4 protein levels in mouse liver

The 5' region of *Fgf21* contains two evolutionarily conserved functional ATF4-binding sequences responsible for its ATF4-dependent transcriptional activation (De Sousa-Coelho et al. 2012). To determine the effect of a LPD on ATF4 expression, we analysed liver protein extracts of mice fed a LPD or a CD for 7 days.

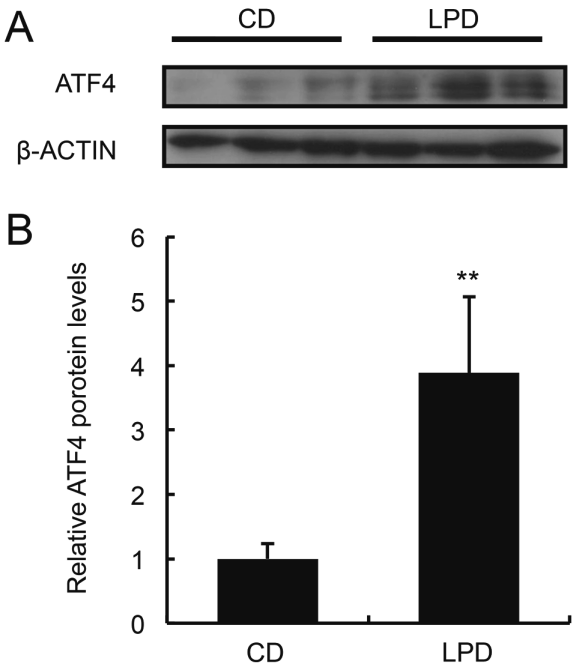

Figure P 3. A LPD increases ATF4 protein levels in liver. ATF4 protein levels were determined by Western blot analysis using hepatic nuclear extracts obtained from *Fgf21*^{LoxP} mice administered a CD or LPD. The experiment was normalized by actin protein levels as loading control and the intensity of the bands were quantified by densitometry with the Image J software (B). Error bars represent the mean ± SEM. ** p<0.01 versus CD. (n=3/group).

ATF4 expression was induced in liver in response to the LPD, as revealed by Western blot assays (Figure P2A-B). These results are consistent with previous published data reporting that ATF4 triggers the expression of FGF21 and that Gcn2 -/- mice show a partially blunted induction of FGF21 under protein restriction (Laeger et al. 2014).

4 *Fgf21* deficiency significantly attenuates weight loss under a LPD

Mice fed a LPD present rapid weight loss. Here we addressed whether this phenomenon is dependent on hepatic FGF21. For this purpose, *Fgf21*^{LoxP} and L*Fgf21*KO mice were fed a CD or LPD for 7 days.

4.1 Total body weight after 7 days on a LPD

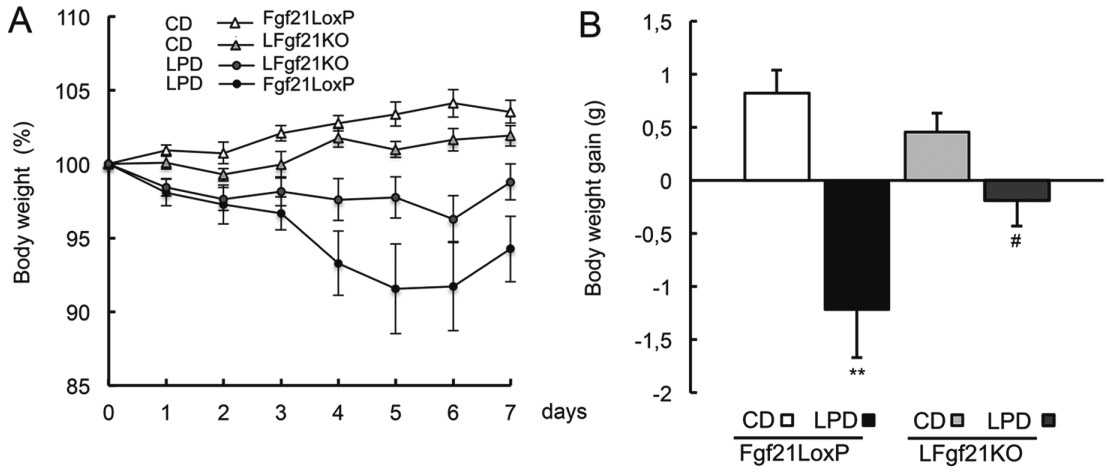

Figure P 4. Hepatic FGF21 expression is required for the weight loss caused by LPD. Body weight progression of mice fed a CD or LPD expressed as percentage of the initial weight, which was considered 100% (A). Total body weight change (g) after 7 days on a CD or LPD (B). Error bars represent the mean ± SEM. ** p<0.01 versus Fgf21LoxP mice fed a CD, # p<0.05 versus LFgf21KO fed a CD; (n=7–9/group).

Our data show that weight loss caused by LPD was partially blunted in L*Fgf21*KO mice (Figure P4A-B). Control mice fed a LPD underwent a 5,75% loss of their initial body weight while *Fgf21*KO animals weight loss reached 1,21%.

4.2 LPD reduces food intake

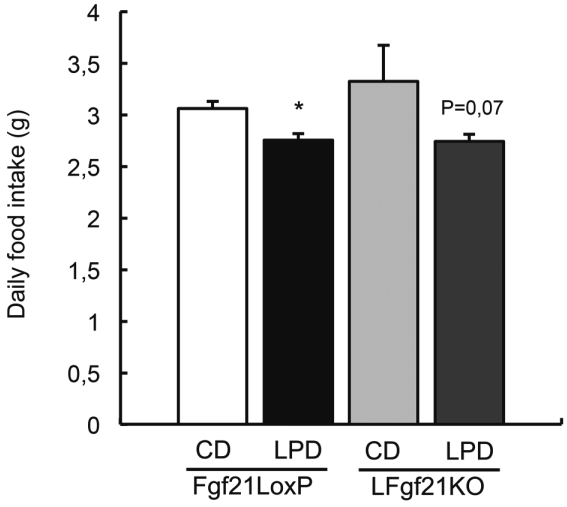

Figure P 5. Hepatic FGF21 does not affect food consumption. Daily food intake. Error bars represent the mean ± SEM. * p<0.05 versus Fgf21LoxP mice fed a CD, 0.07 represents p value versus LFgf21KO mice fed a CD (n=7–9/group).

The reduction in food intake observed under a LPD was unchanged between genotypes (Figure P5). It is remarkable that these results contradict previous publications describing either no change or an increase in food intake in response to protein restriction (Laeger et al. 2014). Nonetheless, the present results are consistent with the decreased food intake described in mice fed leucine-deficient diets (FigureL4).

4.3 Tissue weight after 7 days on a LPD

To determine the importance of each tissue in overall weight loss, we calculated the change in weight of individual tissues.

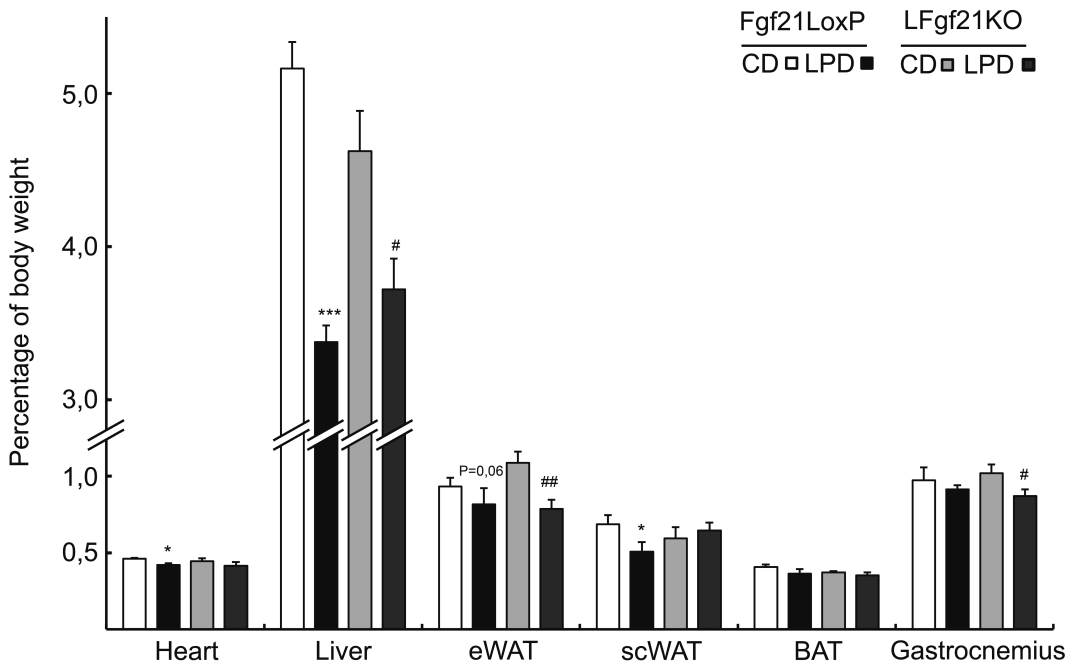

Figure P 6. Hepatic FGF21 is required for the weight loss caused by a LPD. The weight of heart, liver, eWAT, scWAT, BAT and gastrocnemius in mice fed a CD or LPD is presented as the mg of tissue per 100 mg of total body weight. Error bars represent the mean ± SEM. * p<0.05 *** p<0.001 versus *Fgf21*^{LoxP} mice fed a CD; # p<0.05 ## p<0.01 versus L*Fgf21*KO mice fed a CD; 0.06 represents the p value with respect to *Fgf21*^{LoxP} mice fed a CD (n=7–9/group).

All tissues analysed tended to weigh less in mice on the LPD, reaching statistical significance in heart, liver, scWAT and p=0.06 in eWAT (Figure P6). Regarding the role of FGF21, our results show that the weight loss observed in scWAT and heart was dependent on hepatic FGF21 expression, as weight loss was blunted in L*Fgf21*KO mice under the same diet. The effect of the LPD on

liver tissue weight was partially abolished by hepatic *Fgf21* deficiency (Figure P6).

5 FGF21 induces thermogenic genes in response to LPD in scWAT, but not in BAT or eWAT

Since hepatic FGF21 exerts its effects mainly in WAT and BAT through regulating lipid metabolism, the following experiments are focused on describing the role of LPD-induced FGF21 on the metabolic response of adipose depots.

Thermogenesis in BAT is mediated by the upregulation of UCP1 (Matthias et al. 2000) and FGF21 upregulates *Ucp1* in BAT in response to leucine deficiency (De Sousa-Coelho et al. 2013). In addition, FGF21 induces browning of scWAT (Fisher et al. 2012). Consequently, we evaluated the expression of thermogenic genes in BAT, eWAT and scWAT of *Fgf21*^{LoxP} and L*Fgf21*KO mice on a CD or LPD.

5.1 Thermogenic genes in BAT and eWAT of mice on a LPD

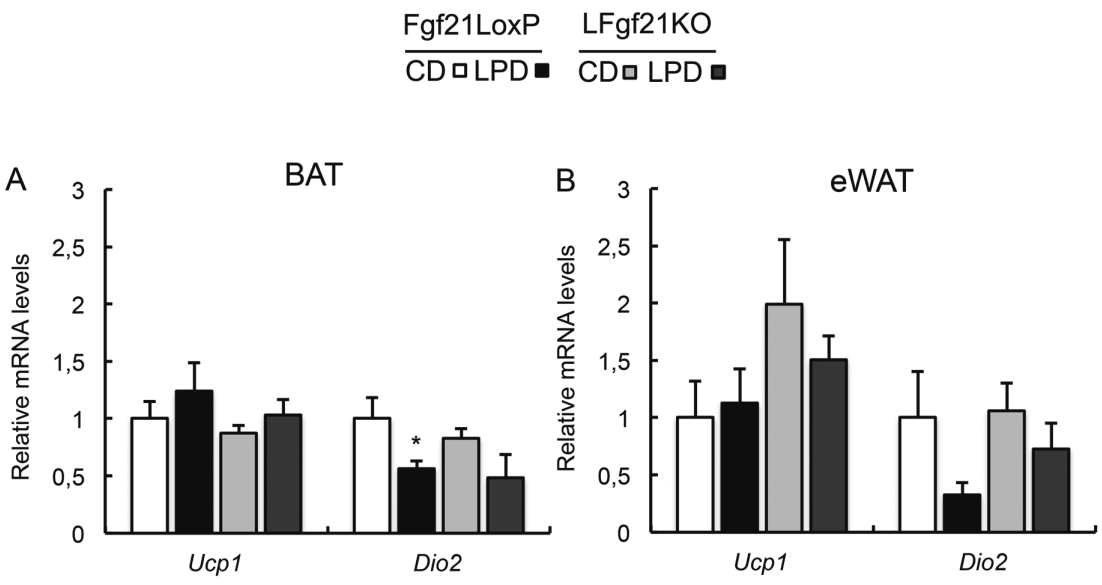

Figure P 7. A LPD does not alter thermogenic genes in BAT or eWAT. *Ucp1* and *Dio2* expression was measured by qRT-PCR in mouse BAT and eWAT. Error bars represent the mean ± SEM. * p<0.05 versus *Fgf21*^{LoxP} mice fed a CD (n=7–9/group).

Contrary to activation of the thermogenic programme reported under leucine deprivation, no statistically significant induction of *Ucp1* or *Dio2* mRNA levels were observed in BAT or eWAT of control mice under a LPD (Figure P7A-B).

5.2 Thermogenic genes in scWAT of mice on LPD

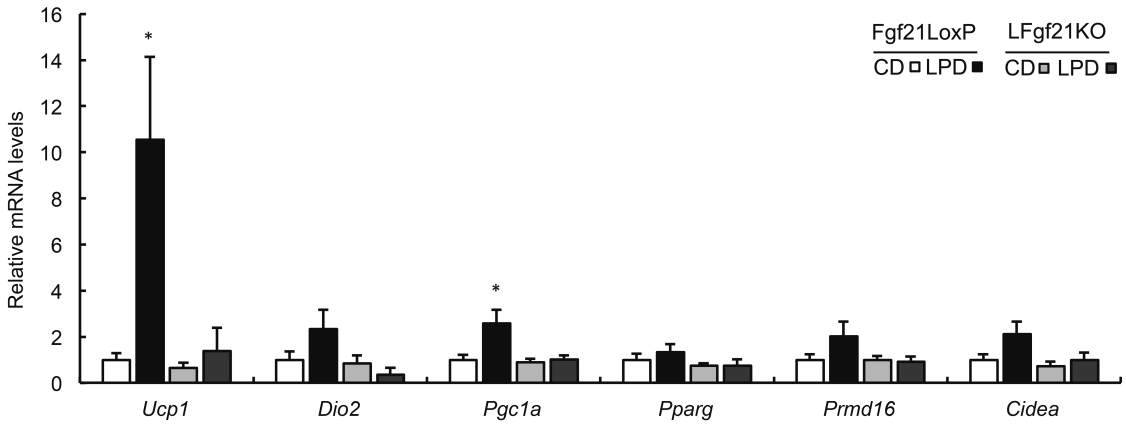

Figure P 8. Hepatic FGF21 is required for inducing thermogenic gene expression during a LPD. *Ucp1, Dio2, Pgc1a, Pparg, Prmd16* and *Cidea* expression was measured by qRT-PCR in mouse scWAT. Error bars represent the mean ± SEM. * p<0.05 versus $Fgf21^{LoxP}$ mice fed a CD (n=7–9/group).

In contrast, the analysis of gene expression in scWAT revealed that the LPD induced the expression of *Ucp1, Pgc1a*, *Cidea* and PR domain containing 16 *(Prdm16),* reaching a statistically significant value for *Ucp1* and *Pgc1a* (Figure P8). This expression pattern was not detected in the L*Fgf21*KO mice (Figure P8), thereby indicating the role of FGF21 in the metabolic adaptation of scWAT to protein restriction.

6 FGF21 signalling in the CNS of protein restricted mice

FGF21 has the potential to act in the central nervous system (CNS) since FGFRs are widely expressed in this tissue and KLB is specifically expressed in certain regions. (Fon Tacer et al. 2010; Bookout et al. 2013; Liang et al. 2014). In addition, FGF21 crosses the blood brain barrier and is present in the cerebrospinal fluid in a linear relationship with serum levels (Tan et al. 2011).

Recent studies point to the CNS as a mediator of the effects of FGF21 on EE and browning of WAT (Douris et al. 2015; Owen et al. 2014).

Given the capacity of FGF21 to modulate signalling pathways in the CNS to increase BAT activation, we speculated whether weight loss and browning of scWAT observed under the LPD is mediated by FGF21 actions in the CNS. Therefore, we analysed the levels of T3, adrenocorticotropin hormone (ACTH) and noradrenaline in plasma of *Fgf21*^{loxP} and L*Fgf21*KO mice fed the CD or the LPD.

6.1 Liver-derived FGF21 reduces plasmatic free T3 levels upon protein restriction

FGF21 and thyroid hormone show mutual regulatory dependency (Domouzoglou et al. 2014) and leucine deficiency increases T3 serum levels (Cheng et al. 2010). As thyroid system is strictly linked with thermogenesis and EE we analysed free T3 plasmatic levels of *Fgf21*^{loxP} and L*Fgf21*KO mice fed a CD or a LPD.

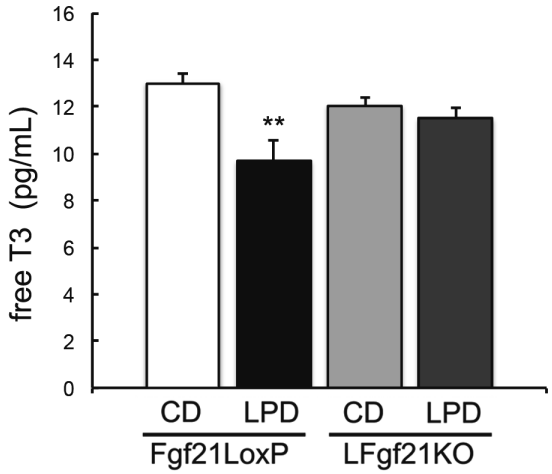

Figure P 9 Hepatic FGF21 induced by a LPD reduces free T3 circulating levels. Plasma concentration of free T3 was measured by ELISA. Error bars represent the mean ± SEM. ** p<0.01 versus Fgf21LoxP mice fed a CD (n=7–9/group).

The LPD caused a significant decrease in circulating free T3 (Figure P9). Hence, the increase of FGF21 levels in plasma (Figure P1) inversely correlates with free T3. This result is consistent with previous data showing that pharmacologic administration of FGF21 decreases free T3 as well as T4 (Coskun et al. 2008). No variations in T3 levels were observed in the L*Fgf21*KO mice on the CD or LPD (Figure P9) indicating an FGF21-mediated effect on circulating T3.

6.2 ACTH plasmatic levels in mice fed a LPD

Corticotropin-releasing factor (Crf) mRNA in hypothalamus and circulating corticosterone concentration are increased in *Fgf21* transgenic mice (Bookout et al. 2013) and acute administration of FGF21 results in increased plasma levels of ACTH (Owen et al. 2014). Moreover, i.c.v. injection of CRF receptor antagonist completely blocks the effect of FGF21 on sympathetic nerve activity in BAT (Owen et al. 2014).

This consistent data led us to hypothesize that FGF21 increase upon protein restriction modulates the hypothalamic–pituitary–adrenal axis. Therefore, we measured plasma ACTH of *Fgf21*^{loxP} and L*Fgf21*KO mice fed the CD or the LPD.

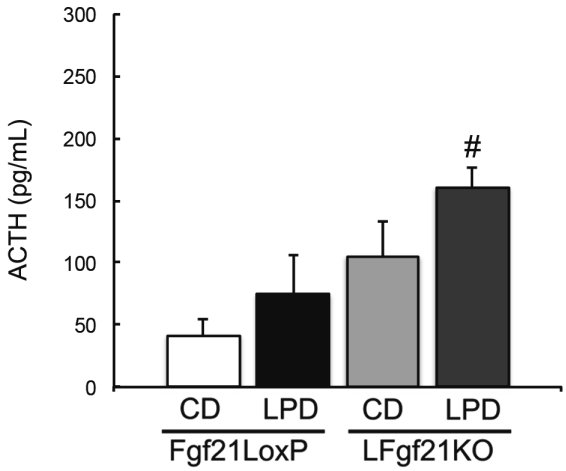

Figure P 10 Hepatic FGF21 deficiency increases ACTH circulating levels. Plasma concentration of ACTH was measured by ELISA. Error bars represent the mean ± SEM. # p<0.05 versus LFgf21KO mice fed a CD (n=7–9/group).

ACTH plasmatic levels presented high variability and no statistical differences could be registered. However, some tendencies may be appreciated, LPD increased ACTH plasmatic levels independently of the genotype and lack of hepatic *Fgf21* rose the basal levels of ACTH.

6.3 Protein restriction increases sympathetic outflow

Finally, we also analysed noradrenaline plasmatic levels in order to study the effect of liver-released FGF21 on the sympathetic tone. Several studies support

our hypothesis that FGF21 acts on the CNS increasing the sympathetic outflow to adipose depots. Centrally FGF21-treated mice present increased browning markers in scWAT and adrenergic blockade prevents the actions of central FGF21 (Douris et al. 2015). Moreover, the specific knockout of *Klb* in the hypothalamus and the dorsal-vagal complex abolishes the effects of the transgenic overexpression of *Fgf21* on thermogenic genes in BAT and scWAT (Owen et al. 2014).

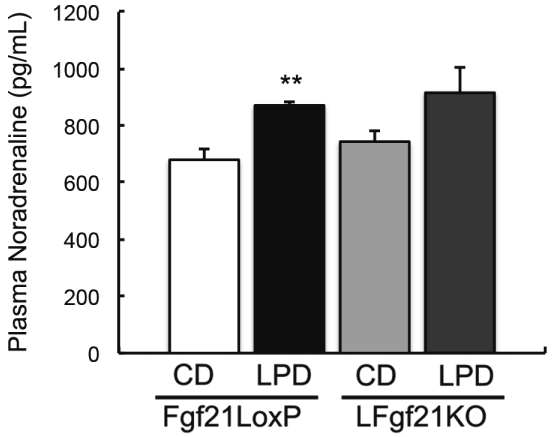

Figure P 11. LPD induces noradrenaline circulating levels. Plasma concentration of noradrenaline was measured by ELISA. Error bars represent the mean ± SEM. ** p<0.01 versus Fgf21LoxP mice fed a CD (n=7–9/group).

LPD increased plasmatic levels of noradrenaline in both *Fgf21*^{loxP} and L*Fgf21*KO mice although the difference only reached statistical significance in the control animals. This result suggests that, beyond FGF21, protein restriction increases the sympathetic tone.

6.4 Blockade of adrenergic receptors diminishes weight differences between mice fed CD or LPD

In order to determine the role of enhanced adrenergic tone in the weight loss observed under a LPD, animals were injected intraperitoneally with the non-selective β-blocker propranolol or the vehicle, and fed CD or LPD for 7 days.

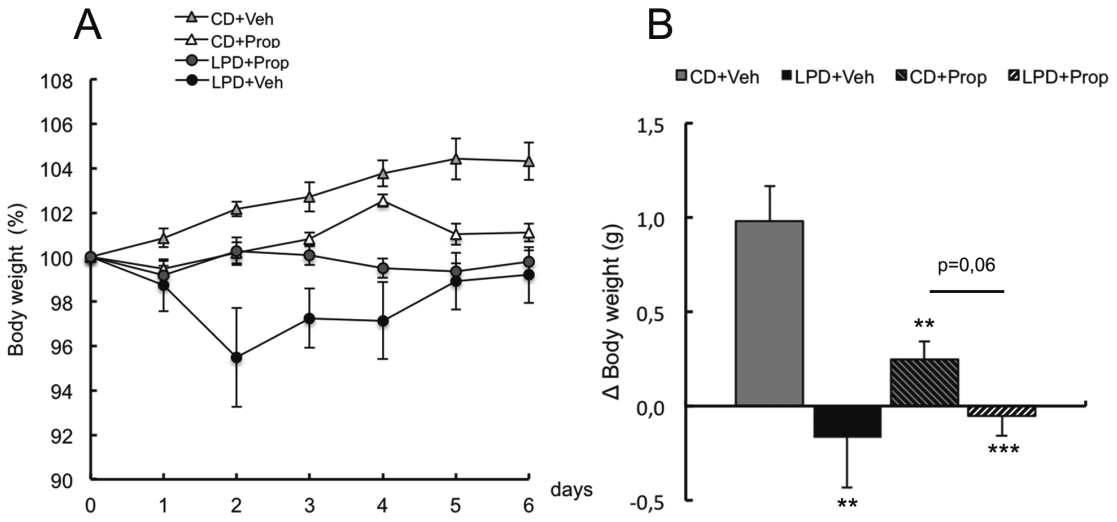

Figure P 12. Propranolol treatment decreased body gain by CD and body weight loss by LPD in mice. Body weight progression of mice fed a CD or LPD, injected with propranolol 5mg/kg/d or the vehicle, expressed as percentage of the initial weight, which was considered 100% (A). Total body weight change (g) after 7 days on a CD or LPD (B). Error bars represent the mean ± SEM. ** p<0.01, *** p<0.001 versus vehicle treated mice fed a CD, 0.06 represents the p value with respect to propranolol treated mice fed a CD (n=6 group).

As previously reported, mice on a LPD lost weight (Figure P12A-B). It is worth to mention that, in this experiment, weight loss registered in animals fed LPD during the first days of the time-course was partially recovered at the conclusion (Figure P12B). No statistical differences were found between propranolol and vehicle-injected mice fed a LPD (Figure P12B). Interestingly, propranolol treatment diminished weight gain in CD animals. This led us to analyse the effect of propranolol treatment on food intake.

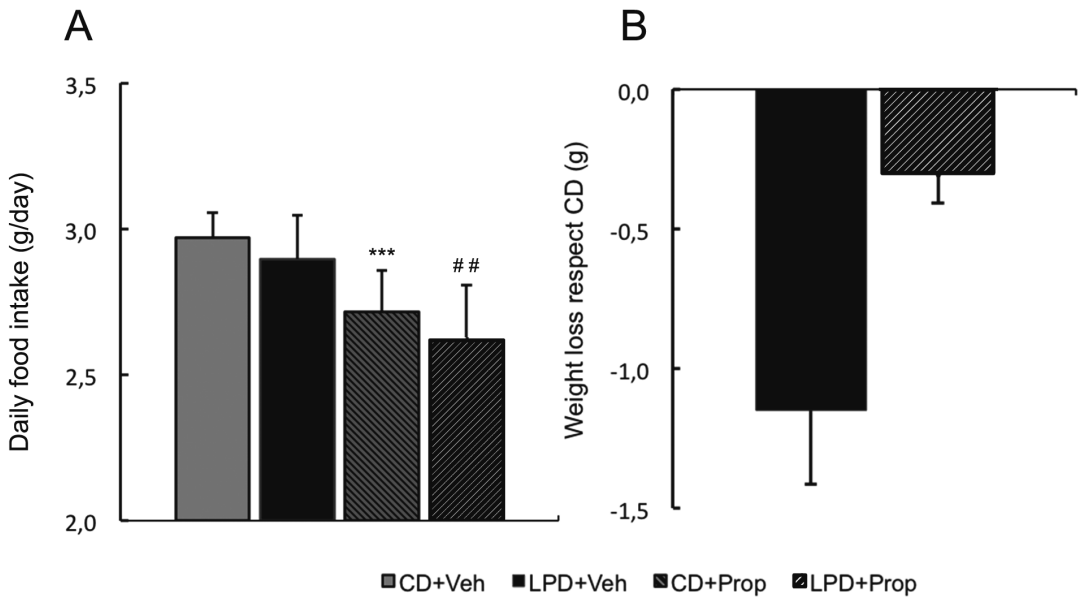

Figure P 13. Propranolol treatment decreased food intake. Daily food intake (g) (A). Weight difference of vehicle or propranolol 5mg/kg/d treated mice on LPD respect their control diet groups. Error bars represent the mean ± SEM. *** p<0.001 versus vehicle treated mice fed a CD (n=6 group).

Propranolol treatment decreased daily food intake in both groups (Figure P13A), which explains blunted weigh gain in propranolol treated mice on CD. When comparing the effect of LPD to their respective control groups, the food intake difference registered in vehicle-treated mice was 1,15g/day, while it was 0,3g/day in propranolol treated animals.

6.5 Adrenergic receptors blockade do not prevent *Ucp1* upregulation in mice on a LPD

The release of noradrenaline by sympathetic nerve activates β-adrenergic receptors inducing the thermogenic response. Since LPD increases plasma noradrenaline (Figure P11) and thermogenic gene expression in scWAT (Figure P8), we speculated that noradrenaline was participating in *Ucp1* induction in scWAT. To determine the contribution of noradrenaline to *Ucp1* induction, we analysed the mRNA levels of mice treated with propranolol or the vehicle, and fed a CD or a LPD.

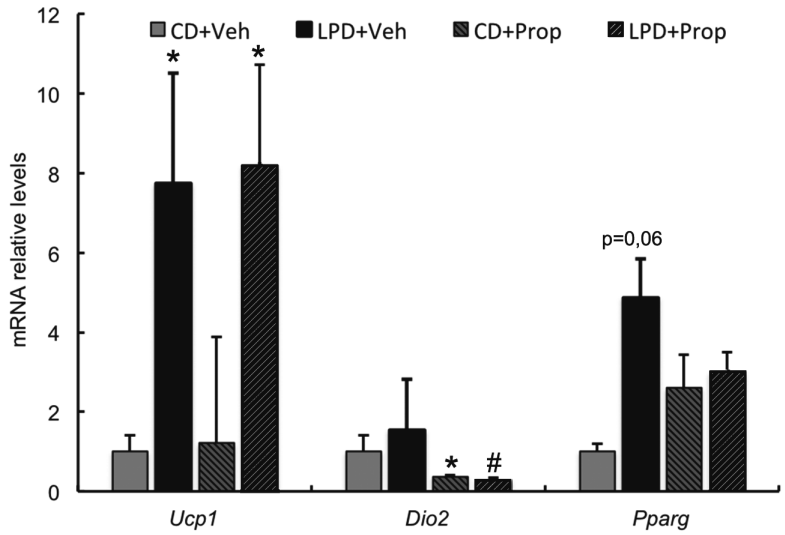

Figure P 14. Propranolol treatment do not block *Ucp1* induction during a LPD. *Ucp1, Dio2 and, Pparg* expression of mice fed a CD or LPD, injected with propranolol 5mg/kg/d or the vehicle, was measured by qRT-PCR in mouse scWAT. Error bars represent the mean ± SEM. * p<0.05 versus vehicle treated mice fed a CD. #p<0.05 versus propranolol treated mice fed a CD 0.06 indicates p value versus vehicle treated mice fed a CD (n=6 group).

Propranolol treatment didn't modified *Ucp1* expression neither on CD nor LPD-fed mice. However, other thermogenic genes were affected by the propranolol treatment. Propranolol downregulated *Dio2* in both diets and blunted *Pparγ* increase caused by LPD. These results are consistent with published data reporting lack of effect of propranolol on *Ucp1* expression when FGF21 is administered peripherally (Douris et al. 2015). The blockade of beta-adrenergic receptors did not interfere with the induction of *Ucp1,* discarding the increase of sympathetic tone in scWAT as the putative mechanism.

7 Hepatic FGF21 deficiency blunts improved glucose tolerance in mice on LPD

FGF21 has been postulated as a potential treatment for diabetes mainly due to its beneficial metabolic effects on insulin sensitivity and glucose tolerance in animal models (Kharitonenkov et al. 2007; Xu et al. 2009). Additionally, leucine- and methionine-restricted mice are protected from insulin resistance (Xiao et al. 2011; Ables et al. 2012). This led us to hypothesise that enhanced *Fgf21* expression upon protein restriction ameliorates glucose metabolism.

7.1 Intraperitoneal Glucose tolerance test (IPGTT)

To evaluate the effect of liver-derived FGF21 on glucose tolerance, *Fgf21*^{loxP} and L*Fgf21*KO mice were maintained on CD or LPD for 7 days and an intraperitoneal glucose tolerance test (IPGTT) was performed.

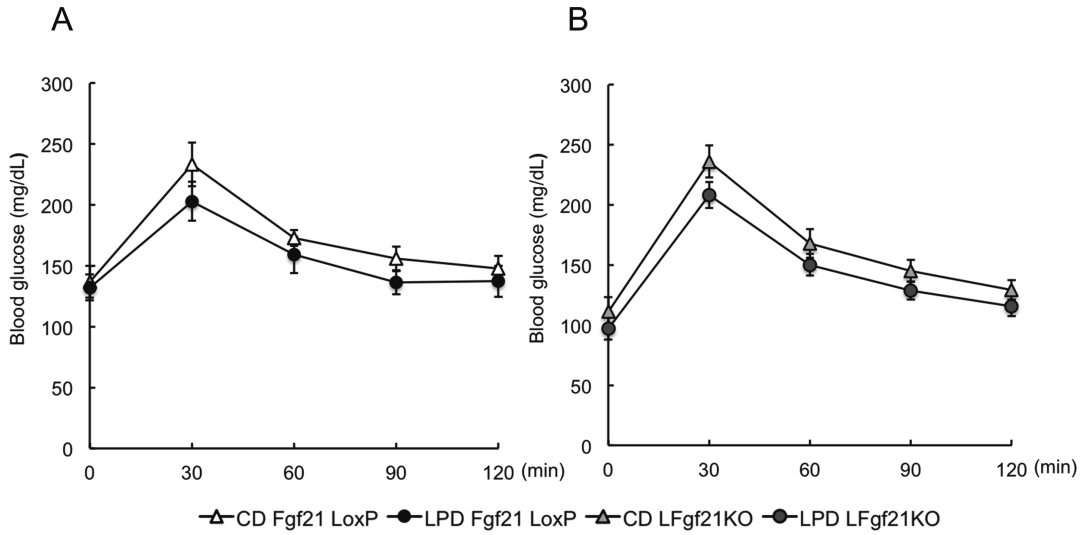

Figure P 15 Intraperitoneal Glucose Tolerance Test (IPTGG) for *Fgf21*^{loxP} mice fed a CD or a LPD (A) or L*Fgf21*KO fed a CD or LPD (B). Mice were fasted for 6h and then injected with glucose (1,5g/kg ip). Blood glucose concentrations were determined with a glucometer using blood taken from cut tail tips at the indicate time points. Error bars represent the mean ± SEM. (n=7 group)

In control mice fed a LPD, blood glucose concentrations were noticeably lower following the intraperitoneal glucose injection (Figure P15A). To simplify the results and evaluate them despite different basal glucose concentrations, we calculated the AUC of the % of basal glucose (Figure P16).

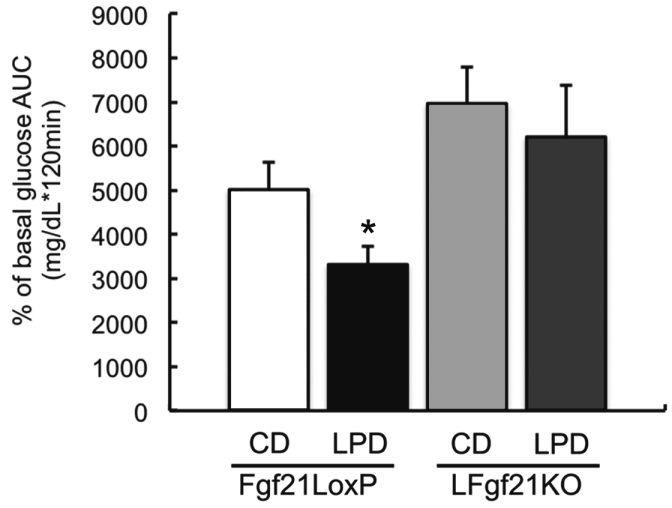

Figure P 16. Area Under the Curve of the percentage of basal glucose for the Intraperitoneal Glucose Tolerance Test (IPTGG) . *Fgf21*^{loxP} or L*Fgf21*KO mice fed a CD or LPD. Area Under the Curve was calculated by the trapezoidal method. Mice were fasted for 6h and then injected with glucose (1,5g/kg ip). Blood glucose concentrations were determined with a glucometer using blood taken from cut tail tips at the indicate time points. Error bars represent the mean ± SEM. * p<0.05 versus *Fgf21*^{LoxP} mice fed a CD (n=7 group)

Lack of hepatic *Fgf21* blunted the improved glucose tolerance of mice on LPD (Figure P16). In addition, L*Fgf21*KO mice showed a tendency to respond poorer to glucose injection. In agreement with the pharmacological effects of FGF21, liver-produced FGF21 in response to LPD improves whole body glucose tolerance.

7.2 Intraperitoneal Insulin Tolerance Test (IPITT)

To further analyse the effect of LPD on glucose metabolism, we performed an IPITT in the same mice.

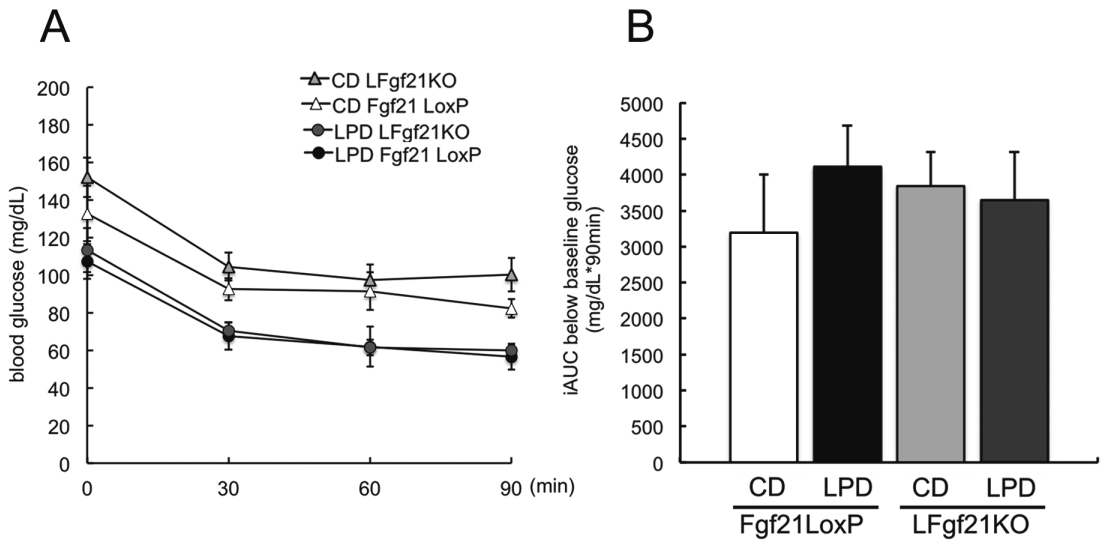

Figure P 17 Intraperitoneal Insulin Tolerance Test (IPTGG) for Fgf21loxP or LFgf21KO mice fed a CD or a LPD (A). Inverse Area Under the Curve below baseline glucose calculated by the trapezoidal method. Mice were fasted for 6h and then injected with insulin (0,75 IU/kg ip). Blood glucose concentrations were determined with a glucometer using blood taken from cut tail tips at the indicate time points. Error bars represent the mean ± SEM. (n=7 group)

The differences in the basal glucose levels complicated the interpretation of the time-course results. When calculating the inverse AUC below baseline glucose, no statistical differences were found between groups.

Regarding insulin sensitivity, the in vitro experiments done both in 3T3-L1 adipocytes and human primary adipocytes show that FGF21 potently stimulates glucose uptake in an insulin-independent manner (Kharitonenkov et al. 2005). Our results agree with these previous data.

7.3 *Glut 1* expression does not change in adipose depots of mice on a LPD

Unlike insulin, FGF21 has no effect on plasma membrane translocation of the glucose transporter GLUT4, but induces the expression of GLUT1 through its transcriptional activation (Kharitonenkov et al. 2005). Thus, we analysed *Glut 1* expression in adipose depots of *Fgf21*^{loxP} and L*Fgf21*KO mice on CD or LPD.

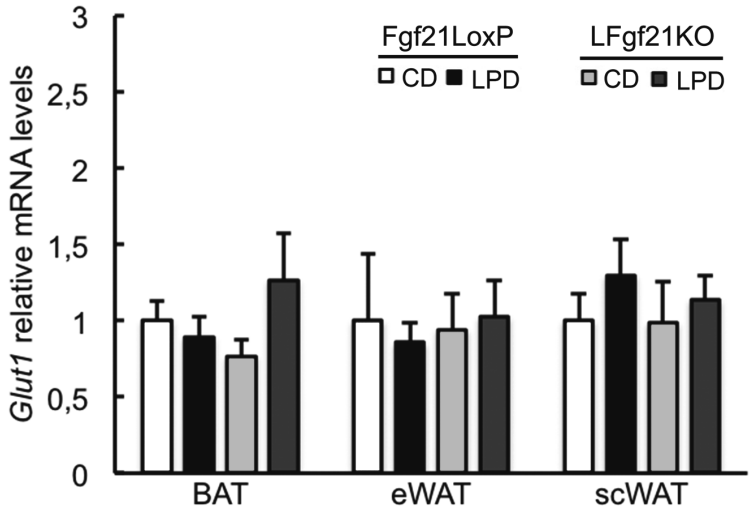

Figure P 18. LPD does not change *Glut1* expression in fat depots. *Glut1* expression was measured by qRT-PCR in mouse BAT, eWAT and scWAT. Error bars represent the mean ± SEM. (n=7–9/group).

No statistical differences were observed in the mRNA levels of *Glut1* between diets or genotypes in any of the tissues analysed. This result discards our hypothesis that FGF21 produced under LPD is improving glucose tolerance by upregulating *Glut1* transporter in adipose depots.

8 FGF21 plasma levels correlate negatively with protein intake in humans

To translate our results to humans, we evaluated the relationship between protein intake and circulating levels of FGF21 in 78 individuals randomly selected from the PREDIMED trial.

Table 2 Multivariable regression analyses with FGF21 (pg/mL) as dependent variable and energy-adjusted protein intake at baseline (g/day) as independent variable.

	Q1	Q2	Q3	Q4	P value[b]
No subjects (78)	19	20	20	19	
Age (years)	67.1±5.9	65.7±4.8	67.0±6.4	65.3±4.0	0.30
Sex (women)	6 (31)	10 (50)	9 (45)	15 (79)	0.03
Body mass index (Kg/m^2)	28.1±3.2	30.0±3.4	27.7±2.7	30.8±2.9	0.006

Energy intake (Kcal/d)	2370±350	2192±603	2227±433	2390±571	0.51
Protein intake (g/day)	80±6	90±2	97±3	110±5	<0.0001
FGF21 (pg/mL)	289±116	276±143	256±117	190±115	0.07

[a]Categorical variables: subjects (percentage), continuous variables: mean ± SD
[b]One-way ANOVA tests (continuous variables) or chi-squared tests (categorical variables).

Baseline data for these subjects are shown in Table 2. Protein intake was obtained from FFQs and was expressed as grams of protein per day (g/day).

Table 3 Multivariable regression analyses with FGF21 (pg/mL) as dependent variable and energy-adjusted protein intake at baseline (g/day) as independent variable.

		β[a]	P value	95% CI
Protein intake (continuous variable)	Model 1[b]	-3.42	0.006	-5.83,-1.02
	Model 2[c]	-3.39	0.007	-5.86, -0.92
Quartiles of protein intake	Model 1[b]	-31.5	0.01	-56.5, -6.5
	Model 2[c]	-30.8	0.02	-56.5, -5.0

CI: Confidence Interval.
[a]Parameter estimates.
[b]Unadjusted.
[c]Adjusted for body mass index (BMI) and total energy intake.

Results from the multiple linear regression analyses showed a significant inverse relationship between plasma FGF21 concentrations and dietary intake of protein. At baseline, FGF21 levels decreased by 3.39 pg/mL for each gram of protein ingested (Table 3). The participants with a high intake of protein showed statistically significant lower values of circulating FGF21.

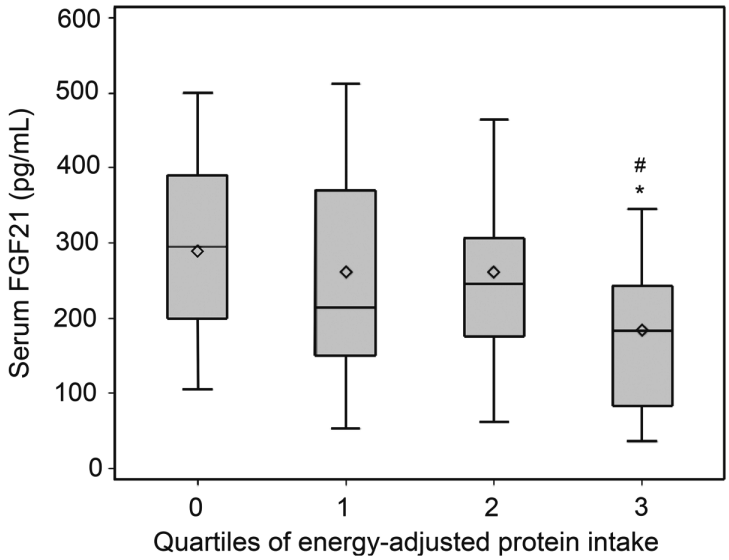

Figure P 19. Circulating FGF21 levels correlate negatively with protein intake. Plasma FGF21 concentration divided into quartiles of protein intake adjusted for the calorie intake of 78 participants in the PREDIMED trial. Error bars represent the mean ± SEM. * p<0.05 from 1st quartile; # p<0.05 from the 2nd quartile.

We also performed regression analyses using quartiles of protein intake and obtained similar results. After adjustment for BMI and calories, FGF21 decreased (-30.7 pg/mL) when moving from the lower to higher quartiles (p=0.015) (Figure 7).

Similarly to the data from mice, these results indicate that the serum concentrations of FGF21 are inversely proportional to dietary protein intake.

DISCUSSION

THE ROLE OF REV-ERBα IN THE INDUCTION OF FGF21 UPON LEUCINE DEPRIVATION

Previous work by our group characterised the ATF4-dependent regulation of FGF21 during amino acid deprivation, concretely during leucine deprivation, and also in response to ER stress inducers (De Sousa-Coelho et al. 2012). In that study, we localised two evolutionarily conserved ATF4-binding sequences in the 5' regulatory region of human *FGF21*. Later studies validated that these binding sequences (Lees et al. 2014; Schaap et al. 2013; Wan et al. 2014).

To delve deeper into the molecular mechanisms that regulate *FGF21* expression during leucine deprivation, we focused on the transcriptional repressor Rev-erbα, which functions both as a core repressive component of the cell autonomous clock and as a regulator of metabolic genes.

Rev-erbα links the circadian clock to liver metabolism (Zhang et al. 2016) and *FGF21* levels inversely correlate to the expression pattern of Rev-Erbα and *ALAS-1* in liver (Kaasik & Lee 2004; Oishi et al. 2008). In addition, PGC-1α negatively regulates hepatic *Fgf21* expression by modulating the heme/Rev-erbα axis (Estall et al. 2009). These lines of evidence led us to consider that Rev-erbα participates in the regulation of *Fgf21* during amino acid deprivation.

To test this hypothesis, first we analysed the expression of *Fgf21, Rev-erb*α and factors involved in Rev-erbα activity in livers of wild-type mice fed Ctl or (-) leu diet. In addition, given that Rev-erbα is involved in *Fgf21* regulation during fasting (Archer et al. 2012; Estall et al. 2009), we also examined the PGC-1α /Rev-erbα in the liver of mice on Ctl or (-)leu diet fasted for 15 h.

According to the bibliography, fasting increased *Fgf21* mRNA levels (Inagaki et al. 2007), and leucine deprivation strikingly did so too in a striking manner. (De Sousa-Coelho et al. 2012). Interestingly, when leucine-deprived mice were fasted, *Fgf21* expression was lower than in leucine-deprived mice fed *ad libitum.* FGF21 serum concentrations paralleled mRNA levels.

Rev-erbα expression was repressed by leucine deprivation and increased by fasting. The increased expression of this repressor during fasting can explain the blunted induction of *Fgf21* in leucine-deprived fasted mice. Thus, we hypothesise that, in this condition, ATF4 activation is counteracted by a corepressor complex recruited by Rev-erbα. In addition, the downregulation of *Rev-erbα* during leucine deprivation boosted ATF4-mediated induction of *Fgf21.*

Along the same line, the expression of *Alas1*, greatly increased by fasting in animals on both diets. According to our hypothesis, the increase in *Alas-1* supplies Rev-erbα with its endogenous ligand heme, and thus enhancing the recruitment of the corepressor complex.

Finally, *Pgc-1α* mRNA levels were also increased by fasting. This observation is consistent with the notion that *PGC-1α* regulates *ALAS-1* expression through the coactivation of NRF-1 and FOXO1 (Handschin et al. 2005).

These results reveal a consistent negative correlation between *Fgf21* and the *Pgc-1α*/heme/Rev-erb*α* axis across various nutritional states. The negative correlation persisted in the eWAT of mice fed a leucine-deficient diet. This observation indicates that the proposed mechanism could be extended to other tissues.

The abovementioned results, together with the analysis of the ChIP-seq findings by Mitchell Lazar's group (Figure R0) that point to the binding of Rev-erbα to the DNA regions containing AAREs of *Fgf21* promoter, led us to propose a model whereby the activator ATF4 and the repressor Rev-erbα compete for occupancy of the Fgf21 promoter.

ATF4 triggers increased transcription by binding to AAREs, which are composed of a half-site for the C/EBP family and a half site for the ATF family of transcription factors (Wolfgang et al. 1997; Fawcett et al. 1999). ATF4 binds to AAREs likely as a heterodimer with members of the C/EBP family although the identity and properties of these proposed heterodimers have not been widely studied. Among C/EBP family members, C/EBPβ has been shown to heterodimerize with ATF4 at AREE sites *in vitro* and *in vivo* (Siu et al. 2002; Lopez et al. 2007; Thiaville et al. 2008; Chen et al. 2004).

Differential mechanisms have been proposed for Rev-erbα to regulate transcription. The direct binding of Rev-erbα to DNA in competition with RORs provides a universal mechanism for the regulation of the molecular clock across all tissues types, whereas the tethering of Rev-erbα by tissue-specific lineage-determining factors determines the expression of metabolic genes. In liver, the Rev-erbα-tethered binding sites are enriched in other transcription factors such as ATF4 and CEBP, among others (Zhang et al. 2016).

In the model we propose, ATF4 and Rev-erbα compete for interaction with their shared partner C/EBPβ in order to exert their function (See Figure D1).

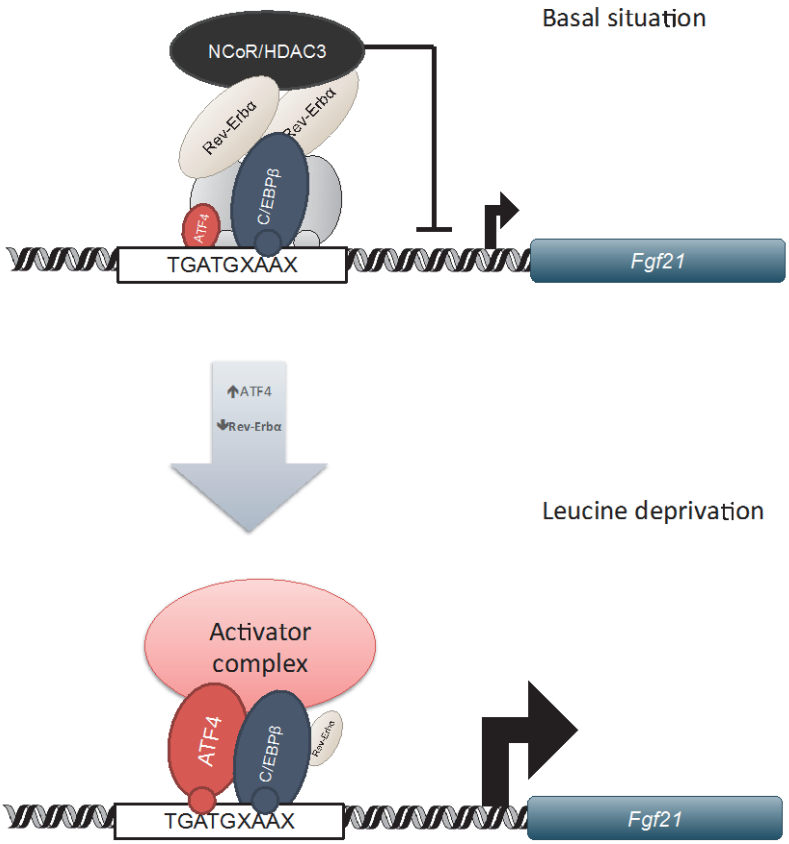

Figure D 1 Proposed molecular mechanism for the activation of *FGF21* promoter during leucine deprivation.

To test this hypothesis we analysed the activity of the human *FGF21* promoter in the presence of ATF4 with or without inhibiting Rev-erbα. The results from the reporter gene assay confirmed that a decrease in Rev-erbα activity enhances the ATF4-mediated upregulation of *Fgf21*. However, we cannot assume from these data that ATF4 and Rev-erbα compete for the same partner

and DNA binding site. Further studies including co-immunoprecipitation (Co-IP), chromatin immunoprecipitation (ChIP), and electrophoretic mobility shift assay (EMSA) are needed to confirm the model. In this regard, ChIP is currently being set up with this purpose.

Along the same line, the study of the mouse *Fgf21* promoter activity in the presence of ATF4, C/EBPβ and Rev-erbα revealed that C/EBPβ blocks the ATF4-induced activation of the *Fgf21* promoter. When transfected alone, Rev-erbα did not produce any change in ATF4 activation. C/EBPβ interaction with ATF4 may seem paradoxical. Low levels of C/EBPβ are constitutively bound to AAREs to heterodimerize with ATF4, thus facilitating its activity; however, when levels of C/EBPβ increase after the initial response to amino acid deprivation (4-6h), it antagonises ATF4 (Kilberg et al. 2009). How C/EBPβ antagonises ATF4 actions is not well understood. A feasible explanation of the blockade produced by C/EBPβ is that it tethered endogenous Rev-erbα present in HepG2 cells. When transfected alone, Rev-erbα had no effect because its tethering to the promoter can only occur when C/EBPβ is present.

Finally, we propose *Egr*-1 as a candidate for the downregulation of *Rev-erbα* during amino acid limitation. During leucine deprivation, *Egr-1* is highly induced in cultured cells in a GCN2-partially dependent manner (Deval et al. 2009) and the adenoviral overexpression of *EGR-1* in primary hepatocytes downregulates *Rev-erbα* (Tao et al. 2015). Along the same line, our results showed that *Egr-1* was upregulated in liver of leucine-deprived mice and that *Rev-erbα* promoter activity decreased in the presence of EGR-1.

Interestingly, *Egr-1* is downstream of the MAPK signalling cascade initiated by the FGF21 binding to its receptor. In fact, *Egr-1* expression is commonly used as an indicator of correct FGF21 signalling. This notion led us to propose a positive feedback mechanism in which FGF21 represses the repressor *Rev-erbα* through the activation of *Egr-1* (See Figure D2). In support of this idea, recent data indicate that a MEK-dependent transcriptional programme regulates the activation of EGR-1 during amino acid limitation (Shan et al. 2014).

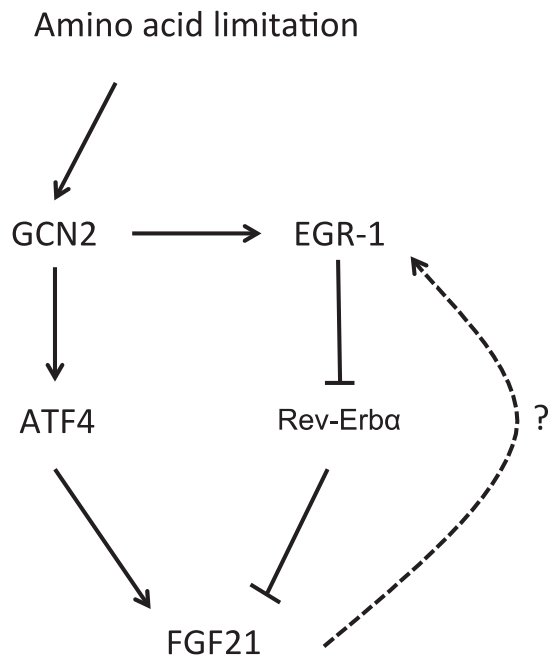

Figure D 2 Proposed signalling pathways involved in *FGF21* regulation during amino acid limitation

The induction of ATF4 occurs very early in the AAR and decreases progressively. The results presented herein describe the mechanisms of *Fgf21* regulation after seven days of leucine deprivation. To improve knowledge of *Fgf21* regulation, it would be interesting to analyse the time-course of the different factors involved. ATF4 could be the initial signal through which *Fgf21* is boosted, and the repression of *Rev-erbα* could be a long-term mechanism to maintain the induction.

To sum up, we propose a model whereby the induction of *Fgf21* upon leucine deprivation is the consequence of the sum of two factors: binding of the activator ATF4 to the promoter and the absence of the repressor Rev-erbα.

THE ROLE OF FGF21 IN THE METABOLIC RESPONSE TO LEUCINE DEPRIVATION

We have previously shown that leucine deprivation significantly increases FGF21 hepatic expression and serum protein levels (De Sousa-Coelho et al. 2012), thereby pointing to a key role of this hormone in the amino acid starvation phenotype. In the current study, we demonstrate that weight loss, downregulation of key lipogenic genes in liver and WAT, and BAT activation in response to leucine deprivation are partly FGF21-dependent.

We found that FGF21 serum levels positively correlated with the mRNA levels measured in liver. BAT mRNA levels remained unchanged whereas in eWAT, *Fgf21* expression was repressed. These results are consistent with liver being the main source of FGF21, and they suggest that the effects of FGF21 on BAT and eWAT derive from the endocrine actions of liver-derived FGF21.

We observed that FGF21 deficiency significantly attenuated weight loss under leucine deprivation. A leucine-deficient diet caused a reduction in food intake in wild-type mice and also in FGF21 null mice. This observation implies that FGF21 is, at least in part, responsible for weight loss in mice subjected to amino acid deprivation, independently of food intake. Consistent with our observation, previous studies have shown that FGF21-transgenic mice are resistant to diet-induced obesity (DIO) and that FGF21 treatment triggers weight loss in genetically obese (Ob/Ob) mice (Kharitonenkov et al. 2005; Coskun et al. 2008). The established reduction in food intake induced by the (-)leu diet was not changed by the absence of FGF21 or by disrupted leptin signalling (Ob/Ob mice). These observations indicate that neither FGF21 nor leptin are responsible for the food aversion produced by leucine deficiency.

It has been shown that white adipocytes from FGF21 transgenic mice are substantially smaller than those from wild-type counterparts (Inagaki et al. 2007; Kharitonenkov et al. 2005). Here we demonstrate that the reduction in adipocyte volume and eWAT mass that occurs under leucine deprivation is

determined by the increased FGF21 expression and secretion that occur in response to this diet.

We found that the levels of phosphorylated (P)-HSL were increased in eWAT upon (-)leu feeding, as had been described (Cheng et al. 2009).Therefore, activation of HSL, probably allowed increased lipolysis. Interestingly, our results show that lack of FGF21 significantly decreased P-HSL levels in the eWAT of (-)leu-fed mice. These findings thus points to a key role of FGF21 in leucine deprivation-induced lipolysis.

The analysis of blood biochemical parameters, however, did not show significant changes in NEFA levels, possibly because of increased fatty acid utilisation by other tissues. We assume that glucagon signalling increases under leucine deprivation as indicated by the increased PKA-dependent HSL Ser660 phosphorylation in WAT. In addition, a reduction in insulin levels under leucine deprivation was observed in wild-type but not in knockout mice. These changes were well correlated with the differences observed in body weight and fat mass.

Adiponectin has recently been shown to mediate part of the metabolic actions of FGF21 (Holland et al. 2013; Lin et al. 2013). In contrast to the effects of pharmacological administration of adiponectin, we found that adiponectin concentration in serum was not changed by a (-)leu diet, despite the increased FGF21 concentration. This observation rules out adiponectin as a mediator of FGF21 actions upon leucine deprivation.

We also examined whether the impaired reduction in body weight observed in FGF21-KO mice under leucine deprivation was related not only to lipolysis in WAT, but also to other factors that influence adipose tissue mass, such as lipogenesis. We observed a significant reduction in FASN protein and mRNA levels in eWAT upon (-)leu feeding. This reduction was totally blocked in FGF21-KO mice. Srebp1c and Acc1 mRNA levels presented the same pattern, although with distinct statistical significance. The same pattern was observed in 3T3L1 cells treated with recombinant FGF21, thereby suggesting a direct effect of FGF21 on adipose tissue.

The endocrine effect of FGF21 on WAT under leucine deprivation that we observed here differs from the recently described autocrine effect of this hormone on this tissue in a fed state, in which FGF21 induces lipogenesis through the regulation of PPARγ activity (Dutchak et al. 2012). The decreased *Fgf21* expression in WAT under leucine deprivation also contrasts with its observed induction after one day of fasting (Muise et al. 2008). FGF21 administration to DIO mice leads to a dramatic decrease in the WAT *Fgf21* transcript. However, controversially, it induces an increase in the expression of adipogenic genes (Coskun et al. 2008). It seems, therefore, that the response to increased levels of FGF21 is determined by the origin of this hormone and also other factors, which may reflect the metabolic state and the energy requirements of the organism.

Regarding the autocrine effects of FGF21 on liver, this protein has already been described to inhibit lipid synthesis (Xu et al. 2009). In this regard, the reduction of hepatic triglyceride levels is associated with FGF21 inhibition of *Srebpc1c* and the expression of an extended array of genes involved in fatty acid and triglyceride synthesis (Zhang et al. 2011). Accordingly, in the livers of FGF21-KO mice, we did not observed the expected reduction in the mRNA levels of *Srebp1c*, *Fasn* and *Acc1* in response to (-)leu diet. The analysis of SREBP1C, FASN and ACC1 protein abundance corroborated the abovementioned observations in mRNA levels. As a result, lipid accumulation was decreased by leucine deprivation in wild type mice but not in the FGF21-KO mice.

The absence of *Fgf21* itself reduced the hepatic expression of genes involved in fatty acid uptake (*Cd36* and *Fabp4*) and oxidation (*Acadm*, *Acadl*, *Cpt1a*) in animals on both diets. This observation underlines the constitutive role of *Fgf21* in the lipid homeostasis in liver.

In the liver from FGF21-KO mice, the induction of *Asns* expression, for which the gene product catalyses the glutamine and ATP-dependent conversion of aspartic acid to asparagine, suggests that FGF21 is not involved in the regulation of amino acid metabolism under amino acid starvation. We have also observed that contrary to the induction of ERK1/2 phosphorylation in the liver and WAT of mice acutely treated with FGF21 (Fisher et al. 2011), the FGF21-

dependent phenotype under leucine deprivation is unexpectedly not related to the MAPK-ERK1/2 signalling pathway both in liver or WAT.

Keeping with FGF21 signalling, the expression of *Fgfr1* and *Klb* in eWAT tended to increase during leucine deficiency in wild type mice and was statistically higher in FGF21-KO animals. However, these findings were not true in BAT, thereby suggesting that the effects of FGF21 on eWAT upon leucine deprivation are modulated by both the increase in circulating FGF21 and the upregulation of the receptor complex. The significant increase in *Fgfr1* and *Klb* mRNA levels in leucine-deprived FGF21-KO mice could be a compensatory mechanism in response to the lack of FGF21 when this hormone is required.

BAT is a major site of adaptive thermogenesis, and it is used to preserve both thermal and caloric homeostasis, in response to environmental temperature or diet (Tseng et al. 2010). FGF21-KO mice under leucine deprivation exhibited decreased induction of genes defining BAT identity (i.e. Ucp1 and Dio2), while the FGF21 transcriptional regulators *Pgc1α* and *Pparγ* were induced in the same manner in both wild-type and FGF21-KO mice. Increased *Ucp1* expression may be regulated by the SNS through the activation of β-adrenergic receptors. We found that the mRNA expression of *Adrb3* was induced by leucine deprivation in BAT, although there were no significant changes between genotypes. The β3-adrenergenic receptor stimulates p38 mitogen-activated protein kinase (p38 MAPK), which is required for the βAR-dependent increase in *Ucp1* expression in brown adipocytes (Cao et al. 2001). Nevertheless, p38 phosphorylation levels were not affected by leucine deprivation in wild-type mice or FGF21-KO mice when compared to controls. One of the best-known inducers of brown adipose tissue and its function is norepinephrine (Cannon & Nedergaard 2004), which has also been shown to be induced in (-)leu-deprived mice (Cheng et al. 2009). These findings raise the possibility that FGF21 induces *Ucp1* (and also *Dio2*) through an indirect mechanism involving the CNS. Of interest, it has recently been proposed that transgenic overexpression (Owen et al. 2014) and pharmacological administration (Douris et al. 2015) of FGF21 increase the sympathetic action. However, a more extensive analysis of other candidate factors should be performed, and further research will be

required to determine the exact mechanism by which FGF21 induces BAT activation.

Feeding obese mice (Ob/Ob) with a (-)leu diet resulted in restrained effects on weight loss, *Fgf21* induction in liver and *Ucp1* induction in BAT. Of note, FGF21 serum concentration was already elevated in the pair-fed control group, an observation that is consistent with obesity as an FGF21-resistant state (M. Fisher et al. 2010). Nevertheless, the serum FGF21 concentration was lower in leucine-deprived obese mice than in leucine-deprived lean counterparts. Proper *Asns* induction in obese mice discards trunked AAR as the mechanism underlying lower FGF21 serum concentration. Interestingly, it has been recently proposed that the c-Jun NH2-terminal kinase (JNK) pathway, which is involved in the development of obesity and insulin resistance, causes an increase in the expression of the repressor NCoR1 to inhibit *Fgf21* expression. Therefore, increased JNK activity may impair *Fgf21* induction in leucine-deprived obese mice.

In summary, we found that FGF21 is an important factor, although not the only one, in mediating the changes in lipid metabolism observed upon leucine deprivation (Figure D3). We demonstrate that Fgf21-deficient mice under these circumstances show unrepressed lipogenesis in liver and WAT, decreased phosphorylation of HSL in WAT (thus indicating impaired lipolysis), and impaired induction of *Ucp1* expression in BAT. Thus, our results support the notion that FGF21 plays a key role in the regulation of lipid metabolism during amino acid starvation.

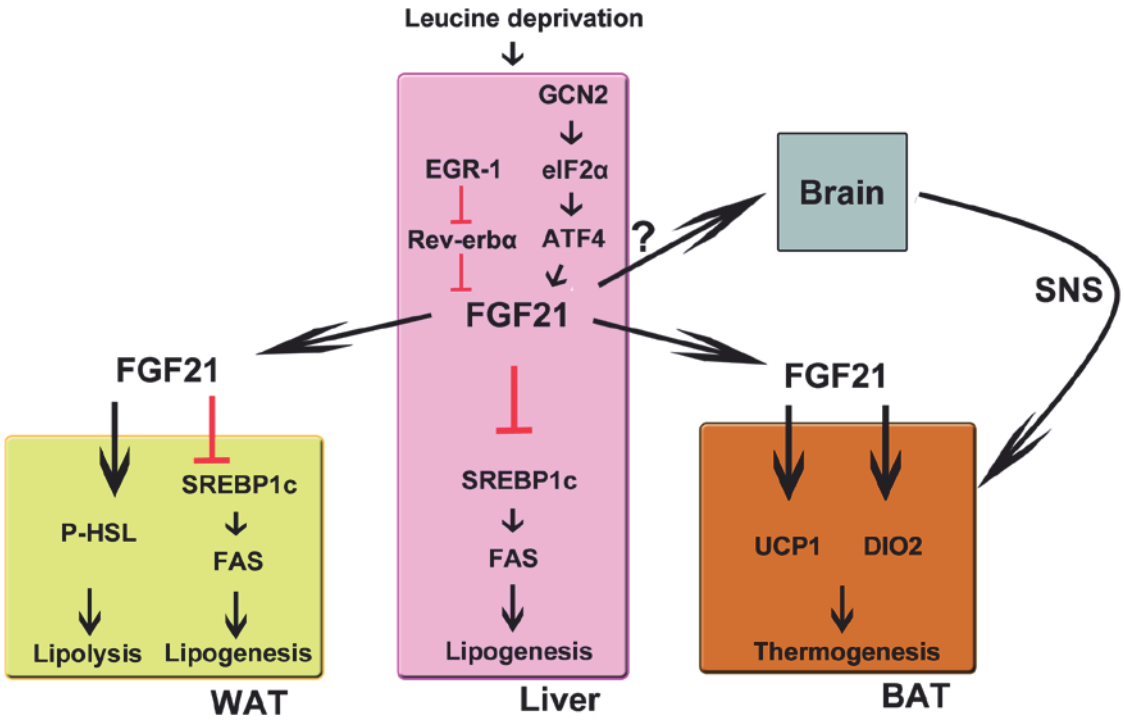

Figure D 3 FGF21 mediates lipid metabolism in response to leucine deprivation in liver, WAT and BAT

THE ROLE OF FGF21 IN THE METABOLIC RESPONSE TO PROTEIN RESTRICTION

Given the unfeasibility to translate single amino acid deprivation to humans, we focussed on low-protein diets (LPDs) as a more realistic approach. The aim of our study was to address whether LPDs cause similar metabolic effects to leucine deprivation. In addition, using the liver-specific *Fgf21* KO mouse we determined the role of liver-derived FGF21 in the response to protein restriction.

The LPD increased circulating FGF21 levels with an associated upregulated expression in liver. This KO model revealed that protein restriction almost exclusively affected the hepatic expression of FGF21 and that there was no compensatory response in other tissues, such as BAT or WAT. Analysis of serum human samples from the PREDIMED study extended the correlation between LPD and FGF21 to humans.

Regarding the molecular basis of *Fgf21* regulation during protein restriction, we have observed a clear induction of ATF4 protein levels in the liver of mice on the LPD. Our results support the notion that the GCN2-ATF4 pathway is the main mechanism underlying hepatic FGF21 overexpression upon protein restriction (Laeger et al. 2014).

GCN2-independent mechanisms that induce hepatic FGF21 in response to methionine-restricted diets have recently been described (Wanders et al. 2016). This observation points to a different response programme in liver via the non-canonical PERK/nuclear respiratory factor 2 (NRF2) pathway. This alternative pathway may effectively sense and translate the metabolic responses to methionine restriction in the absence of GCN2. In parallel, it has also been demonstrated that the absence of GCN2 during long-term dietary protein restriction do not completely blunt *Fgf21* induction (Laeger et al. 2014). In conclusion, the impact of alternative pathways on stimulating FGF21 expression under a LPD, whether they involve ATF4 or not, should be addressed in greater depth.

The ATF4-mediated upregulation of *Fgf21* in liver was partially responsible for

the weight loss observed in mice fed a LPD, since the L*Fgf21*KO mice were partially protected from this loss. The observed reduction in food intake in protein-restricted mice contrasts with studies on rats, which reported no changes (Ozaki et al. 2015) or increased consumption (Laeger et al. 2014) were registered. However, the decrease was consistent with the reduced food intake produced by a leucine-deficient diet. Minor changes in diet composition affecting amino acid bioavailability may explain these discrepancies. Moreover, although FGF21 has the potential to modulate food preferences (Talukdar et al. 2016; von Holstein-Rathlou et al. 2016), in our mouse model it did not contribute to the food aversion caused by the LPD.

When analysing the weight loss data, a global negative tendency was observed across tissues of mice on the LPD. However, only in heart and scWAT the weight loss was clearly dependent of FGF21.

Focusing on the effects of FGF21 on scWAT and given the capacity of FGF21 to produce the browning of white fat depots (Fisher et al. 2012), we examined the activation of the thermogenic programme in this tissue. Accordingly, scWAT browning caused by the LPD did not occur in mice lacking hepatic *Fgf21*. As UCP1 activity is related to EE, the blunted induction of *Ucp1* in the LPD-fed L*Fgf21*KO mice, may contribute to the reduction in weight loss observed in this mouse model under these circumstances.

Contrary to data indicating an increase in *Ucp1* expression in BAT of protein-restricted obese rats (Ozaki et al. 2015) and leucine-deprived mice (De Sousa-Coelho et al. 2013), we did not observe significant changes in *Ucp1* expression in BAT of protein-restricted mice. Nevertheless, the induction of the thermogenic programme in scWAT may be sufficient to affect body weight.

An increasing body of evidence supports the capacity of FGF21 to modulate CNS signalling pathways that regulate a broad range of physiological functions. Processes such as female reproduction (Owen et al. 2013), sugar and alcohol preferences (Talukdar et al. 2016), gluconeogenesis in liver (Patel et al. 2015), circadian behaviour (Bookout et al. 2013) and the sympathetic outflow (Douris et al. 2015; Owen et al. 2014) have been described to be modulated by the

action of FGF21 in various regions of the brain. To further define the mechanisms activating *Ucp1* expression in scWAT under protein restriction we analysed the plasma concentration of several candidate factors related to FGF21 and thermogenesis. We found that, among analysed factors, only variation in free T3 was clearly dependent on FGF21, whereas ACTH and noradrenaline increased in response to protein restriction in both genotypes.

Although leucine deprivation increases free T3 levels (Cheng et al. 2009), we have observed a significant decrease in animals on the LPD, which is consistent with the effect of pharmacological administration of FGF21 on free T3 levels (Coskun et al. 2008). This result reinforces the idea of a mutual regulatory dependency (Domouzoglou et al. 2014) and suggests a negative feedback loop between FGF21 and the thyroid system. However, it discards T3 as a mediator of the effects of FGF21 on thermogenesis.

Increased levels of both FGF21 and noradrenaline are widely reported to induce UCP1 expression (Tseng et al. 2010; Fisher et al. 2012). The administration of the β-blocker propranolol to protein-restricted mice allowed us to distinguish between the roles of FGF21 and noradrenaline. While *Ucp1* expression was upregulated independently of adrenergic signalling, *Dio2* and *Pparγ* expression was blunted by propranolol treatment. These results point to the induction of *Ucp1* as a direct effect of liver-delivered FGF21 on scWAT and discard a CNS-mediated effect. Interestingly, our results agree with reported data indicating that adrenergic receptor blockade prevents the actions of central administered FGF21 but not those of peripheral administration (Owen et al. 2014). It has been proposed that FGF21 exerts a dual effect on thermogenesis by both increasing sympathetic outflow and acting directly on adipocytes (Douris et al. 2015). Although we cannot totally discard an effect of FGF21 on sympathetic outflow upon protein restriction, the increase in noradrenaline levels caused by the LPD appeared to be independent of FGF21 levels. In this regard, although our results do not directly link FGF21 to adrenergic signalling, both signals appear to participate in the activation of the thermogenic programme in scWAT.

Consequently, the effects of the LPD on *Ucp1* expression are explained by a direct effect of FGF21 on scWAT. In addition, our mouse model let us to propose that, under a LPD, the endocrine effects of liver-derived FGF21 on scWAT are predominant, consequently discarding any autocrine effect.

Finally, since FGF21 is proposed as a candidate for the treatment of diabetes due to its beneficial effects on glucose metabolism, we analysed the role of this hormone in the glucose tolerance during protein restriction. The GTT showed that FGF21 is involved in the improved glucose tolerance observed in LPD-fed mice. However, the insulin response was not statistically improved, and *Glut1* mRNA levels in fat depots did not change in these animals. To further understand the metabolic changes regarding improved glucose tolerance, parameters such as fasted insulin levels or insulin signalling should be determined. Moreover, *Glut1* mRNA levels in skeletal muscle would be also valuable information.

BAT and BeAT have a powerful machinery for the oxidation of metabolic substrates, and correspondingly, robust enzymatic machinery for lipid and glucose uptake (Cannon & Nedergaard 2004). Due to this role of BAT/BeAT in the regulation of circulating lipids and glucose, browning of scWAT during protein restriction is probably responsible for the improved glucose tolerance

To sum up, our results, together with the abovementioned published data (Ozaki et al. 2015; Laeger et al. 2014), provide a consistent evidence that protein restriction brings about weight loss and an increase in EE. In addition, the LPD improves glucose tolerance. All these observations are tightly linked to the increase in serum concentrations of FGF21 in rodents on a LPD. Our findings show that the effects of a LPD depend, at least in part, on the circulating levels of FGF21 and consequently on the liver production of this growth factor. The L*Fgf21*KO mice revealed the relevance of FGF21 in the response to a LPD.

Given the parallelism between the results of our study in humans and those in mice, we postulate that modulation of dietary protein content can bring about changes in the circulating levels of FGF21 in mice and humans. Furthermore,

we propose that in mice this nutritional intervention modulates FGF21 activity in the target tissues, especially scWAT. The present work describes the molecular mechanisms through which a LPD—via FGF21— contributes to restoring lipid/glucose homeostasis. The last question would be to define a nutritional recommendation based on a reduction in protein intake as a non-invasive approach to induce the hepatic expression of FGF21.

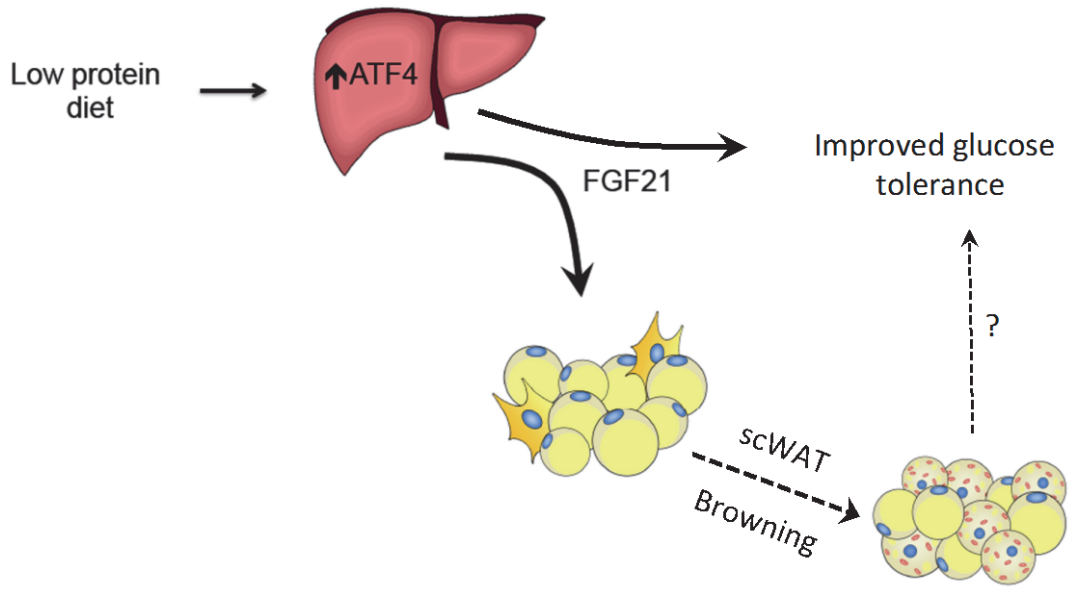

Figure D 4 FGF21 mediates browning of scWAT and improves glucose tolerance in response to protein restriction

GLOBAL DISCUSSION

Given the multiple beneficial metabolic effects of FGF21, this growth factor emerges as an attractive drug candidate for the treatment of metabolic conditions such as cardiovascular disease, obesity and type 2 diabetes.

Knowledge of the molecular basis regulating a drug candidate like FGF21 is relevant for the design of therapeutic strategies. In this study, we sought to further our understanding of *Fgf21* regulation upon amino acid deficiency by adding the repressor Rev-erbα to *Fgf21* regulating factors. On the basis of our findings we propose that an increase in ATF4 and decrease in Rev-erbα act additively to boost *Fgf21* expression during amino acid deficiency. However, how Rev-erbα is tethered to the *Fgf21* promoter is not clear, and further studies will be devoted to this point. This question is especially relevant because targeting the binding of Rev-erbα to the tethering factor would more specifically modulate *Fgf21* expression than generically targeting Rev-erbα, which would affect the entire clock machinery.

Here we also demonstrate that the weight loss, downregulation of key lipogenic genes in liver and WAT, and BAT activation in response to leucine deprivation, are partly FGF21-dependent. Our results show that FGF21 serum levels positively correlate with the mRNA levels measured in liver but not in BAT or WAT, where they were not affected or even downregulated in response to leucine deprivation. All these results demonstrate that FGF21 mediates the response of the lipid metabolism to amino acid starvation.

In the context of a dietary intervention approach and in order to translate our findings to humans, we analysed the role of FGF21 in response to protein restriction instead of to the deficiency of a single amino acid.

Our results demonstrate that the effects of a LPD on body weight, browning of scWAT, and glucose tolerance depend, at least in part, on the circulating levels of FGF21 and consequently on the liver production of this growth factor. The L*Fgf21*KO mice revealed the relevance of FGF21 in the response to a LPD, but

also in the metabolic and transcriptional pathways activated or repressed by protein restriction.

We expected to find similar phenotypes between leucine deprivation and protein restriction. Indeed, we observed similarities regarding the induction of FGF21 and its contribution to weight loss. However, the LPD did not reproduce the robust induction of *Ucp1* observed during leucine deprivation in mouse BAT. In addition, preliminary studies discarded changes in lipogenic genes in liver and eWAT and led us to focus on the metabolic effects observed on scWAT.

These discrepancies not only underlie the different roles of each single amino acid in the metabolic response but also the important differences between protein restriction and amino acid deprivation. Taking into account these considerations, the contribution of each amino acid to the modulation of FGF21 and the way in which a deficiency in specific types of dietary protein alters FGF21 expression gain relevance. In this regard, future studies should addressed these questions.

During leucine deprivation, the FGF21 concentration in serum was higher than during protein restriction. Circulating FGF21 levels may partly explain the different phenotypes observed in leucine-deprived and protein-restricted mice. The concentration of peripheral FGF21 may be critical to ensure its capacity to cross the blood-brain barrier and thus, for its CNS-mediated effects. This observation would explain, for example, the induction of *Ucp1* during leucine deprivation through increased sympathetic outflow to BAT. Circulating FGF21 levels reached under protein restriction would not be higher enough to allow this hormone to cross the blood-brain barrier. Consequently, it would not be able to exert its actions on the CNS to increase *Ucp1* expression in BAT. Along the same lines of this hypothesis, it has been proposed that differences between the effects of endogenous FGF21 and pharmacological treatment are due to the higher levels reached by the latter. Furthermore, our results demonstrate that precise mechanisms regulate *Fgf21* expression during fasting, amino acid deprivation, or both, resulting in variations in FGF21 serum concentrations. This observation supports the notion that a fine-tuning of FGF21 serum concentrations is critical to determine its actions.

As previously mentioned, amino acid deficiency and protein restriction increased *Ucp1* expression and EE. It may seem contradictory that under nutrient deficiency the organism would channel energy into thermogenesis. In this regard, we have questioned the purpose of this process. On the one hand, the uncoupled oxidation in BAT (or BeAT) may provide the metabolic precursors needed to adapt to a new metabolic state. On the other hand, the cold seasons usually coincide with a decrease in food availability, which can cause nutritional deficiencies in some amino acids. The induction of the thermogenic programme in response to amino acid restriction could be the result of an evolutionary adaptation, preparing the organism for the cold to come.

Undoubtedly, a diet that naturally increases the secretion of a candidate factor for the treatment of the metabolic syndrome is very attractive and establishes the modulation of dietary protein content as an inexpensive and viable approach. However, some limitations may lower the potential of this strategy. Our results in Ob/Ob mice suggest that the physiological increase of FGF21 in a context of obesity, which has been described as an FGF21-resistant state (F. M. Fisher et al. 2010), may not be sufficient to produce the expected benefits. The increase in the sensitivity of the target tissues should be a goal in parallel to the increase in circulating FGF21 levels. In this regard, some published data and unpublished results from our group show that bioactive dietary compounds such as polyphenols, improve the FGF21 signalling. Therefore, LPD rich in polyphenols, could satisfy both conditions, namely increased circulating FGF21 levels and enhanced target tissues sensitivity.

Studies performed in humans provide contradictory results regarding the correlation between plasma levels of FGF21, BMI, and insulin resistance (Zhang et al. 2008; Chavez et al. 2009; Chen et al. 2008). Also, the FGF21-resistant state described in mice is not well established in humans, and the beneficial effects of FGF21 induction have yet to be demonstrated in the latter. Further studies will be needed to evaluate the effects of a LPD / FGF21 induction on the metabolic profile of obese and insulin-resistant subjects. Also, potential long-term undesired effects such as impact on muscle mass or bone density require attention.

There is an array of possibilities to extend the strategy to increase the endogenous production of FGF21 as an alternative to exogenous administration. In this context, several scenarios that alter aminoacidemia also lead to an increase in FGF21 expression. The absence of slc6a19 (neutral amino acid transporter) causes a lack of systemic neutral amino acids, resulting in an increase in FGF21 transcription (Jiang et al. 2015). Treatment with the antileukemic agent asparaginase depletes circulating asparagine and glutamine levels, thereby promoting FGF21 expression (Wilson et al. 2015), and the skeletal muscle-specific knockout mice for glucocorticoid receptor (GR) show reduced alanine flux from skeletal muscle during fasting, resulting in an increase in FGF21 plasma levels (Shimizu et al. 2015). Hence, it is likely that many other contexts that lead to a reduction in amino acid availability also trigger FGF21 expression. In this regard, we propose the following as examples: reducing amino acid absorption by inhibiting amino acid transporters in the intestinal tract, increasing amino acid catabolism, and partially blocking tRNAs to initiate the AAR. Furthermore, in addition to amino acids, other nutritional impacts can modulate *FGF21* expression (Pérez-Martí et al. 2016).

In summary, the results from the current study, together with a growing number of publications, highlight the role of FGF21 in metabolic adaptation to a wide variety of stress conditions, including amino acid starvation and protein restriction. Our findings provide new insight into the modulation of dietary protein as a strategy to induce elevated serum concentrations of this therapeutic candidate.

CONCLUSIONS

THE ROLE OF REV-ERBα IN THE INDUCTION OF FGF21 UPON LEUCINE DEPRIVATION

- Decreased Rev-erbα expression and activity enhances FGF21 expression during leucine deprivation.
- EGR-1 represses the promoter activity of Rev-erbα.

THE ROLE OF FGF21 IN THE METABOLIC RESPONSE TO LEUCINE DEPRIVATION

- FGF21 partly mediates the weight loss under leucine deprivation.
- FGF21 mediates increased lipolysis, decreased expression of lipogenic genes and reduction of adipocytes size in eWAT upon leucine deprivation.
- FGF21 mediates diminished expression of lipogenic genes and reduction in lipid content in liver upon leucine deprivation.
- FGF21 mediates upregulation of thermogenesis machinery in BAT upon leucine deprivation.
- The FGF21-dependent effects are not regulated through the MAPK ERK1/2 pathway during leucine deprivation.
- Obese mice (ob/ob) are partially resistant to leucine deprivation effects concerning weight loss, FGF21 circulating levels and *Ucp1* expression in BAT.

THE ROLE OF FGF21 IN THE METABOLIC RESPONSE TO PROTEIN RESTRICTION

- Protein restriction increases ATF4 protein levels and FGF21 expression in liver that couples with increased circulating FGF21.
- In humans, dietary protein intake inversely correlates with plasma FGF21 concentration.
- Liver-derived FGF21 induces browning of scWAT where Ucp1 expression is upregulated independently of the adrenergic signalling.
- Hepatic FGF21 mediates the improved glucose tolerance under protein restriction.

REFERENCES

A

Ables, G.P. et al., 2012. Methionine-restricted C57BL/6J mice are resistant to diet-induced obesity and insulin resistance but have low bone density. *PloS one*, 7(12), p.e51357.

Adams, A.C. et al., 2012. Fundamentals of FGF19 & FGF21 action in vitro and in vivo. *PloS one*, 7(5), p.e38438.

Adams, A.C. et al., 2010. Thyroid hormone regulates hepatic expression of fibroblast growth factor 21 in a PPARalpha-dependent manner. *The Journal of biological chemistry*, 285(19), pp.14078–82.

Anthony, T.G. et al., 2004. Preservation of liver protein synthesis during dietary leucine deprivation occurs at the expense of skeletal muscle mass in mice deleted for eIF2 kinase GCN2. *The Journal of biological chemistry*, 279(35), pp.36553–36561.

Arase, K. et al., 1988. Effects of corticotropin-releasing factor on food intake and brown adipose tissue thermogenesis in rats. *The American Journal of Physiology*, 255, pp.255–259.

Archer, A. et al., 2012. Fasting-induced FGF21 is repressed by LXR activation via recruitment of an HDAC3 corepressor complex in mice. *Molecular endocrinology (Baltimore, Md.)*, 26(12), pp.1980–90.

Arner, P. et al., 2008. FGF21 attenuates lipolysis in human adipocytes - a possible link to improved insulin sensitivity. *FEBS letters*, 582(12), pp.1725–1730.

B

Badman, M.K. et al., 2009. Fibroblast growth factor 21-deficient mice demonstrate impaired adaptation to ketosis. *Endocrinology*, 150(11), pp.4931–4940.

Badman, M.K. et al., 2007. Hepatic fibroblast growth factor 21 is regulated by PPARalpha and is a key mediator of hepatic lipid metabolism in ketotic states. *Cell metabolism*, 5(6), pp.426–437.

Bernardo, B. et al., 2015. FGF21 does not require interscapular brown adipose tissue and improves liver metabolic profile in animal models of obesity and

insulin-resistance. *Scientific reports*, 5, p.11382.

Bookout, A.L. et al., 2013. FGF21 regulates metabolism and circadian behavior by acting on the nervous system. *Nature medicine*, 19(9), pp.1147–1152.

Bordicchia, M. et al., 2012. Cardiac natriuretic peptides act via p38 MAPK to induce the brown fat thermogenic program in mouse and human adipocytes. *The Journal of clinical investigation*, 122(3), pp.1022–1036.

Bostrom, P. et al., 2012. A PGC1-alpha-dependent myokine that drives brown-fat-like development of white fat and thermogenesis. *Nature*, 481(7382), pp.463–468.

Brahma, M.K. et al., 2014. Fibroblast growth factor 21 is induced upon cardiac stress and alters cardiac lipid homeostasis. *Journal of lipid research*, 55(11), pp.2229–2241.

Camporez, J.P.G. et al., 2013. Cellular mechanisms by which FGF21 improves insulin sensitivity in male mice. *Endocrinology*, 154(9), pp.3099–3109.

Cannon, B. & Nedergaard, J., 2004. Brown adipose tissue: function and physiological significance. *Physiological reviews*, 84(1), pp.277–359.

Cao, W. et al., 2001. beta-Adrenergic activation of p38 MAP kinase in adipocytes: cAMP induction of the uncoupling protein 1 (UCP1) gene requires p38 MAP kinase. *The Journal of biological chemistry*, 276(29), pp.27077–27082.

Cereijo, R., Villarroya, J. & Villarroya, F., 2015. Non-sympathetic control of brown adipose tissue. *International Journal of Obesity Supplements*, 5(S1), pp.S40–S44.

C

Cerri, M. & Morrison, S.F., 2006. Corticotropin releasing factor increases in brown adipose tissue thermogenesis and heart rate through dorsomedial hypothalamus and medullary raphe pallidus. *Neuroscience*, 140(2), pp.711–721.

Chartoumpekis, D. V et al., 2011. Brown adipose tissue responds to cold and adrenergic stimulation by induction of FGF21. *Molecular medicine (Cambridge, Mass.)*, 17(7-8), pp.736–740.

Chaveroux, C. et al., 2010. Molecular mechanisms involved in the adaptation to

amino acid limitation in mammals. *Biochimie*, 92(7), pp.736–745.

Chavez, A.O. et al., 2009. Circulating fibroblast growth factor-21 is elevated in impaired glucose tolerance and type 2 diabetes and correlates with muscle and hepatic insulin resistance. *Diabetes Care*, 32(8), pp.1542–1546.

Chen, H. et al., 2004. Amino acid deprivation induces the transcription rate of the human asparagine synthetase gene through a timed program of expression and promoter binding of nutrient-responsive basic region/leucine zipper transcription factors as well as localized histone . *Journal of Biological Chemistry*, 279(49), pp.50829–50839.

Chen, W.-W. et al., 2008. Circulating FGF-21 levels in normal subjects and in newly diagnose patients with Type 2 diabetes mellitus. *Experimental and clinical endocrinology & diabetes : official journal, German Society of Endocrinology [and] German Diabetes Association*, 116(1), pp.65–68.

Cheng, Y. et al., 2009. Leucine deprivation decreases fat mass by stimulation of lipolysis in WAT and upregulation of UCP1 in BAT. *Diabetes*, 59(January), pp.17–25.

Cheng, Y. et al., 2010. Leucine deprivation decreases fat mass by stimulation of lipolysis in white adipose tissue and upregulation of uncoupling protein 1 (UCP1) in brown adipose tissue. *Diabetes*, 59(January), pp.17–25.

Cherasse, Y. et al., 2007. The p300/CBP-associated factor (PCAF) is a cofactor of ATF4 for amino acid-regulated transcription of CHOP. *Nucleic acids research*, 35(17), pp.5954–5965.

Chu, A.Y. et al., 2013. Novel locus including FGF21 is associated with dietary macronutrient intake. *Human molecular genetics*, 22(9), pp.1895–1902.

Coskun, T. et al., 2008. Fibroblast growth factor 21 corrects obesity in mice. *Endocrinology*, 149(12), pp.6018–6027.

Cypess, A.M. et al., 2009. Identification and importance of brown adipose tissue in adult humans. *The New England journal of medicine*, 360(15), pp.1509–1517.

Cyphert, H. a et al., 2012. Activation of the farnesoid X receptor induces hepatic expression and secretion of fibroblast growth factor 21. *The Journal of biological chemistry*, 287(30), pp.25123–38.

D

Dasarathy, S. et al., 2011. Elevated hepatic fatty acid oxidation, high plasma fibroblast growth factor 21, and fasting bile acids in nonalcoholic steatohepatitis. *European journal of gastroenterology & hepatology*, 23(5), pp.382–388.

Deval, C. et al., 2009. Amino acid limitation regulates the expression of genes involved in several specific biological processes through GCN2-dependent and GCN2-independent pathways. *FEBS Journal*, 276(3), pp.707–718.

Diaz-Delfin, J. et al., 2012. TNF-alpha represses beta-Klotho expression and impairs FGF21 action in adipose cells: involvement of JNK1 in the FGF21 pathway. *Endocrinology*, 153(9), pp.4238–4245.

Ding, X. et al., 2012. betaKlotho is required for fibroblast growth factor 21 effects on growth and metabolism. *Cell metabolism*, 16(3), pp.387–393.

Dogan, S.A. et al., 2014. Tissue-specific loss of DARS2 activates stress responses independently of respiratory chain deficiency in the heart. *Cell Metabolism*, 19(3), pp.458–469.

Domingo, P. et al., 2010. Serum FGF21 levels are elevated in association with lipodystrophy, insulin resistance and biomarkers of liver injury in HIV-1-infected patients. *AIDS (London, England)*, 24(17), pp.2629–2637.

Domouzoglou, E.M. et al., 2014. Fibroblast growth factor 21 and thyroid hormone show mutual regulatory dependency but have independent actions in vivo. *Endocrinology*, 155(5), pp.2031–40.

Douris, N. et al., 2015. Central Fibroblast Growth Factor 21 Browns White Fat via Sympathetic Action in Male Mice. *Endocrinology*, (May), pp.en.2014–2001.

Dushay, J. et al., 2010. Increased fibroblast growth factor 21 in obesity and nonalcoholic fatty liver disease. *Gastroenterology*, 139(2), pp.456–463.

Dushay, J.R. et al., 2015. Fructose ingestion acutely stimulates circulating FGF21 levels in humans. *Molecular Metabolism*, 4(1), pp.51–57.

Dutchak, P.A. et al., 2012. Fibroblast growth factor-21 regulates PPARgamma activity and the antidiabetic actions of thiazolidinediones. *Cell*, 148(3), pp.556–567.

E

Emanuelli, B. et al., 2015. Interplay between FGF21 and insulin action in the liver regulates metabolism. *The Journal of clinical investigation*, 125(1), p.458.

Estall, J.L. et al., 2009. PGC-1alpha negatively regulates hepatic FGF21 expression by modulating the heme/Rev-Erb(alpha) axis. *Proceedings of the National Academy of Sciences of the United States of America*, 106(52), pp.22510–22515.

Estruch, R. et al., 2013. Primary prevention of cardiovascular disease with a Mediterranean diet. *The New England journal of medicine*, 368(14), pp.1279–90

F

Fawcett, T.W. et al., 1999. Complexes containing activating transcription factor (ATF)/cAMP-responsive-element-binding protein (CREB) interact with the CCAAT/enhancer-binding protein (C/EBP)-ATF composite site to regulate Gadd153 expression during the stress response. *The Biochemical journal*, 339 (Pt 1, pp.135–141.

Fisher, F.M. et al., 2012. FGF21 regulates PGC-1α and browning of white adipose tissues in adaptive thermogenesis. *Genes & development*, 26(3), pp.271–81.

Fisher, F.M. et al., 2011. Integrated regulation of hepatic metabolism by fibroblast growth factor 21 (FGF21) in vivo. *Endocrinology*, 152(8), pp.2996–3004.

Fisher, F.M. et al., 2010. Obesity is a fibroblast growth factor 21 (FGF21)-resistant state. *Diabetes*, 59(11), pp.2781–2789.

Fisher, F.M. & Maratos-Flier, E., 2016. Understanding the Physiology of FGF21. *Annual Review of Physiology*, 78(1), pp.annurev–physiol–021115–105339.

Fisher, M. et al., 2010. Obesity Is a Fibroblast Growth Factor 21 Resistant State. , 59(November), pp.2781–2789.

Fon Tacer, K. et al., 2010. Research resource: Comprehensive expression atlas of the fibroblast growth factor system in adult mouse. *Molecular*

endocrinology (Baltimore, Md.), 24(10), pp.2050–2064.

G

Gaich, G. et al., 2013. The effects of LY2405319, an FGF21 Analog, in obese human subjects with type 2 diabetes. *Cell Metabolism*, 18(3), pp.333–340.

Ge, X. et al., 2011. Fibroblast growth factor 21 induces glucose transporter-1 expression through activation of the serum response factor/Ets-like protein-1 in adipocytes. *The Journal of biological chemistry*, 286(40), pp.34533–34541.

Giguere, V. et al., 1994. Isoform-specific amino-terminal domains dictate DNA-binding properties of ROR alpha, a novel family of orphan hormone nuclear receptors. *Genes & development*, 8(5), pp.538–553.

Gimeno, R.E. & Moller, D.E., 2014. FGF21-based pharmacotherapy--potential utility for metabolic disorders. *Trends in endocrinology and metabolism: TEM*, 25(6), pp.303–311.

Grimble, R.F. & Whitehead, R.G., 1970. Fasting serum-aminoacid patterns in kwashiorkor and after administration of different levels of protein. *Lancet (London, England)*, 1(7653), pp.918–920.

Guo, F. & Cavener, D.R., 2007. The GCN2 eIF2alpha kinase regulates fatty-acid homeostasis in the liver during deprivation of an essential amino acid. *Cell metabolism*, 5(2), pp.103–114.

H

Handschin, C. et al., 2005. Nutritional regulation of hepatic heme biosynthesis and porphyria through PGC-1alpha. *Cell*, 122(4), pp.505–515.

Handschin, C. & Spiegelman, B.M., 2006. Peroxisome proliferator-activated receptor gamma coactivator 1 coactivators, energy homeostasis, and metabolism. *Endocrine reviews*, 27(7), pp.728–735.

Hankir, M.K., Cowley, M.A. & Fenske, W.K., 2016. A BAT-Centric Approach to the Treatment of Diabetes: Turn on the Brain. *Cell Metabolism*, 24(1), pp.31–40.

Hany, T.F. et al., 2002. Brown adipose tissue: a factor to consider in

symmetrical tracer uptake in the neck and upper chest region. *European journal of nuclear medicine and molecular imaging*, 29(10), pp.1393–1398.

Hao, L. et al., 2016. Fibroblast Growth Factor 21 (Fgf21) Gene Expression Is Elevated in the Liver of Mice Fed a High-Carbohydrate Liquid Diet and Attenuated by a Lipid Emulsion but Is Not Upregulated in the Liver of Mice Fed a High-Fat Obesogenic Diet. *The Journal of nutrition*, 146(2), pp.184–190.

Hao, S. et al., 2005. Uncharged tRNA and sensing of amino acid deficiency in mammalian piriform cortex. *Science (New York, N.Y.)*, 307(5716), pp.1776–1778.

Harding, H.P. et al., 2003. An integrated stress response regulates amino acid metabolism and resistance to oxidative stress. *Molecular cell*, 11(3), pp.619–633.

Harding, H.P. & Lazar, M.A., 1995. The monomer-binding orphan receptor Rev-Erb represses transcription as a dimer on a novel direct repeat. *Molecular and cellular biology*, 15(9), pp.4791–4802.

Harris, L.-A.L.S. et al., 2015. Perilipin 5-Driven Lipid Droplet Accumulation in Skeletal Muscle Stimulates the Expression of Fibroblast Growth Factor 21. *Diabetes*, 64(8), pp.2757–2768.

Hojman, P. et al., 2009. Fibroblast growth factor-21 is induced in human skeletal muscles by hyperinsulinemia. *Diabetes*, 58(12), pp.2797–2801.

Holland, W.L. et al., 2013. An FGF21-adiponectin-ceramide axis controls energy expenditure and insulin action in mice. *Cell Metabolism*, 17(5), pp.790–797..

von Holstein-Rathlou, S. et al., 2016. FGF21 Mediates Endocrine Control of Simple Sugar Intake and Sweet Taste Preference by the Liver. *Cell metabolism*, 23(2), pp.335–343.

Hondares, E. et al., 2010. Hepatic FGF21 expression is induced at birth via PPARalpha in response to milk intake and contributes to thermogenic activation of neonatal brown fat. *Cell metabolism*, 11(3), pp.206–212.

Hondares, E. et al., 2011. Thermogenic activation induces FGF21 expression and release in brown adipose tissue. *The Journal of biological chemistry*, 286(15), pp.12983–12990.

Hotta, Y. et al., 2009. Fibroblast growth factor 21 regulates lipolysis in white

adipose tissue but is not required for ketogenesis and triglyceride clearance in liver. *Endocrinology*, 150(10), pp.4625–4633.

I

Iizuka, K., Takeda, J. & Horikawa, Y., 2009. Glucose induces FGF21 mRNA expression through ChREBP activation in rat hepatocytes. *FEBS Letters*, 583(17), pp.2882–2886.

Inagaki, T. et al., 2007. Endocrine regulation of the fasting response by PPARalpha-mediated induction of fibroblast growth factor 21. *Cell metabolism*, 5(6), pp.415–425.

Ishida, N., 2009. Role of PPAR in the control of torpor through FGF21-NPY pathway: From circadian clock to seasonal change in mammals. *PPAR Research*.

Izumiya, Y. et al., 2008. FGF21 is an Akt-regulated myokine. *FEBS letters*, 582(27), pp.3805–3810.

J

Jiang, Y. et al., 2015. Mice lacking neutral amino acid transporter B0AT1 (Slc6a19) have elevated levels of FGF21 and GLP-1 and improved glycaemic control. *Molecular Metabolism*, 4(5), pp.406–417.

Johnson, C.L. et al., 2009. Fibroblast Growth Factor 21 Reduces the Severity of Cerulein-Induced Pancreatitis in Mice. *Gastroenterology*, 137(5), pp.1795–1804.

Joki, Y. et al., 2015. FGF21 attenuates pathological myocardial remodeling following myocardial infarction through the adiponectin-dependent mechanism. *Biochemical and Biophysical Research Communications*, 459(1), pp.124–130.

K

Kaasik, K. & Lee, C.C., 2004. Reciprocal regulation of haem biosynthesis and the circadian clock in mammals. *Nature*, 430(6998), pp.467–471.

Kajimura, S., Spiegelman, B.M. & Seale, P., 2015. Brown and Beige Fat: Physiological Roles beyond Heat Generation. *Cell metabolism*, 22(4), pp.546–559.

Keipert, S. et al., 2014. Skeletal muscle mitochondrial uncoupling drives endocrine cross-talk through the induction of FGF21 as a myokine. *American journal of physiology. Endocrinology and metabolism*, 306(5), pp.E469–82.

Kharitonenkov, A. et al., 2005. FGF-21 as a novel metabolic regulator. *The Journal of clinical investigation*, 115(6), pp.1627–1635.

Kharitonenkov, A. et al., 2007. The metabolic state of diabetic monkeys is regulated by fibroblast growth factor-21. *Endocrinology*, 148(2), pp.774–781.

Kharitonenkov, A. & Shanafelt, A.B., 2009. FGF21: a novel prospect for the treatment of metabolic diseases. *Current opinion in investigational drugs (London, England : 2000)*, 10(4), pp.359–364.

Kiefer, F.W. et al., 2012. Retinaldehyde dehydrogenase 1 coordinates hepatic gluconeogenesis and lipid metabolism. *Endocrinology*, 153(7), pp.3089–3099.

Kilberg, M.S., Shan, J. & Su, N., 2009. ATF4-dependent transcription mediates signaling of amino acid limitation. *Trends in Endocrinology and Metabolism*, 20(9), pp.436–443.

Kim, H. et al., 2014. Liver-enriched transcription factor CREBH interacts with peroxisome proliferator-activated receptor ?? to regulate metabolic hormone FGF21. *Endocrinology*, 155(3), pp.769–782.

Kim, K.H., Kim, S.H., et al., 2013. Acute exercise induces FGF21 expression in mice and in healthy humans. *PloS one*, 8(5), p.e63517.

Kim, K.H., Jeong, Y.T., Oh, H., et al., 2013. Autophagy deficiency leads to protection from obesity and insulin resistance by inducing Fgf21 as a mitokine. *Nature medicine*, 19(1), pp.83–92.

Kim, K.H., Jeong, Y.T., Kim, S.H., et al., 2013. Metformin-induced inhibition of the mitochondrial respiratory chain increases FGF21 expression via ATF4 activation. *Biochemical and biophysical research communications*, 440(1), pp.76–81.

Kume, K. et al., 1999. mCRY1 and mCRY2 are essential components of the

negative limb of the circadian clock feedback loop. *Cell*, 98(2), pp.193–205.

L

Laeger, T. et al., 2014. FGF21 is an endocrine signal of protein restriction. *Journal of Clinical Investigation*, 124(9), pp.3913–3922.

Laplante, M. & Sabatini, D.M., 2013. mTOR signaling in growth control and disease. *Cell*, 149(2), pp.274–293.

Lee, J.H. et al., 2011. The transcription factor cyclic AMP-responsive element-binding protein H regulates triglyceride metabolism. *Nature medicine*, 17(7), pp.812–815.

Lee, M.S. et al., 2012. Fibroblast growth factor-21 protects human skeletal muscle myotubes from palmitate-induced insulin resistance by inhibiting stress kinase and NF-kappaB. *Metabolism: clinical and experimental*, 61(8), pp.1142–1151.

Lees, E.K. et al., 2014. Methionine restriction restores a younger metabolic phenotype in adult mice with alterations in fibroblast growth factor 21. *Aging cell*, 13(5), pp.817–827.

Li, X. et al., 2009. Inhibition of lipolysis may contribute to the acute regulation of plasma FFA and glucose by FGF21 in ob/ob mice. *FEBS letters*, 583(19), pp.3230–3234.

Li, Y. et al., 2013. Retinoic acid receptor β stimulates hepatic induction of fibroblast growth factor 21 to promote fatty acid oxidation and control whole-body energy homeostasis in mice. *Journal of Biological Chemistry*, 288(15), pp.10490–10504.

Liang, Q. et al., 2014. FGF21 maintains glucose homeostasis by mediating the cross talk between liver and brain during prolonged fasting. *Diabetes*, 63(12), pp.4064–4075.

Lin, Z. et al., 2013. Adiponectin mediates the metabolic effects of FGF21 on glucose homeostasis and insulin sensitivity in mice. *Cell Metabolism*, 17(5), pp.779–789.

Liu, S.Q. et al., 2013. Endocrine protection of ischemic myocardium by FGF21 from the liver and adipose tissue. *Scientific reports*, 3, p.2767.

Lopez, A.B. et al., 2007. A feedback transcriptional mechanism controls the

level of the arginine/lysine transporter cat-1 during amino acid starvation. *Biochem J*, 402(1), pp.163–173.

Lopez, M. et al., 2010. Hypothalamic AMPK and fatty acid metabolism mediate thyroid regulation of energy balance. *Nature medicine*, 16(9), pp.1001–1008.

Lundåsen, T. et al., 2007. PPARα is a key regulator of hepatic FGF21. *Biochemical and Biophysical Research Communications*, 360(2), pp.437–440.

Lynch, L. et al., 2016. iNKT Cells Induce FGF21 for Thermogenesis and Are Required for Maximal Weight Loss in GLP1 Therapy. *Cell metabolism*, 24(3), pp.510–519.

M

Ma, S. et al., 2012. Activation of the cold-sensing TRPM8 channel triggers UCP1-dependent thermogenesis and prevents obesity. *Journal of molecular cell biology*, 4(2), pp.88–96.

Mai, K. et al., 2009. Free fatty acids link metabolism and regulation of the insulin-sensitizing fibroblast growth factor-21. *Diabetes*, 58(7), pp.1532–1538.

Makela, J. et al., 2014. Fibroblast growth factor-21 enhances mitochondrial functions and increases the activity of PGC-1alpha in human dopaminergic neurons via Sirtuin-1. *SpringerPlus*, 3, p.2.

Markan, K.R. et al., 2014. Circulating FGF21 Is Liver Derived and Enhances Glucose Uptake During Refeeding and Overfeeding. *Diabetes*, 63(12), pp.4057–4063.

van Marken Lichtenbelt, W.D. et al., 2009. Cold-activated brown adipose tissue in healthy men. *The New England journal of medicine*, 360(15), pp.1500–1508.

Mashili, F.L. et al., 2011. Direct effects of FGF21 on glucose uptake in human skeletal muscle: implications for type 2 diabetes and obesity. *Diabetes/metabolism research and reviews*, 27(3), pp.286–297.

Mataix Verdú, J., 2003. *Tabla de composición de alimentos* 5a ed., Granada: Universidad de Granada.

Matthias, A. et al., 2000. Thermogenic responses in brown fat cells are fully UCP1-dependent. UCP2 or UCP3 do not substitute for UCP1 in adrenergically or fatty scid-induced thermogenesis. *The Journal of biological chemistry*, 275(33), pp.25073–81.

Monika, P. & Geetha, A., 2015. The modulating effect of Persea americana fruit extract on the level of expression of fatty acid synthase complex, lipoprotein lipase, fibroblast growth factor-21 and leptin - A biochemical study in rats subjected to experimental hyperlipidemia and obesit. *Phytomedicine*, 22(10), pp.939–945.

Moreno-Aliaga, M.J. et al., 2011. Cardiotrophin-1 is a key regulator of glucose and lipid metabolism. *Cell metabolism*, 14(2), pp.242–253.

Muise, E.S. et al., 2008. Adipose fibroblast growth factor 21 is up-regulated by peroxisome proliferator-activated receptor gamma and altered metabolic states. *Molecular pharmacology*, 74(2), pp.403–412.

N

Nedergaard, J., Bengtsson, T. & Cannon, B., 2007. Unexpected evidence for active brown adipose tissue in adult humans. *American journal of physiology. Endocrinology and metabolism*, 293(2), pp.E444–52.

Nguyen, K.D. et al., 2011. Alternatively activated macrophages produce catecholamines to sustain adaptive thermogenesis. *Nature*, 480(7375), pp.104–108.

O

Oishi, K., Uchida, D. & Ishida, N., 2008. Circadian expression of FGF21 is induced by PPARalpha activation in the mouse liver. *FEBS letters*, 582(25-26), pp.3639–3642.

Owen, B.M. et al., 2014. FGF21 acts centrally to induce sympathetic nerve activity, energy expenditure, and weight loss. *Cell Metabolism*, 20(4), pp.670–677.

Owen, B.M. et al., 2013. FGF21 contributes to neuroendocrine control of female reproduction. *Nature medicine*, 19(9), pp.1153–6.

Ozaki, Y. et al., 2015. Rapid increase in fibroblast growth factor 21 in protein

malnutrition and its impact on growth and lipid metabolism. *British Journal of Nutrition*, 114(09), pp.1410–1418.

P

Pan, Y.-X. et al., 2007. Activation of the ATF3 gene through a co-ordinated amino acid-sensing response programme that controls transcriptional regulation of responsive genes following amino acid limitation. *The Biochemical journal*, 401(1), pp.299–307.

Patel, R. et al., 2015. Glucocorticoids regulate the metabolic hormone FGF21 in a feed-forward loop. *Molecular endocrinology (Baltimore, Md.)*, 29(2), pp.213–223.

Peirce, V., Carobbio, S. & Vidal-Puig, A., 2014. The different shades of fat. *Nature*, 510(7503), pp.76–83.

Peirce, V. & Vidal-Puig, A., 2013. Regulation of glucose homoeostasis by brown adipose tissue. *The lancet. Diabetes & endocrinology*, 1(4), pp.353–360.

Pérez-Martí, A. et al., 2016. Nutritional regulation of fibroblast growth factor 21: from macronutrients to bioactive dietary compounds. *Hormone Molecular Biology and Clinical Investigation*, 0(0).

Pezeshki, A. et al., 2016. Low protein diets produce divergent effects on energy balance. *Scientific reports*, 6, p.25145.

Placko, P. & Graham, G., 1974. Serum proteins and plasma free amino acids in severe malnutrition. *The American journal of clinical nutrition*, 27, pp.733–742.

Planavila, a. et al., 2014. Fibroblast growth factor 21 protects the heart from oxidative stress. *Cardiovascular Research*, 106(1), pp.19–31.

Planavila, A., Redondo-Angulo, I. & Villarroya, F., 2015. FGF21 and Cardiac Physiopathology. *Frontiers in Endocrinology*, 6(August), p.133.

Potthoff, M.J. et al., 2009. FGF21 induces PGC-1alpha and regulates carbohydrate and fatty acid metabolism during the adaptive starvation response. *Proc Natl Acad Sci U S A*, 106(26), pp.10853–10858.

Q

Qiu, H. et al., 2001. The tRNA-binding moiety in GCN2 contains a dimerization domain that interacts with the kinase domain and is required for tRNA binding and kinase activation. *EMBO Journal*, 20(6), pp.1425–1438.

R

Raghuram, S. et al., 2007. Identification of heme as the ligand for the orphan nuclear receptors REV-ERBalpha and REV-ERBbeta. *Nature structural & molecular biology*, 14(12), pp.1207–1213.

S

Samms, R.J. et al., 2015. Discrete Aspects of FGF21 In Vivo Pharmacology Do Not Require UCP1. *Cell reports*, 11(7), pp.991–999.

Schaap, F.G. et al., 2013. Fibroblast growth factor 21 is induced by endoplasmic reticulum stress. *Biochimie*, 95(4), pp.692–9.

Schibler, U. & Sassone-Corsi, P., 2002. A web of circadian pacemakers. *Cell*, 111(7), pp.919–922.

Shan, J. et al., 2014. A mitogen-activated protein kinase/extracellular signal-regulated kinase kinase (MEK)-dependent transcriptional program controls activation of the early growth response 1 (EGR1) gene during amino acid limitation. *The Journal of biological chemistry*, 289(35), pp.24665–79.

Shan, J. et al., 2009. Elevated ATF4 expression, in the absence of other signals, is sufficient for transcriptional induction via CCAAT enhancer-binding protein-activating transcription factor response elements. *The Journal of biological chemistry*, 284(32), pp.21241–21248.

Shimizu, N. et al., 2015. A muscle-liver-fat signalling axis is essential for central control of adaptive adipose remodelling. *Nature communications*, 6, p.6693.

Siu, F. et al., 2002. ATF4 is a mediator of the nutrient-sensing response pathway that activates the human asparagine synthetase gene. *Journal of Biological Chemistry*, 277(27), pp.24120–24127.

So, W.Y. et al., 2013. High glucose represses beta-klotho expression and impairs fibroblast growth factor 21 action in mouse pancreatic islets: involvement of peroxisome proliferator-activated receptor gamma signaling. *Diabetes*, 62(11), pp.3751–3759.

De Sousa-Coelho, A.L. et al., 2013. FGF21 mediates the lipid metabolism response to amino acid starvation. *Journal of lipid research*, 54(7), pp.1786–97.

De Sousa-Coelho, A.L., Marrero, P.F. & Haro, D., 2012. Activating transcription factor 4-dependent induction of FGF21 during amino acid deprivation. *The Biochemical journal*, 443(1), pp.165–171.

T

Talukdar, S., Zhou, Y., et al., 2016. A long-acting FGF21 molecule, PF-05231023, decreases body weight and improves lipid profile in non-human primates and type 2 diabetic subjects. *Cell Metabolism*, 23(3), pp.427–440.

Talukdar, S., Owen, B.M., et al., 2016. FGF21 Regulates Sweet and Alcohol Preference. *Cell metabolism*, 23(2), pp.344–349.

Tan, B.K. et al., 2011. Fibroblast growth factor 21 (FGF21) in human cerebrospinal fluid: relationship with plasma FGF21 and body adiposity. *Diabetes*, 60(11), pp.2758–2762.

Tanaka, T. et al., 2013. Genome-wide meta-analysis of observational studies shows common genetic variants associated with macronutrient intake. *The American journal of clinical nutrition*, 97(6), pp.1395–1402.

Tao, W. et al., 2015. EGR1 regulates hepatic clock gene amplitude by activating Per1 transcription. *Scientific reports*, 5, p.15212.

Thiaville, M.M., Dudenhausen, E.E., et al., 2008. Deprivation of protein or amino acid induces C/EBPbeta synthesis and binding to amino acid response elements, but its action is not an absolute requirement for enhanced transcription. *The Biochemical journal*, 410(3), pp.473–484.

Thiaville, M.M., Pan, Y.-X., et al., 2008. MEK signaling is required for phosphorylation of eIF2alpha following amino acid limitation of HepG2 human hepatoma cells. *The Journal of biological chemistry*, 283(16), pp.10848–10857.

Tseng, Y.-H., Cypess, A.M. & Kahn, C.R., 2010. Cellular bioenergetics as a target for obesity therapy. *Nature reviews. Drug discovery*, 9(6), pp.465–482.

Tyynismaa, H. et al., 2010. Mitochondrial myopathy induces a starvation-like response. *Human molecular genetics*, 19(20), pp.3948–3958.

U

Uonaga, T. et al., 2010. FGF-21 enhances islet engraftment in mouse syngeneic islet transplantation model. *Islets*, 2(4), pp.247–251.

V

Vandanmagsar, B. et al., 2016. Impaired Mitochondrial Fat Oxidation Induces FGF21 in Muscle. *Cell Reports*, 15(8), pp.1686–1699.

Véniant, M.M. et al., 2015. Pharmacologic Effects of FGF21 Are Independent of the “Browning” of White Adipose Tissue. *Cell Metabolism*, 21(5), pp.731–738.

Virtanen, K.A. et al., 2009. Functional brown adipose tissue in healthy adults. *The New England journal of medicine*, 360(15), pp.1518–1525.

Virtue, S. & Vidal-Puig, A., 2010. Adipose tissue expandability, lipotoxicity and the Metabolic Syndrome--an allostatic perspective. *Biochimica et biophysica acta*, 1801(3), pp.338–349.

W

Wan, X.S. et al., 2014. ATF4- and CHOP-dependent induction of FGF21 through endoplasmic reticulum stress. *BioMed Research International*, 2014.

Wanders, D. et al., 2016. Role of GCN2-independent signaling through a non-canonical PERK/NRF2 pathway in the physiological responses to dietary methionine restriction. *Diabetes*, 65(February), p.db151324.

Wang, Y., Solt, L.A. & Burris, T.P., 2010. Regulation of FGF21 expression and secretion by retinoic acid receptor-related orphan receptor ?? *Journal of*

Biological Chemistry, 285(21), pp.15668–15673.

Watanabe, M. et al., 2006. Bile acids induce energy expenditure by promoting intracellular thyroid hormone activation. *Nature*, 439(7075), pp.484–489.

Wei, W. et al., 2012. Fibroblast growth factor 21 promotes bone loss by potentiating the effects of peroxisome proliferator-activated receptor gamma. *Proceedings of the National Academy of Sciences of the United States of America*, 109(8), pp.3143–3148.

Weng, Y. et al., 2015. Pharmacokinetics (PK), pharmacodynamics (PD) and integrated PK/PD modeling of a novel long acting FGF21 clinical candidate PF-05231023 in diet-induced obese and leptin-deficient obese mice. *PLoS ONE*, 10(3).

Wente, W. et al., 2006. Fibroblast growth factor-21 improves pancreatic beta-cell function and survival by activation of extracellular signal-regulated kinase 1/2 and Akt signaling pathways. *Diabetes*, 55(9), pp.2470–2478.

Whittle, A.J. et al., 2012. BMP8B increases brown adipose tissue thermogenesis through both central and peripheral actions. *Cell*, 149(4), pp.871–885.

Wilson, G.J. et al., 2015. GCN2 is required to increase fibroblast growth factor 21 and maintain hepatic triglyceride homeostasis during asparaginase treatment. *American journal of physiology. Endocrinology and metabolism*, 308(4), pp.E283–93.

Wolfgang, C.D. et al., 1997. gadd153/Chop10, a potential target gene of the transcriptional repressor ATF3. *Molecular and cellular biology*, 17(11), pp.6700–6707.

Wu, J. et al., 2012. Beige Adipocytes Are a Distinct Type of Thermogenic Fat Cell in Mouse and Human. *Cell*, 150(2), pp.366–376.

Wu, N. et al., 2009. Negative feedback maintenance of heme homeostasis by its receptor, Rev-erbalpha. *Genes & development*, 23(18), pp.2201–2209.

X

Xiao, F. et al., 2011. Leucine deprivation increases hepatic insulin sensitivity via GCN2/mTOR/S6K1 and AMPK pathways. *Diabetes*, 60(3), pp.746–756.

Xu, J., Stanislaus, S., et al., 2009. Acute glucose-lowering and insulin-

sensitizing action of FGF21 in insulin-resistant mouse models--association with liver and adipose tissue effects. *American journal of physiology. Endocrinology and metabolism*, 297(5), pp.E1105–14.

Xu, J., Lloyd, D.J., et al., 2009. Fibroblast growth factor 21 reverses hepatic steatosis, increases energy expenditure, and improves insulin sensitivity in diet-induced obese mice. *Diabetes*, 58(1), pp.250–259.

Y

Yang, C. et al., 2013. Activation of Liver FGF21 in hepatocarcinogenesis and during hepatic stress. *BMC gastroenterology*, 13, p.67.

Yang, C. et al., 2012. Differential specificity of endocrine FGF19 and FGF21 to FGFR1 and FGFR4 in complex with KLB. *PloS one*, 7(3), p.e33870.

Ye, L. et al., 2012. TRPV4 is a regulator of adipose oxidative metabolism, inflammation, and energy homeostasis. *Cell*, 151(1), pp.96–110.

Yie, J. et al., 2012. Understanding the physical interactions in the FGF21/FGFR/beta-Klotho complex: structural requirements and implications in FGF21 signaling. *Chemical biology & drug design*, 79(4), pp.398–410.

Yin, L. et al., 2007. Rev-erbalpha, a heme sensor that coordinates metabolic and circadian pathways. *Science (New York, N.Y.)*, 318(5857), pp.1786–1789.

Yin, L. & Lazar, M.A., 2005. The orphan nuclear receptor Rev-erbalpha recruits the N-CoR/histone deacetylase 3 corepressor to regulate the circadian Bmal1 gene. *Molecular endocrinology (Baltimore, Md.)*, 19(6), pp.1452–1459.

Young, P., Arch, J.R. & Ashwell, M., 1984. Brown adipose tissue in the parametrial fat pad of the mouse. *FEBS letters*, 167(1), pp.10–14.

Yu, J. et al., 2011. Conjugated linoleic acid induces hepatic expression of fibroblast growth factor 21 through PPAR-α. *British Journal of Nutrition*, 107(04), pp.461–465.

Yu, Y. et al., 2013. Bitter melon extract attenuating hepatic steatosis may be mediated by FGF21 and AMPK/Sirt1 signaling in mice. *Scientific reports*, 3, p.3142.

Z

Zhang, X. et al., 2008. Serum FGF21 levels are increased in obesity and are independently associated with the metabolic syndrome in humans. *Diabetes*, 57(5), pp.1246–1253.

Zhang, Y. et al., 2015. GENE REGULATION. Discrete functions of nuclear receptor Rev-erbalpha couple metabolism to the clock. *Science (New York, N.Y.)*, 348(6242), pp.1488–1492.

Zhang, Y. et al., 2016. HNF6 and Rev-erbalpha integrate hepatic lipid metabolism by overlapping and distinct transcriptional mechanisms. *Genes & development*, 30(14), pp.1636–1644.

Zhang, Y. et al., 2011. The link between fibroblast growth factor 21 and sterol regulatory element binding protein 1c during lipogenesis in hepatocytes. *Molecular and cellular endocrinology*, 342(1-2), pp.41–47.

Zhang, Y. et al., 2012. The starvation hormone, fibroblast growth factor-21, extends lifespan in mice. *eLife*, 1, pp.1–14.

ANNEXES

ANNEX1: Diets composition

	Control diet		Low protein diet	
	g (%)	Kcal(%)	g(%)	Kcal(%)
Protein	20	21	5	5
Carbohydrate	66	68	81	83
Fat	5	12	5	12
Total		100		100
Kcal/g	3,90			

Ingredient	g	Kcal	g	Kcal
Casein	200	800	50	200
DL-Methionine	3	12	1	4
Corn Starch	150	600	252	1008
Maltodextrin 10	0	0	50	200
Sucrose	500	2000	500	2000
Cellullose, BW200	50	0	50	0
Corn Oil	50	450	50	450
Mineral Mix S10001	35	0	35	0
Vitamin Mix V10001	10	40	10	40
Choline Bitartate	2	0	2	0
FD&Y Yellow Dye #5	0	0	0,05	0
Total	1000	3902	1000,05	3902

	Control diet		Leucine deficient diet	
	g (%)	Kcal(%)	g(%)	Kcal(%)
Protein	17	18	16	16
Carbohydrate	69	71	70	72
Fat	5	12	5	12
Total		100		100
Kcal/g	3,90		3,90	

Ingredient	g(%)	Kcal(%)	g(%)	Kcal(%)
L-Arginine	10	40	10	40
L-Histidine-HCl-H2O	6	24	6	24
L-Isoleucine	8	32	8	32
L-Leucine	12	48	0	0
L-Lysine-HCl-H2O	14	56	14	56
L-Methionine	6	24	6	24
L-Phenylalanine	8	32	8	32
L-Threonine	8	32	8	32
L-Tryptophan	2	8	2	8
L-Valine	8	32	8	32
L-Alanine	10	40	10	40
L-Asparagine-H2O	5	20	5	20
L-Aspartate	10	40	10	40
L-Cysteine	4	16	4	16
L-Glutamic Acid	30	120	30	120
L-Glutamine	5	20	5	20
Glycine	10	40	10	40
L-Proline	5	20	5	20
L-Serine	5	20	5	20
L-Tyrosine	4	16	4	16
Total L-Amino Acids	170	0	158	0
Corn Starch	550,5	2202	562,5	2250
Maltodextrin 10	125	500	125	500
Cellulose	50	0	50	0
Corn Oil	50	450	50	450
Mineral Mix S10001	35	0	35	0
Sodium Bicarbonate	7,5	0	7,5	0
Vitamin Mix V10001	10	40	10	40
Choline Bitrartrate	2	0	2	0
Red Dye, FD&C#40	0	0	0,025	0
Blue Dye, FD&C#1	0,05	0	0	0
Yellow Dye, FD&C#5	0	0	0,025	0
Total	1000,05	3872	1000,05	3872

ANNEX 2: Promoters sequences

MOUSE *FGF21* PROMOTER

GGGCCCAGCTGTTACTTTTTAGATTGGTAAATACAGCAAATAACTTTTTTTCTG
GCCAGAAGGAGGAAAGAGAGTGTTTTCAACATTCTTTTTAGACAGGCCTCTGAA
GTGAGGCTGGAGACAAAGGTTCTCCCACGGTTCCTTCCGGAGCCCATTAATTAA
TCGCATGGAGTCGGGGCCTGAAGCCTCACCTTGACACCTTAAAAGACTCAGAAA
TTCCACTTGGCTAGCCCAAGATGAGATCATTTCTTCACACTGCAGAGTTCCAGG
GCCACATCAGTTCTAAAGGTCCACTCCCCAGCCTCCTCCCCTTAGATGCTCCTT
GGGACTTAGGGGTCAGTGCTCCAGTCTCACTCCCAAGAGTCCTTGCTCAGGGTT
CCTCCTAGAAATCCAAACTCGGCCCCAGCGCCTTTGACTGCAGGAAACAACCCA
GCTCTTCCCCTTCACCGAGCCTAATCCTCCCACCCCCCAAAGCATCTGGAGAGC
ACCTGTGCAGGACGCTGTCTGGTGAAAGAAGCACTAGGATTGCATCAGGGAGGA
CAGCAGCTGAGCACAAGGCCCGAATGCTAAGCAGGGGTTGGTGAGGGTGACTGG
CCTGTGGCCAGCTGGGAGACTTCCACCTGCTGGGCTGAGGACTCCTCTTACACA
CTGCTGATACAGCTCTCCTGATGAAAGAAAGCCTCAGACACGCCCCCCCCCCAA
AGCACCTTGAAGCTTAAAATTCCAAAAGGATGAACCACACCAGCTCAGTTGCTT
ACACAGAAAGTCTGAAGCCCCAGGTTCCTTCTTAGTACCCAAGAGCCAGACCCT
AGCCTCCTCCCTCAGACCCAAGAGCTAGATCCCAGCCTCCTCCCTCAGACCCAA
GAGCCAGACCCTAGCCTCCTCCCTCAGATCCAGGAATACAGACCCCAGCCACCT
CCCTCAGACCCAGAACTGCAGAGCCCAGCCACCTTCAGACCCAGGAGTGTAGAC
TTCAGTCTCCTACCTCAGACCCAGAACTGCAGACCCCAGCTACCTTCAGACCCA
GGAGTGTAGACCCCAGCCTCCTCCTTCAGACTCAGGAGTGTAGACCCCAGCCTC
CTCCCTCAGACTCAGGAGTGCAGACCCTAGCCTCCTCCCTCAGACTCAGGAGTG
CAGACCCCAGCCTCCTCCTTCAGACTCAGGAGTGCAGACAAGTCCCCTTCCTTA
GACCCAAGGCCCCAAACCCCATCTTTCCTCCCCTCAGATACTAAGGTGAAGATC
CCAACCTCCTCCAGAGTCCAACCCTCCTCCCTCAGACCAAGGAGCACAGACCCC
AGCCTCCTCCTCCAGATTTAGGAGTGCAGACCCGCCCCCCAGCACTCTTCCCCC
CCAAACCCAGGGGGCCCATGCCTAGCCCTTTTCATTCAGACCCCTGTTGGAAAG
ACCCCCCCCATTGCATCATCCGTCCAGGCCGCCCTGGCCACGGTGGAATTCAGGT
TCCTGCCAAGTGTGTCAAATATCACGCGTCAGGAGTGGGGAGGGCACGTGGGCG
GGCCTGTCTGGGTATAAATTCTGGTATTTCTGCGTTCACCAGACAGCCTTAGTG
TCTTCTCAGCTGGGGATTCAACACAGGAGAAACAGCCATTCACTTTGCCTGAGC
CCCAGTCTGAACCTGACCCATCCCTGCTGGGCACCGGAGTCAGAACACAATTCC

AGCTGCCTTGGCTCCTCAGCCGCTCGCTTGCCAGGGGCTCTCCCGAACGGAGCG

CAGCCCTG**ATG**GAATGGATGAGATCTAGAGTTGGGACCCTGGGACTGTGGGTCC

AARE1→ATTGCATCA
AARE2→ATTGCATCA

Fw primer→ AGTC***CCCGGG***ATTAATTAATCGCATGGAGT
Rv primer→ GCAAT***CTCGAG***GCTGTCTGGTGAACGCAGA

ATG→ Translation start site
AGA→ Transcription start site

HUMAN *FGF21* PROMOTER

CCTACCCTTGCACCCTTAGGGGCTCCAGGAAATTAGCCAACCTGTCTTCCCTCTGGGTG
CCCACTCCAGGGCCTGGCTTGGCTGCCAACTCCAGTCAGGGACTTTCAGCCACCCCTCC
CCCCAGGTTATTTCAGGAGCACCTGCCTGGGCCTGGGATGGCTTCTCTGGTGAAAGAAA
CACCAGGATTGCATCAGGGAGGAGGAGGCTGGGATGTCCAGGGTCTGAGCATCTGAGCA
GGGACAGATGAGGTTGAGGTTGGCCCACGGCCAGGTGAGAGGCTTCCAAGGCAGGATAC
TTGTGTCTCAGATGCGGTCGCTTCTTTCATACAGCAATTGCCGCCTTGCTGAGGATCAA
GGAACCTCAGTGTCAGATCACGCCCTCCCCCCAAACTTAGAAATTCAGATGGGGCGCAG
AAATTTCTCTTGTTCTGCGTGATCTGCATAGATGGTCCAAGAGGTGGTTTTTCCAGGAG
CCCAGCACCCCTCCTCCCTCCGACTCAGGTGCTTGAGACCCCAGATCCTTCTCTCTGAG
ACTCAGGAATGTGGGCCCCCAGCCCCTTTCACCTGGGTCCCAGCTAACCCGATCCTCCC
CTCCCTCATCCCCTAGACCCAGGAGTCTGGCCCTCCATTGAAAGGACCCCAGGTTACAT
CATCCATTCAGGCTGCCCTTGCCACGATGGAATTCTGTAGCTCCTGCCAAATGGGTCAA
ATATCATGGTTCAGGCGCAGGGAGGGTGATTGGGCGGGCCTGTCTGGGTATAAATTCTG
GAGCTTCTGCATCTATCCCAAAAAACAAGGGTGTTCTGTCAGCTGAGGATCCAGCCGAA
AGAGGAGCCAGGCACTCAGGCCACCTGAGTCTACTCACCTGGACAACTGGAATCTGGCA
CCAATTCTAAACCACTCAGCTTCTCCGAGCTCACACCCCGGAGATCACCTGAGGACCCG
AGCCATTG**ATG**GACTCGGACGAGACCGGGTTCGAGCACTCAGGACTGTGGGTTTCTGTG
CTGGCTGGTCTTCTGCTGGGAGCCTGCCAGGCACACCCCATCCCTGACTCCAGTCCTCT
CCTGCAATTCGGGGGCCAAGTCCGGCAGCGGTACCTCTACACAGATGATGCCCAGCAGA
CAGAAGCCCACCTGGAGATCAGGGAGGATGGGACGGTGGGGGGCGCTGCTGACCAGAGC
CCCGAAAGTGAGTGTGGGCCAGAGCCTGGGTCTGAGGGAGGAGGGGCTGTGGGTCTGGA
TTCCTGGGTCTGAGGGAGGAGGGGCTGGGGGCCTTGGCCCCTGGGTCTGAGGGAGGAGG
GGCTGGGGATCTGGACTCCTGGGTCTGAGGGAGGAGGGGCTGGGGATCTGGGCCCCTGG
GTCTGAGGGAGGAGGGGCTGGGTCTGGACCCCTGGGTCTGAGGGAGGAGGGGCTGGG

AARE1→ATTGCATCA
AARE2→GTTACATCA

Fw primer: ***GGTACC***AGCCAACCTGTCTTCCCTCT
Rv primer: CTCTGGCCCACACTCACTTT

GAGCTC→SacI restriction site

ATG→ Translation start site
CTG→ Transcription start site

MOUSE *REV-ERB ALPHA* PROMOTER

TCGGGGAGTTGAGGGGTGGGAGTTAAATGATCCTCATGTTCTCCCTAAACTGTGGGCTT
CTTCTGCTATCATGAAGCCCTGCAGAGAGCAGACCCCCCTCTCTCTATGAGGACCTCAG
AGCACTTTCCCTTTGTTCTCCTTTTTATTTCCCAGACAAAGGGAAATGACTCACCCCAA
AGTCACTTGAGTGGGCAGTGTGGTGTCATATAAGCAAACAGGGAGTCCCTAGGGATATC
CCCGTGCTATGCCAGTCCTACCCGTGGGGGCTGGGGTTAGGGTGAAGAAGAGAAAGGGG
TTTTATTTACACTGCTTGTCGCCCACCTTGTCACCATAGCAAAAGATGCTTAAGTTCTT
GATTTAAGGGAAATCTCTCCTCCCAGCTTGTCTTTCTCCCCCTAGTCACCACTAACCTC
AGGGTGAGGTCAGTTCTCCAATCACGTGAAGCTCTCACGTTTGCTAGGTTTGCAGAAAG
GGCCTTTTAGCTTTGATCTTCCACGGAGCAGTAAAGCTTGCCAGGCCCTCCCCAGGAAT
TCACATGCCCTTGCCATACAAGGCTTTCCAAACACGCCACCCTGACTCTTCAGAAAACC
CCACCCCAGTCCACTTTCAGCTCCTCCCCGCTGCCAGCAAGCACTTTTGCAAAGCAGAA
AAGGAATAGGCACACTCCACCTACATTGTCAGTAGACTACAAATCCCAACAATCCTGGC
GGTGCGCAGGCGCACAGATCTCAACGTGCCGGCTGCTGGAAAAGTGTGTCACTGGGGCA
CGAGGCGCTCCCTGGAATCACATGGTACCTGCTCCAGTGCCGCGTGCGGCCCGGGAACC
CTGGGCTGCTGGCGCCTGCGCAGAGCCCTCTGTCCCAGGGAAAGGCTCGGGCAAAAGGC
GGTTGAGATTGGCAGAGTGAAATATTACTGCTGAGGAAACGTAGCAGGGCACACGTCTC
TCTTTGCGTCCTGGTGCCTCATTTCTCCATCACCTACTTACTTCCTGGTTGCAGCTTCT
CTTCCTTTGGGACTTTTGCACCCGGAGCTCCAGATTCATTACCCTGCTTCACTGCGGAG
CCTTCAGGAGTGGCATCCGGTGCACTGCAGAGACCCGACTCTCCTTGCTACCTTATAGC
CAGAACTGCTGCAGGCTGATTCTTCACACACACACTCTCTGCTCTTCCCATGCAAATCA
GATCTCAGGTGCCTCAGCGTCCTACCCTTCTGGAGGGCTGCAGTATAGCCACCCCAAGA
CCTTACTGCTCAGTGCCTGGAATCCTGATTGCGAACTGCGGGGCTCACTCGTCTCCCTC
AGCCATTGCCCAGGGGGCGAGAGAGGCCATCACAACCTCCAGTTTGTGTCAAGGTCCAG
TTTGAATGACCGCTTTCAGCTGGTGAAGAC**ATG**ACGACCCTGGACTCCAATAACAACAC
AGGTACTGAGATTCTTATCTTTGCTCTGTCACTGTCTCCATTTCCATCCAAGGCTTATG
AGAGGAACTTTGTAAGGGATTGGGGATTCCCTCTGGC

GTGCGCAGGCGC Conserved EGR-1response element conserved in mice and human.

ACT → Transcription start site
ATG → Translation sart site

Fw primer 5'-AA***ACGCGT***AATCTCTCCTCCCAGCTTGT-3'

Rv primer 5'-AA***CTCGAG***GTCTTCACCAGCTGAAAGCG-3'

ANNEX 3: Nutritional regulation of fibroblast growth factor 21: from macronutrients to bioactive dietary compounds. (Review article)

DE GRUYTER Horm Mol Biol Clin Invest 2016; aop

Albert Pérez-Martí, Viviana Sandoval, Pedro F. Marrero, Diego Haro* and Joana Relat*

Nutritional regulation of fibroblast growth factor 21: from macronutrients to bioactive dietary compounds

DOI 10.1515/hmbci-2016-0034
Received July 1, 2016; accepted July 21, 2016

Abstract: Obesity is a worldwide health problem mainly due to its associated comorbidities. Fibroblast growth factor 21 (FGF21) is a peptide hormone involved in metabolic homeostasis in healthy individuals and considered a promising therapeutic candidate for the treatment of obesity. FGF21 is predominantly produced by the liver but also by other tissues, such as white adipose tissue (WAT), brown adipose tissue (BAT), skeletal muscle, and pancreas in response to different stimuli such as cold and different nutritional challenges that include fasting, high-fat diets (HFDs), ketogenic diets, some amino acid-deficient diets, low protein diets, high carbohydrate diets or specific dietary bioactive compounds. Its target tissues are essentially WAT, BAT, skeletal muscle, heart and brain. The effects of FGF21 in extra hepatic tissues occur through the fibroblast growth factor receptor (FGFR)-1c together with the co-receptor β-klotho (KLB). Mechanistically, FGF21 interacts directly with the extracellular domain of the membrane bound cofactor KLB in the FGF21- KLB-FGFR complex to activate FGFR substrate 2α and ERK1/2 phosphorylation. Mice lacking KLB are resistant to both acute and chronic effects of FGF21. Moreover, the acute insulin sensitizing effects of FGF21 are also absent in mice with specific deletion of adipose KLB or FGFR1. Most of the data show that pharmacological administration of FGF21 has metabolic beneficial effects. The objective of this review is to compile existing information about the mechanisms that could allow the control of endogenous FGF21 levels in order to obtain the beneficial metabolic effects of FGF21 by inducing its production instead of doing it by pharmacological administration.

Keywords: beta-klotho; diet; energy metabolism; fibroblast growth factor 21; obesity.

***Corresponding authors: Diego Haro and Joana Relat,** Department of Nutrition, Food Sciences and Gastronomy, Food Campus (Torribera), School of Pharmacy, University of Barcelona, Av Prat de la Riba 171, 08921 Santa Coloma de Gramenet, Barcelona, Spain; and Institute of Biomedicine from University of Barcelona (IBUB), Barcelona, Spain, E-mail: dharo@ub.edu (D. Haro), jrelat@ub.edu (J. Relat)

Albert Pérez-Martí, Viviana Sandoval and Pedro F. Marrero: Department of Nutrition, Food Sciences and Gastronomy, Food Campus (Torribera), School of Pharmacy, University of Barcelona, Santa Coloma de Gramenet, Barcelona, Spain; and Institute of Biomedicine from University of Barcelona (IBUB), Barcelona, Spain

Introduction

Fibroblast growth factor 21 (FGF21) increases energy expenditure. It thus has beneficial effects on glucose/lipid homeostasis and on body weight control and emerges as a novel therapeutic agent for the treatment of metabolic diseases such as obesity, type 2 diabetes and metabolic syndrome. In rodent and primate models of the aforementioned conditions, FGF21 has the capacity to restore glycemia and lipid profile, and to improve insulin resistance [1, 2].

It is widely accepted that FGF21 participates in metabolic homeostasis in health but its action takes on greater relevance in diseases.

To date, the pharmacological use of FGF21 is limited due to its half-life of around 1–2 h. In order to improve the pharmacokinetics, selectivity, and potency of FGF21, several laboratories have focused on designing FGF21 analogs. Two such analogs (LY2405319 and PF05231023) are currently being tested in clinical trials and have yielded similar results: benign toxicology, decreased plasma TGs and low-density lipoprotein cholesterol, increased high-density lipoprotein cholesterol, modest weight loss, elevated adiponectin, reduced insulin levels, and elevated plasma ketones. Surprisingly, no glucose-lowering effect was registered in any trial. This is a major setback as both compounds were assessed mainly as anti-diabetic drugs. However, the results of these two trials highlight the capacity of FGF21 to ameliorate lipid and cholesterol metabolism [3–5].

Nutritional signals play an important role in controlling gene expression in mammals. Macronutrients

[carbohydrates, fatty acids (FAs), proteins], micronutrients (minerals and vitamins), and some bioactive dietary compounds have the capacity to regulate gene expression and thus metabolic homeostasis. In this context, it has been described that endogenous FGF21 levels are regulated by various nutritional challenges such as high-fat diets (HFDs), low-protein diets (LPDs), amino acid-deficient diets, fasting, and polyphenols [6, 7] (Figure 1). However, the levels of this molecule are also determined by metabolic stress, including obesity, type 2 diabetes (T2DM), and non-alcoholic fatty liver disease (NAFLD) [8]. In this regard, this review summarizes how various nutrient stimuli and diet components regulate the expression of FGF21, and it also seeks to shed light on the molecular mechanisms and the clinical implications of the crosstalk between diet composition FGF21 levels and signaling.

FGF21 signal transduction

FGF21, together with FGF15/19 and FGF23, is an atypical member of the fibroblast growth factor (FGF) family. With endocrine, paracrine and autocrine properties, FGF21 lacks the heparin domain present in the rest of the family members, thus allowing it to be secreted. Defined as a hepatokine, myokine, and adipokine, FGF21 is expressed in several tissues, including the liver, pancreas, thymus, heart, testis, skeletal muscle, white adipose tissue (WAT), brown adipose tissue (BAT), heart, and brain. It also exerts action on multiple target tissues, ranging from peripheral to central [9].

FGF21 acts as a hormone-like peptide and its signaling pathway requires FGF21 binding to a fibroblast growth factor receptor (FGFR). FGFRs are tyrosine kinase receptors, and seven isoforms have been described (1b, 1c, 2b, 2c, 3b, 3c and 4). FGFR1c has been defined as the main mediator of FGF21 response in vivo [10] through an obligate dimerization with the co-receptor β-klotho (KLB) [11]. The co-expression of these two receptors determines the sensitivity of a tissue or organ to FGF21 signaling.

Regarding the signal transduction pathway, the binding of FGF21 to the FGFR-KLB dimer stimulates the phosphorylation of FGFR substrate 2α (FRS2α) and the activation of extracellular signal-regulated kinase 1/2 (ERK1/2) and Akt [12].

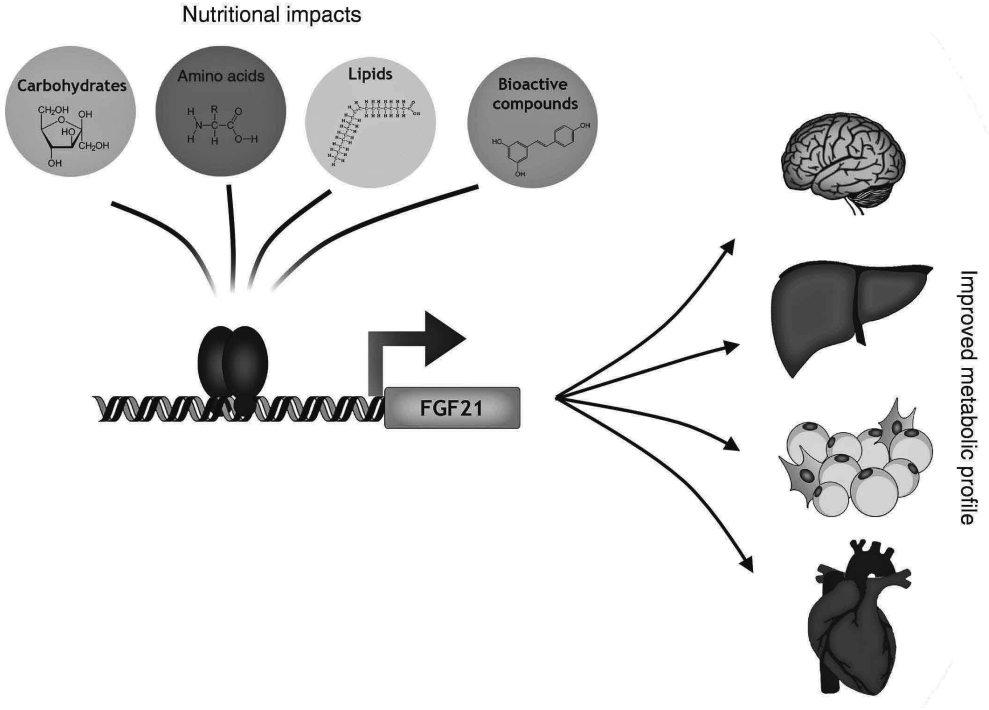

Figure 1: FGF21 expression is regulated by diet and its effects are widely distributed.
Endogenous levels of FGF21 are regulated by different macronutrients and bioactive dietary compounds. Acting as a hormone, FGF21 impacts on several tissues where regulates mainly lipid and glucose metabolism.

FGF21 as a hepatokine, myokine, adipokine and other kines

Liver production and secretion

The main source of FGF21 is the liver, where its expression is induced in response to stress. FGF21 was initially described as a fasting-adaptation hormone, as its hepatic production coupled to plasma levels is dramatically increased during prolonged fasting [13, 14]. It is now known that hepatic FGF21 expression is also induced in other liver-stress circumstances such as in obesity, specific nutritional conditions, liver injury, viral infection, chemical insult, hepatosteatosis, steatohepatitis, NAFLD, cirrhosis, and liver cancer [8, 15–18].

Hepatic overexpression of FGF21 triggers ketogenesis, gluconeogenesis, and FA oxidation (FAO) and suppresses lipogenesis in the liver [15, 19]. However, the autocrine effects of FGF21 on this organ are still under debate. FGFR4 is the predominant isoform in the liver, but the FGFR4-KLB complex cannot activate the FGF21 transduction pathway [10]. In contrast, hepatic FGFR1 levels are low, and it is unclear whether they are enough to ensure FGF21 signaling. Later studies reported contradictory results regarding the role of FGF21 in ketogenesis, thereby suggesting that the physiological effects of this molecule may differ from the pharmacological ones.

As a hepatokine, FGF21 affects WAT and BAT, tissues in which it regulates lipid metabolism – mainly by inducing lipolysis and browning and by increasing thermogenic capacity [20, 21]. It also exerts action in the brain, where it is able to reduce physical activity, induce torpor, and regulate circadian behavior [22, 23]. In conclusion, all data indicate that FGF21 is produced and secreted by the liver when the function of this organ is compromised by stress and that it is responsible for restoring and maintaining metabolic homeostasis. Hepatic FGF21 expression is highly sensitive to nutritional status, and the molecular mechanisms that modulate its expression in the liver will be reviewed in the following chapter.

White adipose tissue: autocrine and paracrine effects

Adipose tissue is the main target tissue of FGF21 and the major mediator of its beneficial effects. While the physiological effects of FGF21 during fasting remain elusive, most data on its signaling in WAT derive from studies in which it was pharmacologically administered or overexpressed in obese mice. Nevertheless, FGF21 shows paradoxical actions on WAT depending on its source. *Fgf21*-overexpressing mice show induced lipolysis [13, 24]. In contrast, *Fgf21*-knockout mice present enhanced lipolysis in late fasting [21]. In addition, while FGF21 suppresses lipolysis in mouse and human adipocytes [25], it is induced by peroxisome proliferator activating receptor g (PPARg) in WAT upon feeding, thus stimulating adipogenesis [26, 27].

Regarding glucose metabolism, FGF21 induces glucose uptake in 3T3L1 adipocytes by increasing glucose transporter 1 (GLUT1) independently of insulin action [2, 28]. Moreover, later studies showed increased glucose uptake in both WAT and BAT of lean mice infused with FGF21 and fed a chow diet [29].

In summary, in WAT, FGF21 induces genes involved in glucose uptake, lipogenesis and lipolysis, depending on the metabolic state of the adipocytes. These apparently contradictory effects may be due to compensatory effects of genetic modifications in mice, different nutritional status and different FGF21 concentrations reached between pharmacological administration and physiological secretion.

WAT is not only a FGF21 target tissue but also a mediator of the effects of this growth factor. In this regard, the glucose- and insulin-sensitizing effects of FGF21 require the production and secretion of adiponectin from WAT. Accordingly, FGF21 stimulates this mechanism in rodents, and adiponectin-knockout mice fail to reproduce the sensitizing effects of FGF21 [30]. Similarly, FGF21 also reduces the levels of the sphingolipid ceramide. Sphingolipid ceramides have been associated with insulin resistance caused by lipotoxicity. By inducing adiponectin secretion, FGF21 diminishes the accumulation of ceramides in obese animals [31]. Overall, despite some contradictory effects of FGF21 in adipose fat depots, adipose tissue is considered indispensable for the physiological and pharmacological effects of FGF21.

Finally, FGF21 induces the expression of uncoupling protein 1 (Ucp1), thus producing the so-called browning process of WAT in an autocrine, paracrine or endocrine fashion [20, 32]. Browning occurs in multilocular beige adipocytes in specific susceptible WAT depots, such as inguinal and perirenal tissue, through an increase in the expression of genes involved in thermogenesis and confers a brown fat-like phenotype to white adipocytes.

Brown adipose tissue: FGF21 induces thermogenic capacity

BAT is a FGF21 target tissue since it expresses FGFR1 and KLB; however, it is also a source of FGF21. In BAT, FGF21

stimulates glucose uptake and thermogenesis through the induction of UCP1 in the interscapular depot in an autocrine and paracrine fashion [33]. Upon cold exposure, FGF21 expression is increased in BAT and other cold-sensitive fat depots in the β-adrenergic/ATF2-dependent pathway [32–34]. In this regard, Fgf21-deficient mice respond poorly to cold exposure and show greater shivering [32]. The mechanisms underlying the action of FGF21 on BAT/WAT are still not well understood. Part of the FGF21-induced activation of the thermogenic program is driven by PGC1a, as FGF21 increases the protein levels of this molecule. Similarly, Pgc1a-knockout mice show an impaired response to FGF21 [32].

Furthermore, hepatic FGF21-mediated thermogenesis has also been described in response to maternal milk consumption in neonatal pups [35], and also in situations of metabolic stress, for example upon amino acid restriction [20]. These observations suggest that the hepatic FGF21-mediated increase in thermogenic capacity is an adaptive response to metabolic stress.

It has been proposed that the effect of FGF21 on energy expenditure and weight loss may be due to an increased thermogenic capacity of BAT and WAT (browning). However, recent experiments in Ucp1-null mice and interscapular BAT-excised mice show that when FGF21 is administered pharmacologically, UCP1 is not required for the improvement of the glucose, cholesterol, and free FA profile. Nonetheless, the increment in metabolic rate associated with the administration of FGF21 is diminished in these mice [36–38]. These data suggest that the metabolic benefits of FGF21 are partly UCP1-independent.

Skeletal muscle: FGF21 is produced in response to mitochondrial dysfunction

FGF21 expression in muscle was first described in Akt1 transgenic mice in which the mRNA and serum levels of FGF21 were induced [39]. In normal conditions, basal expression of FGF21 in skeletal muscle is low but its expression is increased by insulin [39, 40], exercise [41], mitochondrial myopathies [42], impaired mitochondrial FAO [43], muscle-specific autophagy deficiency [44] and transgenic overexpression of Akt1, perilipin-5 [45] or Ucp1 [46] in skeletal muscle. The induction of FGF21 in muscle due to a metabolic dysfunction is driven by the transcription factor ATF4, which is activated by endoplasmic reticulum (ER) stress. The AMPK and PI3K/Akt1 signaling pathways are also able to increase FGF21 expression [43].

The impact of FGF21 on skeletal muscle is not clear, as the expression levels of KLB do not seem to be sufficient to respond to FGF21. Several studies suggest that FGF21 administration can improve glucose uptake in vitro [47, 48], and a model of impaired mitochondrial FAO has recently shown the same in vivo [43].

In contrast, the role of FGF21 as a myokine is more evident. In the abovementioned conditions where FGF21 is overexpressed in muscle, the plasma levels of this growth factor also increase. The metabolic effects of this increase include the reduction of fat content in liver, increased FAO, resistance to a HFD and browning of WAT. These results show that FGF21 can act as a myokine when secreted in response to muscle stress and that it exerts its effects on metabolism in an endocrine fashion.

Heart: FGF21 exerts cardioprotective actions

Initially, the heart was discarded as a target tissue or source of FGF21 due to the low levels of FGF21 and KLB mRNA detected in this organ. However, later studies showed that FGF21 is expressed and secreted by cardiac cells in response to various stress conditions, including obesity, type 1 diabetes, fasting, ER stress, inflammation, infarct or hypertrophy, and some cardiovascular diseases [49, 50]. In the heart, FGFR1 and KLB have been detected in cardiac cells, where FGF21 exerts protective effects in an autocrine and endocrine fashion. The mRNA expression of FGF21 in these cells is driven by the transcriptional activation of Sirtuin1 – peroxisome proliferator-activated receptor a (Sirt1-PPARa) [50]; however, it can also be regulated by ATF4, especially when FGF21 induction is caused by ER or oxidative stress [49, 51].

It is now well established that FGF21 plays a key role in cardiac remodeling and pathophysiology. FGF21 protects cardiomyocytes from hypertrophy through a mechanism that involves the activation of the cAMP responsive element binding protein (CREB), the induction of PGC1a expression, and the reduction of the NF-kB pro-inflammatory pathway [50]. Cardiac FGF21 also induces the expression of anti-oxidant genes such as Ucp3 and superoxide dismutase (Sod2), thus preventing the production of reactive oxygen species (ROS) in cardiac cells and oxidative stress in the heart [52]. In an autocrine fashion, FGF21 modulates cardiac lipid homeostasis [49] and protects against diabetes-induced cardiomyopathy by activating the ERK-p38MAPK-AMPK pathway [50]. Finally, as an endocrine peptide, FGF21 can also inhibit cardiomyocyte apoptosis, thus reducing damage to the heart [53, 54].

Central nervous system: target tissue of FGF21

FGF21 has the potential to act in the central nervous system (CNS) since FGFRs are widely expressed in this tissue and KLB is specifically expressed in the suprachiasmatic nucleus, the dorsal vagal complex of the hindbrain, the area postrema, the nucleus tractus solitari, the nodose ganglia, and the paraventricular nucleus [22, 55, 56]. Immunoblotting experiments have revealed that FGF21 is expressed in several regions of the brain, such as the substantia nigra, striatum, hippocampus, and cortex [57]; however, this growth factor also crosses the blood brain barrier and is present in the cerebrospinal fluid in a linear relationship with serum levels [58]. FGF21 modulates circadian rhythm and fertility [22, 59], but current data point to the CNS as a mediator of the effects of FGF21 on energy expenditure and browning [60]. However, in all cases, the presence of KLB appears to be required for FGF21 to exert its effects. This observation thus indicates that this growth factor is an endocrine signal. Regarding the effects of FGF21 on energy expenditure and browning, experiments with diet-induced obese (DIO) mice show that the lack of KLB in the CNS abrogates all the effects of FGF21 on body weight, insulin sensitivity, metabolic regulation in liver, WAT, and BAT. These data suggest that direct signaling in the CNS causes an increase in the sympathetic outflow.

In the hypothalamus, FGF21 affects the expression of corticotropin-releasing factor. Intracerebroventricular injection of FGF21 in Fgf21-KO mice restores the metabolic effects of FGF21 essentially through the corticotropin-releasing hormone (CRH) and the activation of CREB, which finally enhances hepatic gluconeogenesis and sympathetic nerve activity in BAT [56, 61, 62]. According to that, lack of KLB in the brain blunts these effects [56, 60, 61]. Finally, treatment with the b-blocker propranolol diminishes the effects of FGF21 when it is centrally administered but not when delivered peripherally [60].

Given the wide range of biological processes regulated by the CNS and the capacity of FGF21 to act in the brain, it is likely that future studies will reveal new actions of FGF21 signaling through the CNS.

Pancreas: FGF21 preserves b-cell function

FGF21 is highly expressed in the pancreas and has protective effects against cerulein-induced pancreatitis [63]. Supporting data show that FGF21-deficient mice are more susceptible to damage, and FGF21-overexpressing mice are partly protected. In addition, FGF21 may be involved in enhancing islet engraftment [64] and in the preservation of b-cell function and survival [65]. Another point is that KLB expression is critical for these beneficial effects, but the expression of KLB is reduced when islets are treated with high glucose concentrations [66]. In the pancreas, FGF21 increases insulin content and glucose-dependent secretion and inhibits glucagon release in isolated islets [65].

Other effects of FGF21

In addition, and consistent with its metabolic benefits, FGF21 transgenic overexpression extends lifespan in mice. The authors of that study proposed that inhibition of the GH/IGF-1 signaling pathway would explain life extension in Fgf21 transgenic mice. Furthermore, microarray analysis showed that FGF21 modulates gene expression in the liver in a similar manner to caloric restriction (which is known to extend lifespan in mammals). These data suggest that FGF21 extends lifespan by acting as a selective caloric restriction mimetic in the liver [67].

Interestingly, FGF21 appears to be not only a metabolic regulator but also a nutrient intake and taste regulator. Both pharmacologic administration and hepatic secretion of FGF21 produce a satiety signal that suppresses the intake of “sweets” [68, 69]. In addition, two genome-wide meta-analyses associated genetic variations in a locus including Fgf21 with significant differences in macronutrient intake [6, 70].

While FGF21 boasts numerous beneficial effects, a major adverse effect is a decrease in bone mass. Both genetic overexpression of *Fgf21* and pharmacological administration of this molecule lead to the inhibition of osteoblastogenesis and the stimulation of adipogenesis. In contrast, the absence of *Fgf21* leads to a high bone mass phenotype. The mechanism underlying bone mass loss is the potentiation of PPARg activity [71]. Although this non-desirable effect has been described only in rodents, it has to be taken into account when considering FGF21 as a potential drug candidate.

FGF21 expression is regulated by nutrition

Fasting and feeding

FGF21 is expressed and produced by multiple tissues. However, under normal physiological conditions, all circulating protein appears to derive from the liver [72]. FGF21 was initially described as a protein induced in the liver to control metabolic adaptation to long periods of

starvation. This mRNA induction goes through the PPARa [13, 73, 74] and CREBH [75, 76]. Later, several studies showed that FGF21 expression is regulated not only by fasting but also by other nutritional states [77]. In addition to PPARa and CREBH FGF21 expression responds to the retinoic acid (RA) receptor b (RARb) [78], the RA receptor-related orphan receptor a (RORa) [79], the thyroid hormone receptor b (TRb) [80], the activating transcription factor-4 (ATF4) [81], the farnesoid X receptor (FXR) [82], and the carbohydrate responsive element binding protein (ChREBP) [83]. The following chapter will summarize the effects of various macronutrients and bioactive dietary components on FGF21 expression, the metabolic consequences and the putative signaling transduction pathways involved.

Carbohydrates upregulate FGF21 expression

Hepatic FGF21 is induced by prolonged fasting and also by refeeding with a high carbohydrate diet (HCD) (mixed sugar and starch) [84]. Rats starved for 24 h and refed with a HCD for 12 h show an increase in hepatic mRNA and serum levels of FGF21 and metabolic adaptations in the liver and WAT. Specifically in liver, there is an induction of lipogenesis, glucose uptake and metabolism, and a reduction of FA uptake and FAO. Similarly, in WAT, refeeding with a HCD induces lipogenesis, glucose uptake and metabolism, and lipolysis [84]. These results support the hypothesis that FGF21 is produced to compensate any imbalanced nutritional states.

Hepatic FGF21 mRNA expression and plasma levels are also induced in male C57BL/6 mice fed a HC diet containing 77% of energy as dextrose, 0.5% as fat and 22.5% as protein [85]. These results agree with previous studies performed in isolated rat hepatocytes cultured with high glucose [86]. Under this dextrose-rich diet, the liver induction of FGF21 increases de novo lipogenesis, probably as a result of excess carbohydrate intake. In contrast, the same diet supplemented with exogenous lipids [a soybean oil-based emulsion that is rich in C-18:1 and C-18:2 (n−6) unsaturated FAs] reduces FGF21 mRNA levels and de novo lipogenesis.

In rodents and humans, glucose is not the only molecule able to induce FGF21 expression in vitro. The human promoter of FGF21 responds to xylitol [77] and fructose [87] through the transcription factor ChREBP, which binds to a carbohydrate response element (ChoRE) present in human and mouse promoters [77, 83]. These data again reveal the independent mechanisms that regulate the expression of FGF21 downstream of fasting and feeding signals. In vivo, both in humans and rodents, fructose ingestion, but not glucose, leads to an increase of FGF21 serum levels, which peak 2 h after an acute load [87]. In this case, the remaining question is how and why FGF21, which is considered a metabolic positive hormone, is induced by a metabolically pernicious sugar such as fructose.

Finally, it has also been demonstrated that FGF21 expression is regulated by dietary fiber. The intake of such fiber facilitates weight loss and improves lipid and glucose profiles. Sugarcane fiber (SCF: 85% insoluble fiber, 70% particles <1 μM) administered to mice fed a HFD for 12 weeks enhances insulin sensitivity, diminishes fasting plasma glucose and TGs, and attenuates weight [88]. Without altering caloric intake, SCF regulates leptin and glucagon-like peptide 1 (GLP-1) in these mice. In the liver, SCF decreases TGs, cholesterol content, and FGF21 expression, but induces mRNA levels of KLB, FGFR1, FGFR3 and PPARa, thus enhancing FGF21 signaling and ameliorating the obesity observed in the FGF21-resistant state. In parallel SCF also increases AMPK signaling [88].

High-fat diets induce FGF21 resistance

The notion of crosstalk between HFDs and FGF21 expression is controversial probably because of the variety of FAs included in diets. For example, mice fed a corn-oil based HFD (cHFD) for 5 weeks express more FGF21 in liver than those fed a HFD in which corn-oil is replaced by a fish-derived long-chain polyunsaturated n-3 FA (PUFA) [89]. Moreover, another study reported that mice fed a HFD for 16 weeks show no differences in FGF21 mRNA levels versus those fed a low-fat diet [85].

In HepG2 cells, oleate, linoleate and trans-10, cis-12 conjugated linoleic acid (t-10, c-12-CLA) induce FGF21 expression and secretion while palmitate has no effect [90, 91]. Lipid infusion in humans increases the circulating levels of FGF21 [90]. Similarly, in neonatal mice, hepatic FGF21 expression is induced at the initiation of suckling, mainly due to the high FA content of milk [35]. In this case, the FGF21 secreted induces the thermogenic program in BAT.

In the abovementioned situations, mRNA induction occurs through the activation of PPARa and causes an increase in serum levels of FGF21.

In addition to long-chain FAs, butyrate and α-lipoic acid also modulate FGF21 expression in the liver. The former is produced mainly by bacterial fermentation of dietary fiber in the large intestine, and its effect on FGF21 expression seems to be due to its capacity to inhibit histone deacetylase-3 (HDAC3) [92]. Another short FA,

α-lipoic acid, is also involved in the regulation of FGF21. α-lipoic acid can be obtained from the diet (leafy green vegetables and red meats), and its dietary supplementation induces hepatic and plasma levels of FGF21 in vivo and in vitro [93, 94]. The effect of α-lipoic acid on FGF21 expression depends on a CREBH-dependent mechanism that includes the induction of its expression and an increase in its binding to the FGF21 promoter [95].

Finally, several models of obesity in rodents, primates and humans showed that FGF21 levels are higher than in normal weight littermates [17, 96, 97]. In this context, obesity can be defined as an "FGF21-resistant state" [98]. The hepatic induction of FGF21 mRNA in DIO mice positively correlates with an attenuated responsiveness in liver and WAT as a result of a reduction in FGFR1, FGFR4 and KLB levels.

Amino acid-deficient and low-protein diets increase energy expenditure

Several studies have described that hepatic FGF21 is regulated by protein intake. In general, LPDs or diets deficient in a specific amino acid (i.e. leucine or methionine) cause an increase in the hepatic expression and serum levels of FGF21. In this regard, diets with a relatively low content of essential amino acids, such as many vegan diets, are known to be protective against cancer, autoimmunity, obesity, and diabetes. These benefits could be partly due to increased circulating levels of FGF21 [99]. Several studies have demonstrated that FGF21 is the link between imbalanced amino acid intake and adaptive metabolic response and that it serves to restore metabolic homeostasis.

In liver – but not in WAT or BAT–, FGF21 is induced by leucine deprivation. In wild-type mice, the metabolic response to leucine deprivation includes dramatic changes in lipid metabolism. In liver, such deprivation inhibits FA synthase (FAS) activity, decreases the expression of lipogenic genes, and increases the mobilization of lipid stores. In WAT, it decreases FAS activity and the expression of lipogenic genes and increases the expression of FAO genes. Finally, there is an induction of UCP1 expression in BAT [20, 100, 101]. In contrast, in *Fgf21*-deficient mice this metabolic response to leucine is impaired, thus indicating that FGF21 is a key hormone in the regulation of lipid metabolism during leucine deprivation [20, 81].

In the same way, methionine-deprived mice show a comparable phenotype to that of leucine deprivation. The metabolic response to methionine deficiency includes resistance to diet-induced obesity, improved glucose homeostasis, increased FA activation and oxidation in liver, increased lipolysis in WAT, and increased Ucp1 expression in BAT [102–104]. All these effects are coupled to an increase in FGF21 levels.

The metabolic response to protein restriction is similar to that observed under leucine or methionine restriction [7]. Serum levels of FGF21 increase in both rodents and humans upon exposure to LPDs, regardless of overall caloric intake [105, 106]. Protein restriction is accompanied by weight loss and an increase in both food intake and energy expenditure. Remarkably, neither food intake nor energy expenditure of *Fgf21*-deficient mice are altered by the administration of LPDs [7]. Moreover, ketogenic diets (KDs), which are widely known to induce FGF21 expression, are usually low in carbohydrates and proteins but rich in fat. The protein content of KDs underlies the increased levels of circulating FGF21, since protein supplementation but not carbohydrate supplementation blunts the induction [107]. This effect could also explain the induction of FGF21 observed in HCDs, which are characterized by a low protein content.

Protein undernutrition caused by LPDs or imbalanced diets (which are common in mammals confronted with deficient sources of certain amino acids like legumes, grains or corn) strongly affects aminoacidemia. Additionally, pathological situations caused by various forms of stress, such as trauma, thermal burning, sepsis and fever, can lead to a negative nitrogen balance. In this context, several scenarios that alter aminoacidemia also lead to an increase in FGF21 expression. The absence of slc6a19 (neutral amino acid transporter) causes a lack of systemic neutral amino acids, resulting in an increase in FGF21 transcription [108]. The treatment with the antileukemic agent asparaginase depletes circulating asparagine and glutamine levels, promoting FGF21 expression [109], and the skeletal muscle-specific knockout mice for glucocorticoid receptor (GR) show reduced alanine flux from skeletal muscle during fasting, resulting in an increase in FGF21 plasma levels [110]. Hence, it is likely that many other situations that reduce amino acid availability also lead to an induction of FGF21 expression.

GCN2, a kinase that acts as a sensor of amino acid supply [111], and PPARa are indispensable for the induction of FGF21 in response to protein restriction. In this regard, the respective knockout mice present blunted induction of FGF21 when fed a LPD. Nevertheless, it is worth mentioning that in both Ppara-KO and Gcn2-KO mice, the LPD still induces FGF21 expression [7]. This observation suggests that additional signaling pathways are involved in triggering the increase in FGF21 expression in response to protein restriction.

To date, there is no evidence of PPARa activation in response to a LPD, thus suggesting that PPARa plays a role in the constitutive expression of FGF21. In contrast, the LPD increases GCN2-dependent phosphorylation of eIF2a, resulting in greater ATF4 protein levels [100, 112]. Therefore, the GCN2/eIF2a/ATF4 cascade emerges as the main signaling pathway in the induction of FGF21 by protein restriction. ATF4 directly or indirectly induces the transcription of a subset of specific target genes, including FGF21, to modulate many cellular processes to adapt to amino acid deficiency [81, 113, 114]. The 5′ regulatory region of the human FGF21 gene contains two evolutionarily conserved functional ATF4-binding sequences (AARE), which are responsible for ATF4-dependent transcriptional activation in response to ER stress or amino acid restriction [81, 115].

Hepatic mTORC1 activity is also related to FGF21 expression. The mTOR signaling pathway monitors amino acid sufficiency and promotes protein translation and cell growth, among other processes [116]. In this case, L-Tsc1 KO mice, which present mTORC1 hyperactivity in the liver, show increased expression of FGF21 and depleted levels of glutamine [117]. Moreover, when these animals are treated with rapamycin (mTORC1 inhibitor) or glutamine, the increase in FGF21 is blunted. Finally, in human hepatic tumors, mTORC1 activation also correlates with FGF21 levels [117]. It has been proposed that the mechanism underling the increase in FGF21 expression occurs through PGC1a; however, additional mechanisms could be involved and it is feasible that depleted glutamine levels trigger an amino acid response (AAR).

In summary, amino acid-deficient diets diminish aminoacidemia and trigger AAR, thereby resulting in elevated FGF21 levels. The contribution of each single amino acid to the modulation of FGF21 and how a deficiency in specific types of dietary protein alters FGF21 expression require further study.

Bioactive dietary compounds affect FGF21 expression and signaling

Polyphenols are the most abundant phytochemicals in nature. These bioactive compounds are synthesized as secondary metabolites by plants and are thus abundant in fruits, vegetables, legumes, cocoa and some beverages, such as tea, coffee and wine. Polyphenols comprise a large heterogeneous group of chemical structures, all with a phenolic ring with one or more hydroxyl groups, and they are classified mainly into two families, namely flavonoids and non-flavonoids, and also into many subfamilies. Flavonoids are the most abundant polyphenols and consequently those most greatly ingested in human diets.

Due to the diversity of polyphenols, their absorption in the body is dose- and type-dependent and their effects are related to their bioavailability and pharmacokinetics. It is estimated that most of the polyphenols ingested go directly to the colon and only between 5 and 10% are absorbed in small intestine. The effects of polyphenols in the colon have been related to a prebiotic capacity, as they are believed to induce the growth and activity of some bacteria, such as *Bifidobacterium*, *Enterococcus* and *Prevotella*. Furthermore, once absorbed, polyphenols enter portal circulation and are metabolized in the liver. Finally, the conjugate metabolites reach the bloodstream and the target tissues [118, 119].

Various epidemiological studies have reported that the regular consumption of polyphenols has beneficial effects in obesity, insulin resistance, cardiovascular diseases, and cancer. Several lines of evidence support the notion that polyphenol-rich diets play a key role in regulating lipid and glucose metabolism and are thus pivotal in the prevention and treatment of pathologies related to energy homeostasis [120–123].

It has been described that resveratrol has a protective effect on cardiovascular risk associated to ROS overproduction but also on the prevention of hepatic steatosis and the improvement of insulin resistance [124]. Green tea polyphenols, mainly epigallocatechin-3-gallate (EGCG), reduce the LDL and increase HDL levels in humans and improve insulin sensitivity in genetic models of insulin resistance, thus exerting a beneficial effect on body weight and lipid profile [125, 126]. Isoflavones and polyphenol-rich grape extract can partially prevent hepatic steatosis associated with obesity by restoring the correct secretion of adipokines – mainly leptin and adiponectin, by up-regulating FAO, and by down-regulating lipogenesis in adipose tissue [127, 128].

For many years, the health benefits of polyphenols were attributed to their anti-oxidant capacity as free radical scavengers. It has recently been described that polyphenols activate cell-signaling pathways that are not related to ROS production but rather those involved in metabolic regulation. It is remarkable that most of these pathways are downstream of FGF21. It has been reported that, in vitro, polyphenols downregulate SREBP-1c and its main target genes in lipogenesis, namely FAS and acetyl-CoA carboxylase (ACC) [129]. Stilbens, mainly resveratrol, exert their effects by promoting the phosphorylation and activation of the AMP-activated protein kinase (AMPK) and the activity of SIRT and PGC1a, thus inducing FA catabolism through the AMPK/SIRT1/PGC1a axis [130, 131]. On

the other hand, an anthocyanin-rich juice extract up-regulates PPARa activity in mice on a HFD and down-regulates lipogenic gene expression in liver by promoting FA consumption. Coffee polyphenols and resveratrol also induce FAO in rats through PPARa and PGC1a-dependent mechanisms [132]. Chalcones and flavokawain cardamonin type B inhibit lipid accumulation and adipocyte differentiation by increasing the phosphorylation of the ERK in the early phase of adipogenesis [133].

In summary, polyphenols exert beneficial metabolic effects especially in obese and in insulin-resistant animal models, and FGF21 restores homeostasis in scenarios of metabolic stress. The crosstalk between the two signals remains unclear, but a positive correlation between the beneficial effects of polyphenol-rich fruit extracts and FGF21 activity has been described in various rodent models of diet-induced obesity. In some cases, the effects of polyphenols were due to an induction of FGF21 levels in liver [134, 135] but also to an enhancement of FGF21 signaling by increasing the expression of FGF21 receptors and KLB, [136, 137]. Moreover, flavokawain B and cardamonin also modulate the secretion of FGF21 in mature adipocytes [133].

FGF21 in humans

After the identification of rodent FGF21 as an endocrine regulator induced downstream of PPARa and its agonists by both fasting and a KD [13, 73], it was shown that fasting FGF21 levels are significantly increased in patients with T2DM without a correlation with BMI, thereby pointing to a potential role of FGF21 in the pathogenesis of insulin resistance and T2DM [138].

Later, in contrast to previously published data, it was described that serum FGF21 levels in overweight and in obese subjects are significantly higher than in lean individuals and that they correlate positively with adiposity and the metabolic syndrome [17, 139]. Also, an increase in plasma levels of FGF21 in hepatic- and muscle-insulin resistant states and a correlation with BMI have been reported [140].

Accordingly, a study performed in 2010 again showed a positive correlation between FGF21 expression and BMI; however, the authors did not find that fasting and refeeding or 12 days of a KD regulated the hormone in humans [8]. Moreover, FGF21 concentrations are reversibly increased and are related to leptin and free FAs in obese children. However, the results of that study do not support a significant relationship between FGF21, insulin resistance, and features of metabolic syndrome or NAFLD in this age group [141]. The same pattern of FGF21 expression was described in obese adolescents with T2DM compared with obese adolescents without. As in rodents, this increment in FGF21 levels in obesity and T2DM points to a FGF21-resistant state and an impaired capacity of FGF21 to improve insulin sensitivity [142]. No significant association between FGF21 and growth or IGF-1 was found in either cross-sectional or longitudinal analyses; these findings do not support a relationship between FGF21 and growth in obese children [143].

In contrast, in the pubertal transition, it was found that FGF21 concentrations do not differ by obesity status or by sex. An inverse association between FGF21 and bone mineral content (BMC) among non-obese individuals and an inverse association between FGF21 and lean mass among females were observed, which were both independent of fat mass. FGF21 was inversely associated with HOMA-IR in males but not in females. The existence of relationships between FGF21, musculoskeletal parameters, and insulin resistance raises the possibility of crosstalk between these systems. These data suggest that circulating FGF21 differs in its association with bone, lean mass and insulin resistance depending on the sex and weight of the individual [144].

Globally, several studies have proposed FGF21 as a biomarker for metabolic pathologies such as cardiovascular diseases, NAFLD, and mitochondrial disease [8, 145]. Serum FGF21 concentrations are significantly elevated in patients with mitochondrial disease. This prospective study established serum FGF21 levels as a sensitive biomarker of mitochondrial disease and demonstrated that they are the best predictor of this disorder when compared to serum levels of other classical indicators [146]. In the same way, a cross-sectional study with a large well-characterized sample (913 subjects) assessed the interaction between clinical parameters (renal function, metabolic, hepatic and vascular risk markers), as well as growth hormone (GH) status, with FGF21 levels. Those authors concluded that FGF21 serum concentrations are associated with several aspects of the metabolic syndrome, hepatocellular function, as well as with GH status [147].

In a healthy population, there is also an age-related increase in serum FGF21 levels. This observation highlights a potential age effect in response to metabolic demands during the lifespan. FGF21 levels increase with age independently of body composition. At lower levels of FGF21, bone mineral density (BMD), but not other body composition parameters, attenuates the association between FGF21 levels and age, thereby suggesting that the metabolic demands of the skeleton serve to link FGF21 and energy metabolism [148].

Regarding the nutritional regulation of FGF21 in humans, the data are less clear than in rodents. Increased levels of FGF21 in human serum after extreme fasting (7 days) and PPARa activation have been described in healthy non-diabetic individuals but with a wide inter-individual variation. The induction of ketogenesis independently of FGF21 levels suggests that the physiological role of FGF21 in humans differs from that in mice [149]. Although FGF21 is elevated in response to pharmacological activation of PPARa and PPARd, the absence of variation in human plasma during fasting and refeeding and the decrease after a 3-month KD confirm that FGF21 does not play a major role in regulating fasting response or ketosis in humans [150].

Unlike mice, which showed an increase in circulating FGF21 after only 6 h of fasting, human subjects did not have a notable surge in FGF21 until 7–10 days of fasting. Moreover, FGF21 induction was associated with decreased thermogenesis and adiponectin, an observation that contrasts with previous reports based on supraphysiological dosing. In addition, FGF21 levels increased after ketone induction, thereby demonstrating that endogenous FGF21 does not drive starvation-mediated ketogenesis in humans. Instead, a longitudinal analysis of biologically relevant variables identified serum transaminase markers of tissue breakdown as predictors of FGF21. These data establish FGF21 as a fasting-induced hormone in humans and indicate that it contributes to the late stages of adaptation to starvation, when it may regulate the utilization of fuel derived from tissue breakdown [151].

A large number of studies have shown that dietary protein content markedly influences food intake and metabolism. In this context, in humans, circulating FGF21 levels increase dramatically after 28 days on a LPD, thereby suggesting that FGF21 is a signal of protein restriction and providing an explanation of the effect of dietary protein deficiency on metabolism [7].

As mentioned earlier, FGF21 levels increase rapidly following fructose ingestion and return to baseline within 5 h. Moreover, both baseline and fructose-stimulated FGF21 levels are 2–3 fold higher in subjects with metabolic syndrome compared to those in healthy subjects. In contrast, FGF21 does not increase in the first 2 h after the ingestion of a glucose load, although a modest increase is observed after 3–4 h. These data suggest that FGF21 plays a key role in fructose metabolism in humans [87].

Other nutritional challenges that affect FGF21 levels are fish oil supplements and betaine. The inclusion of the former in a diet for 3 months markedly reduces the circulating levels of FGF21 and other biomarkers, combined with decreases in serum lipids, glucose, liver enzymes, and other NAFLD risk factors. These results suggest that fish oil might contribute to reversing FGF21 resistance [152]. Regarding betaine, it is known that plasma betaine levels are reduced in insulin-resistant humans and that they correlate closely with insulin sensitivity. In this context, in addition to the beneficial metabolic effects of betaine, supplementation with this compound robustly increases hepatic and circulating FGF21 levels in mice. On the basis of these observations, betaine supplementation merits further investigation for the treatment or prevention of T2DM in humans [153].

Circulating levels of FGF21 can also be boosted by exercise. Increased levels of the protein were observed in the serum of healthy male volunteers performing a treadmill run at 50 or 80% VO_2max. These results suggest that FGF21 is also associated with exercise-induced lipolysis [41].

Finally, in healthy human volunteers, the injection of natural glucagon increased plasma FGF21 within hours, showing for the first time that glucagon regulates glucose, energy, and lipid metabolism, at least in part via FGF21-dependent pathways [154].

Expert opinion

FGF21 is a peptide hormone involved in metabolic homeostasis and considered a promising therapeutic candidate for the treatment of obesity and associated comorbidities such insulin resistance, T2DM, and cardiovascular diseases. Although the effects of FGF21 in humans seems to be weaker than in mice and interindividual variability in the levels of this growth factor are observed, it is obvious that FGF21 exerts beneficial effects on metabolic homeostasis in both species. To date, the therapies related to FGF21 overexpression have involved pharmacological administration; however, this approach has considerable limitations due to the kinetics and bioavailability of the compound. Recently, several studies have demonstrated that specific macronutrients and bioactive dietary compounds can modulate endogenous FGF21 expression and signaling, thereby opening up the possibility to induce FGF21 production or increase activity through dietary intervention. The most feasible approaches to define a nutritional intervention able to induce FGF21 activity and reduce obesity and associated-comorbidities are probably through protein restriction and polyphenol-enriched diets. However, more research is needed in order to establish the role of FGF21 as the link between the dietary components. It is also important to highlight that all these nutritional interventions must be done in compliance

with a balanced diet in order to prevent the loss of muscle mass or BMD and essential nutrient deficiencies.

Outlook

To design therapeutic approaches based on a nutritional intervention it is essential to determine the molecular mechanisms through which macronutrients, micronutrients, and bioactive dietary compounds affect FGF21 expression and signaling. It is likely that the metabolic effects of certain diets such as vegan or the beneficial effects of established healthy diets, such as the Mediterranean diet, occur at least in part through FGF21. Further studies in humans will be required to define the effect of a nutritional profile on FGF21 levels and signaling in healthy, obese and T2DM patients. Also it will be important to define if there are any differential effects between the pharmacological administration of FGF21 and its endogenous overproduction. Moreover, obesity that is one of the possible diseases treatable with FGF21 is also a FGF21-resistant state. In this context it will be strictly necessary to study the way to overcome this resistance, thus increasing the levels of the FGF21 receptors in its target tissues. Some studies have revealed that some nutritional interventions are able to induce the expression of FGFR and KLB.

In summary, FGF21 is a promising therapeutic candidate against metabolic pathologies such as obesity or T2DM and its expression and signaling are highly regulated by different nutritional states. The remaining question is how we can increase the responsiveness to FGF21 in obese or T2DM patient just through a dietary intervention.

Highlights

In animal models has been is well described that:

- The liver is the main organ in contributing to serum levels of FGF21.
- The transcription factors network responsible for the control of FGF21 gene expression is highly complicated. Both, positive and negative factors have been described.
- The expression of hepatic FGF21 responds to several stimuli, mainly metabolic stress signals.
- The hepatic expression of FGF21 can be modified by dietary components. Mainly high fat diet, high carbohydrate diet, low protein diet or amino acid restricted diets.

In order to confirm FGF21 as a therapeutic candidate against metabolic pathologies such as obesity or T2DM:

- The role of FGF21 as the link between the dietary components and its metabolic effects has to be set precisely.
- The effect of dietary bioactive compounds on the expression of hepatic FGF21 needs further studies.
- The mechanisms responsible for the establishment of the FGF21-resistant state have to be proven.
- The effect of different dietary interventions on the expression of FGF21 receptors in target tissues needs future evaluation.

Acknowledgments: This project was supported by grants SAF2010-15217 (to DH) and SAF2013-41093 (to PM and DH) from Spain's Ministerio de Ciencia e Inovación and Ministerio de Economia y Competitividad, respectively, and by funding from the Catalan government (Ajut de Suport als Grups de Recerca de Catalunya 2009SGR163 and 2014SGR916). APM was supported by Scholarship from Spain's Ministerio de Educación Cultura y Deporte**.** VS was supported by Scholarship from Chile's Ministerio de Educación (Conicyt).

Funding: Authors state no funding involved.
Conflict of interest: Authors state no conflict of interest.
Material and methods: Informed consent: Informed consent is not applicable.
Ethical approval: The conducted research is not related to either human or animals use.

References

1. Kharitonenkov A, Shanafelt AB. FGF21: a novel prospect for the treatment of metabolic diseases. Curr Opin Investig Drugs 2009;10:359–64.
2. Kharitonenkov A, Shiyanova TL, Koester A, Ford AM, Micanovic R, Galbreath EJ, Sandusky GE, Hammond LJ, Moyers JS, Owens RA, Gromada J, Brozinick JT, Hawkins ED, Wroblewski VJ, Li DS, Mehrbod F, Jaskunas SR, Shanafelt AB. FGF-21 as a novel metabolic regulator. J Clin Invest 2005;115:1627–35.
3. Gaich G, Chien JY, Fu H, Glass LC, Deeg MA, Holland WL, Kharitonenkov A, Bumol T, Schilske HK, Moller DE. The effects of LY2405319, an FGF21 analog, in obese human subjects with type 2 diabetes. Cell Metab 2013;18:333–40.
4. Weng Y, Chabot JR, Bernardo B, Yan Q, Zhu Y, Brenner MB, Vage C, Logan A, Calle R, Talukdar S. Pharmacokinetics (PK), pharmacodynamics (PD) and integrated PK/PD modeling of a novel long acting FGF21 clinical candidate PF-05231023 in diet-induced obese and leptin-deficient obese mice. PLoS One 2015;10:e0119104.
5. Talukdar S, Zhou Y, Li D, Rossulek M, Dong J, Somayaji V, Weng Y, Clark R, Lanba A, Owen BM, Brenner MB, Trimmer JK, Gropp KE,

Chabot JR, Erion DM, Rolph TP, Goodwin B, Calle RA. A long-acting FGF21 molecule, PF-05231023, decreases body weight and improves lipid profile in non-human primates and type 2 diabetic subjects. Cell Metab 2016;23:427–40.
6. Chu AY, Workalemahu T, Paynter NP, Rose LM, Giulianini F, Tanaka T, Ngwa JS; CHARGE Nutrition Working Group, Qi Q, Curhan GC, Rimm EB, Hunter DJ, Pasquale LR, Ridker PM, Hu FB, Chasman DI, Qi L; DietGen Consortium. Novel locus including FGF21 is associated with dietary macronutrient intake. Hum Mol Genet 2013;22:1895–902.
7. Laeger T, Henagan TM, Albarado DC, Redman LM, Bray GA, Noland RC, Münzberg H, Hutson SM, Gettys TW, Schwartz MW, Morrison CD. FGF21 is an endocrine signal of protein restriction. J Clin Invest 2014;124:3913–22.
8. Dushay J, Chui PC, Gopalakrishnan GS, Varela-Rey M, Crawley M, Fisher FM, Badman MK, Martinez-Chantar ML, Maratos-Flier E. Increased fibroblast growth factor 21 in obesity and nonalcoholic fatty liver disease. Gastroenterology 2010;139:456–63.
9. Itoh N. FGF21 as a hepatokine, adipokine, and myokine in metabolism and diseases. Front Endocrinol (Lausanne) 2014;5:107.
10. Yang C, Jin C, Li X, Wang F, McKeehan WL, Luo Y. Differential specificity of endocrine FGF19 and FGF21 to FGFR1 and FGFR4 in complex with KLB. PLoS One 2012;7:e33870.
11. Ding X, Boney-Montoya J, Owen BM, Bookout AL, Coate KC, Mangelsdorf DJ, Kliewer SA. betaKlotho is required for fibroblast growth factor 21 effects on growth and metabolism. Cell Metab 2012;16:387–93.
12. Fisher FM, Maratos-Flier E. Understanding the physiology of FGF21. Annu Rev Physiol 2016;78:223–41.
13. Inagaki T, Dutchak P, Zhao G, Ding X, Gautron L, Parameswara V, Li Y, Goetz R, Mohammadi M, Esser V, Elmquist JK, Gerard RD, Burgess SC, Hammer RE, Mangelsdorf DJ, Kliewer SA. Endocrine regulation of the fasting response by PPARalpha-mediated induction of fibroblast growth factor 21. Cell Metab 2007;5:415–25.
14. Potthoff MJ, Inagaki T, Satapati S, Ding X, He T, Goetz R, Mohammadi M, Finck BN, Mangelsdorf DJ, Kliewer SA, Burgess SC. FGF21 induces PGC-1alpha and regulates carbohydrate and fatty acid metabolism during the adaptive starvation response. Proc Natl Acad Sci USA 2009;106:10853–8.
15. Dasarathy S, Yang Y, McCullough AJ, Marczewski S, Bennett C, Kalhan SC. Elevated hepatic fatty acid oxidation, high plasma fibroblast growth factor 21, and fasting bile acids in nonalcoholic steatohepatitis. Eur J Gastroenterol Hepatol 2011;23:382–8.
16. Domingo P, Gallego-Escuredo JM, Domingo JC, Gutiérrez Mdel M, Mateo MG, Fernández I, Vidal F, Giralt M, Villarroya F. Serum FGF21 levels are elevated in association with lipodystrophy, insulin resistance and biomarkers of liver injury in HIV-1-infected patients. AIDS 2010;24:2629–37.
17. Zhang X, Yeung DC, Karpisek M, Stejskal D, Zhou ZG, Liu F, Wong RL, Chow WS, Tso AW, Lam KS, Xu A. Serum FGF21 levels are increased in obesity and are independently associated with the metabolic syndrome in humans. Diabetes 2008;57:1246–53.
18. Yang C, Lu W, Lin T, You P, Ye M, Huang Y, Jiang X, Wang C, Wang F, Lee MH, Yeung SC, Johnson RL, Wei C, Tsai RY, Frazier ML, McKeehan WL, Luo Y. Activation of Liver FGF21 in hepatocarcinogenesis and during hepatic stress. BMC Gastroenterol 2013;13:67.
19. Fisher FM, Estall JL, Adams AC, Antonellis PJ, Bina HA, Flier JS, Kharitonenkov A, Spiegelman BM, Maratos-Flier E. Integrated regulation of hepatic metabolism by fibroblast growth factor 21 (FGF21) in vivo. Endocrinology 2011;152:2996–3004.
20. De Sousa-Coelho AL, Relat J, Hondares E, Pérez-Martí A, Ribas F, Villarroya F, Marrero PF, Haro D. FGF21 mediates the lipid metabolism response to amino acid starvation. J Lipid Res 2013;54:1786–97.
21. Hotta Y, Nakamura H, Konishi M, Murata Y, Takagi H, Matsumura S, Inoue K, Fushiki T, Itoh N. Fibroblast growth factor 21 regulates lipolysis in white adipose tissue but is not required for ketogenesis and triglyceride clearance in liver. Endocrinology 2009;150:4625–33.
22. Bookout AL, de Groot MH, Owen BM, Lee S, Gautron L, Lawrence HL, Ding X, Elmquist JK, Takahashi JS, Mangelsdorf DJ, Kliewer SA. FGF21 regulates metabolism and circadian behavior by acting on the nervous system. Nat Med 2013;19:1147–52.
23. Ishida N. Role of PPAR in the control of torpor through FGF21-NPY pathway: from circadian clock to seasonal change in mammals. PPAR Res 2009;2009:412949.
24. Li X, Ge H, Weiszmann J, Hecht R, Li YS, Véniant MM, Xu J, Wu X, Lindberg R, Li Y. Inhibition of lipolysis may contribute to the acute regulation of plasma FFA and glucose by FGF21 in ob/ob mice. FEBS Lett 2009;583:3230–4.
25. Arner P, Pettersson A, Mitchell PJ, Dunbar JD, Kharitonenkov A, Ryden M. FGF21 attenuates lipolysis in human adipocytes – a possible link to improved insulin sensitivity. FEBS Lett 2008;582:1725–30.
26. Dutchak PA, Katafuchi T, Bookout AL, Choi JH, Yu RT, Mangelsdorf DJ, Kliewer SA. Fibroblast growth factor-21 regulates PPARgamma activity and the antidiabetic actions of thiazolidinediones. Cell 2012;148:556–67.
27. Muise ES, Azzolina B, Kuo DW, El-Sherbeini M, Tan Y, Yuan X, Mu J, Thompson JR, Berger JP, Wong KK. Adipose fibroblast growth factor 21 is up-regulated by peroxisome proliferator-activated receptor gamma and altered metabolic states. Mol Pharmacol 2008;74:403–12.
28. Ge X, Chen C, Hui X, Wang Y, Lam KSL, Xu A. Fibroblast growth factor 21 induces glucose transporter-1 expression through activation of the serum response factor/Ets-like protein-1 in adipocytes. J Biol Chem 2011;286:34533–41.
29. Camporez JP, Jornayvaz FR, Petersen MC, Pesta D, Guigni BA, Serr J, Zhang D, Kahn M, Samuel VT, Jurczak MJ, Shulman GI. Cellular mechanisms by which FGF21 improves insulin sensitivity in male mice. Endocrinology 2013;154:3099–109.
30. Lin Z, Tian H, Lam KS, Lin S, Hoo RC, Konishi M, Itoh N, Wang Y, Bornstein SR, Xu A, Li X. Adiponectin mediates the metabolic effects of FGF21 on glucose homeostasis and insulin sensitivity in mice. Cell Metab 2013;17:779–89.
31. Holland WL, Adams AC, Brozinick JT, Bui HH, Miyauchi Y, Kusminski CM, Bauer SM, Wade M, Singhal E, Cheng CC, Volk K, Kuo MS, Gordillo R, Kharitonenkov A, Scherer PE. An FGF21-adiponectin-ceramide axis controls energy expenditure and insulin action in mice. Cell Metab 2013;17:790–7.
32. Fisher FM, Kleiner S, Douris N, Fox EC, Mepani RJ, Verdeguer F, Wu J, Kharitonenkov A, Flier JS, Maratos-Flier E, Spiegelman BM. FGF21 regulates PGC-1α and browning of white adipose tissues in adaptive thermogenesis. Genes Dev 2012;26:271–81.
33. Iglesias R, Giralt A, Gonzalez FJ, Giralt M, Mampel T, Villarroya F. Thermogenic activation induces FGF21 expression and release in brown adipose tissue. J Biol Chem 2011;286:12983–90.

34. Chartoumpekis DV, Habeos IG, Ziros PG, Psyrogiannis AI, Kyriazopoulou VE, Papavassiliou AG. Brown adipose tissue responds to cold and adrenergic stimulation by induction of FGF21. Mol Med 2011;17:736–40.
35. Hondares E, Rosell M, Gonzalez FJ, Giralt M, Iglesias R, Villarroya F. Hepatic FGF21 expression is induced at birth via PPARalpha in response to milk intake and contributes to thermogenic activation of neonatal brown fat. Cell Metab 2010;11:206–12.
36. Samms RJ, Smith DP, Cheng CC, Antonellis PP, Perfield JW, Kharitonenkov A, Gimeno RE, Adams AC. Discrete aspects of FGF21 in vivo pharmacology do not require UCP1. Cell Rep 2015;11:991–9.
37. Véniant MM, Sivits G, Helmering J, Komorowski R, Lee J, Fan W, Moyer C, Lloyd DJ. Pharmacologic effects of FGF21 are independent of the "Browning" of white adipose tissue. Cell Metab 2015;21:731–8.
38. Bernardo B, Lu M, Bandyopadhyay G, Li P, Zhou Y, Huang J, Levin N, Tomas EM, Calle RA, Erion DM, Rolph TP, Brenner M, Talukdar S. FGF21 does not require interscapular brown adipose tissue and improves liver metabolic profile in animal models of obesity and insulin-resistance. Sci Rep 2015;5:11382.
39. Izumiya Y, Bina HA, Ouchi N, Akasaki Y, Kharitonenkov A, Walsh K. FGF21 is an Akt-regulated myokine. FEBS Lett 2008;582:3805–10.
40. Hojman P, Pedersen M, Nielsen AR, Krogh-Madsen R, Yfanti C, Akerstrom T, Nielsen S, Pedersen BK. Fibroblast growth factor-21 is induced in human skeletal muscles by hyperinsulinemia. Diabetes 2009;58:2797–801.
41. Kim KH, Kim SH, Min Y-K, Yang H-M, Lee J-B, Lee M-S. Acute exercise induces FGF21 expression in mice and in healthy humans. PLoS One 2013;8:e63517.
42. Tyynismaa H, Carroll CJ, Raimundo N, Ahola-Erkkilä S, Wenz T, Ruhanen H, Guse K, Hemminki A, Peltola-Mjøsund KE, Tulkki V, Oresic M, Moraes CT, Pietiläinen K, Hovatta I, Suomalainen A. Mitochondrial myopathy induces a starvation-like response. Hum Mol Genet 2010;19:3948–58.
43. Vandanmagsar B, Warfel JD, Wicks SE, Ghosh S, Salbaum JM, Burk D, Dubuisson OS, Mendoza TM, Zhang J, Noland RC, Mynatt RL. Impaired mitochondrial fat oxidation induces FGF21 in muscle. Cell Rep 2016;15:1686–99.
44. Kim KH, Jeong YT, Oh H, Kim SH, Cho JM, Kim YN, Kim SS, Kim do H, Hur KY, Kim HK, Ko T, Han J, Kim HL, Kim J, Back SH, Komatsu M, Chen H, Chan DC, Konishi M, Itoh N, Choi CS, Lee MS. Autophagy deficiency leads to protection from obesity and insulin resistance by inducing Fgf21 as a mitokine. Nat Med 2013;19:83–92.
45. Harris L-ALS, Skinner JR, Shew TM, Pietka TA, Abumrad NA, Wolins NE. Perilipin 5-driven lipid droplet accumulation in skeletal muscle stimulates the expression of fibroblast growth factor 21. Diabetes 2015;64:2757–68.
46. Keipert S, Ost M, Johann K, Imber F, Jastroch M, van Schothorst EM, Keijer J, Klaus S. Skeletal muscle mitochondrial uncoupling drives endocrine cross-talk through the induction of FGF21 as a myokine. Am J Physiol Endocrinol Metab 2014;306:E469–82.
47. Lee MS, Choi SE, Ha ES, An SY, Kim TH, Han SJ, Kim HJ, Kim DJ, Kang Y, Lee KW. Fibroblast growth factor-21 protects human skeletal muscle myotubes from palmitate-induced insulin resistance by inhibiting stress kinase and NF-kappaB. Metabolism 2012;61:1142–51.
48. Mashili FL, Austin RL, Deshmukh AS, Fritz T, Caidahl K, Bergdahl K, Zierath JR, Chibalin AV, Moller DE, Kharitonenkov A, Krook A. Direct effects of FGF21 on glucose uptake in human skeletal muscle: implications for type 2 diabetes and obesity. Diabetes Metab Res Rev 2011;27:286–97.
49. Brahma MK, Adam RC, Pollak NM, Jaeger D, Zierler KA, Pöcher N, Schreiber R, Romauch M, Moustafa T, Eder S, Ruelicke T, Preiss-Landl K, Lass A, Zechner R, Haemmerle G. Fibroblast growth factor 21 is induced upon cardiac stress and alters cardiac lipid homeostasis. J Lipid Res 2014;55:2229–41.
50. Planavila A, Redondo-Angulo I, Villarroya F. FGF21 and cardiac physiopathology. Front Endocrinol 2015;6:133.
51. Dogan SA, Pujol C, Maiti P, Kukat A, Wang S, Hermans S, Senft K, Wibom R, Rugarli EI, Trifunovic A. Tissue-specific loss of DARS2 activates stress responses independently of respiratory chain deficiency in the heart. Cell Metab 2014;19:458–69.
52. Planavila A, Redondo-Angulo I, Ribas F, Garrabou G, Casademont J, Giralt M, Villarroya F. Fibroblast growth factor 21 protects the heart from oxidative stress. Cardiovasc Res 2014;106:19–31.
53. Liu SQ, Roberts D, Kharitonenkov A, Zhang B, Hanson SM, Li YC, Zhang LQ, Wu YH. Endocrine protection of ischemic myocardium by FGF21 from the liver and adipose tissue. Sci Rep 2013;3:2767.
54. Joki Y, Ohashi K, Yuasa D, Shibata R, Ito M, Matsuo K, Kambara T, Uemura Y, Hayakawa S, Hiramatsu-Ito M, Kanemura N, Ogawa H, Daida H, Murohara T, Ouchi N. FGF21 attenuates pathological myocardial remodeling following myocardial infarction through the adiponectin-dependent mechanism. Biochem Biophys Res Commun 2015;459:124–30.
55. Fon Tacer K, Bookout AL, Ding X, Kurosu H, John GB, Wang L, Zhang LQ, Wu YH. Research resource: comprehensive expression atlas of the fibroblast growth factor system in adult mouse. Mol Endocrinol 2010;24:2050–64.
56. Liang Q, Zhong L, Zhang J, Wang Y, Bornstein SR, Triggle CR, Ding H, Lam KS, Xu A. FGF21 maintains glucose homeostasis by mediating the cross talk between liver and brain during prolonged fasting. Diabetes 2014;63:4064–75.
57. Mäkelä J, Tselykh TV, Maiorana F, Eriksson O, Do HT, Mudò G, Korhonen LT, Belluardo N, Lindholm D. Fibroblast growth factor-21 enhances mitochondrial functions and increases the activity of PGC-1alpha in human dopaminergic neurons via Sirtuin-1. Springerplus 2014;3:2.
58. Tan BK, Hallschmid M, Adya R, Kern W, Lehnert H, Randeva HS. Fibroblast growth factor 21 (FGF21) in human cerebrospinal fluid: relationship with plasma FGF21 and body adiposity. Diabetes 2011;60:2758–62.
59. Owen BM, Bookout AL, Ding X, Lin VY, Atkin SD, Gautron L, Kliewer SA, Mangelsdorf DJ. FGF21 contributes to neuroendocrine control of female reproduction. Nat Med 2013;19:1153–6.
60. Douris N, Stevanovic D, Fisher FM, Cisu TI, Chee MJ, Ly Nguyen N, Zarebidaki E, Adams AC, Kharitonenkov A, Flier JS, Bartness TJ, Maratos-Flier E. Central fibroblast growth factor 21 browns white fat via sympathetic action in male mice. Endocrinology 2015;156:2470–81.
61. Owen BM, Bookout AL, Ding X, Lin VY, Atkin SD, Gautron L, Kliewer SA, Mangelsdorf DJ. FGF21 acts centrally to induce sympathetic nerve activity, energy expenditure, and weight loss. Cell Metab 2014;20:670–7.
62. Arase K, York D, Shimizu H, Shargill N, Bray G. Effects of corticotropin-releasing factor on food intake and brown adipose tissue thermogenesis in rats. Am J Physiol 1988;255:255–9.
63. Johnson CL, Weston JY, Chadi SA, Fazio EN, Huff MW, Kharitonenkov A, Köester A, Pin CL. Fibroblast growth factor 21 reduces the

severity of cerulein-induced pancreatitis in mice. Gastroenterology 2009;137:1795–804.
64. Uonaga T, Toyoda K, Okitsu T, Zhuang X, Yamane S, Uemoto S, Inagaki N. FGF-21 enhances islet engraftment in mouse syngeneic islet transplantation model. Islets 2010;2:247–51.
65. Wente W, Efanov AM, Brenner M, Kharitonenkov A, Köster A, Sandusky GE, Sewing S, Treinies I, Zitzer H, Gromada J. Fibroblast growth factor-21 improves pancreatic beta-cell function and survival by activation of extracellular signal-regulated kinase 1/2 and Akt signaling pathways. Diabetes 2006;55:2470–8.
66. So WY, Cheng Q, Chen L, Evans-Molina C, Xu A, Lam KS, Leung PS. High glucose represses beta-klotho expression and impairs fibroblast growth factor 21 action in mouse pancreatic islets: involvement of peroxisome proliferator-activated receptor gamma signaling. Diabetes 2013;62:3751–9.
67. Zhang Y, Xie Y, Berglund ED, Coate KC, He TT, Katafuchi T, Xiao G, Potthoff MJ, Wei W, Wan Y, Yu RT, Evans RM, Kliewer SA, Mangelsdorf DJ. The starvation hormone, fibroblast growth factor-21, extends lifespan in mice. Elife 2012;1:1–14.
68. von Holstein-Rathlou S, BonDurant LD, Peltekian L, Naber MC, Yin TC, Claflin KE, Urizar AI, Madsen AN, Ratner C, Holst B, Karstoft K, Vandenbeuch A, Anderson CB, Cassell MD, Thompson AP, Solomon TP, Rahmouni K, Kinnamon SC, Pieper AA, Gillum MP, Potthoff MJ. FGF21 mediates endocrine control of simple sugar intake and sweet taste preference by the liver. Cell Metab 2016;23:335–43.
69. Talukdar S, Owen BM, Song P, Hernandez G, Zhang Y, Zhou Y, Scott WT, Paratala B, Turner T, Smith A, Bernardo B, Müller CP, Tang H, Mangelsdorf DJ, Goodwin B, Kliewer SA. FGF21 regulates sweet and alcohol preference. Cell Metab 2016;23:344–9.
70. Tanaka T, Ngwa JS, van Rooij FJ, Zillikens MC, Wojczynski MK, Frazier-Wood AC, Houston DK, Kanoni S, Lemaitre RN, Luan J, Mikkilä V, Renstrom F, Sonestedt E, Zhao JH, Chu AY, Qi L, Chasman DI, de Oliveira Otto MC, Dhurandhar EJ, Feitosa MF, Johansson I, Khaw KT, Lohman KK, Manichaikul A, McKeown NM, Mozaffarian D, Singleton A, Stirrups K, Viikari J, Ye Z, Bandinelli S, Barroso I, Deloukas P, Forouhi NG, Hofman A, Liu Y, Lyytikäinen LP, North KE, Dimitriou M, Hallmans G, Kähönen M, Langenberg C, Ordovas JM, Uitterlinden AG, Hu FB, Kalafati IP, Raitakari O, Franco OH, Johnson A, Emilsson V, Schrack JA, Semba RD, Siscovick DS, Arnett DK, Borecki IB, Franks PW, Kritchevsky SB, Lehtimäki T, Loos RJ, Orho-Melander M, Rotter JI, Wareham NJ, Witteman JC, Ferrucci L, Dedoussis G, Cupples LA, Nettleton JA. Genome-wide meta-analysis of observational studies shows common genetic variants associated with macronutrient intake. Am J Clin Nutr 2013;97:1395–402.
71. Wei W, Dutchak PA, Wang X, Ding X, Wang X, Bookout AL, Goetz R, Mohammadi M, Gerard RD, Dechow PC, Mangelsdorf DJ, Kliewer SA, Wan Y. Fibroblast growth factor 21 promotes bone loss by potentiating the effects of peroxisome proliferator-activated receptor gamma. Proc Natl Acad Sci USA 2012;109:3143–8.
72. Markan KR, Naber MC, Ameka MK, Anderegg MD, Mangelsdorf DJ, Kliewer SA, Mohammadi M, Potthoff MJ. Circulating FGF21 is liver derived and enhances glucose uptake during refeeding and overfeeding. Diabetes 2014;63:4057–63.
73. Badman MK, Pissios P, Kennedy AR, Koukos G, Flier JS, Maratos-Flier E. Hepatic fibroblast growth factor 21 is regulated by PPARalpha and is a key mediator of hepatic lipid metabolism in ketotic states. Cell Metab 2007;5:426–37.
74. Lundåsen T, Hunt MC, Nilsson LM, Sanyal S, Angelin B, Alexson SE, Rudling M. PPARα is a key regulator of hepatic FGF21. Biochem Biophys Res Commun 2007;360:437–40.
75. Kim H, Mendez R, Zheng Z, Chang L, Cai J, Zhang R, Zhang K. Liver-enriched transcription factor CREBH interacts with peroxisome proliferator-activated receptor a to regulate metabolic hormone FGF21. Endocrinology 2014;155:769–82.
76. Lee JH, Giannikopoulos P, Duncan SA, Wang J, Johansen CT, Brown JD, Plutzky J, Hegele RA, Glimcher LH, Lee AH. The transcription factor cyclic AMP-responsive element-binding protein H regulates triglyceride metabolism. Nat Med 2011;17:812–5.
77. Uebanso T, Taketani Y, Yamamoto H, Amo K, Ominami H, Arai H, Takei Y, Masuda M, Tanimura A, Harada N, Yamanaka-Okumura H, Takeda E. Paradoxical regulation of human FGF21 by both fasting and feeding signals: is FGF21 a nutritional adaptation factor? PLoS One 2011;6:e22976.
78. Li Y, Wong K, Walsh K, Gao B, Zang M. Retinoic acid receptor β stimulates hepatic induction of fibroblast growth factor 21 to promote fatty acid oxidation and control whole-body energy homeostasis in mice. J Biol Chem 2013;288:10490–504.
79. Wang Y, Solt LA, Burris TP. Regulation of FGF21 expression and secretion by retinoic acid receptor-related orphan receptor alpha. J Biol Chem 2010;285:15668–73.
80. Adams AC, Astapova I, Fisher FM, Badman MK, Kurgansky KE, Flier JS, Hollenberg AN, Maratos-Flier E. Thyroid hormone regulates hepatic expression of fibroblast growth factor 21 in a PPARalpha-dependent manner. J Biol Chem 2010;285:14078–82.
81. De Sousa-Coelho AL, Marrero PF, Haro D. Activating transcription factor 4 dependent induction of FGF21 during amino acid deprivation. Biochem J 2012;443:165–71.
82. Cyphert HA, Ge X, Kohan AB, Salati LM, Zhang Y, Hillgartner FB. Activation of the farnesoid X receptor induces hepatic expression and secretion of fibroblast growth factor 21. J Biol Chem 2012;287:25123–38.
83. Iizuka K, Takeda J, Horikawa Y. Glucose induces FGF21 mRNA expression through ChREBP activation in rat hepatocytes. FEBS Lett 2009;583:2882–6.
84. Sánchez J, Palou A, Picó C. Response to carbohydrate and fat refeeding in the expression of genes involved in nutrient partitioning and metabolism: striking effects on fibroblast growth factor-21 induction. Endocrinology 2009;150:5341–50.
85. Hao L, Huang KH, Ito K, Sae-Tan S, Lambert JD, Ross AC. Fibroblast growth factor 21 (Fgf21) gene expression is elevated in the liver of mice fed a high-carbohydrate liquid diet and attenuated by a lipid emulsion but is not upregulated in the liver of mice fed a high-fat obesogenic diet. J Nutr 2016;146:184–90.
86. Ma L, Robinson LN, Towle HC. ChREBP*Mlx is the principal mediator of glucose-induced gene expression in the liver. J Biol Chem 2006;281:28721–30.
87. Dushay JR, Toschi E, Mitten EK, Fisher FM, Herman MA, Maratos-Flier E. Fructose ingestion acutely stimulates circulating FGF21 levels in humans. Mol Metab 2015;4:51–7.
88. Wang ZQ, Yu Y, Zhang XH, Elizabeth Floyd Z, Boudreau A, Lian K, Cefalu WT. Comparing the effects of nano-sized sugarcane fiber with cellulose and psyllium on hepatic cellular signaling in mice. Int J Nanomedicine 2012;7:2999–3012.
89. Villarroya J, Flachs P, Redondo-Angulo I, Giralt M, Medrikova D, Villarroya F, Kopecky J, Planavila A. Fibroblast growth factor-21 and the beneficial effects of long-chain n-3 polyunsaturated fatty acids. Lipids 2014;49:1081–9.

90. Mai K, Andres J, Biedasek K, Weicht J, Bobbert T, Sabath M, Meinus S, Reinecke F, Möhlig M, Weickert MO, Clemenz M, Pfeiffer AF, Kintscher U, Spuler S, Spranger J. Free fatty acids link metabolism and regulation of the insulin-sensitizing fibroblast growth factor-21. Diabetes 2009;58:1532–8.
91. Yu J, Yu B, Jiang H, Chen D. Conjugated linoleic acid induces hepatic expression of fibroblast growth factor 21 through PPAR-α. Br J Nutr 2011;107:461–5.
92. Li H, Gao Z, Zhang J, Ye X, Xu A, Ye J, Jia W. Sodium butyrate stimulates expression of fibroblast growth factor 21 in liver by inhibition of histone deacetylase 3. Diabetes 2012;61:797–806.
93. Xia M, Erickson A, Yi X, Moreau R. Mapping the response of human fibroblast growth factor 21 (FGF21) promoter to serum availability and lipoic acid in HepG2 hepatoma cells. Biochim Biophys Acta 2016;1860:498–507.
94. Yi X, Pashaj A, Xia M, Moreau R. Reversal of obesity-induced hypertriglyceridemia by (R)-a-lipoic acid in ZDF (fa/fa) rats. Biochem Biophys Res Commun 2013;439:390–5.
95. Bae KH, Min AK, Kim JG, Lee IK, Park KG. Alpha lipoic acid induces hepatic fibroblast growth factor 21 expression via up-regulation of CREBH. Biochem Biophys Res Commun 2014;455:212–7.
96. Badman MK, Kennedy AR, Adams AC, Pissios P, Maratos-Flier E. A very low carbohydrate ketogenic diet improves glucose tolerance in ob/ob mice independently of weight loss. Am J Physiol Endocrinol Metab 2009;297:E1197–204.
97. Nygaard EB, Møller CL, Kievit P, Grove KL, Andersen B. Increased fibroblast growth factor 21 expression in high-fat diet-sensitive non-human primates (Macaca mulatta). Int J Obes 2014;38:183–91.
98. Fisher FM, Chui PC, Antonellis PJ, Bina HA, Kharitonenkov A, Flier JS, Maratos-Flier E. Obesity is a fibroblast growth factor 21 (FGF21)-resistant state. Diabetes 2010;59:2781–9.
99. McCarty MF. GCN2 and FGF21 are likely mediators of the protection from cancer, autoimmunity, obesity, and diabetes afforded by vegan diets. Med Hypotheses 2014;83:365–71.
100. Guo F, Cavener DR. The GCN2 eIF2alpha kinase regulates fatty-acid homeostasis in the liver during deprivation of an essential amino acid. Cell Metab 2007;5:103–14.
101. Cheng Y, Meng Q, Wang C, Li H, Huang Z, Chen S, Xiao F, Guo F. Leucine deprivation decreases fat mass by stimulation of lipolysis in white adipose tissue and upregulation of uncoupling protein 1 (UCP1) in brown adipose tissue. Diabetes 2010;59:17–25.
102. Ables GP, Perrone CE, Orentreich D, Orentreich N. Methionine-restricted C57BL/6J mice are resistant to diet-induced obesity and insulin resistance but have low bone density. PLoS One 2012;7:1–12.
103. Lees EK, Król E, Grant L, Shearer K, Wyse C, Moncur E, Bykowska AS, Mody N, Gettys TW, Delibegovic M. Methionine restriction restores a younger metabolic phenotype in adult mice with alterations in fibroblast growth factor 21. Aging Cell 2014;13:817–27.
104. Stone KP, Wanders D, Orgeron M, Cortez CC, Gettys TW. Mechanisms of increased in vivo insulin sensitivity by dietary methionine restriction in mice. Diabetes 2014;63:1–28.
105. Morrison CD, Laeger T. Protein-dependent regulation of feeding and metabolism. Trends Endocrinol Metab 2015;26:256–62.
106. Ozaki Y, Saito K, Nakazawa K, Konishi M, Itoh N, Hakuno F, Takahashi S, Kato H, Takenaka A. Rapid increase in fibroblast growth factor 21 in protein malnutrition and its impact on growth and lipid metabolism. Br J Nutr 2015;114:1410–8.
107. Bielohuby M, Menhofer D, Kirchner H, Stoehr BJM, Muller TD, Stock P, Hempel M, Stemmer K, Pfluger PT, Kienzle E, Christ B, Tschöp MH, Bidlingmaier M. Induction of ketosis in rats fed low-carbohydrate, high-fat diets depends on the relative abundance of dietary fat and protein. Am J Physiol Endocrinol Metab 2011;300:E65–76.
108. Jiang Y, Rose AJ, Sijmonsma TP, Bröer A, Pfenninger A, Herzig S, Schmoll D, Bröer S. Mice lacking neutral amino acid transporter B0AT1 (Slc6a19) have elevated levels of FGF21 and GLP-1 and improved glycaemic control. Mol Metab 2015;4:406–17.
109. Wilson GJ, Lennox BA, She P, Mirek ET, Al Baghdadi RJT, Fusakio ME, Dixon JL, Henderson GC, Wek RC, Anthony TG. GCN2 is required to increase fibroblast growth factor 21 and maintain hepatic triglyceride homeostasis during asparaginase treatment. Am J Physiol Endocrinol Metab 2015;308:E283–93.
110. Shimizu N, Maruyama T, Yoshikawa N, Matsumiya R, Ma Y, Ito N, Tasaka Y, Kuribara-Souta A, Miyata K, Oike Y, Berger S, Schütz G, Takeda S, Tanaka H. A muscle-liver-fat signalling axis is essential for central control of adaptive adipose remodelling. Nat Commun 2015;6:6693.
111. Qiu H, Dong J, Hu C, Francklyn CS, Hinnebusch AG. The tRNA-binding moiety in GCN2 contains a dimerization domain that interacts with the kinase domain and is required for tRNA binding and kinase activation. EMBO J 2001;20:1425–38.
112. Anthony TG, McDaniel BJ, Byerley RL, McGrath BC, Cavener DR, McNurlan MA, Wek RC. Preservation of liver protein synthesis during dietary leucine deprivation occurs at the expense of skeletal muscle mass in mice deleted for eIF2 kinase GCN2. J Biol Chem 2004;279:36553–61.
113. Harding HP, Zhang Y, Zeng H, Novoa I, Lu PD, Calfon M, Sadri N, Yun C, Popko B, Paules R, Stojdl DF, Bell JC, Hettmann T, Leiden JM, Ron D. An integrated stress response regulates amino acid metabolism and resistance to oxidative stress. Mol Cell 2003;11:619–33.
114. Shan J, Ord D, Ord T, Kilberg MS. Elevated ATF4 expression, in the absence of other signals, is sufficient for transcriptional induction via CCAAT enhancer-binding protein-activating transcription factor response elements. J Biol Chem 2009;284:21241–8.
115. Wan XS, Lu XH, Xiao YC, Lin Y, Zhu H, Ding T, Yang Y, Huang Y, Zhang Y, Liu YL, Xu ZM, Xiao J, Li XK. ATF4- and CHOP-dependent induction of FGF21 through endoplasmic reticulum stress. Biomed Res Int 2014;2014:807874.
116. Laplante M, Sabatini DM. Regulation of mTORC1 and its impact on gene expression at a glance. J Cell Sci 2013;126(Pt 8):1713–9.
117. Cornu M, Oppliger W, Albert V, Robitaille AM, Trapani F, Quagliata L, Fuhrer T, Sauer U, Terracciano L, Hall MN. Hepatic mTORC1 controls locomotor activity, body temperature, and lipid metabolism through FGF21. Proc Natl Acad Sci USA 2014;111:11592–9.
118. Monagas M, Urpi-Sarda M, Sánchez-Patán F, Llorach R, Garrido I, Gómez-Cordovés C, Andres-Lacueva C, Bartolomé B. Insights into the metabolism and microbial biotransformation of dietary flavan-3-ols and the bioactivity of their metabolites. Food Funct 2010;1:233–53.
119. Cardona F, Andrés-Lacueva C, Tulipani S, Tinahones FJ, Queipo-Ortuño MI. Benefits of polyphenols on gut micro-

biota and implications in human health. J Nutr Biochem 2013;24:1415–22.
120. Arranz S, Chiva-Blanch G, Valderas-Martínez P, Medina-Remón A, Lamuela-Raventós RM, Estruch R. Wine, beer, alcohol and polyphenols on cardiovascular disease and cancer. Nutrients 2012;4:759–81.
121. Dembinska-Kiec A, Mykkänen O, Kiec-Wilk B, Mykkänen H. Antioxidant phytochemicals against type 2 diabetes. Br J Nutr 2008;99E(Suppl):ES109–17.
122. Xiao JB, Högger P. Dietary polyphenols and type 2 diabetes: current insights and future perspectives. Curr Med Chem 2015;22:23–38.
123. Wang S, Moustaid-Moussa N, Chen L, Mo H, Shastri A, Su R, Bapat P, Kwun I, Shen CL. Novel insights of dietary polyphenols and obesity. J Nutr Biochem 2014;25:1–18.
124. Pan Q-R, Ren Y-L, Liu W-X, Hu Y-J, Zheng J-S, Xu Y, Wang G. Resveratrol prevents hepatic steatosis and endoplasmic reticulum stress and regulates the expression of genes involved in lipid metabolism, insulin resistance, and inflammation in rats. Nutr Res 2015;35:576–84.
125. Chen I-J, Liu C-Y, Chiu J-P, Hsu C-H. Therapeutic effect of high-dose green tea extract on weight reduction: a randomized, double-blind, placebo-controlled clinical trial. Clin Nutr 2016;35:592–9.
126. Ueno T, Torimura T, Nakamura T, Sivakumar R, Nakayama H, Otabe S, Yuan X, Yamada K, Hashimoto O, Inoue K, Koga H, Sata M. Epigallocatechin-3-gallate improves nonalcoholic steatohepatitis model mice expressing nuclear sterol regulatory element binding protein-1c in adipose tissue. Int J Mol Med 2009;24:17–22.
127. Kim M-H, Kang K-S, Lee Y-S. The inhibitory effect of genistein on hepatic steatosis is linked to visceral adipocyte metabolism in mice with diet-induced non-alcoholic fatty liver disease. Br J Nutr 2010;104:1333–42.
128. Park HJ, Jung UJ, Lee MK, Cho SJ, Jung HK, Hong JH, Park YB, Kim SR, Shim S, Jung J, Choi MS. Modulation of lipid metabolism by polyphenol-rich grape skin extract improves liver steatosis and adiposity in high fat fed mice. Mol Nutr Food Res 2013;57:360–4.
129. Murase T, Misawa K, Minegishi Y, Aoki M, Ominami H, Suzuki Y, Shibuya Y, Hase T. Coffee polyphenols suppress diet-induced body fat accumulation by downregulating SREBP-1c and related molecules in C57BL/6J mice. Am J Physiol Endocrinol Metab 2011;300:E122–33.
130. Zang M, Xu S, Maitland-Toolan KA, Zuccollo A, Hou X, Jiang B, Wierzbicki M, Verbeuren TJ, Cohen RA. Polyphenols stimulate AMP-activated protein kinase, lower lipids, and inhibit accelerated atherosclerosis in diabetic LDL receptor-deficient mice. Diabetes 2006;55:2180–91.
131. Hou X, Xu S, Maitland-Toolan KA, Sato K, Jiang B, Ido Y, Lan F, Walsh K, Wierzbicki M, Verbeuren TJ, Cohen RA, Zang M. SIRT1 regulates hepatocyte lipid metabolism through activating AMP-activated protein kinase. J Biol Chem 2008;283:20015–26.
132. Rodriguez-Ramiro I, Vauzour D, Minihane AM. Polyphenols and non-alcoholic fatty liver disease: impact and mechanisms. Proc Nutr Soc 2016;75:47–60.
133. Zhang T, Yamamoto N, Yamashita Y, Ashida H. The chalcones cardamonin and flavokawain B inhibit the differentiation of preadipocytes to adipocytes by activating ERK. Arch Biochem Biophys 2014;554:44–54.
134. Monika P, Geetha A. The modulating effect of Persea americana fruit extract on the level of expression of fatty acid synthase complex, lipoprotein lipase, fibroblast growth factor-21 and leptin – a biochemical study in rats subjected to experimental hyperlipidemia and obesit. Phytomedicine 2015;22:939–45.
135. Tian L, Zeng K, Shao W, Yang BB, Fantus IG, Weng J, Jin T. Short-term curcumin gavage sensitizes insulin signaling in dexamethasone-treated C57BL/6 mice. J Nutr 2015;145:2300–7.
136. Song H, Zheng Z, Wu J, Lai J, Chu Q, Zheng X. White pitaya (Hylocereus undatus) juice attenuates insulin resistance and hepatic steatosis in diet-induced obese mice. PLoS One 2016;11:e0149670.
137. Yu Y, Zhang XH, Ebersole B, Ribnicky D, Wang ZQ. Bitter melon extract attenuating hepatic steatosis may be mediated by FGF21 and AMPK/Sirt1 signaling in mice. Sci Rep 2013;3:3142.
138. Chen W-W, Li L, Yang G-Y, Li K, Qi X-Y, Zhu W, Tang Y, Liu H, Boden G. Circulating FGF-21 levels in normal subjects and in newly diagnose patients with Type 2 diabetes mellitus. Exp Clin Endocrinol Diabetes 2008;116:65–8.
139. Zhang X1, Yeung DC, Karpisek M, Stejskal D, Zhou ZG, Liu F, Wong RL, Chow WS, Tso AW, Lam KS, Xu A. Serum FGF21 levels are increased in obesity and are independently associated with the metabolic syndrome in humans. Diabetes 2008;57:1246–53.
140. Chavez AO, Molina-Carrion M, Abdul-Ghani MA, Folli F, DeFronzo RA, Tripathy D. Circulating fibroblast growth factor-21 is elevated in impaired glucose tolerance and type 2 diabetes and correlates with muscle and hepatic insulin resistance. Diabetes Care 2009;32:1542–6.
141. Reinehr T, Woelfle J, Wunsch R, Roth CL. Fibroblast growth factor 21 (FGF-21) and its relation to obesity, metabolic syndrome, and nonalcoholic fatty liver in children: a longitudinal analysis. J Clin Endocrinol Metab 2012;97:2143–50.
142. Reinehr T, Karges B, Meissner T, Wiegand S, Fritsch M, Holl RW, Woelfle J. Fibroblast growth factor 21 and fetuin-a in obese adolescents with and without type 2 diabetes. J Clin Endocrinol Metab 2015;100:3004–10.
143. Reinehr T, Roth CL, Woelfle J. Fibroblast growth factor 21 (FGF-21) in obese children: no relationship to growth, IGF-1, and IGFBP-3. Horm Mol Biol Clin Investig 2016 [Epub ahead of print].
144. Hanks LJ, Casazza K, Ashraf AP, Wallace S, Gutiérrez OM. Fibroblast growth factor-21, body composition, and insulin resistance in pre-pubertal and early pubertal males and females. Clin Endocrinol 2015;82:550–6.
145. Li H, Fang Q, Gao F, Fan J, Zhou J, Wang X, Zhang H, Pan X, Bao Y, Xiang K, Xu A, Jia W. Fibroblast growth factor 21 levels are increased in nonalcoholic fatty liver disease patients and are correlated with hepatic triglyceride. J Hepatol 2010;53:934–40.
146. Davis RL, Liang C, Edema-Hildebrand F, Riley C, Needham M, Sue CM. Fibroblast growth factor 21 is a sensitive biomarker of mitochondrial disease. Neurology 2013;81:1819–26.
147. Kralisch S, Tönjes A, Krause K, Richter J, Lossner U, Kovacs P, Ebert T, Blüher M, Stumvoll M, Fasshauer M. Fibroblast growth factor-21 serum concentrations are associated with metabolic and hepatic markers in humans. J Endocrinol 2013;216:135–43.
148. Hanks LJ, Gutiérrez OM, Bamman MM, Ashraf A, McCormick KL, Casazza K. Circulating levels of fibroblast growth factor-21 increase with age independently of body

composition indices among healthy individuals. J Clin Transl Endocrinol 2015;2:72–82.
149. Gälman C, Lundåsen T, Kharitonenkov A, Bina HA, Eriksson M, Hafström I, Dahlin M, Amark P, Angelin B, Rudling M. The circulating metabolic regulator FGF21 is induced by prolonged fasting and PPARα activation in man. Cell Metab 2008;8:169–74.
150. Christodoulides C, Dyson P, Sprecher D, Tsintzas K, Karpe F. Circulating fibroblast growth factor 21 is induced by peroxisome proliferator-activated receptor agonists but not ketosis in man. J Clin Endocrinol Metab 2009;94:3594–601.
151. Fazeli PK, Lun M, Kim SM, Bredella MA, Wright S, Zhang Y, Lee H, Catana C, Klibanski A, Patwari P, Steinhauser ML. FGF21 and the late adaptive response to starvation in humans. J Clin Invest 2015;125:4601–11.
152. Qin Y, Zhou Y, Chen SH, Zhao XL, Ran L, Zeng XL, Wu Y, Chen JL, Kang C, Shu FR, Zhang QY, Mi MT. Fish oil supplements lower serum lipids and glucose in correlation with a reduction in plasma fibroblast growth factor 21 and prostaglandin E2 in nonalcoholic fatty liver disease associated with hyperlipidemia: a randomized clinical trial. PLoS One 2015;10:1–13.
153. Ejaz A, Martinez-Guino L, Goldfine AB, Ribas-Aulinas F, De Nigris V, Ribó S, Gonzalez-Franquesa A, Garcia-Roves PM, Li E, Dreyfuss JM, Gall W, Kim JK, Bottiglieri T, Villarroya F, Gerszten RE, Patti ME, Lerin C. Dietary betaine supplementation increases Fgf21 levels to improve glucose homeostasis and reduce hepatic lipid accumulation in mice. Diabetes 2016;65:902–12.
154. Habegger KM, Stemmer K, Cheng C, Müller TD, Heppner KM, Ottaway N, Holland J, Hembree JL, Smiley D, Gelfanov V, Krishna R, Arafat AM, Konkar A, Belli S, Kapps M, Woods SC, Hofmann SM, D'Alessio D, Pfluger PT, Perez-Tilve D, Seeley RJ, Konishi M, Itoh N, Kharitonenkov A, Spranger J, DiMarchi RD, Tschöp MH. Fibroblast growth factor 21 mediates specific glucagon actions. Diabetes 2013;62:1453–63.

ANNEX 4: FGF21 mediates the lipid metabolism response to amino acid starvation. (Article 1)

FGF21 mediates the lipid metabolism response to amino acid starvation

Ana Luísa De Sousa-Coelho,[*,†] Joana Relat,[*,†] Elayne Hondares,[†,§] Albert Pérez-Martí,[*,†] Francesc Ribas,[†,§] Francesc Villarroya,[†,§] Pedro F. Marrero,[*,†] and Diego Haro[1,*,†]

Departament de Bioquímica i Biologia Molecular,* Facultat de Farmàcia, Universitat de Barcelona, 08028 Barcelona, Spain; Institut de Biomedicina de la Universitat de Barcelona (IBUB),† 08028 Barcelona, Spain; and Departament de Bioquímica i Biologia Molecular,§ Facultat de Biologia, Universitat de Barcelona and CIBER Fisiopatología de la Obesidad y Nutrición, 08028 Barcelona, Spain

Abstract Lipogenic gene expression in liver is repressed in mice upon leucine deprivation. The hormone fibroblast growth factor 21 (FGF21), which is critical to the adaptive metabolic response to starvation, is also induced under amino acid deprivation. Upon leucine deprivation, we found that FGF21 is needed to repress expression of lipogenic genes in liver and white adipose tissue, and stimulate phosphorylation of hormone-sensitive lipase in white adipose tissue. The increased expression of *Ucp1* in brown adipose tissue under these circumstances is also impaired in FGF21-deficient mice. Our results demonstrate the important role of FGF21 in the regulation of lipid metabolism during amino acid starvation.—De Sousa-Coelho, A. L., J. Relat, E. Hondares, A. Pérez-Martí, F. Ribas, F. Villarroya, P. F. Marrero, and D. Haro. **FGF21 mediates the lipid metabolism response to amino acid starvation. *J. Lipid Res*. 2013.** 54: **1786–1797.**

Supplementary key words brown adipose tissue • fibroblast growth factor 21 • leucine deprivation • liver • white adipose tissue

Amino acid starvation initiates a signal transduction cascade, starting with the activation of the general control nonderepressible 2 (GCN2) kinase, phosphorylation of eukaryotic initiation factor 2 (eIF2), and increased synthesis of activating transcription factor 4 (ATF4) (1). We have recently found that fibroblast growth factor 21 (*Fgf21*) is a target gene for ATF4. Consequently, FGF21 is induced by amino acid deprivation both in mouse liver and HepG2 cells as part of the transcriptional program initiated by increased levels of ATF4 (2).

FGF21 is a member of the FGF family with endocrine properties. It is predominantly produced by the liver, but is also produced by other tissues such as white adipose tissue (WAT), brown adipose tissue (BAT), skeletal muscle, and pancreas (3–6). FGF21 expression in liver is under tight control by peroxisome proliferator-activated receptor (PPAR) α (7–10). It is induced in the liver during fasting and its expression induces a metabolic state that mimics long-term fasting. Thus, FGF21 is critical for the induction of hepatic fat oxidation, ketogenesis, and gluconeogenesis, which are metabolic processes critical for the adaptive metabolic response to starvation (11). *Fgf21* is also a target of the liver X receptor that represses its induction during fasting (12, 13). Significantly, FGF21 extends life span in transgenic mice to a similar extent as dietary restriction (14).

A dietary amino acid imbalance alters metabolic pathways beyond protein homeostasis. GCN2-dependent inhibition of fatty acid synthase (FASN) activity, expression of lipogenic genes in liver, and increased mobilization of lipid stores occur in response to leucine deprivation in mice (15). In addition, the following have been observed: increased expression of β-oxidation genes, decreased expression of lipogenic genes and activation of FASN in WAT, and increased expression of uncoupling protein 1 (*Ucp1*) in BAT (16, 17).

This work was supported by the Ministerio de Educación y Ciencia (SAF2010-15217 to D.H. and SAF2011-23636 to F.V.) and the Ajut de Suport als Grups de Recerca de Catalunya (2009 SGR163). A.L.D.S-C. was supported by Fundação para a Ciência e a Tecnologia (FCT) from Portuguese Government.

Manuscript received 18 October 2012 and in revised form 6 May 2013.

Published, JLR Papers in Press, May 9, 2013
DOI 10.1194/jlr.M033415

Abbreviations: ACC1, acetyl-CoA carboxylase 1; β3AR, β3-adrenergenic receptor; ASNS, asparagine synthetase; ATF4, activating transcription factor 4; Atgl, adipose triglyceride lipase; BAT, brown adipose tissue; Cd36; cluster of differentiation 36; Cpt1a, carnitine palmitoyltransferase 1a; Ctl, control; DIO, diet-induced obesity; Dio2, type 2 deiodinase; eIF2, eukaryotic initiation factor 2; eWAT, epididymal white adipose tissue; Fabp4, fatty acid binding protein 4; FASN, fatty acid synthase; FGF21, fibroblast growth factor 21; FGFR1, fibroblast growth factor receptor 1; GCN2, general control nonderepressible 2; H and E, hematoxylin and eosin; HSL, hormone-sensitive lipase; KO, knockout; (−)leu, leucine-deficient; MAPK, mitogen-activated protein kinase; MEK, mitogen-activated protein/ERK kinase; PGC1, peroxisome proliferator-activated receptor γ coactivator 1; Plin1, perilipin 1; PPAR, peroxisome proliferator-activated receptor; qRT-PCR, quantitative RT-PCR; SREBP1c, sterol regulatory element binding protein 1c; Ucp1, uncoupling protein 1; WAT, white adipose tissue; WT, wild-type.

[1]To whom correspondence should be addressed.
e-mail: dharo@ub.edu.

The coincidence between the metabolic response to essential amino acid deprivation and to FGF21, the induction of *Fgf21* under amino acid deprivation (2), together with the repression of the transcription and maturation of sterol regulatory element binding protein 1c (SREBP1c) induced by FGF21 in HepG2 cells (18), led us to consider that FGF21 could be an important mediator between amino acid deprivation and lipid metabolism in liver, WAT, and BAT.

To investigate this hypothesis, we examined the response of FGF21-deficient mice to deprivation of the essential amino acid leucine. As expected, we found a huge increase in *Fgf21* expression in the liver of wild-type (WT) animals, along with a repression of lipogenic genes after 7 days of leucine deprivation. In this condition, FGF21-deficient mice developed liver steatosis caused by unrepressed expression of lipogenic genes. In WAT, the expression of lipogenic genes was also repressed and the phosphorylation of hormone-sensitive lipase (HSL) was increased under leucine deprivation. The absence of leucine also induced an increase in the expression of *Ucp1* and type 2 deiodinase (*Dio2*) in BAT. We found that all these effects in WAT and BAT were also impaired in FGF21-deficient mice. Here, we show the involvement of FGF21 in the regulation of lipid metabolism during amino acid starvation, thus reinforcing its important role as an endocrine factor in coordinating energy homeostasis under a variety of nutritional conditions.

MATERIALS AND METHODS

Animals and diets

Male WT and *Fgf21*-null mice (B6N; 129 S5-Fgf21tm1Lex/Mmucd), obtained from the Mutant Mouse Regional Resource Center, were housed in a temperature-controlled room (22 ± 1°C) on a 12/12 h light/dark cycle and were provided free access to commercial rodent chow and tap water prior to the experiments. Control (nutritionally complete amino acid) and leucine-deficient [(−)leu] diets were obtained from Research Diets, Inc. (New Brunswick, NJ). All diets were isocaloric and compositionally the same in terms of carbohydrate and lipid components. At the beginning of the feeding experiment, 12–15 week old male mice were first acclimated to the control diet for 7 days, and then randomly assigned to either the control diet group, with continued free access to the nutritionally complete diet, or the (−)leu diet group, with free access to the diet devoid of the essential amino acid leucine for 7 days. Food intake and body weight were recorded at least every 2 days. Animals were anesthetized by isoflurane inhalation, and blood was collected from the heart for the assay described below. After euthanization, tissues were isolated and immediately snap-frozen and stored at −80°C for future analysis. The Animal Ethics Committee of the University of Barcelona approved these experiments.

Cell culture and treatment conditions

HepG2 cells were cultured in Eagle's Minimal Essential Medium (MEM) (GIBCO, Invitrogen) supplemented to contain 1× nonessential amino acids, 4 mM glutamine, 100 μg/ml streptomycin sulfate, 100 units/ml penicillin G, and 10% (v/v) fetal bovine serum. Cells were maintained at 37°C in a 5% CO_2/95% air incubator, and cultures were replenished with fresh MEM medium and serum for approximately 16 h prior to initiating all treatments to ensure that the cells were in the basal ("fed") state. Amino acid deprivation was induced by transfer of cells to culture medium containing 2 mM histidinol (HisOH) for 8 h, which blocks charging of histidine onto the corresponding tRNA and thus mimics histidine deprivation and triggers activation of the AAR cascade (19). For mitogen-activated protein/ERK kinase (MEK) inhibition, the direct upstream kinases of ERK1/2, cells were treated with 30 μM PD98059 (PD98) for approximately 16 h before harvesting. HisOH (H6647) and PD98059 (P215) were purchased from Sigma-Aldrich (St. Louis, MO). Primary BAT adipocytes were obtained and maintained as previously described (20). Mouse 3T3-L1 adipocytes were cultured and differentiated as described previously (21).

Serum measurements. Serum was obtained by centrifugation of clotted blood and stored at −80°C. A mouse FGF21 enzyme-linked immunosorbent assay (ELISA) kit was obtained from Millipore for the quantification of FGF21 in mouse serum. The assay was conducted according to the manufacturer's protocol. Briefly, a calibration curve was constructed by plotting the difference in absorbance values at 450 and 590 nm versus the FGF21 concentrations of the calibrators, and concentrations of unknown samples (performed in duplicate) were determined using this calibration curve (22). The Veterinary Service of Clinical Biochemistry at the Universitat Autònoma de Barcelona determined blood biochemical parameters.

RNA isolation and relative quantitative RT-PCR. Total RNA was extracted from the frozen tissues [liver, epididymal white adipose tissue (eWAT), and BAT] or cells (3T3L1 and primary brown adipocytes) using TRI reagent solution (Ambion) followed by DNase I treatment (Ambion) to eliminate genomic DNA contamination. To measure the relative mRNA levels, quantitative (q)RT-PCR was performed using TaqMan reagents. cDNA was synthesized from 1 μg of total RNA by MLV reverse transcriptase (Invitrogen) with random hexamers (Roche Diagnostics) according to the manufacturer's instructions. TaqMan Gene Expression Master Mix and TaqMan Gene Expression assays (Invitrogen/Applied Biosystems) were used for the PCR step. Amplification and detection were performed using the Step-One Plus Real-Time PCR System. Each mRNA from a single sample was measured in duplicate, using 18S rRNA as an internal control. Results were obtained by the comparative threshold cycle (Ct) method and expressed as fold of the experimental control.

Protein extract preparation. Whole-cell lysates from HepG2 cells were isolated using NP40 lysis buffer [50 mM Tris-HCl (pH 8), 150 mM NaCl, 1% Nonidet P-40]. To obtain liver nuclear extracts, frozen liver was triturated within a mortar in liquid nitrogen and immediately homogenized with a Dounce homogenizer in 1 ml of HB buffer [15 mM Tris-HCl (pH 8), 15 mM NaCl, 60 mM KCl, 0.5 mM EDTA], and centrifuged at 800 *g* for 5 min. The resulting pellet was resuspended in 100 μl of HB buffer supplemented with 0.05% Triton X-100 (Sigma), and centrifuged for 10 min at 1,000 *g*. Nuclear pellets were washed with 1 ml of HB buffer supplemented with 0.05% Triton X-100 and 1 ml of HB buffer. Nuclei were incubated at 4°C for 30 min in 50 μl of HB buffer containing 360 mM KCl and centrifuged for 5 min at 10,000 *g*. The supernatant corresponding to the nuclear extract was collected, frozen, and stored at −80°C. To obtain liver, WAT, and BAT total extracts, tissues were homogenized in RIPA buffer and centrifuged at 12,000 *g* for 15 min at 4°C. The supernatant was collected and frozen at −80°C until analysis. Protein concentration was assayed using Bio-Rad reagent. All of the buffers were

supplemented with a mixture of protease inhibitors (Sigma-Aldrich), 0.1 mM phenylmethylsulfonyl fluoride (PMSF), and a phosphatase inhibitor cocktail (IPC3, Sigma-Aldrich).

Immunoblotting. Total and nuclear proteins were resolved by SDS-polyacrylamide gel electrophoresis and transferred onto a Hybond-P PVDF membrane (Millipore). Membranes were blocked for 1 h at room temperature. The blots were then incubated with primary antibody in blocking solution overnight at 4°C. Antibodies were diluted according to the manufacturer's instructions. The blots were washed three times and incubated with horseradish peroxidase-conjugated secondary antibody in blocking buffer for 2 h at room temperature. After three washes, the blots were developed using the EZ-ECL Chemiluminescence Detection Kit for HRP (Biological Industries). The quantification of phosphorylation was performed by densitometry of phosphorylated protein normalized to total protein using Image J software.

Antibodies. HSL (#4107), phospho HSL (#4126), ERK1/2 (#4695), phospho-ERK1/2 (#4370), and phospho-p38 (#9211) antibodies were purchased from Cell Signaling Technology. ATF4 (sc-200), p38α/β (A-12, sc-7972), and SREBP1c (C-20, sc-36) antibodies were from Santa Cruz Biotechnology, Inc. (Santa Cruz, CA); FASN (ab128870) antibody was from Abcam; acetyl-CoA carboxylase 1 (ACC1) (04-322) and phospho-ACC1 (07-303) antibodies were from Millipore; actin antibody (A2066) was from Sigma-Aldrich; and tubulin antibody (#CP06) was from Calbiochem.

Histological examinations. For the histological analysis, tissues (liver and eWAT) were fixed in 10% formalin (Sigma-Aldrich) and embedded in paraffin. Then, 4 μm thick sections were cut and stained with hematoxylin and eosin (H and E). Images were acquired using a Leica CTR 4000 microscope. Quantitative data were obtained using the IMAT program developed in the Science and Technology Center of the University of Barcelona. The selection of the test objects was performed according to color and choosing the same limits for binarization for all images. Adipocyte size and lipid accumulation were measured using at least three different randomly chosen fields of eWAT and liver sections, respectively, from each mouse.

Lipolysis assay. Lipolysis assay was performed after 24 h treatment with FGF21 using the Free Glycerol Determination Kit (Sigma).

Data analysis/statistics. All data are expressed as means ± SEM. Significant differences were assessed by a two-tailed Student's *t*-test. $P < 0.05$ was considered statistically significant. *a*, $P < 0.05$ versus control (Ctl) WT mice (or DMSO-treated HepG2 cells); *b*, $P < 0.05$ versus Ctl *Fgf21*-knockout (KO) mice; *c*, $P < 0.05$ versus (−)leu WT (or HisOH-treated HepG2 cells) (n = 6 per group of mice, or at least three independent experiments with HepG2 cells).

RESULTS

FGF21 gene expression is induced by leucine deprivation specifically in liver but not in BAT or WAT

According to our previously reported results (2), mice maintained on a (−)leu diet show a dramatic increase in FGF21 circulating levels (**Fig. 1A**). To check the origin of this circulating FGF21 we analyzed *Fgf21* gene expression in several tissues. Consistent with the liver as the main site of FGF21 production and release into the blood, *Fgf21* mRNA levels in liver paralleled those in serum, whereas mRNA levels were unchanged in BAT and, unexpectedly, significantly decreased in eWAT in WT mice maintained on a (−)leu diet (Fig. 1B). As expected, *Fgf21* mRNA levels were undetectable in any analyzed tissue in the *Fgf21*-KO mice. In accordance with previous reports (23), the circulating levels of FGF21 in KO mice were below the threshold for correct quantification.

FGF21 deficiency significantly attenuates weight loss under leucine deprivation

When fed a leucine-deprived diet, mice undergo rapid weight loss (16). The goal of the present study is to investigate whether this phenomenon is FGF21 dependent. For this purpose, WT and *Fgf21*-KO mice were fed a control or (−)leu diet for 7 days. Together with total body weight

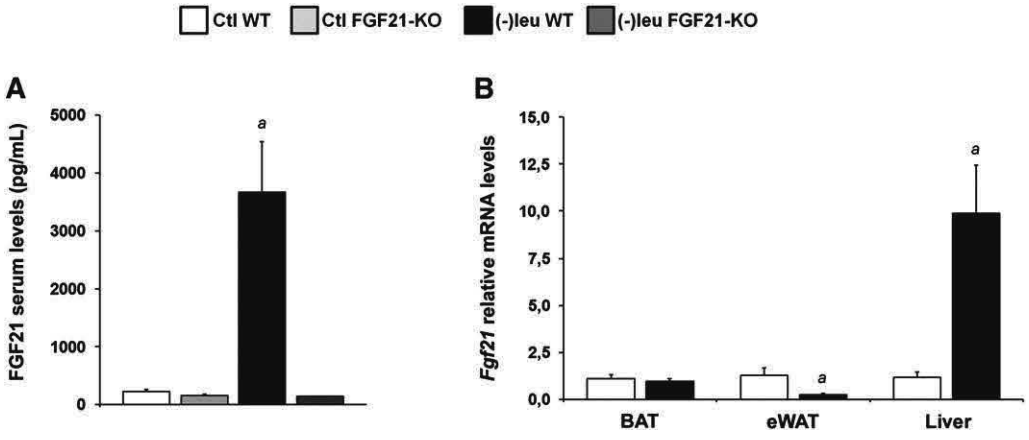

Fig. 1. FGF21 is differently regulated by leucine deprivation in liver and adipose tissues. A: Serum FGF21 protein concentrations were measured by ELISA. B: *Fgf21* mRNA in BAT, eWAT, and liver was measured by qRT-PCR. Error bars represent the mean ± SEM. *a*, $P < 0.05$ versus Ctl WT.

loss (**Figs. 2A, B**), mice fed a leucine-deprived diet undergo a fat mass loss, both epididymal and subcutaneous (Fig. 2D). We found that these effects were partially blunted in *Fgf21*-KO mice (Figs. 2A, B, D), while the reduction in food intake caused by leucine deprivation (~30%) was unchanged between genotypes (Fig. 2C).

The reported observation that white adipocytes from FGF21 transgenic mice are substantially smaller than those from WT mice (8, 24) and that leucine deprivation decreased adipocyte volume (16), led us to examine whether this effect was FGF21 dependent. A histological analysis of eWAT (**Fig. 3A**) showed that leucine deprivation resulted in a reduction in adipocyte volume compared with mice fed a control diet. By contrast, the adipocyte volume was only slightly reduced in (−)leu-fed *Fgf21*-KO mice and remained unchanged in *Fgf21*-KO mice on the control diet (Fig. 3A). We note that other groups reported increased (25) or decreased (26) adipocyte size in *Fgf21*-KO mice on regular diets. We have no explanation for these discrepancies beyond potential minor differences in the composition of the diet.

Increased phosphorylation of HSL under leucine deprivation is FGF21 dependent

It has been previously described that leucine deprivation increases lipolysis in WAT (16). It has also been suggested that FGF21 stimulates lipolysis in WAT during normal feeding, but inhibits it during fasting (25). Therefore, to examine the role of FGF21 in lipolysis, we evaluated the mRNA levels of adipose triglyceride lipase (*Atgl*), *Hsl*, and perilipin 1 (*Plin1*), and the levels of phosphorylated HSL. We did not find any statistically significant changes in *Atgl*, *Hsl*, or *Plin1* mRNA levels upon leucine deprivation (Fig. 3B). Consistent with changes in body weight, lack of FGF21 significantly decreased levels of phosphorylated HSL in WAT under leucine deprivation (Fig. 3C), which suggests that lipolysis was impaired in these mice. Despite the evidence of increased lipolysis under leucine deprivation, levels of free fatty acids in serum were not significantly altered in the conditions analyzed (**Table 1**), suggesting increased fatty acid utilization by other tissues.

FGF21 deficiency prevents changes in liver and WAT in leucine-deprived mice

A link between FGF21 and SREBP1c during lipogenesis in cultured hepatocytes has recently been proposed (18). As lipogenic genes are downregulated in the liver of mice deprived of leucine (15), we speculated that FGF21 might regulate their expression. To investigate this possibility, we examined the expression of genes involved in the regulation of lipid metabolism in the liver

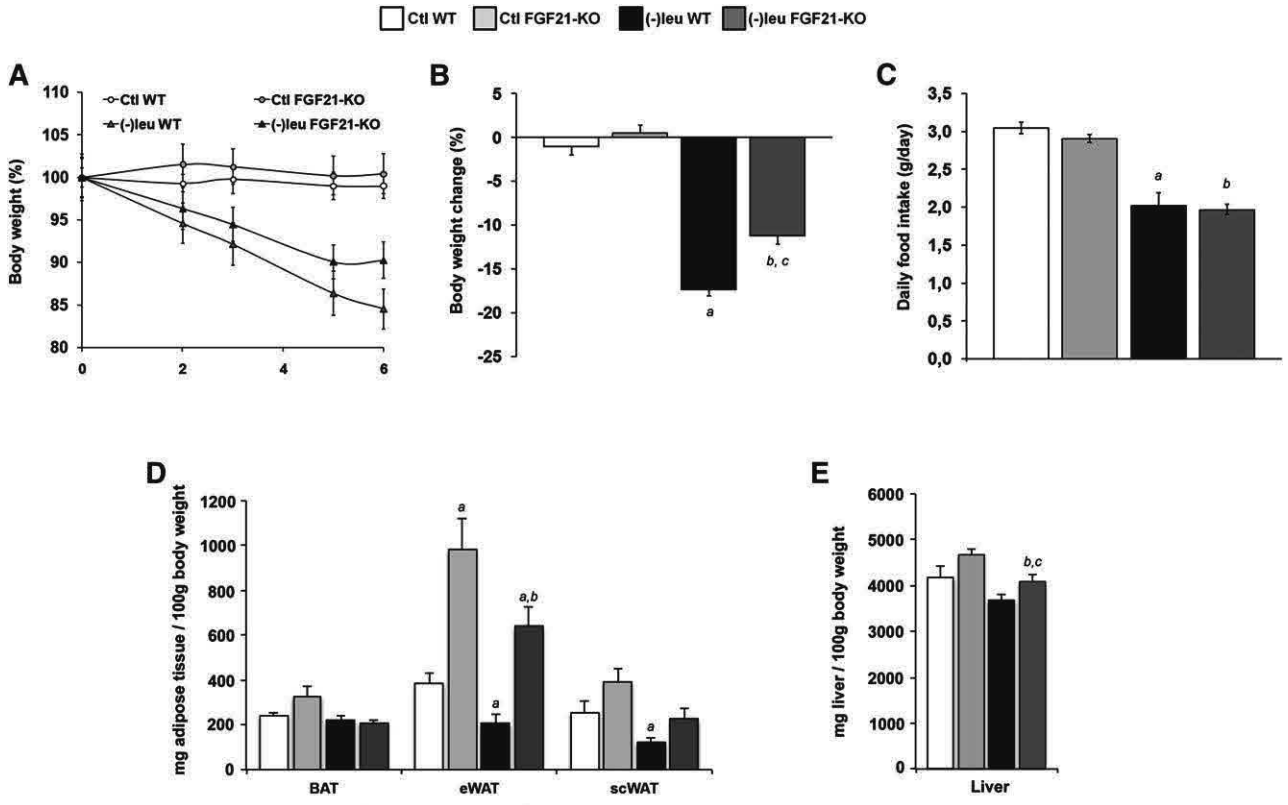

Fig. 2. FGF21 is required for (−)leu diet effects on body weight without affecting food consumption. A: Body weight of mice fed with Ctl or (−)leu diet. The weight on the first day was considered 100%. B: Body weight change (%) after 7 days of feeding the Ctl or (−)leu diet. C: Daily food intake. D: BAT, eWAT, and scWAT weight of mice fed with Ctl or (−)leu diet related to 100 mg of body weight. E: Liver weight of mice fed with Ctl or (−)leu diet related to 100 mg of body weight. Error bars represent the mean ± SEM. *a*, $P < 0.05$ versus Ctl WT mice; *b*, $P < 0.05$ versus Ctl FGF21-KO mice; *c*, $P < 0.05$ versus (−)leu WT mice (n = 6/group).

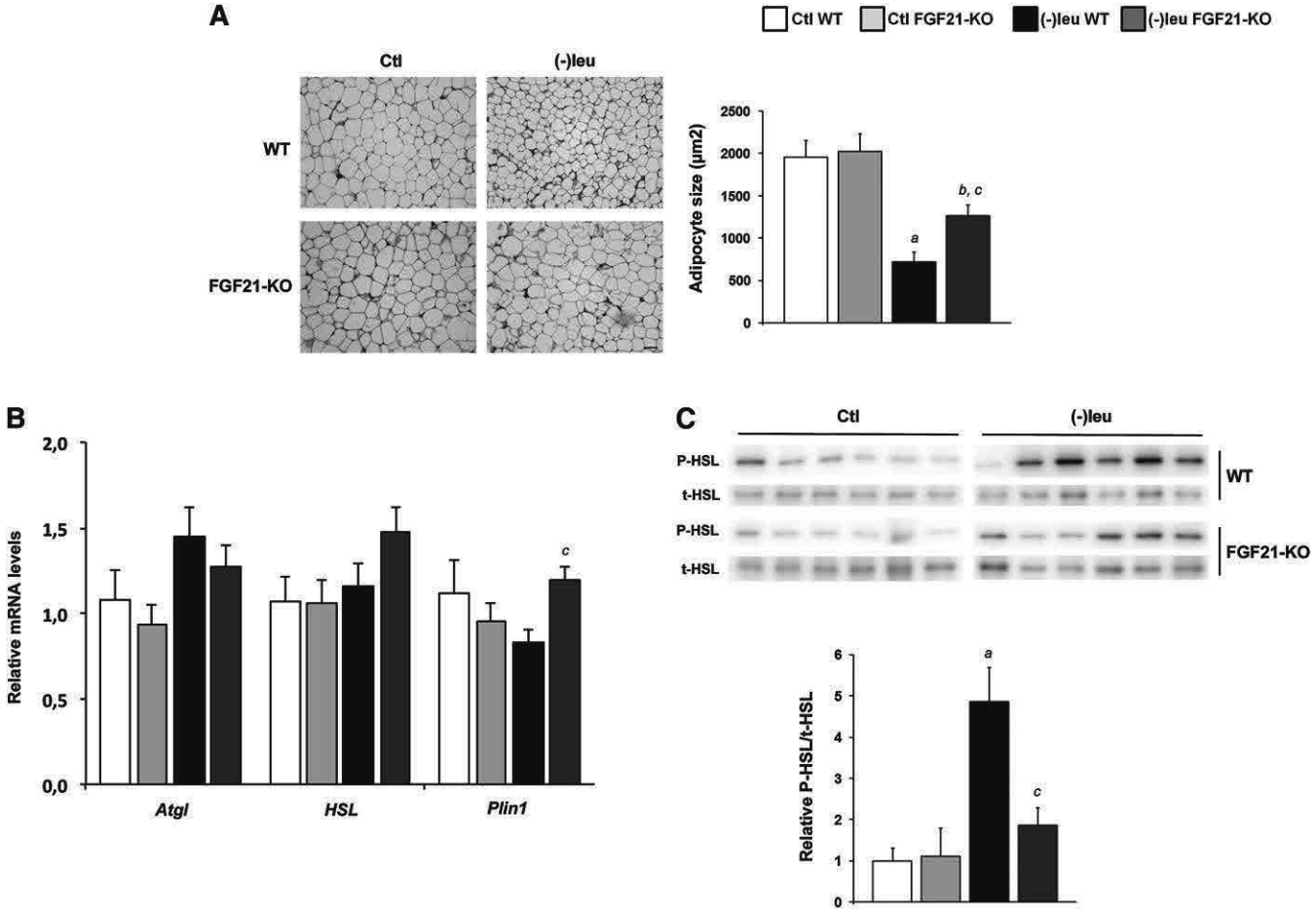

Fig. 3. The (−)leu diet effects on adipocyte size and lipid metabolism in WAT are FGF21 dependent. A: Representative H and E-stained eWAT sections from WT and FGF21-KO mice (×20 magnification). Scale bar, 50 µM. Adipocyte size (right panel) was measured as described in Materials and Methods, using at least three different randomly chosen fields of eWAT sections from each mouse. B: *Atgl*, *Hsl*, and *Plin1* gene expression was measured by qRT-PCR in mouse eWAT. C: Phosphorylated HSL (P-HSL) and total HSL (t-HSL) protein levels were measured in WT and FGF21-KO eWAT homogenates by Western blot analysis. The bottom panel shows quantification by densitometry of phosphorylated HSL normalized to total HSL using Image J software. Error bars represent the mean ± SEM. *a*, $P < 0.05$ versus Ctl WT mice; *b*, $P < 0.05$ versus Ctl FGF21-KO mice; *c*, $P < 0.05$ versus (−)leu WT mice (n = 6/group). P-HSL, phosphorylated HSL.

of WT and *Fgf21*-KO mice maintained either on the control or (−)leu diet. As expected, levels of *Fasn*, *Srebp1c*, and *Acc1* mRNA were significantly decreased on the (−) leu diet. However, in mice lacking FGF21, the reduced expression of *Fasn* was statistically significantly increased, and, although not statistically significant, showed a tendency to increase in both *Srebp1c* and *Acc1* (**Fig. 4A**). The expression of other genes involved in fatty acid uptake [cluster of differentiation 36 (*Cd36*) and fatty acid binding protein 4 (*Fabp4*)] or oxidation [carnitine palmitoyltransferase 1a (*Cpt1a*)] was decreased in the absence of *Fgf21*. The analysis of FASN, SREBP1c, and ACC1 protein abundance showed a good correlation with the gene expression data (Fig. 4B). By contrast ACC1 phosphorylation was decreased under leucine deprivation in both WT and *Fgf21*-KO mice.

TABLE 1. Serum measurements in mice maintained on different diets

	WT Ctl	FGF21-KO Ctl	WT leu(−)	FGF21-KO leu(−)
NEFA (nmol/l)	0.79 ± 0.11	1.05 ± 0.11	0.73 ± 0.09	0.82 ± 0.06
TG (mg/dl)	95.79 ± 7.18	153.73 ± 11.62[a]	99.39 ± 15.36	186.08 ± 27.38[a,c]
Cholesterol (mg/dl)	101.13 ± 13,13	147.65 ± 4.21[a]	96.40 ± 7.69	122.55 ± 3.08[b,c]
Glucose (mg/dl)	209.43 ± 10.45	212.90 ± 7.88	185.53 ± 14.87	187.02 ± 9.55
Glycerol (µmol/l)	393.50 ± 38.32	520.95 ± 23.10[a]	313.93 ± 26.56	372.16 ± 19.99[b]
Insulin (µg/l)	1.26 ± 0.23	2.01 ± 0.52	0.41 ± 0.04[a]	1.21 ± 0.20[c]

All data are expressed as means ± SEM. Significant differences were assessed by a two-tailed Student's *t*-test. $P < 0.05$ was considered statistically significant. n = 6/group of mice. TG, triglycerides.

[a] $P < 0.05$ versus Ctl WT mice.

[b] $P < 0.05$ versus Ctl FGF21-KO mice.

[c] $P < 0.05$ versus (−)leu WT mice.

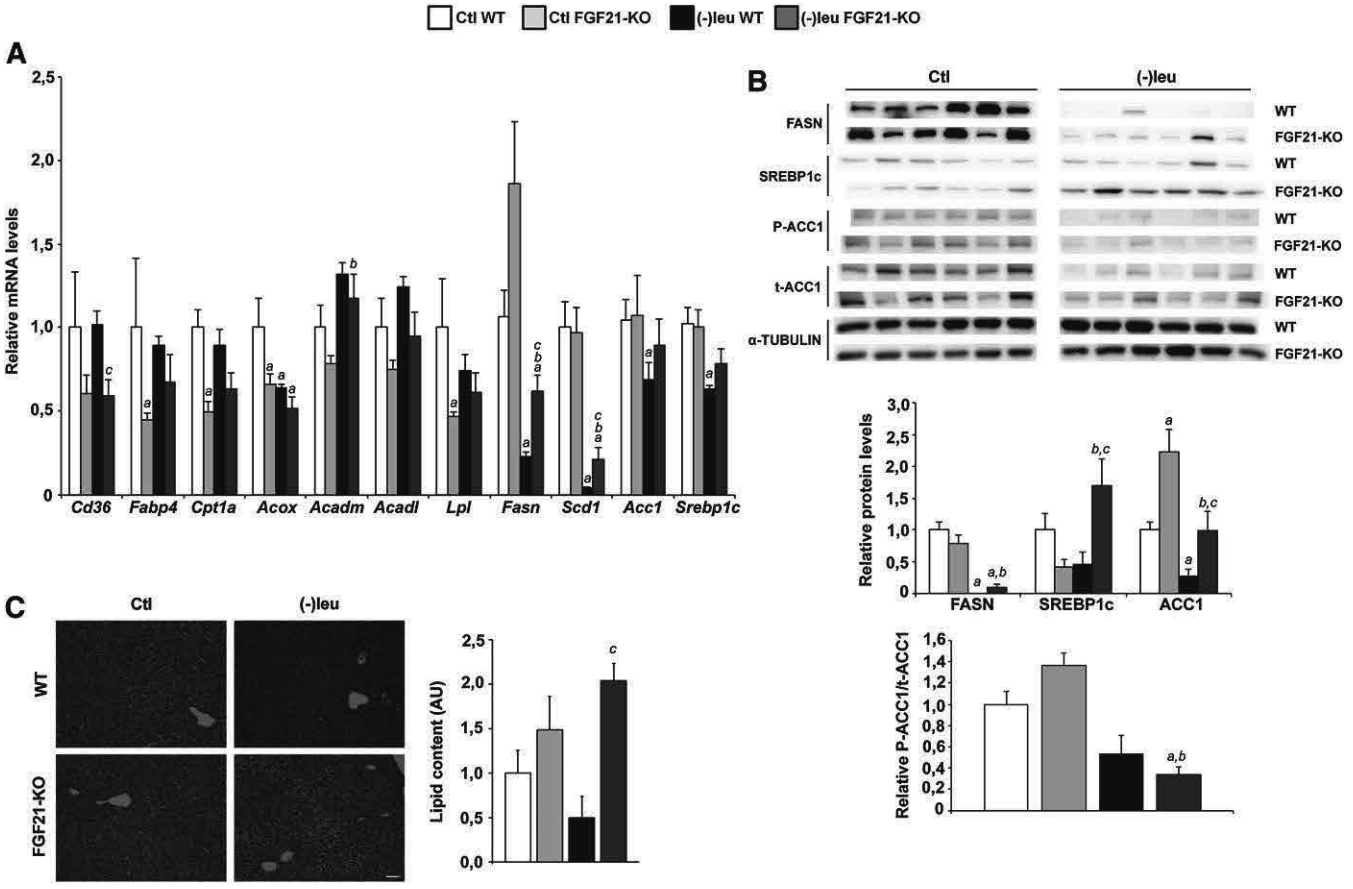

Fig. 4. FGF21-KO liver has impaired lipid metabolism and lipid accumulation in response to leucine deprivation. A: Expression of genes related with lipid handling was measured by qRT-PCR in mouse liver. B: FASN, SREBP1c, phosphorylated ACC1 (P-ACC1), and total ACC1 (t-ACC1) protein levels were detected by Western blot analysis in mouse liver. The bottom panel shows quantification by densitometry of the immunoblotted proteins using Image J software. Error bars represent the mean ± SEM. *a*, $P < 0.05$ versus Ctl WT mice; *b*, $P < 0.05$ versus Ctl FGF21-KO mice; *c*, $P < 0.05$ versus (−)leu WT mice (n = 6/group). C: Histological appearance and hepatic lipid accumulation of H and E liver staining of WT and FGF21-KO mice maintained either on a Ctl or a (−)leu diet. Representative H and E-stained hepatocytes are shown (×20 magnification). Scale bar, 50 μM. Lipid accumulation (right panel) was measured as described in Materials and Methods, using at least three different randomly chosen fields of liver sections from each mouse. Acadm, medium-chain acyl-CoA dehydrogenase; Acadl, long-chain acyl-CoA dehydrogenase; Acox, acetyl-CoA oxidase; Lpl, lipoprotein lipase; Scd1, stearoyl-CoA desaturase 1.

Although liver triglyceride levels, measured by extraction and posterior quantification, did not reflect the expression pattern of the lipid synthesis genes, H and E staining revealed it. This suggested a decreased lipid accumulation under leucine deprivation in WT animals that does not seem to occur in the *Fgf21*-KO mice (Fig. 4C).

As expected, gene expression analysis in eWAT revealed that the mRNA levels of the lipogenic genes *Fasn*, *Srebp1c*, and *Acc1* were also lower in this tissue in mice maintained on the (−)leu diet. These changes were blunted in the *Fgf21*-KO mice, particularly for *Fasn* (**Fig. 5A**). The analysis of FASN protein abundance showed a good correlation with the gene expression data (Fig. 5B).

We have analyzed the expression of the FGF21-receptor complex β-Klotho and fibroblast growth factor receptor 1 (FGFR1) in WAT. There was a significant increase in both β-Klotho and *Fgfr1* mRNA levels induced by both *Fgf21* knockout and leucine deprivation (Figs. 5C).

To further confirm the results obtained in mice, we have analyzed the expression of lipogenic and lipolytic genes in 3T3L1 treated with FGF21. This treatment induced a decrease in the expression of *Fasn*, *Srebp1c*, and *Acc1* and also of *Atgl* and *Plin* (Fig. 5D).

The FGF21-dependent phenotype during leucine deprivation is not related with the mitogen-activated protein kinase ERK1/2 signaling pathway

As described, mitogen-activated protein kinase (MAPK) ERK1/2 signaling is required for the amino acid starvation response (27, 28). Accordingly, histidinol treatment of HepG2 cells, which blocks charging of histidine onto the corresponding tRNA and thus mimics histidine deprivation, induced the phosphorylation of ERK1/2 (**Fig. 6A**). In addition, increased *FGF21* and asparagine synthetase (*ASNS*), mRNA levels (Fig. 6C), as well as increased ATF4 protein levels in HisOH-treated cells (Fig. 6B) were reduced in the presence of the MEK inhibitor PD98. In these cells, *FASN* expression is opposed to that of *FGF21* (Fig. 6D), mimicking what we observed in leucine-deprived WT (high FGF21) or *Fgf21*-null mice (Fig. 4A).

As it has been described that exogenous FGF21 is able to induce ERK1/2 phosphorylation in the liver and WAT

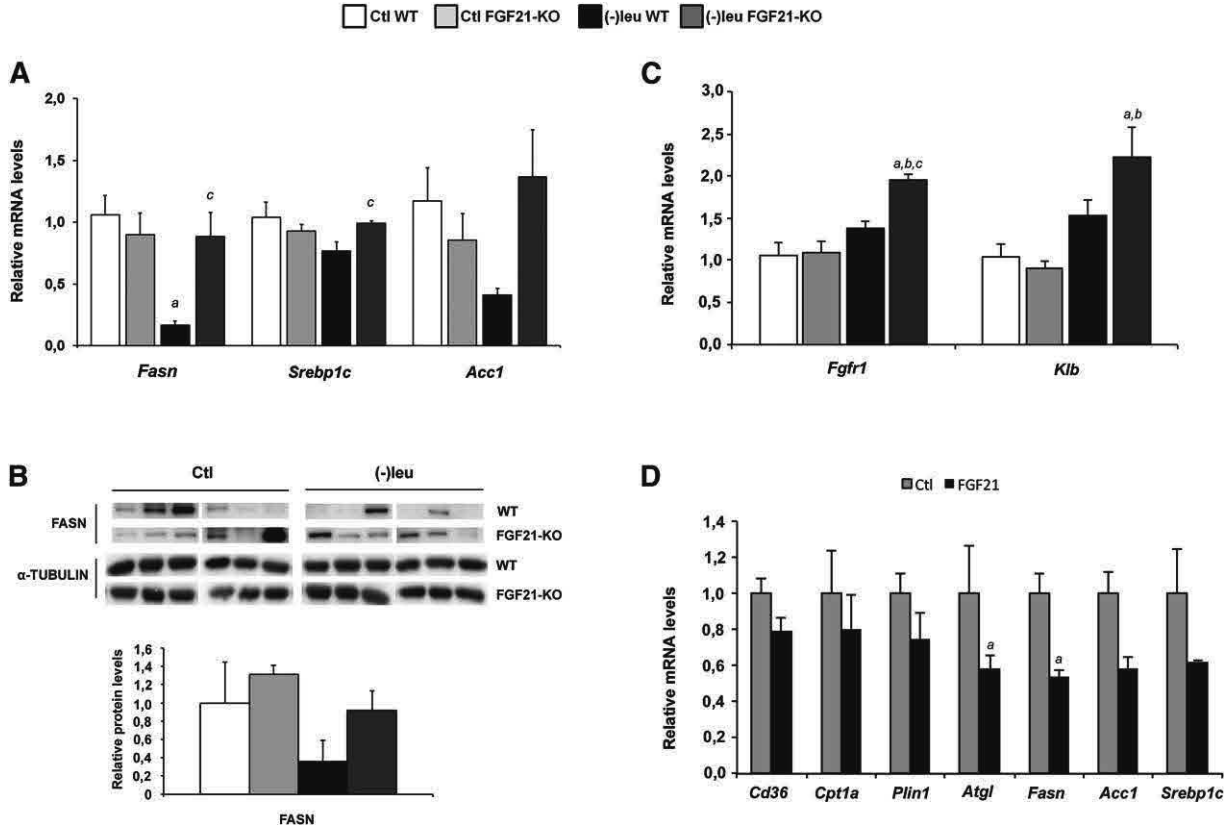

Fig. 5. FGF21-KO eWAT has altered lipogenic pathway in response to leucine deprivation. A: *Fasn*, *Srebp1c*, and *Acc1* gene expression was measured by qRT-PCR in mouse eWAT. B: FASN protein levels were detected by Western blot analysis in mouse liver. The bottom panel shows quantification by densitometry of the immunoblotted proteins using Image J software. Error bars represent the mean ± SEM. *a*, $P < 0.05$ versus Ctl WT mice; *b*, $P < 0.05$ versus Ctl FGF21-KO mice; *c*, $P < 0.05$ versus (−)leu WT mice (n = 6/group). C: *FgfR1* and β-Klotho gene expression was measured by qRT-PCR in mouse eWAT. D: The expression of genes related with lipid metabolism pathways was measured by qRT-PCR in 3T3L1 adipocytes treated with recombinant FGF21 (100 nM) for 24 h. Error bars represent the mean ± SEM. *a*, $P < 0.05$ versus Ctl WT mice; *b*, $P < 0.05$ versus Ctl FGF21-KO mice; *c*, $P < 0.05$ versus (−)leu WT mice (n = 6/group).

of acutely treated mice (29); we checked ERK1/2 phosphorylation in leucine-deprived WT and FGF21-null mice. Effectively, ERK1/2 phosphorylation was induced in the liver of leucine-deprived mice, although there were no differences between genotypes (Fig. 6E). Accordingly, the amino acid starvation response program was correctly initiated in *Fgf21*-KO mice, as shown by the increased levels of ATF4 protein and *Asns*, a prototypical ATF4 target gene, mRNA levels (Fig. 6F). Moreover, despite the fact that FGF21 serum levels are highly increased in leucine-deprived mice (Fig. 1A), ERK1/2 phosphorylation is not modified in WAT (Fig. 6G).

FGF21 deficiency prevents increases in BAT activation in leucine-deprived mice

Thermogenesis in BAT is mediated by the upregulation of UCP1 (30). It has been proposed that the induction of FGF21 production by the liver mediates direct activation of brown fat thermogenesis during the fetal-to-neonatal transition (20). FGF21 also regulates PPARγ coactivator 1 (PGC1) α and browning of WAT in adaptive thermogenesis (31). Consistent with previous results (16), leucine deprivation increased levels of *Ucp1* and *Dio2* mRNAs in the BAT of WT mice. These changes were blocked in *Fgf21*-KO mice (**Fig. 7A**). Because UCP1 expression is related to energy expenditure, the absence of induction of *Ucp1* in *Fgf21*-KO mice under leucine deprivation may contribute to the decrease in weight loss observed under these circumstances. mRNA levels of *Pgc1α*, which regulates the expression of UCP1 (32), were also increased. However, they did not differ between WT and *Fgf21*-KO mice under either control or (−)leu diet conditions (Fig. 7B). The same pattern as for *Pparγ* and *Pgc1α* was observed for *Adrb3* mRNA levels (Fig. 7C). We tested the possibility that the activation of p38 MAPK by the β3-adrenergic receptor (β3AR) participated in the induction of the *Ucp1* gene in BAT under this situation. However, although p38 phosphorylation, but not PKA activity, is induced in primary brown adipocytes treated with recombinant FGF21 (data not shown), phosphorylated p38 levels remained unchanged between diets and genotypes in BAT (Fig. 7C).

We have also analyzed the expression of lipogenic and lipolytic genes and glycerol release in primary brown adipocytes treated with FGF21. This treatment decreased the expression of *Fasn* and increased glycerol release without significant changes in the expression of *Atgl* and *Plin*

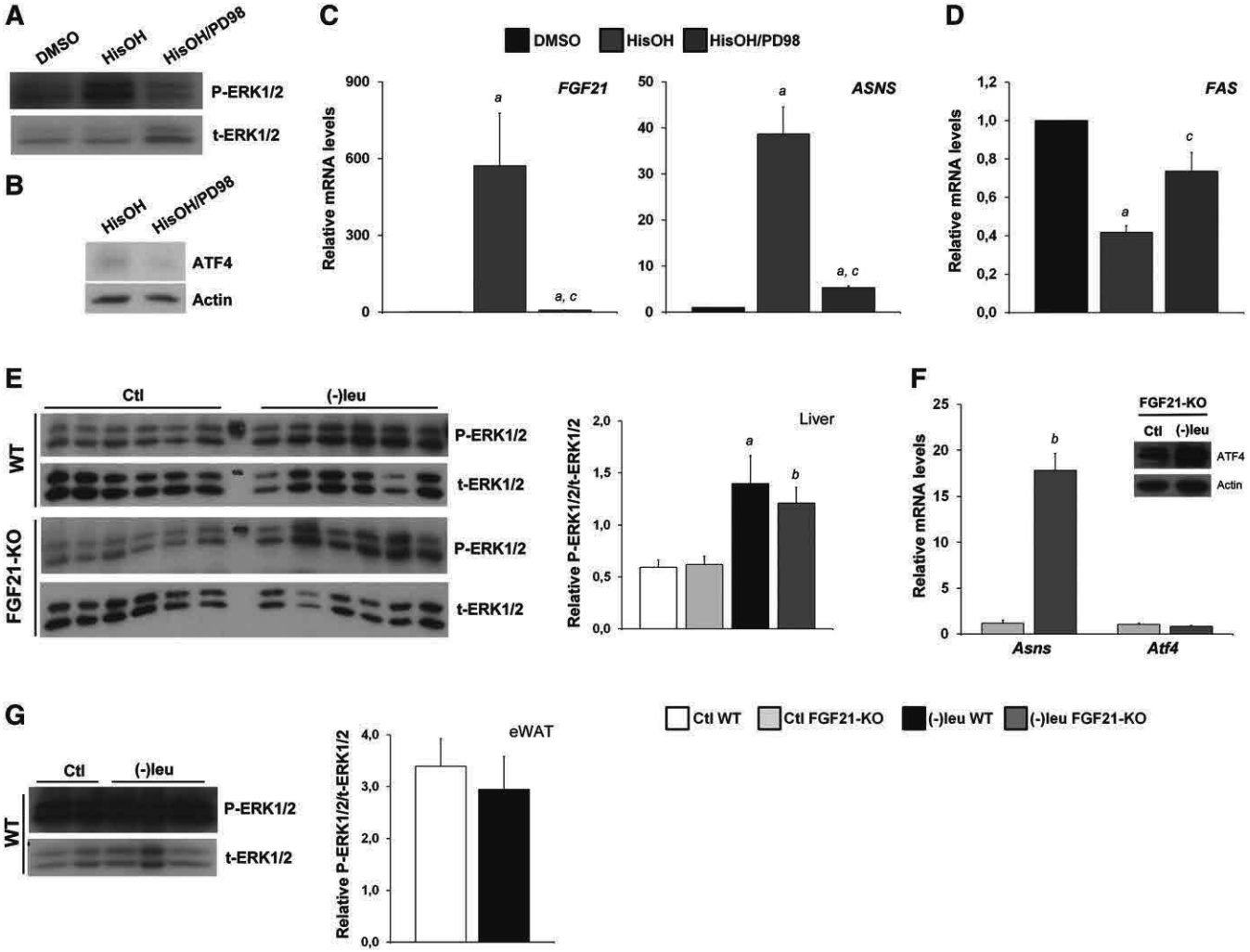

Fig. 6. Activation of the MEK/ERK pathway in the liver by leucine deprivation is independent of FGF21. HepG2 cells were incubated for 8 h with HisOH (2 mM) and the MEK inihibitor PD98 (30 μM), when indicated. Phosphorylation of ERK1/2 (A) and ATF4 protein levels (B) were analyzed by Western blot in total and nuclear HepG2 extracts, respectively. mRNA levels for *FGF21*, *ASNS* (C), and *FASN* (D) were analyzed by qRT-PCR. E: Phosphorylated ERK1/2 (P-ERK1/2) and total ERK1/2 (t-ERK1/2) levels were measured in liver extracts of WT and FGF21-KO mice by Western blot analysis. The right panel shows quantification by densitometry of phosphorylated ERK1/2 normalized to total ERK1/2 using Image J software. F: *Asns* and *Atf4* mRNA levels and nuclear ATF4 protein levels (insert), were measured in FGF21-KO mouse liver by qRT-PCR and Western blot, respectively. Actin was used as a loading control. A representative blot is shown. G: Phosphorylated and total ERK1/2 levels were measured in WT mouse eWAT homogenates by Western blot analysis. The right panel shows quantification by densitometry of phosphorylated ERK1/2 normalized to total ERK1/2 using Image J software. Error bars represent the mean ± SEM. *a*, $P < 0.05$ versus Ctl WT mice; *b*, $P < 0.05$ versus Ctl FGF21-KO mice; *c*, $P < 0.05$ versus (−)leu WT mice (n = 6/group).

(Fig. 7E, F). Accordingly, mRNA levels of *Hsl* and *Atgl* as well as HSL phosphorylation did not change in BAT of *Fgf21*-deficient mice (Fig. 7B, D).

DISCUSSION

We have previously shown that leucine deprivation significantly increased FGF21 hepatic expression and serum protein levels (2), suggesting an important role of this hormone in the amino acid starvation phenotype. In the current study, we demonstrate that in response to leucine deprivation, weight loss, downregulation of liver and WAT key lipogenic genes, as well as BAT activation are partly FGF21 dependent. Our results show that the FGF21 serum levels positively correlate with the mRNA levels measured in liver but not in BAT or WAT where they were not affected or even downregulated.

We have seen that FGF21 deficiency significantly attenuates weight loss under leucine deprivation; although the established reduction in food intake induced by a leucine-deprived diet was not changed by the absence of FGF21. This means that FGF21 is in part responsible for the loss of weight under amino acid deprivation, independently of food intake. Consistent with our observation, previous studies have shown that FGF21 transgenic mice are resistant to diet-induced obesity (DIO) and that FGF21 treatment induced weight loss in genetically obese (ob/ob) mice (24, 33, 34).

It has been shown that white adipocytes from FGF21 transgenic mice are substantially smaller than those from WT mice (8, 24). Here, we demonstrate that the reduction

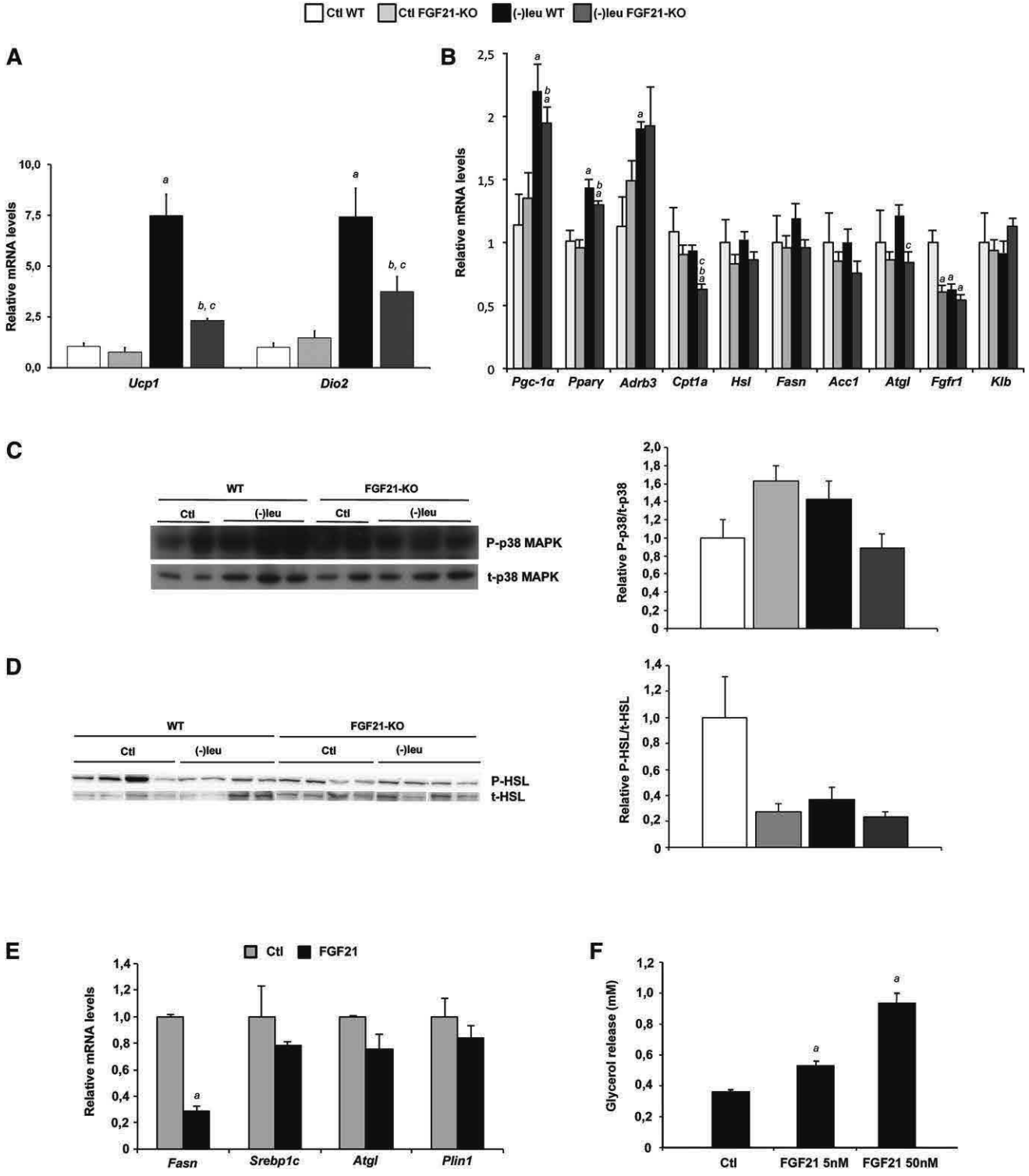

Fig. 7. FGF21 is required for inducing BAT activation during amino acid deprivation. A: *Ucp1* and *Dio2* gene expression was measured by qRT-PCR in mouse BAT. B: The expression of genes related with lipid metabolism was measured by qRT-PCR in mouse BAT. C: Phosphorylated p38 MAPK (P-p38 MAPK) and total p38 MAPK (t-p38 MAPK) levels were measured in WT and FGF21-KO mouse liver extracts by Western blot analysis. The right panel shows quantification by densitometry of phosphorylated p38 MAPK normalized to total p38 MAPK using Image J software. D: Phosphorylated and total HSL protein levels were measured in WT and FGF21-KO eWAT homogenates by Western blot analysis. The right panel shows quantification by densitometry of phosphorylated HSL normalized to total HSL, using Image J software. A representative blot is shown. E: *Fasn, Srebp1c, Atgl* and *Plin1* gene expression was measured by qRT-PCR in differentiated primary BAT treated with FGF21 (50nM) for 24h. F: Glycerol release in differentiated primary BAT treated with FGF21 (5nM and 50nM) for 24h. Error bars represent the mean ± standard error of the mean (SEM). Error bars represent the mean ± SEM. A representative blot is shown. *a*, $P < 0.05$ versus Ctl WT mice; *b*, $P < 0.05$ versus Ctl FGF21-KO mice; *c*, $P < 0.05$ versus (−)leu WT mice (n = 6/group).

in the adipocyte volume that occurs under leucine deprivation depends on the increased FGF21 expression and secretion that takes place under this diet.

We have found that the levels of phosphorylated (P)-HSL were increased upon (−)leu feeding in eWAT, as it was described in (16), so activation of the HSL protein probably allowed increased lipolysis. Interestingly, our results show that lack of FGF21 significantly decreases phosphorylated HSL levels in the eWAT of (−)leu-fed mice, suggesting an important role of FGF21 action on leucine deprivation-induced lipolysis.

The analysis of blood biochemical parameters, however, did not show significant changes in NEFA levels, likely due to increased fatty acid utilization by other tissues. We assume that there is an increased glucagon signaling under leucine deprivation, indicated by the increased PKA-dependent HSL Ser660 phosphorylation in WAT. Additionally, a reduction in insulin levels under leucine deprivation is observed in WT but not in KO mice; these changes are well correlated with the differences observed in body weight and fat mass.

We have also examined whether the impaired reduction in body weight observed in *Fgf21*-KO mice under leucine deprivation was not only related to lipolysis in WAT, but also to other factors that influence adipose tissue mass as lipogenesis. We have observed a significant reduction in *Fasn* mRNA levels in eWAT upon (−)leu feeding that was totally blocked in *Fgf21*-KO mice. *Srebp1c* and *Acc1* mRNA levels presented the same pattern, although with distinct statistical significances. The endocrine effect of FGF21 on WAT under leucine deprivation that we observe here is different from the recently described autocrine effect on this tissue in a fed state, in which FGF21 induces lipogenesis through the regulation of PPARγ activity (26). The decreased *Fgf21* expression in WAT under leucine deprivation also contrasts with its observed induction after one day of fasting (35). FGF21 administration to DIO mice leads to a dramatic decrease in the WAT *Fgf21* transcript. However, controversially, it induces an increase in the expression of adipogenic genes (33). It seems, therefore, that the response to increased levels of FGF21 depends on its origin and other factors, which may reflect the metabolic state and the energy requirements of the organism.

An inhibitory action in the lipid synthesis had been already described for FGF21 (36). It was demonstrated that the reduction of hepatic triglyceride levels was associated with FGF21 inhibition of nuclear sterol regulatory element binding protein 1c (*Srebp1c*) and the expression of an extended array of genes involved in fatty acid and triglyceride synthesis. Accordingly, in liver, we have seen that the expected reduction in the mRNA levels of *Srebp1c*, *Fasn*, and *Acc1* by (−)leu diet was not observed in *Fgf21*-KO mice. We have also seen a direct effect in lipogenic gene expression in both 3T3L1 cells and primary brown adipocytes treated with recombinant FGF21.

The induction, in liver from *Fgf21*-KO mice, of *Asns* expression, for which the gene product catalyzes the glutamine and ATP-dependent conversion of aspartic acid to asparagine, suggests that FGF21 is not involved in the control of amino acid metabolism under amino acid starvation. We have also observed that contrary to the exogenous FGF21 induction of ERK1/2 phosphorylation in the liver and WAT of acutely treated mice (29), the FGF21-dependent phenotype in leucine deprivation is unexpectedly not related with the MAPK ERK1/2 signaling pathway both in liver and WAT.

BAT is a major site of adaptive thermogenesis, and it is used to preserve both thermal and caloric homeostasis in response to environmental temperature or diet (37). *Fgf21*-KO mice under leucine deprivation exhibited decreased induction of genes defining BAT identity (i.e., *Ucp1* and *Dio2*), while its transcriptional regulators *Pgc1α* and *Pparγ* were identically induced in both WT and *Fgf21*-KO mice. Increased *Ucp1* expression may be regulated by the sympathetic nervous system through the activation of β-adrenergic receptors. We found that the mRNA expression of *Adrb3* was induced by leucine deprivation in BAT, although there were no significant changes between genotypes. The β3AR stimulates p38 MAPK, which is required for the βAR-dependent increase in *Ucp1* expression in brown adipocytes (38). Nevertheless, p38 phosphorylation levels were not affected by leucine deprivation compared with control, both in the WT

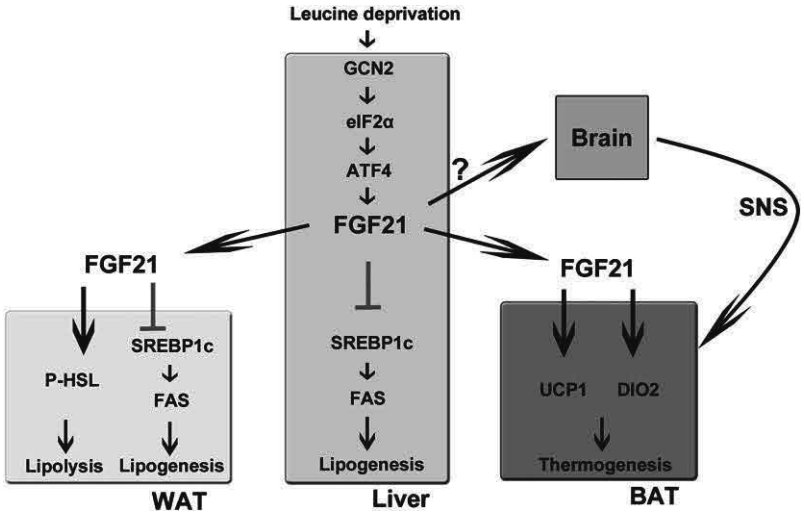

Fig. 8. Working model of the FGF21 regulatory pathway under leucine deprivation.

and *Fgf21*-KO mice. One of the best-known inducers of BAT and its function is norepinephrine (39), which has also been shown to be induced in leucine-deprived mice (16). These findings raise the possibility that FGF21 might induce *Ucp1* (and also *Dio2*) through an indirect mechanism involving the central nervous system. Of interest, it has been recently proposed that increased expression of FGF21 secreted from liver enters the brain and stimulates the hypothalamic-pituitary-adrenal axis (40). However, a more extensive analysis of other candidate factors should be performed in the future, and further investigation will be required to determine the exact mechanism by which FGF21 induces BAT activation.

In summary, we found that FGF21 is an important factor, although not the only one, in mediating the changes in lipid metabolism observed upon leucine deprivation (**Fig. 8**). We have shown that *Fgf21*-deficient mice under these circumstances showed unrepressed lipogenesis in liver and WAT, decreased phosphorylation of HSL in WAT indicating impaired lipolysis, and impaired induction of *Ucp1* expression in BAT. Thus, our results suggest that FGF21 plays an important role in the regulation of lipid metabolism during amino acid starvation.

While this work was under revision, a study was published (41) that showed the Atf4-dependent induction of FGF21 in mice with autophagy deficiency in skeletal muscle or liver. As a result of this induction, these mice are protected from diet-induced obesity and insulin resistance. In the supplementary results of this paper, the authors confirm that the ATF4-FGF21 axis also has a physiologically relevant role under conditions of leucine deprivation. In agreement with our results, they also show how the effects of leucine deprivation on body weight, fat weight, and blood glucose are partially diminished in *Fgf21*-KO mice.

REFERENCES

1. Kilberg, M. S., J. Shan, and N. Su. 2009. ATF4-dependent transcription mediates signaling of amino acid limitation. *Trends Endocrinol. Metab.* **20:** 436–443.
2. De Sousa-Coelho, A. L., P. F. Marrero, and D. Haro. 2012. Activating transcription factor 4-dependent induction of FGF21 during amino acid deprivation. *Biochem. J.* **443:** 165–171.
3. Nishimura, T., Y. Nakatake, M. Konishi, and N. Itoh. 2000. Identification of a novel FGF, FGF-21, preferentially expressed in the liver. *Biochim. Biophys. Acta.* **1492:** 203–206.
4. Johnson, C. L., J. Y. Weston, S. A. Chadi, E. N. Fazio, M. W. Huff, A. Kharitonenkov, A. Köester, and C. L. Pin. 2009. Fibroblast growth factor 21 reduces the severity of cerulein-induced pancreatitis in mice. *Gastroenterology.* **137:** 1795–1804.
5. Izumiya, Y., H. A. Bina, N. Ouchi, Y. Akasaki, A. Kharitonenkov, and K. Walsh. 2008. FGF21 is an Akt-regulated myokine. *FEBS Lett.* **582:** 3805–3810.
6. Hondares, E., R. Iglesias, A. Giralt, F. J. Gonzalez, M. Giralt, T. Mampel, and F. Villarroya. 2011. Thermogenic activation induces FGF21 expression and release in brown adipose tissue. *J. Biol. Chem.* **286:** 12983–12990.
7. Badman, M. K., P. Pissios, A. R. Kennedy, G. Koukos, J. S. Flier, and E. Maratos-Flier. 2007. Hepatic fibroblast growth factor 21 is regulated by PPARalpha and is a key mediator of hepatic lipid metabolism in ketotic states. *Cell Metab.* **5:** 426–437.
8. Inagaki, T., P. Dutchak, G. Zhao, X. Ding, L. Gautron, V. Parameswara, Y. Li, R. Goetz, M. Mohammadi, V. Esser, et al. 2007. Endocrine regulation of the fasting response by PPARalpha-mediated induction of fibroblast growth factor 21. *Cell Metab.* **5:** 415–425.
9. Gälman, C., T. Lundåsen, A. Kharitonenkov, H. A. Bina, M. Eriksson, I. Hafström, M. Dahlin, P. Amark, B. Angelin, and M. Rudling. 2008. The circulating metabolic regulator FGF21 is induced by prolonged fasting and PPARalpha activation in man. *Cell Metab.* **8:** 169–174.
10. Lundåsen, T., M. C. Hunt, L. M. Nilsson, S. Sanyal, B. Angelin, S. E. Alexson, and M. Rudling. 2007. PPARalpha is a key regulator of hepatic FGF21. *Biochem. Biophys. Res. Commun.* **360:** 437–440.
11. Reitman, M. L. 2007. FGF21: a missing link in the biology of fasting. *Cell Metab.* **5:** 405–407.
12. Uebanso, T., Y. Taketani, H. Yamamoto, K. Amo, S. Tanaka, H. Arai, Y. Takei, M. Masuda, H. Yamanaka-Okumura, and E. Takeda. 2012. Liver X receptor negatively regulates fibroblast growth factor 21 in the fatty liver induced by cholesterol-enriched diet. *J. Nutr. Biochem.* **23:** 785–790.
13. Archer, A., N. Venteclef, A. Mode, M. Pedrelli, C. Gabbi, K. Clément, P. Parini, J. Gustafsson, and M. Korach-André. 2012. Fasting-induced FGF21 is repressed by LXR activation via recruitment of an HDAC3 corepressor complex in mice. *Mol. Endocrinol.* **26:** 1980–1990.
14. Zhang, Y., Y. Xie, E. D. Berglund, K. C. Coate, T. T. He, T. Katafuchi, G. Xiao, M. J. Potthoff, W. Wei, Y. Wan, et al. 2012. The starvation hormone, fibroblast growth factor-21, extends lifespan in mice. *Elife.* **1:** e00065.
15. Guo, F., and D. R. Cavener. 2007. The GCN2 eIF2alpha kinase regulates fatty-acid homeostasis in the liver during deprivation of an essential amino acid. *Cell Metab.* **5:** 103–114.
16. Cheng, Y., Q. Meng, C. Wang, H. Li, Z. Huang, S. Chen, F. Xiao, and F. Guo. 2010. Leucine deprivation decreases fat mass by stimulation of lipolysis in white adipose tissue and upregulation of uncoupling protein 1 (UCP1) in brown adipose tissue. *Diabetes.* **59:** 17–25.
17. Cheng, Y., Q. Zhang, Q. Meng, T. Xia, Z. Huang, C. Wang, B. Liu, S. Chen, F. Xiao, Y. Du, et al. 2011. Leucine deprivation stimulates fat loss via increasing CRH expression in the hypothalamus and activating the sympathetic nervous system. *Mol. Endocrinol.* **25:** 1624–1635.
18. Zhang, Y., T. Lei, J. F. Huang, S. B. Wang, L. L. Zhou, Z. Q. Yang, and X. D. Chen. 2011. The link between fibroblast growth factor 21 and sterol regulatory element binding protein 1c during lipogenesis in hepatocytes. *Mol. Cell. Endocrinol.* **342:** 41–47.
19. Hansen, B. S., M. H. Vaughan, and L. Wang. 1972. Reversible inhibition by histidinol of protein synthesis in human cells at the activation of histidine. *J. Biol. Chem.* **247:** 3854–3857.
20. Hondares, E., M. Rosell, F. J. Gonzalez, M. Giralt, R. Iglesias, and F. Villarroya. 2010. Hepatic FGF21 expression is induced at birth via PPARalpha in response to milk intake and contributes to thermogenic activation of neonatal brown fat. *Cell Metab.* **11:** 206–212.
21. Díaz-Delfín, J., E. Hondares, R. Iglesias, M. Giralt, C. Caelles, and F. Villarroya. 2012. TNF-α represses β-Klotho expression and impairs FGF21 action in adipose cells: involvement of JNK1 in the FGF21 pathway. *Endocrinology.* **153:** 4238–4245.
22. Vilà-Brau, A., A. L. De Sousa-Coelho, C. Mayordomo, D. Haro, and P. F. Marrero. 2011. Human HMGCS2 regulates mitochondrial fatty acid oxidation and FGF21 expression in HepG2 cell line. *J. Biol. Chem.* **286:** 20423–20430.
23. Badman, M. K., A. Koester, J. S. Flier, A. Kharitonenkov, and E. Maratos-Flier. 2009. Fibroblast growth factor 21-deficient mice demonstrate impaired adaptation to ketosis. *Endocrinology.* **150:** 4931–4940.
24. Kharitonenkov, A., T. L. Shiyanova, A. Koester, A. M. Ford, R. Micanovic, E. J. Galbreath, G. E. Sandusky, L. J. Hammond, J. S. Moyers, R. A. Owens, et al. 2005. FGF-21 as a novel metabolic regulator. *J. Clin. Invest.* **115:** 1627–1635.
25. Hotta, Y., H. Nakamura, M. Konishi, Y. Murata, H. Takagi, S. Matsumura, K. Inoue, T. Fushiki, and N. Itoh. 2009. Fibroblast growth factor 21 regulates lipolysis in white adipose tissue but is not required for ketogenesis and triglyceride clearance in liver. *Endocrinology.* **150:** 4625–4633.
26. Dutchak, P. A., T. Katafuchi, A. L. Bookout, J. H. Choi, R. T. Yu, D. J. Mangelsdorf, and S. A. Kliewer. 2012. Fibroblast growth factor-21 regulates PPARγ activity and the antidiabetic actions of thiazolidinediones. *Cell.* **148:** 556–567.
27. Thiaville, M. M., Y. X. Pan, A. Gjymishka, C. Zhong, R. J. Kaufman, and M. S. Kilberg. 2008. MEK signaling is required for phosphorylation of eIF2alpha following amino acid limitation of HepG2 human hepatoma cells. *J. Biol. Chem.* **283:** 10848–10857.

28. Pan, Y. X., H. Chen, M. M. Thiaville, and M. S. Kilberg. 2007. Activation of the ATF3 gene through a co-ordinated amino acid-sensing response programme that controls transcriptional regulation of responsive genes following amino acid limitation. *Biochem. J.* **401:** 299–307.
29. Fisher, F. M., J. L. Estall, A. C. Adams, P. J. Antonellis, H. A. Bina, J. S. Flier, A. Kharitonenkov, B. M. Spiegelman, and E. Maratos-Flier. 2011. Integrated regulation of hepatic metabolism by fibroblast growth factor 21 (FGF21) in vivo. *Endocrinology.* **152:** 2996–3004.
30. Matthias, A., K. B. Ohlson, J. M. Fredriksson, A. Jacobsson, J. Nedergaard, and B. Cannon. 2000. Thermogenic responses in brown fat cells are fully UCP1-dependent. UCP2 or UCP3 do not substitute for UCP1 in adrenergically or fatty scid-induced thermogenesis. *J. Biol. Chem.* **275:** 25073–25081.
31. Fisher, F. M., S. Kleiner, N. Douris, E. C. Fox, R. J. Mepani, F. Verdeguer, J. Wu, A. Kharitonenkov, J. S. Flier, E. Maratos-Flier, et al. 2012. FGF21 regulates PGC-1α and browning of white adipose tissues in adaptive thermogenesis. *Genes Dev.* **26:** 271–281.
32. Handschin, C., and B. M. Spiegelman. 2006. Peroxisome proliferator-activated receptor gamma coactivator 1 coactivators, energy homeostasis, and metabolism. *Endocr. Rev.* **27:** 728–735.
33. Coskun, T., H. A. Bina, M. A. Schneider, J. D. Dunbar, C. C. Hu, Y. Chen, D. E. Moller, and A. Kharitonenkov. 2008. Fibroblast growth factor 21 corrects obesity in mice. *Endocrinology.* **149:** 6018–6027.
34. Xu, J., D. J. Lloyd, C. Hale, S. Stanislaus, M. Chen, G. Sivits, S. Vonderfecht, R. Hecht, Y. S. Li, R. A. Lindberg, et al. 2009. Fibroblast growth factor 21 reverses hepatic steatosis, increases energy expenditure, and improves insulin sensitivity in diet-induced obese mice. *Diabetes.* **58:** 250–259.
35. Muise, E. S., B. Azzolina, D. W. Kuo, M. El-Sherbeini, Y. Tan, X. Yuan, J. Mu, J. R. Thompson, J. P. Berger, and K. K. Wong. 2008. Adipose fibroblast growth factor 21 is up-regulated by peroxisome proliferator-activated receptor gamma and altered metabolic states. *Mol. Pharmacol.* **74:** 403–412.
36. Xu, J., S. Stanislaus, N. Chinookoswong, Y. Y. Lau, T. Hager, J. Patel, H. Ge, J. Weiszmann, S. C. Lu, M. Graham, et al. 2009. Acute glucose-lowering and insulin-sensitizing action of FGF21 in insulin resistant mouse models–association with liver and adipose tissue effects. *Am. J. Physiol. Endocrinol. Metab.* **297:** E1105–E1114.
37. Tseng, Y. H., A. M. Cypess, and C. R. Kahn. 2010. Cellular bioenergetics as a target for obesity therapy. *Nat. Rev. Drug Discov.* **9:** 465–482.
38. Cao, W., A. V. Medvedev, K. W. Daniel, and S. Collins. 2001. beta-Adrenergic activation of p38 MAP kinase in adipocytes: cAMP induction of the uncoupling protein 1 (UCP1) gene requires p38 MAP kinase. *J. Biol. Chem.* **276:** 27077–27082.
39. Cannon, B., and J. Nedergaard. 2004. Brown adipose tissue: function and physiological significance. *Physiol. Rev.* **84:** 277–359.
40. Wang, T., Y. M. Shah, T. Matsubara, Y. Zhen, T. Tanabe, T. Nagano, S. Fotso, K. W. Krausz, T. M. Zabriskie, J. R. Idle, et al. 2010. Control of steroid 21-oic acid synthesis by peroxisome proliferator-activated receptor alpha and role of the hypothalamic-pituitary-adrenal axis. *J. Biol. Chem.* **285:** 7670–7685.
41. Kim, K. H., Y. T. Jeong, H. Oh, S. H. Kim, J. M. Cho, Y. N. Kim, S. S. Kim, H. Kim, K. Y. Hur, H. K. Kim, et al. 2013. Autophagy deficiency leads to protection from obesity and insulin resistance by inducing Fgf21 as a mitokine. *Nat. Med.* **19:** 83–92.

ANNEX 5: A low-protein diet induces body weight loss and browning of subcutaneous white adipose tissue through enhanced expression of hepatic Fibroblast Growth Factor 21 (FGF21). (Article 2)

APTARA | MNFR Journal | mnfr201600725 MSP No. | Dispatch: January 20, 2017 No. of pages: 10

Mol. Nutr. Food Res. 0, 0, 2017, 1600725 DOI 10.1002/mnfr.201600725 (1 of 10) 1600725

RESEARCH ARTICLE

A low-protein diet induces body weight loss and browning of subcutaneous white adipose tissue through enhanced expression of hepatic fibroblast growth factor 21 (FGF21)

Albert Pérez-Martí[1,2], *Maite Garcia-Guasch*[1,2], *Anna Tresserra-Rimbau*[1,3,4], *Alexandra Carrilho-Do-Rosário*[1,2], *Ramon Estruch*[4,5], *Jordi Salas-Salvadó*[4,6], *Miguel Ángel Martínez-González*[4,7], *Rosa Lamuela-Raventós*[1,3,4], *Pedro F. Marrero*[1,2], *Diego Haro*[1,2] and *Joana Relat*[1,2]*

[1] Department of Nutrition, Food Sciences and Gastronomy, School of Pharmacy and Food Science, University of Barcelona, Torribera Food Campus, Santa Coloma de Gramenet, Barcelona, Spain
[2] Institute of Biomedicine of the University of Barcelona (IBUB)
[3] Insitute of Nutrition and Food Safety of the University of Barcelona (INSA-UB)
[4] CIBEROBN, Instituto de Salud Carlos III, Madrid, Spain
[5] Department of Internal Medicine, Hospital Clinic, IDIBAPS, University of Barcelona, Spain
[6] Human Nutrition Department, Hospital Universitari Sant Joan, Institut d'Investigació Sanitària Pere Virgili, University Rovira i Virgili, Reus (Tarragona), Spain
[7] Department of Preventive Medicine and Public Health, Universidad de Navarra-Institute of Health Research of Navarra (IDISNA), Pamplona, Spain

Received: August 18, 2016
Revised: November 22, 2016
Accepted: December 21, 2016

Scope: Fibroblast growth factor 21 (FGF21) is considered a promising therapeutic candidate for the treatment of obesity. Since FGF21 production is regulated by various nutritional factors, we analyze the impact of low protein intake on circulating levels of this growth hormone in mice and in a sub cohort of the PREDIMED (*Prevención con Dieta Mediterránea*) trial. We also describe the role of hepatic FGF21 in metabolic adaptation to a low-protein diet (LPD).

Methods and results: We fed control and liver-specific *Fgf21* knockout (L*Fgf21*KO) mice a LPD. This diet increased FGF21 production by inducing its overexpression in liver, and this correlated with a body weight decrease without changes in food intake. The LPD also caused FGF21-dependent browning in subcutaneous white adipose tissue (scWAT), as indicated by an increase in the expression of uncoupling protein 1 (UCP1). In a subgroup of 78 individuals from the PREDIMED trial, we observed an inverse correlation between protein intake and circulating FGF21 levels.

Conclusion: Our results reinforce the involvement of FGF21 in coordinating energy homeostasis under a range of nutritional conditions. Moreover, here we describe an approach to increase the endogenous production of FGF21, which if demonstrated functional in humans, could generate a treatment for obesity.

Keywords:
Adipose tissue / Browning / Fibroblast growth factor 21 / Low-protein diet / Uncoupling protein 1

Additional supporting information may be found in the online version of this article at the publisher's web-site

Correspondence: Dr. Diego Haro
E-mail: dharo@ub.edu

Abbreviations: **(FGF21)**, Fibroblast growth factor 21; **(LPD)**, Low-protein diet; **(WAT)**, white adipose tissue; **(UCP1)**, Uncoupling protein 1; **(EE)**, Energy expenditure; **(DIO2)**, Type 2 iodothyronine deiodinase protein 2; **(BAT)**, Brown adipose tissue; **(PPAR)**, Peroxisome proliferator-activated receptor; **(FAO)**, Fatty acid oxidation; **(ATF4)**, Activating transcription factor 4; **(DIO)**, Diet-induced obesity; **(HFD)**, High fat diet; **(CD)**, Control diet; **(FFQ)**, Quantitative food frequency questionnaire; **(PGC1a)**, Peroxisome proliferator-activated receptor gamma coactivator 1-alpha; **(PRDM16)**, PR domain containing 16

*Additional correspondence: Joana Relat
E-mail: jrelat@ub.edu

1 Introduction

FGF21 (Fibroblast growth factor 21) is considered a promising therapeutic candidate for the treatment of obesity and type-2 diabetes. Its administration to obese rodents and monkeys leads to decreased plasma concentrations of glucose, insulin, triglycerides and cholesterol, as well as a reduction in body weight through increased energy expenditure (EE) [1]. The injection of FGF21 in experimental animals induces increased thermogenic capacity by stimulating the expression of uncoupling protein 1 (UCP1) and type 2 iodothyronine deiodinase protein 2 (DIO2) in brown adipose tissue (BAT), and UCP1 in white adipose tissue (WAT), where it produces the so-called browning process [2, 3]. Although most of the effects of FGF21 have been related to UCP1 expression, it has also been reported that *Ucp1*-null mice respond positively to the pharmacological administration of this growth factor [4, 5].

FGF21 is a member of the FGF family, which is characterized by endocrine properties. It is produced mainly by the liver, but also by other tissues such as WAT, BAT, skeletal muscle, and pancreas [6–9]. Expression of FGF21 in the liver is induced by fasting, and its transcriptional activity is tightly controlled by peroxisome proliferator-activated receptor alpha (PPAR-α) [10–13]. The expression of this growth factor in liver activates fatty acid oxidation (FAO), ketogenesis, and gluconeogenesis in this organ, thereby triggering a metabolic state that mimics long-term fasting [14].

In addition to fasting, FGF21 expression is also induced in various tissues in response to a number of nutritional challenges and also to cold exposure. In this regard, FGF21 expression in BAT is produced in response to cold temperature [9,15], although it is unclear whether BAT-derived FGF21 acts as an endocrine factor or whether it is simply an autocrine factor in the adipose tissue itself.

In mouse liver and HepG2 cells, FGF21 is induced by leucine-deprivation as part of the transcriptional program initiated by increased levels of activating transcription factor 4 (ATF4) [16]. The ATF4-dependent increase in FGF21 expression has been confirmed in mice with autophagy deficiency in skeletal muscle and in liver [17]. Interestingly, these mice are protected from diet-induced obesity (DIO) and insulin resistance. The similarities in the metabolic responses between the effects to leucine-deprivation [18] and to FGF21 overexpression allowed us to consider FGF21 as a key mediator between amino acid deprivation and lipid metabolism in liver, WAT, and BAT. In this regard, results from the evaluation of the metabolic response of *Fgf21*-deficient mice to a leucine-deficient diet previously led us to conclude that, as expected, most of the effects caused by leucine deprivation in liver, WAT, and BAT are impaired in the absence of this growth factor [19].

Likewise, methionine-deprived mice show a phenotype comparable to that of leucine-deprivation, including resistance to a high-fat diet (HFD), improved glucose homeostasis, increased fatty acid activation and FAO in liver, enhanced lipolysis in WAT, and increased UCP1 expression in BAT [20, 21]. Of note, the induction of hepatic FGF21 expression under leucine- or methionine-restricted diets was found to be accompanied by an increase in FGF21 protein levels in serum.

In order to facilitate the translation of these findings to humans, here we focussed on low-protein diets (LPD) instead of amino acid-deficient diets. Protein restriction brings about weight loss and an increase in both food intake and EE [22]. Moreover, a LPD induces thermogenic markers in BAT of obese rats [23]. Moreover, serum concentrations of FGF21 in both rodents and humans increase upon exposure to an LPD, regardless of total calorie intake. This observation thus reveals that FGF21 is likely to be involved in the metabolic response to protein-restricted diets [24].

Here we addressed whether a LPD exerts similar effects on lipid metabolism to those of a leucine-deficient diet and whether these effects are dependent on hepatic FGF21 production. To this end, we examined the metabolic response of wild-type and *Fgf21* liver-specific knockout mice (L*Fgf21*KO) to a LPD (up to 5% of energy as protein). A decreased in dietary protein content induced a huge increase in FGF21 serum levels, significant weight loss, and an increase in the expression of UCP1 in the subcutaneous WAT (scWAT) of wild-type mice. Remarkably, no effects were observed in *Fgf21*-deficient mice, thereby indicating that the absence of FGF21 blunts or completely blocks the response to a LPD in this mouse model.

To corroborate these results in humans, we evaluated whether protein intake is associated with circulating levels of FGF21. We calculated protein intake through nutritional questionnaires and determined the serum levels of FGF21 in 78 individuals randomly selected from two nodes of the PREDIMED (*Prevención con Dieta Mediterránea*) trial. As with the animal model, an inverse correlation between circulating FGF21 levels and protein intake was observed.

To summarize, here we define the molecular mechanisms by which a LPD exerts its metabolic effects through the induction of hepatic FGF21 expression and browning of scWAT. Furthermore, the data collected from humans raises the possibility of investigate the dietary modulation of circulating levels of FGF21 as an alternative approach to its pharmacological administration. In this regard, we propose the modification of protein intake to enhance FGF21 production.

2 Material and methods

2.1 Animals

To generate the L*Fgf21*KO mice, $Fgf21^{loxP}$ mice ($Fgf21^{tm1.2Djm}$/J) that have *Fgf21* flanked by two *loxP* sites (Jackson Laboratory, USA) were crossed with Albumin-cre (Tg(Alb1-cre)1Dlr/J) mice (kindly provided by Dr. A. Zorzano). The latter express the CRE recombinase enzyme under control of albumin promoter/enhancer elements, thus allowing liver-specific gene deletions [25]. $Fgf21^{LoxP}$

mice were used as controls. Animals were housed in a temperature-controlled room (22 ± 1°C) on a 12/12 h light/dark cycle and were provided free access to commercial rodent chow and tap water prior to the experiments.

2.1.1 Dietary intervention

The control diet (CD) (Ref. D10001) and LPD (Ref. D12010401) were obtained from Research Diets, Inc. (USA). Both diets were isocaloric. They had the following composition (in percentage of mass): 20% protein, 66% carbohydrates and 5% fat for the CD, and 5% protein, 81% carbohydrates and 5% fat for the LPD (detailed composition shown in Supporting Information Table 1). For the feeding experiment, 8-week-old male mice were first fed the CD for 7 days and then randomly assigned to either the CD or LPD group with free access to food and water for 7 days. Food intake and body weight were recorded daily. Animals were then anesthetized by isoflurane inhalation, and blood was collected by cardiac puncture. After euthanizing the animals, tissues were isolated and immediately snap-frozen and stored at −80°C for future analysis. The Animal Ethics Committee of the University of Barcelona approved these experiments (CEEA register: 48/15)

2.1.2 Human samples for plasma measurements

We used plasma samples from 78 men and women randomly selected from the participants of the centers in Hospital Clinic (Barcelona) and Reus (Tarragona) of the PREDIMED trial (www.predimed.es). This study was a 5-year randomized clinical trial to compare the effects of either a Mediterranean diet supplemented with extra virgin olive oil or nuts versus a low-fat control diet. A total of 7447 asymptomatic men but at high cardiovascular risk (aged 55–80 years) and women (aged 60–80 years) were recruited. All participants had type 2 diabetes or three or more cardiovascular risk factors. Details of the recruitment method and study design have been described elsewhere [26] and are also available at www.predimed.es. In addition to the plasma samples, we also gathered information from these 78 individuals, including a 137-item semi-quantitative food frequency questionnaire (FFQ), and a general questionnaire that provided data on lifestyle habits, concurrent diseases, anthropometry, and medication use. Total energy intake and nutrient intake were calculated on the basis of Spanish food composition tables [27]. The study protocol was approved by the institutional review boards of the participating centers (ISRCTN35739639).

2.1.3 Plasma measurements

Mouse plasma samples were obtained by centrifuging whole blood collected in EDTA-treated tube. The plasma was stored at −80°C. FGF21 in mouse and human plasma was measured by means of a Human (ref. EZHFGF21-19K) and Mouse/Rat (ref. EZRMFGF21-26K) FGF21 ELISA obtained from EMD Millipore (Germany). The assay was conducted following the manufacturer's protocol. Briefly, a calibration curve was constructed by plotting the difference in absorbance values at 450 and 590 nm versus the FGF21 concentrations of the calibrators, and concentrations of unknown samples (performed in duplicate) were determined using this calibration curve. Free fatty acids (non-esterified fatty acids, NEFA) were determined in mice plasma by an enzymatic colorimetric assay. The Free fatty acids, Half-micro test (ref. 11383175001) was obtained from Sigma-Aldrich (USA). The measure was performed according to the manufacturers' instructions.

2.1.4 RNA isolation and relative quantitative RT-PCR

Total RNA was extracted from the frozen tissues [liver, epididymal WAT (eWAT), BAT and inguinal scWAT] using TRI reagent solution (ref. AM9738 Ambion, Thermo Fisher Scientific, USA) followed by DNase I treatment (ref. AM1906, Ambion, Thermo Fisher Scientific, USA) to eliminate genomic DNA contamination. To measure the relative mRNA levels, quantitative (q)RT-PCR was performed using SYBR Green or TaqMan reagents. cDNA was synthesized from 1 μg of total RNA by MLV reverse transcriptase (ref. 28025021, Invitrogen, Thermo Fisher Scientific, USA) with random hexamers (ref. 11034731001, Roche Diagnostics, Germany), following the manufacturer's instructions. The TaqMan Gene Expression Master Mix (ref. 4369514) and SYBR® Green PCR Master Mix (ref. 4364344), supplied by Applied Biosystems (ThermoFisher Scientific, USA), were used for the PCR step. Amplification and detection were performed using the StepOne Plus Real-Time PCR System (Applied Biosystems, ThermoFisher Scientific, USA). Each mRNA from a single sample was measured in duplicate, using 18S, Beta-Actin, and 36b4 as housekeeping genes. The primer sequences are shown in Supporting Information Table 2. Results were obtained by the Relative Standard Curve Method and expressed as fold increase versus the experimental control.

2.1.5 Protein extracts preparation

To obtain liver nuclear extracts, frozen liver was triturated with a mortar in liquid nitrogen and immediately homogenized with a Dounce in 1 mL of HB buffer [15 mM Tris-HCl (pH 8), 15 mM NaCl, 60 mM KCl, 0.5 mM EDTA], and centrifuged at 800 × *g* for 5 min. The resulting pellet was resuspended in 100 μL of HB buffer supplemented with 0.05% Triton X-100 (Sigma, USA) and centrifuged for 10 min at 1000 × *g*. Nuclear pellets were washed with 1 mL of HB buffer supplemented with 0.05% Triton X-100 and 1 mL of HB buffer. Nuclei were incubated at 4°C for 30 min in 50 μL of HB buffer containing 360 mM of KCl and then centrifuged for 5 min at 10 000 × *g*. The supernatants corresponding to the

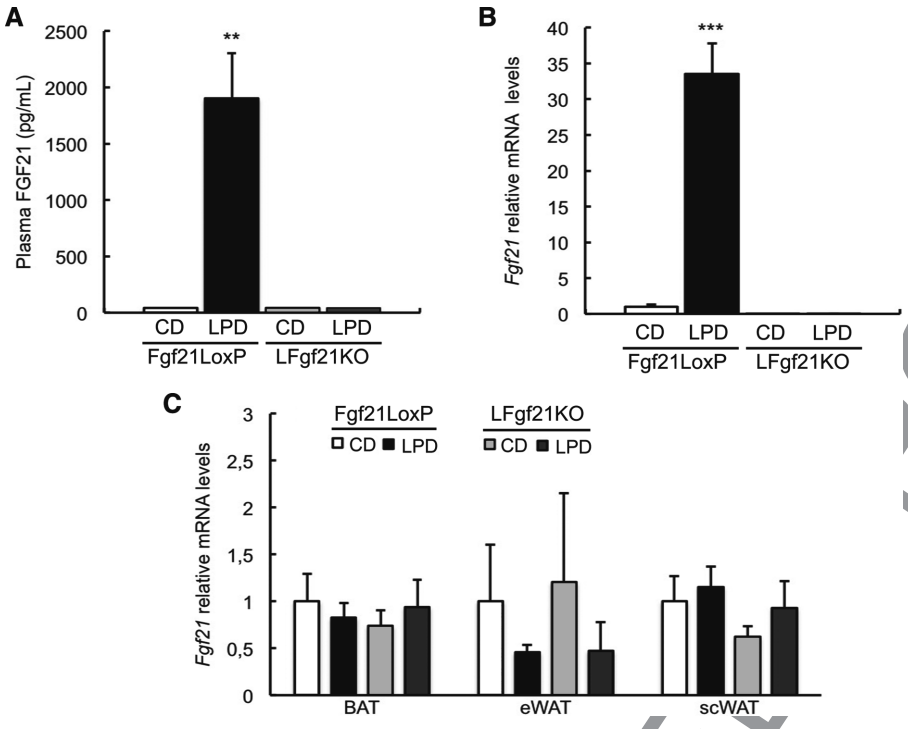

Figure 1. FGF21 is induced by an LPD in liver but not in BAT or WAT, and this induction correlates positively with plasma concentration in mice. Plasma protein concentration of FGF21 was measured by ELISA (A). Fgf21 mRNA levels in liver (B) and WAT and BAT (C) were measured by qRT-PCR. Error bars represent the mean ± SEM. $^{**}p<0.01$ $^{***}p<0.001$ versus $Fgf21^{LoxP}$ mice fed a CD ($n = 7$–9/group).

nuclear extracts were collected, frozen, and stored at −80°C. Protein concentration was determined using the Bio-Rad Protein Assay Dye Reagent Concentrate (Ref. 5000006, Bio Rad, USA). All buffers were supplemented with a mixture of protease inhibitors (Ref. P8340, Sigma-Aldrich, USA), 0.1 mM of PMSF, and a phosphatase inhibitor cocktail 3 (Ref. P0044, Sigma-Aldrich, USA).

2.1.6 Immunoblotting

Nuclear proteins were resolved by SDS-polyacrylamide gel electrophoresis and transferred onto a Hybond-P PVDF membrane (Millipore). Membranes were blocked (Tris-HCl 50 mM pH 8, 150 mM, 5% skimmed milk, 0.1% Tween) for 1 h at room temperature. The blots were then incubated with ATF4 primary antibody (sc-200, Santa Cruz Biotechnology, Inc., USA) in blocking solution (1:200). After an overnight incubation at 4°C, the blots were washed and incubated with an anti-rabbit horseradish peroxidase-conjugated secondary antibody (ref. NA934, Amersham, GE Healthcare, UK) in blocking buffer for 2 h at room temperature. The blots were developed using the EZ-ECL Chemiluminescence Detection Kit for HRP (ref. 20-500-500, Biological Industries, Israel). Quantification was performed using Image J software.

2.1.7 Data analysis/statistics

For human samples, baseline characteristics are presented as means ± standard error of the mean (SEM) for continuous variables, frequencies and percentages for categorical variables across quartiles of protein intake at baseline. Differences between quartiles were tested by a 1-factor ANOVA test for continuous variables and by the chi-square test for the categorical ones. We performed multiple linear regressions to evaluate the relationship between protein intake (exposure variable) and FGF21 hormone levels (dependent variable). Protein intake was previously adjusted for calories using the residual method. Regression analyses were unadjusted (model 1) or adjusted by body mass index (BMI) and total energy intake (model 2).

All statistical analyses were conducted using SAS software, version 9.3 (SAS Institute, Inc., USA). All t tests were two-sided and p values below 0.05 were considered statistically significant.

3 Results and discussion

3.1 A LPD induces FGF21 gene expression in the liver of control mice, but not in BAT or WAT

According to previously reported results, mice on an LPD show a dramatic increase in serum levels of FGF21 [22–24] (Fig. 1A). To check the origin of this FGF21, we analyzed the *Fgf21* mRNA levels in several tissues. The liver is the main site of FGF21 production and release into the blood. Accordingly, we observed a great induction of *Fgf21* mRNA synthesis in the liver of mice on the LPD (Fig. 1B). This increase correlated positively with serum levels. In contrast,

Fgf21 expression was unchanged in BAT, eWAT and scWAT of control mice (*Fgf21*^{loxP}) on the same diet (Fig. 1C).

To determine the specific role of hepatic FGF21 in the metabolic response to a LPD, we fed L*Fgf21*KO mice a LPD diet. As expected, *Fgf21* mRNA levels were undetectable in the livers of these animals (Fig. 1B), while no statistically significant changes were detected in BAT, eWAT, or scWAT when compared to the same tissues in control mice (Fig. 1C).

This mouse model shows that protein restriction almost exclusively affects the hepatic expression of FGF21 and that there is no compensatory response in other tissues, such as BAT or WAT.

We measured the circulating FFA levels as a possible signaling factor for the induction of FGF21 in mice under a low protein diet. The absence of statistically significant changes in FFA (data not shown) allow us to rule out the PPAR-FA axis in the signaling mechanism responsible for the induction of the hepatic expression of FGF21 in these conditions.

3.2 A LPD increases ATF4 protein levels in mouse liver

GCN2 is a kinase that acts as a sensor of amino acid supply [28]. When activated, GCN2 phosphorylates EIF2a, which results in the slowing or stalling of the initiation step of mRNA translation. Hence, phospho-EIF2a reduces general protein synthesis rates. Paradoxically, in these circumstances there is an increase in the translation of discrete mRNAs, including ATF4 [29, 30]. A LPD increases GCN2-dependent phosphorylation of eIF2a, resulting in greater levels of ATF4 protein [31, 32]. ATF4 is a transcriptional factor that directly or indirectly induces a subset of specific genes to regulate metabolic adaptation to amino acid restriction. The 5' region of Fgf21 contains two evolutionarily conserved functional ATF4-binding sequences responsible for its ATF4-dependent transcriptional activation [16, 33]. To determine the effect of an LPD on ATF4 expression, we analyzed liver protein extracts of mice fed an LPD or a CD for 7 days. ATF4 expression was induced in liver in response to the LPD, as revealed by Western blot assays (Fig. 2A and B). These results are consistent with previous published data reporting that ATF4 triggers the expression of FGF21 and that Gcn2 -/- mice show a partially blunted induction of FGF21 under protein restriction [24]. On the basis of the aforementioned published data, our results support the notion that the GCN2-ATF4 pathway is likely to be the main mechanism underlying hepatic FGF21 overexpression upon protein restriction.

GCN2-independent mechanisms that induce hepatic FGF21 in response to methionine-restricted diets have recently been described [34]. This observation points to a different response program in liver via a non-canonical PERK/nuclear respiratory factor 2 (NRF2) pathway. This alternative pathway could effectively sense and translate the metabolic responses to methionine restriction in the absence of GCN2. In parallel, the absence of GCN2 during long-term

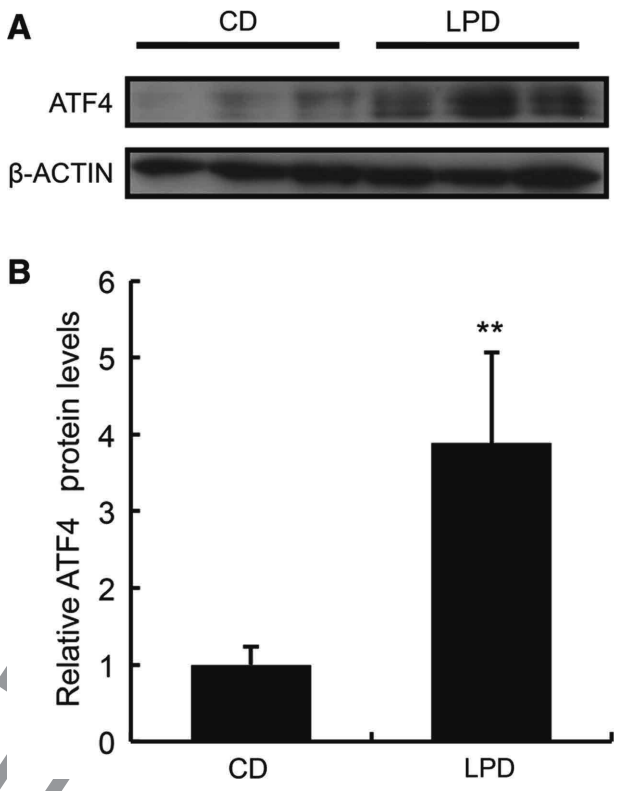

Figure 2. An LPD increases ATF4 protein levels in liver. ATF4 protein levels were determined by Western blot analysis using hepatic nuclear extracts obtained from *Fgf21*^{LoxP} mice administered a CD or LPD (A). The experiment was normalized by actin protein levels as loading control and the intensity of the bands were quantified by densitometry with the Image J software (B). Error bars represent the mean ± SEM. $^{**}p<0.01$ versus CD (n = 3/group).

dietary protein restriction has been reported to be compensated upstream of ATF4 to induce FGF21 [35]. Globally, the impact of alternative pathways to stimulate FGF21 expression under a LPD, whether they involve ATF4 or not, should be addressed in greater depth.

3.3 *Fgf21* deficiency significantly attenuates weight loss under an LPD

Mice fed an LPD presented rapid weight loss. Here we addressed whether this phenomenon is dependent on hepatic FGF21. For this purpose, *Fgf21*^{LoxP} mice and L*Fgf21*KO mice were fed a CD or LPD for 7 days.

Our data showed that weight loss was partially blunted in L*Fgf21*KO mice (Fig. 3A and B). However, the reduction in food intake observed under an LPD, that can account for some of the loss in body weight, was unchanged between genotypes (Fig. 3C). It is remarkable that these results contradicted previous publications describing either no change or an increase in food intake in response to protein restriction

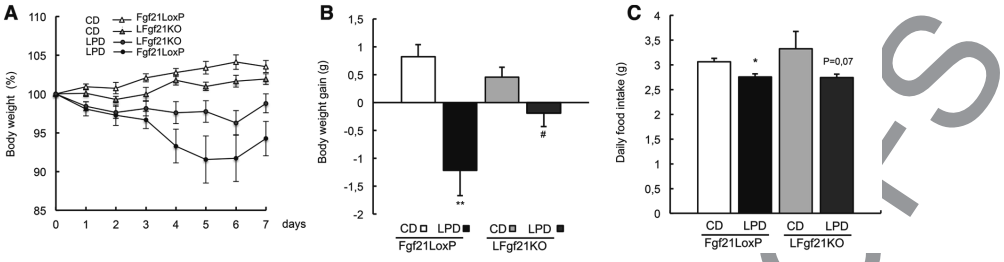

Figure 3. Hepatic FGF21 expression is required for the weight loss caused by LPD but does not affect food consumption. Body weight progression of mice fed a CD or LPD expressed as percentage of the initial weight, which was considered 100% (A). Total body weight change (g) after 7 days on a CD or LPD (B). Daily food intake (C). Error bars represent the mean ± SEM. $^{**}p<0.01$ versus *Fgf21*^{LoxP} mice fed a CD, $^{\#}p<0.05$ versus L*Fgf21*KO fed a CD; 0.07 represents *p* value versus L*Fgf21*KO mice fed a CD ($n = 7$–9/group).

[24]. Nonetheless, the present results are consistent with the decreased food intake described in mice fed leucine-deficient diets [19]. Minor changes in diet composition affecting amino acid bioavailability may explain these discrepancies. Moreover, although FGF21 has the potential to modulate food preferences [36, 37]. In our mouse model this FGF21 did not contribute to the food aversion caused by the LPD.

To determine the importance of each tissue in overall weight loss, we calculated the change in weight of individual tissues. All tissues analyzed tended to weigh less in mice on the LPD, reaching statistical significance in heart, liver, scWAT and $p = 0.06$ in eWAT (Fig. 4). Regarding the role of FGF21, our results show that the weight loss observed in scWAT and heart was dependent on hepatic FGF21 expression, as weight loss was blunted in L*Fgf21*KO mice under the same diet. The effect of the LPD on liver tissue weight was partially abolished by hepatic *Fgf21* deficiency (Fig. 4).

Taken together, FGF21 produced by the liver is, at least in part, responsible for the body weight loss experienced by the mice on the LPD. Our results point to scWAT as one of the target tissues of hepatic FGF21 regarding the weight loss effect. Since hepatic FGF21 exerts its effects mainly in WAT and BAT through regulating lipid metabolism, the following experiments are focused on describing the role of LPD-induced FGF21 on the metabolic response of adipose depots.

3.4 LPD induces metabolic changes in response to FGF21 in scWAT, but not in eWAT or BAT

Thermogenesis in BAT is mediated by the upregulation of UCP1 [38]. It has been proposed that the induction of FGF21 production by the liver mediates direct activation of brown fat thermogenesis during the fetal-to-neonatal transition [39]. FGF21 also regulates peroxisome proliferator-activated receptor gamma coactivator 1-alpha (PGC1a) and browning of WAT in adaptive thermogenesis [40].

Contrary to what happens under leucine deprivation [19], no statistically significant induction of *Ucp1* or *Dio2* mRNA levels were observed in BAT or eWAT of control mice under the LPD (Fig. 5A and B). In contrast, the analysis of gene expression in scWAT revealed that the LPD induced the expression of *Ucp1, Pgc1a, Cidea* and PR domain containing 16 (*Prdm16*), reaching a statistically significant value for *Ucp1* and *Pgc1a* (Fig. 6). This expression pattern was not detected in the L*Fgf21*KO mice (Fig. 6), thereby indicating the role

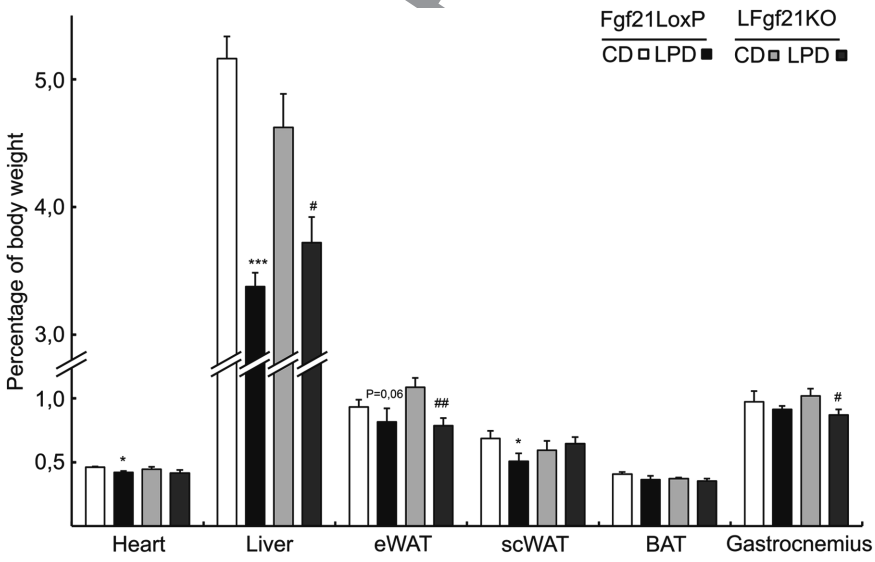

Figure 4. Hepatic FGF21 is required for the weight loss caused by an LPD. The weight of heart, liver, eWAT, scWAT, BAT, and gastrocnemius in mice fed a CD or LPD is presented as the mg of tissue per 100 mg of total body weight. Error bars represent the mean ± SEM. $^{*}p<0.05$, $^{***}p<0.001$ versus *Fgf21*^{LoxP} mice fed a CD; $^{\#}p<0.05$, $^{\#\#}p<0.01$ versus L*Fgf21*KO mice fed a CD; 0.06 represents the *p* value with respect to *Fgf21*^{LoxP} mice fed a CD ($n = 7$–9/group).

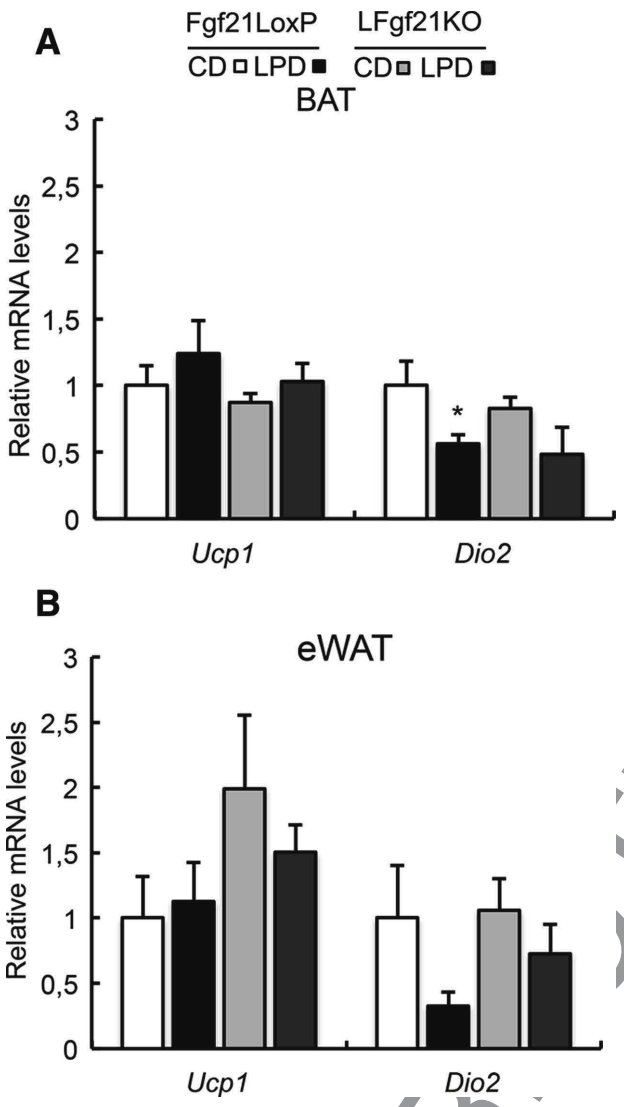

Figure 5. A LPD does not alter thermogenic genes in BAT or eWAT. *Ucp1* and *Dio2* expression was measured by qRT-PCR in mouse BAT and eWAT. Error bars represent the mean ± SEM. $^{*}p<0.05$ versus $Fgf21^{LoxP}$ mice fed a CD ($n = 7$–9/group).

of FGF21 in the metabolic adaptation of scWAT to protein restriction.

As UCP1 activity is related to EE, the blunted induction of UCP1 in the L*Fgf21*KO mice under LPD may contribute to the lower weight loss observed in this mouse model under these circumstances. In conclusion, hepatic FGF21 induces the browning of scWAT and increases the thermogenic capacity of mice on an LPD.

3.5 FGF21 plasma levels correlate negatively with protein intake in humans

To translate our results to humans, we evaluated the relationship between protein intake and circulating levels of FGF21 in 78 individuals randomly selected from the PREDIMED trial. Baseline data for these subjects are shown in Table 1. Protein intake was obtained from FFQs and was expressed as grams of protein per day (g/day). We used baseline samples (T = 0). Results from the multiple linear regression analyses showed a significant inverse relationship between plasma FGF21 concentrations and dietary intake of protein. At baseline, FGF21 levels decreased by 3.39 pg/mL for each gram of protein ingested (Table 2). The participants with a high intake of protein showed statistically significant lower values of circulating FGF21.

We also performed regression analyses using quartiles of protein intake and obtained similar results. After adjustment for BMI and total energy intake, FGF21 decreased (−30.7 pg/mL) when moving from the lower to higher quartiles ($p = 0.015$)(Fig. 7).

Similarly to the data from mice, these results indicate that the serum concentrations of FGF21 are inversely proportional to dietary protein intake.

4 Concluding remarks

Here we addressed the role of hepatic FGF21 in the metabolic changes triggered by an LPD. Our results demonstrate that the effects of an LPD depend, at least in part, on the circulating levels of FGF21 and consequently on the liver production of

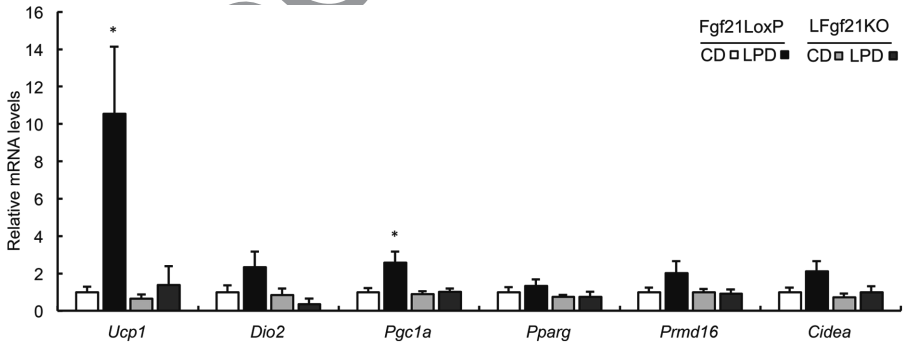

Figure 6. Hepatic FGF21 is required for inducing thermogenic gene expression during an LPD. *Ucp1, Dio2, Pgc1a, Pparg, Prmd16,* and *Cidea* expression was measured by qRT-PCR in mouse scWAT. Error bars represent the mean ± SEM. $^{*}p<0.05$ versus $Fgf21^{LoxP}$ mice fed a CD ($n = 7$–9/group).

Table 1. Baseline characteristics of participants from the PREDIMED cohort included in this study, divided into quartiles of energy-adjusted protein intake at baseline[a)]

	Quartiles of energy-adjusted protein intake				*p* value[b)]
	Q1	Q2	Q3	Q4	
No subjects (78)	19	20	20	19	
Age (years)	67.1 ± 5.9	65.7 ± 4.8	67.0 ± 6.4	65.3 ± 4.0	0.30
Sex (women)	6 (31)	10 (50)	9 (45)	15 (79)	0.03
Body mass index (kg/m^2)	28.1 ± 3.2	30.0 ± 3.4	27.7 ± 2.7	30.8 ± 2.9	0.006
Energy intake (kcal/day)	2370 ± 350	2192 ± 603	2227 ± 433	2390 ± 571	0.51
Protein intake (g/day)	80 ± 6	90 ± 2	97 ± 3	110 ± 5	<0.0001
FGF21 (pg/mL)	289 ± 116	276 ± 143	256 ± 117	190 ± 115	0.07

[a)]Categorical variables: subjects (percentage), continuous variables: mean ± SD
[b)]One-way ANOVA tests (continuous variables) or chi-squared tests (categorical variables).

Table 2. Multivariable regression analyses with FGF21 (pg/mL) as dependent variable and energy-adjusted protein intake at baseline (g/day) as independent variable

		β[a)]	*p* value	95% CI
Protein intake (continuous variable)	Model 1[b)]	−3.42	0.006	−5.83, −1.02
	Model 2[c)]	−3.39	0.007	−5.86, −0.92
Quartiles of protein intake	Model 1[b)]	−31.5	0.01	−56.5, −6.5
	Model 2[c)]	−30.8	0.02	−56.5, −5.0

CI: Confidence interval.
[a)]Parameter estimates.
[b)]Unadjusted.
[c)]Adjusted for body mass index (BMI) and total energy intake.

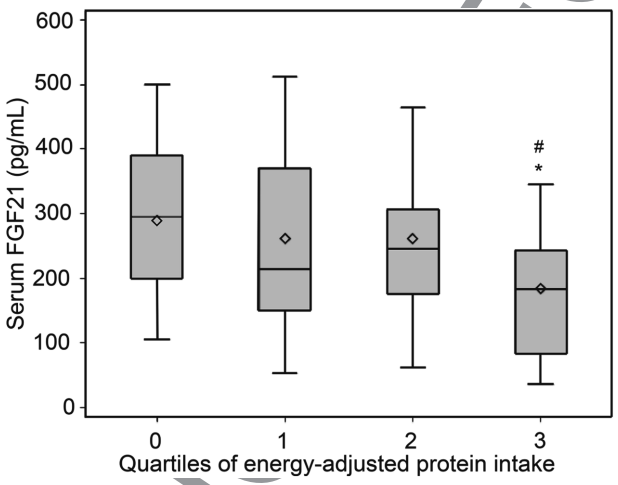

Figure 7. Circulating FGF21 levels correlate negatively with protein intake. Plasma FGF21 concentration divided into quartiles of protein intake adjusted for the calorie intake of 78 participants in the PREDIMED trial. Error bars represent the mean ± SEM. $^{*}p<0{,}05$ from first quartile; $^{\#}p<0{,}05$ from the second quartile.

this growth factor. The L*Fgf21*KO mice revealed the relevance of FGF21 in the response to an LPD, but also in the metabolic and transcriptional pathways activated or repressed by protein restriction.

Given the parallelism between the results of our study in humans and those in mice, we postulate that dietary protein content is crucial for the modulation of circulating FGF21 levels and thus for the activity of this hormone in target tissues in mice and that it could also be in humans. We propose to investigate a dietary intervention consisting of a reduction in protein intake as a non-invasive approach to induce the hepatic expression of FGF21. We also describe the molecular mechanisms through which a LPD—via FGF21—could be beneficial to restore lipid/glucose homeostasis.

Studies performed in humans provide contradictory results regarding the correlation between plasma levels of FGF21, BMI, and insulin resistance [41–43]. Also, the FGF21-resistant state described in mice [44] is not well established in humans and the beneficial effects of FGF21 induction have yet to be demonstrated in the latter.

Our findings provide new insight into the modulation of dietary protein as a strategy to induce elevated serum concentrations of FGF21. Further studies will be needed to evaluate the effects of an LPD / FGF21 induction on the metabolic profile of obese and insulin-resistant subjects.

~~*This project was supported by grant SAF2013-41093 (to P.F.M. and D.H.) from Spain's Ministerio de Economía y Competitividad, and by funding from the Catalan government (Ajut de Suport als Grups de Recerca de Catalunya 2014SGR916). A.P.M. was supported by Scholarship from Spain's Ministerio de Educación Cultura y Deporte. ACDR was supported by Scholarship from University of Barcelona.*~~

A.P.M. performed the experiments with mice. M.G.G. performed the ELISA and the statistical analysis of human samples. A.T.R. performed the statistical analysis of human samples with M.G.G. A.C.D.R. has made the FFA analysis during the revision of the manuscript. R.E., J.S.S., M.A.M.G. provided the human samples P.F.M., D.H., J.R. conceived the project and wrote the

paper. All authors read, approved and contributed with important intellectual content to the final version of the manuscript.

The authors have declared no conflict of interest.

5 References

[1] Kharitonenkov, A., Shanafelt, A.-B., FGF21: a novel prospect for the treatment of metabolic diseases. *Curr. Opin. Investig. Drugs.* 2009, *10*, 359–364.

[2] Fisher, F.-M., Kleiner, S., Douris, N., Fox, E.-C. et al., FGF21 regulates PGC-1α and browning of white adipose tissues in adaptive thermogenesis. *Genes Dev.* 2012, *26*, 271–281.

[3] Lee, P., Swarbrick, M.-M., Greenfield, J.-R., The sum of all browning in FGF21 therapeutics. *Cell Metab.* 2015, *21*, 795–796.

[4] Véniant, M.-M., Sivits, G., Helmering, J., Komorowski, R. et al., Pharmacologic effects of FGF21 are independent of the 'browning' of white adipose tissue. *Cell Metab.* 2015, *21*, 731–738.

[5] Samms, R.-J., Smith, D.-P., Cheng, C.-C., Antonellis, P.-P. et al., Discrete aspects of FGF21 in vivo pharmacology do not require UCP1. *Cell Rep.* 2015, *11*, 991–999.

[6] Nishimura, T., Nakatake, Y., Konishi, M., and Itoh, N., Identification of a novel FGF, FGF-21, preferentially expressed in the liver. *Biochim. Biophys. Acta - Gene Struct. Expr.* 2000, *1492*, 203–206.

[7] Johnson, C.-L., Weston, J.-Y., Chadi, S.-A., Fazio, E.-N. et al., Fibroblast growth factor 21 reduces the severity of cerulein-induced pancreatitis in mice. *Gastroenterology.* 2009, *137*, 1795–1804.

[8] Izumiya, Y., Bina, H.-A., Ouchi, N., Akasaki, Y. et al., FGF21 is an Akt-regulated myokine. *FEBS Lett.* 2008, *582*, 3805–3810.

[9] Hondares, E., Iglesias, R., Giralt, A., Gonzalez, F.-J. et al., Thermogenic activation induces FGF21 expression and release in brown adipose tissue. *J. Biol. Chem.* 2011, *286*, 12983–12990.

[10] Badman, M.-K., Pissios, P., Kennedy, A.-R., Koukos, G., Hepatic fibroblast growth factor 21 is regulated by PPARa and is a key mediator of hepatic lipid metabolism in ketotic states. *Cell Metab.* 2007, *5*, 426–437.

[11] Inagaki, T., Dutchak, P., Zhao, G., Ding, X. et al., Endocrine regulation of the fasting response by PPARa-mediated induction of fibroblast growth factor 21. *Cell Metab.* 2007, *5*, 415–425.

[12] Gälman, C., Lundåsen, T., Kharitonenkov, A., Bina, H.-A., et al,. The circulating metabolic regulator FGF21 is induced by prolonged fasting and PPARα activation in man. *Cell Metab.* 2008, *8*, 169–174.

[13] Lundåsen, T., Hunt, M.-C., Nilsson, L.-M., Sanyal, S. et al., PPARα is a key regulator of hepatic FGF21. *Biochem. Biophys. Res. Commun.* 2007, *360*, 437–440.

[14] Reitman, M.-L., FGF21: a missing link in the biology of fasting. *Cell Metabolism* 2007, *5*, 405–407.

[15] Chartoumpekis, D.-V., Habeos, I.-G., Ziros, P.-G., Psyrogiannis, A.-I. et al., Brown adipose tissue responds to cold and adrenergic stimulation by induction of FGF21. *Mol. Med.*, 2011, *17*, 736–740.

[16] De Sousa-Coelho, A.-L., Marrero, P.-F., Haro, D., Activating transcription factor 4-dependent induction of FGF21 during amino acid deprivation. *Biochem. J.*, 2012, *443*, 165–171.

[17] Kim, K.-H., Jeong, Y.-T., Oh, H., Kim, S.-H. et al., Autophagy deficiency leads to protection from obesity and insulin resistance by inducing Fgf21 as a mitokine. *Nat Med.* 2013, *19*, 83–92.

[18] Cheng, Y., Meng, Q., Wang, C., Li, H. et al., Leucine deprivation decreases fat mass by stimulation of lipolysis in white adipose tissue and upregulation of uncoupling protein 1 (UCP1) in brown adipose tissue. *Diabetes*, 2010, *59*, 17–25.

[19] De Sousa-Coelho, A.-L., Relat, J., Hondares, E., Pérez-Martí, A. et al., FGF21 mediates the lipid metabolism response to amino acid starvation. *J. Lipid Res.* 2013, *54*, 1786–1797.

[20] Ables, G.-P., Perrone, C.-E., Orentreich, D., Orentreich, N., Methionine-restricted C57BL/6J mice are resistant to diet-induced obesity and insulin resistance but have low bone density. *PLoS One.* 2012, *7*.

[21] Stone, K.-P., Wanders, D., Orgeron, M., Cortez, C.-C. et al., Mechanisms of increased in vivo insulin sensitivity by dietary methionine restriction in mice. *Diabetes.* 2014, *63*, 1–28.

[22] Ozaki, Y., Saito, K., Nakazawa, K., Konishi, M. et al., Rapid increase in fibroblast growth factor 21 in protein malnutrition and its impact on growth and lipid metabolism. *Br. J. Nutr.* 2015, *114*, 1410–1418.

[23] Pezeshki, A., Zapata, R.-C., Singh, A., Yee, N.-J. et al., Low protein diets produce divergent effects on energy balance. *Sci. Rep.* 2016, *6*, 25145.

[24] Laeger, T., Henagan, T.-M., Albarado, D.-C., Redman, L.-M. et al., FGF21 is an endocrine signal of protein restriction. *J. Clin. Invest.* 2014, *124*, 3913–3922.

[25] Yakar, S., Liu, J.-L., Stannard, B., Butler, A. et al., Normal growth and development in the absence of hepatic insulin-like growth factor I. *Proc. Natl. Acad. Sci.* 1999, *96*, 7324–7329.

[26] Estruch, R., Ros, E., Salas-Salvadó, J., Covas, M.-I. et al., Primary prevention of cardiovascular disease with a Mediterranean diet. *N. Engl. J. Med.* 2013, *368*, 1279–1290.

[27] Mataix, J., *Tabla de composición de alimentos*. 2003, 5a ed. Granada: Universidad de Granada.

[28] Qiu, H., Dong, J., Hu, C., Francklyn, C.-S. et al., The tRNA-binding moiety in GCN2 contains a dimerization domain that interacts with the kinase domain and is required for tRNA binding and kinase activation. *EMBO J.*, 2001, *20*, 1425–1438.

[29] Hao, S., Sharp, J.-W., Ross-Inta, C.-M., McDaniel, B.-J. et al., Uncharged tRNA and sensing of amino acid deficiency in mammalian piriform cortex. *Science* 2005, *307*, 1776–1778.

[30] Shan, J., Ord, D., Ord, T., Kilberg, M.-S., Elevated ATF4 expression, in the absence of other signals, is sufficient for transcriptional induction via CCAAT enhancer-binding protein-activating transcription factor response elements. *J. Biol. Chem.* 2009, *284*, 21241–21248.

[31] Anthony, T.-G., McDaniel, B.-J., Byerley, R.-L., McGrath, B.-C. et al., Preservation of liver protein synthesis during dietary leucine deprivation occurs at the expense of skeletal muscle

mass in mice deleted for eIF2 kinase GCN2. *J. Biol. Chem.* 2004, *279*, 36553–36561.

[32] Guo, F., Cavener, D.-R., The GCN2 eIF2a kinase regulates fatty-acid homeostasis in the liver during deprivation of an essential amino acid. *Cell Metab.*, 2007, *5*, 103–114.

[33] Wan, X.-S., Lu, X.-H., Xiao, Y.-C., Lin, Y. et al., ATF4- and CHOP-dependent induction of FGF21 through endoplasmic reticulum stress. *Biomed Res. Int.*, vol. 2014, >*2014*, 807874.

[34] Wanders, D., Stone, K.-P., Forney, L.-A., Cortez et al., Role of GCN2-independent signaling through a non-canonical PERK/NRF2 pathway in the physiological responses to dietary methionine restriction. *Diabetes*, 2016, *65*, db151324.

[35] Laeger, T., Albarado, D.-C., Burke, S.-J., Trosclair, L. et al., Metabolic responses to dietary protein restriction require an increase in FGF21 that is delayed by the absence of GCN2. *Cell Rep.*, 2016, *16*, 707–716.

[36] von Holstein-Rathlou, S., BonDurant, L.-D., Peltekian, L., Naber, M.-C. et al., FGF21 mediates endocrine control of simple sugar intake and sweet taste preference by the liver. *Cell Metab.* 2016, *23*, 335–343.

[37] Chu, A.-Y., Workalemahu, T., Paynter, N.-P., Rose, L.-M. et al., Novel locus including FGF21 is associated with dietary macronutrient intake. *Hum. Mol. Genet.* 2013, *22*, 1895–1902.

[38] Matthias, A., Ohlson, K.-B., Fredriksson, J.-M., Jacobsson, A. et al., Thermogenic responses in brown fat cells are fully UCP1-dependent. UCP2 or UCP3 do not substitute for UCP1 in adrenergically or fatty SCID-induced thermogenesis. *J. Biol. Chem.* 2000, *275*, 25073–25081.

[39] Hondares, E., Rosell, M., Gonzalez, F.-J., Giralt, M. et al., Hepatic FGF21 expression is induced at birth via PPARalpha in response to milk intake and contributes to thermogenic activation of neonatal brown fat. *Cell Metab.* 2010, *11*, 206–212.

[40] Fisher, F.-F., Kleiner, S., Douris, N., Fox, E.-C. et al., FGF21 regulates PGC-1a and browning of white adipose tissues in adaptive thermogenesis. *Genes Dev.* 2012, *26*, 271–281.

[41] Zhang, X., Yeung, D.-C.-Y., Karpisek, M., Stejskal, D. et al., Serum FGF21 levels are increased in obesity and are independently associated with the metabolic syndrome in humans. *Diabetes.* 2008, *57*, 1246–1253.

[42] Chen, W.-W., Li, L., Yang, G.-Y., Li, K. et al., Circulating FGF-21 levels in normal subjects and in newly diagnose patients with Type 2 diabetes mellitus. *Exp. Clin. Endocrinol. Diabetes.* 2008, *116*, 65–68.

[43] Chavez, A.-O., Molina-Carrion, M., Abdul-Ghani, M.-A., Folli, F. et al., Circulating fibroblast growth factor-21 is elevated in impaired glucose tolerance and type 2 diabetes and correlates with muscle and hepatic insulin resistance. *Diabetes Care* 2009, *32*, 1542–1546.

[44] Fisher, F.-M., Chui, P.-C., Antonellis, P.-J., Bina, H.-A. et al., Obesity is a fibroblast growth factor 21 (FGF21)-resistant state. *Diabetes* 2010, *59*, 2781–2789.

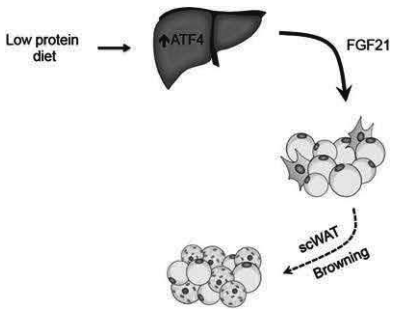

In mice, a low protein diet induces a huge increase in liver FGF21 expression and serum levels, which correlates with enhanced ATF4 protein levels. Also, this diet caused an FGF21-dependent browning of subcutaneous white adipose tissue. The observation of an inverse relationship between serum levels of FGF21 and dietary protein content also in humans suggests that the induction of hepatic FGF21 expression by a low protein diet could offer an effective treatment for obesity and type 2 diabetes.

Page 1–10

Albert Pérez-Martí, Maite Garcia-Guasch, Anna Tresserra-Rimbau, Alexandra Carrilho-Do-Rosário, Ramon Estruch, Jordi Salas-Salvadó, Miguel Ángel Martínez-González, Rosa Lamuela-Raventós, Pedro F. Marrero, Diego Haro and Joana Relat

A low-protein diet induces body weight loss and browning of subcutaneous white adipose tissue through enhanced expression of hepatic fibroblast growth factor 21 (FGF21)

ANNEX 6: Abbreviations

(-)leu	Leucine deficient
AAR	Amino Acid Response
AARE	Amino Acid Response Element
ACACA	Acetyl-CoA Carboxylase Alpha (Aso ACC1)
ACADM	Acyl-CoA dehydrogenase, C-4 to C-12 straight chain (Medium-Chain Acyl-CoA Dehydrogenase - MCAD)
ACC1	Acetyl-CoA carboxylase 1
ACOX	Acyl-CoA Oxidase
ACTH	Adenocorticotropic Hormone
ADRB3	Adrenoceptor Beta 3
AKT1	RAC-alpha serine/threonine-protein kinase 1
ALAS-1	Delta-Aminolevulinate Synthase 1
ANOVA	ANalysis Of VAriance
ANP	Atrial Natriuretic Peptide
ASNS	Asparagine Synthetase
ATF3	Activating Transcription Factor 3
ATF4	Activating Transcription Factor 4
ATGL	Adipose triglyceride lipase (Also PNLPA2 - Patatin Like Phospholipase Domain Containing 2)
AUC	Aerea Under the Curve
BAT	Brown Adipose Tissue
BeAT	Beige Adipose Tissue
BLAST	Basic Local Aligment Search Tool
BMI	Body Mass Index
bp	base pairs
C/EBP	CCAAT/enhancer-binding protein
CARE	C/ebp-Atf Response Element
CD	Control Diet
ChIP	Chromatin Immunoprecipitation
CHOP	CCAAT-enhancer-binding protein Homologous Protein
ChREBP	Carbohydrate-Responsive Element-Binding Protein
CIDEA	Cell Death-Inducing DFFA-Like Effector A
CNS	Central Nervous System
CPT1A	Carnitine Palmitoyltransferase 1A
CREB	cAMP-responsive element binding protein
CREBH	cAMP-responsive element binding protein, hepatocyte specific (Also CREB3L3 cAMP responsive element binding protein 3-like 3)
CRH	Corticotropin-Releasing Hormone
Ctl	Control
DIO	Diet Induced Obesity

DIO2	Type II Iodothyronine Deiodinase
DMEM	Dubecco'a Modified Eagle's Medium
DMT2	Diabetes Mellitus Type 2
dNTPs	Deoxynucleotides
dsDNA	double stranded DNA
EE	Energy Expenditure
EGR1	Early growth response protein 1
eiF2	Eukaryotic Initiation Factor 2
ELISA	Enzyme-Linked ImmunoSorbent Assay
ER	Endoplasmic Reticulum
ERK1/2	Extracellular Signal-Regulated
eWAT	epididymal White Adipose Tissue
FA	Fatty Acid
FABP4	Fatty Acid Binding Protein 4
FAO	Fatty Acid Oxidation
FASN	Fatty Acid Synthase
FBS	Fetal Bovine Serum
FFA	Free Fatty Acids
FFQ	Food Frequency Questionnaire
FGF	Fibroblast Growth Factor
FGFR	Fibroblast Growth Factor Receptor
FOXO1	Forkhead box O1
FRS2α	Fibroblast growth factor receptor substrate 2
FXR	Farnesoid X Receptor
GCN2	General Control Nonderepressible 2)
gDNA	genomic DNA
GH	Growth Hormone
GLUT1	Glucose Transporter 1
GLUT4	Glucose Transporter 4
GR	Glucocorticoid Receptor
GTT	Glucose Tolerance Test
H&E	Hematoxylin and Eosin
HDAC3	Histone deacetylase 3
HFD	High Fat Diet
hisOH	Histidinol
HNF6	Hepatocyte Nuclear Factor 6
HRP	Horseradish Peroxidase
HSL	Hormone Sensitive Lipase
iBAT	interscapular Brown Adipose Tissue
Ig	Immunoglobulin
IGF-1	Insulin Growth Factor 1
IP	Immunoprecipitation

ip	intraperitoneal
ITT	Insulin Tolerance Test
JNK	cJun NH-terminal Kinase
KLB	Beta-Klotho
KO	Knockout
LPD	Low protein Diet
LPL	Lipoprotein Lipase
LXR	Liver X Receptor
MAPK	Mitogen-Activated Protein Kinase
MEM	Minimum Essential Medium
mTOR	mammalian Target Of Rapamycin
MW	Multiwell
NA	Noradrenaline
NAFLD	Non Alcoholic Fatty Liver Disease
NCoR	Nuclear Receptor CoRepressor
NEFAs	Non Esterified Fatty Acids
NFY	Nuclear Transcription Factor Y
NR1D1	Nuclear Receptor Subfamily 1 Group D Member 1 (Also Rev-Erb alpha)
NRF-1	**Nuclear Respiratory Factor 1**
PBS	Phosphate-Buffered Saline
PCR	Polymerase Chain Reaction
PERK	Protein kinase RNA-like Endoplasmic Reticulum kinase
PGC-1	Peroxisome proliferator-activated receptor gamma coactivator 1
PI3K	Phosphatidylinositide 3-kinases
PKA	Protein Kinase A
PKR	Protein Kinase R
PLIN1	Perilipin 1
PPAR	Peroxisome Proliferator-Activated Receptor
PPARE	PPAR Response Element
PRDM16	PR domain containing 16
PREDIMED	Primary Prevention of Cardiovascular Disease with a Mediterranean Diet
Prop	Propranolol
Q1	First Quartile
Q2	Second Quartile
Q3	Third Quartile
Q4	Fourth Quartile
qPCR	quantitative Polymerase Chain Reaction
RAR	Retinoic Acid Receptor
ROR	RAR-related orphan receptor

RORE	ROR/REV-ERB-response element
RT	Reverse Transcription
RT	Real Temperature (≈ 25ºC)
scWAT	Subcutaneous White Adipose Tissue
SEM	Standard Error of the Mean
SIRT1	Sirtuin1
SNAT2	Sodium-dependent neutral amino acid transporter-2
SNS	Sympathetic Nervous System
SOD2	Superoxide Dismutase 2
SP1	Specific Protein 1
SREBP1	Sterol Regulatory Element-Binding Protein 1
supBAT	supraclavicular Brown Adipose Tissue
TBS	Tris-Buffered Saline
TGF	Transforming Growth Factor
TGs	Triglyceride’s
TRPM8	Transient Receptor Potential Melastin 8
TRVP-4	Transient Receptor Potential Vainilloid 4
UCP1	Uncoupling Protein 1
UCP3	Uncoupling Protein 3
VNP	Ventricular Natriuretic Peptide
WB	Western Blot
ZT	Zeitgeber Time